Titre: Title:	Diagnostic des machines dans le plan temps-fréquence
Auteur: Author:	M. S. Safizadeh
Date:	1999
Type:	Mémoire ou thèse / Dissertation or Thesis
Référence: Citation:	Safizadeh, M. S. (1999). Diagnostic des machines dans le plan temps-fréquence [Thèse de doctorat, École Polytechnique de Montréal]. PolyPublie. https://publications.polymtl.ca/8838/

UNIVERSITÉ DE MONTRÉAL

DIAGNOSTIC DES MACHINES DANS LE PLAN TEMPS-FRÉQUENCE

MIR-SAEED SAFIZADEH

DÉPARTEMENT DE GÉNIE MÉCANIQUE

ÉCOLE POLYTECHNIQUE DE MONTRÉAL

THÈSE PRÉSENTÉE EN VUE DE L'OBTENTION

DU DIPLÔME DE PHILOSOPHIAE DOCTOR

(GÉNIE MÉCANIQUE)

AOÛT 1999

UNIVERSITÉ DE MONTRÉAL

ÉCOLE POLYTECHNIQUE DE MONTRÉAL

Cette thèse intitulée:

DIAGNOSTIC DES MACHINES DANS

LE PLAN TEMPS-FRÉQUENCE

présentée par: SAFIZADEH Mir-Saeed

en vue de l'obtention du diplôme de : Philosophiae Doctor

a été dûment acceptée par le jury d'examen constitué de:

M. OSTIGUY Germain, Ph.D., président

M. LAKIS Aouni A., Ph.D., membre et directeur de recherche

M. DE SANTIS Romano M., Ph.D., membre

M. SMAÏL Mohamad, Ph.D., membre

À ma famille et
À mes parents

REMERCIEMENTS

Je tiens à adresser mes remerciements les plus sincères à mon directeur de recherche, Monsieur le professeur Aouni A. Lakis, pour son apport et son soutien constant au cours de ce travail.

En second lieu, je veux remercier Monsieur le professeur Mark Thomas de l'École de technologie supérieure pour son support lors de l'exécution des essais expérimentaux. Je remercie également Monsieur René Archambault pour son aide dans l'obtention des signaux industriels. Finalement, mes remerciements vont aux membres de jury de cette thèse, Messieurs les professeurs Germain Ostiguy, Romano De Santis et Mohamad Esmaïl.

Le support financier alloué par M.C.H.E. (Ministry of Culture and Higher Education of Iran) et mon professeur est grandement apprécié.

En dernier lieu, je remercie vivement mes parents et mon épouse pour avoir souhaité avec moi cet instant et pour m'avoir soutenu par leurs encouragements et leur confiance durant ces années de travail.

RÉSUMÉ

Ces dernières années, la surveillance et le diagnostic des machines par l'analyse des vibrations sont devenus un outil efficace pour détecter précocement les défauts et en suivre l'évolution dans le temps. La maintenance des machines nécessite une bonne compréhension des phénomènes liés à l'apparition et au développement des défauts. Détecter l'apparition à un stade précoce d'un défaut et suivre son évolution présente un grand intérêt. De fait, il existe un vaste choix de techniques de traitement de signal appliquées au diagnostic des machines, mais l'opinion générale est que ces techniques ne sont pas suffisamment efficaces et fiables. L'intérêt économique de mettre en place une méthode de maintenance prévisionnelle favorise les programmes de recherche en techniques de traitement du signal.

Les techniques de traitement du signal dans le domaine temporel et dans le domaine fréquentiel peuvent être utilisées pour identifier et isoler les défauts dans une machine tournante. Alors que l'analyse de spectre peut nous aider à détecter l'apparition d'un défaut, la décomposition du signal dans le temps peut nous fournir la nature et la position du défaut dans la machine tournante.

Cependant, bien que ces techniques puissent s'avérer très utiles dans des cas simples ou permettre la formulation rapide d'un pré diagnostic, elles présentent un certain nombre

d'inconvénients. Ces inconvénients conduisent souvent à des pertes de temps considérables ou à la formulation de diagnostics erronés. La localisation de l'origine des chocs et des phénomènes de modulation et, en particulier, des événements non stationnaires ou cyclo-stationnaires nécessite la mise en oeuvre de techniques encore plus élaborées, basées sur l'analyse tridimensionnelle (temps-fréquence-amplitude).

Ce travail consiste à étudier, comparer, modifier et adapter des techniques de représentation temps-fréquence qui peuvent être utilisées pour étudier le contenu fréquentiel d'un processus non stationnaire.

Dans la première partie de ce travail, les méthodes courantes de diagnostic des machines basées sur le temps ou la fréquence sont présentées et les avantages et désavantages de chaque méthode sont notés. Ensuite, on discute de la nécessité de la recherche dans le domaine des techniques de traitement du signal appropriées pour résoudre les problèmes de surveillance et de diagnostic des machines.

Finalement, l'application de la transformée de Fourier à fenêtre glissante (Short-time Fourier Transform), la plus simple et la plus rapide des méthodes temps-fréquence, au diagnostic de machine est présentée. Les avantages et les inconvénients de cette méthode sont également expliqués et une solution pour améliorer la performance de la transformée de Fournier à fenêtre glissante est proposée. En bref, cette partie montre l'efficacité des méthodes temps-fréquence et particulièrement l'efficacité de la transformée de Fourier à fenêtre glissante par

rapport aux méthodes traditionnelles de surveillance et de diagnostic des machines.

Dans la deuxième partie du travail, les différentes techniques des méthodes temps-fréquence, comme la distribution Wigner-Ville, la distribution Choi-Williams et la distribution RID, sont brièvement expliquées et leur avantages et désavantages examinés avec un "programme maison" (in-house program). D'abord, on s'est servi de signaux créés par ordinateur pour vérifier l'efficacité et la marche du programme. Ensuite, les signaux enregistrés durant les essais expérimentaux ont été utilisés pour vérifier la performance de chaque méthode. Finalement, les signaux enregistrés durant les essais industriels sur une boîte d'engrenage défectueuse et sur un séchoir de machine à papier ont été évalués.

Dans la troisième partie de cette recherche, les plus récentes méthodes pour une présentation temps-fréquence, soit les méthodes temps-échelle, sont expliquées. L'une de ces méthodes, la transformée en ondelettes, donne la possibilité de compenser les faiblesses des méthodes temps-fréquence. La transformée en ondelettes a une caractéristique particulière dans le plan temps-fréquence par laquelle elle est devenue un outil très efficace pour l'analyse des événements transitoires et variables dans le temps.

Cette partie du travail présente les différentes méthodes temps-échelle, comme la transformée en ondelettes, la transformée en paquet d'ondelettes et les transformées en ondelettes adaptatives. Les exemples donnés dans cette partie montrent les avantages et les désavantages des méthodes temps-échelle. Enfin, l'efficacité de ces méthodes pour la

surveillance et le diagnostic des machines est vérifiée par des signaux expérimentaux et des signaux industriels.

La quatrième partie de cette thèse présente un logiciel temps-fréquence convivial qui est développé pour faire le pont entre le bureau de recherche et le service d'ingénierie de la maintenance. Pour utiliser le programme, il suffit de choisir le signal à analyser puis de répondre aux quelques questions concernant les caractéristiques du signal telles que la fréquence d'échantillonnage, la taille du signal et les paramètres d'analyse. Ensuite, on peut visualiser la représentation temps-fréquence de chacune des méthodes temps-fréquence et temps-échelle.

Ce logiciel est équipé selon une nouvelle méthode qui s'appelle "Zoom in Wavelet Transform" pour obtenir plus de résolution fréquentielle par rapport à la transformée en ondelettes. Le logiciel exploite aussi deux nouvelles méthodes de "de-noising" par des transformées en odelettes.

L'environnement de fenêtrage de ce programme et l'affichage en couleurs de la représentation temps-fréquence font de l'outil un logiciel professionnel et puissant pour l'analyse temps-fréquence.

ABSTRACT

The analysis of vibration signals has proven to be a powerful and effective tool for the early detection of developing failure in rotating machines. The detection and diagnosis of rotating/reciprocating machines can be achieved by analyzing the vibration generated by defects. The benefits obtained in predicting failures in rotating/reciprocating machines in critical plant is needless to say, wide-ranging. A variety of signal processing techniques has been used for this purpose but a complete consensus on their effectiveness does not yet exist. The growing interest in the application of advanced methods of signal processing, emphasizes further the need for additional studies in this area.

Signal analysis techniques in time and frequency domains can be applied to identify and isolate abnormalities in rotating/reciprocating machines. While spectrum analysis aids indicating the presence of an abnormality, decomposition of the time domain signal into periodic and position locked components can be used to isolate the location of the abnormality in the machine.

Although the traditional techniques are useful in simple cases and may provide a pre-diagnostic in the complex machine but they have several limitations which reduce their performance. These limitations may often mislead us. The application of conventional

methods to the diagnostic of rotating machines for which the stationary or pseudo-stationary vibration signals cannot be assumed yields incorrect results. The analysis of non-stationary, cylco-stationary or time-varying signals needs advance methods capable to represent signals in time-frequency-amplitude domain.

The objective of the present work is to study, compare, modify and adapt the time-frequency representation techniques which can be used to analyses non-stationary phenomena.

In the first part of this thesis the classical vibration techniques in time domain and in frequency domain are presented and the advantages and disadvantages of each technique are described. In fact, in certain cases such as transient events in a machine or varying speed rotating machinery, traditional vibration analysis methods in time or in frequency are incapable of reflecting changes in the operating conditions of machines. Time-frequency methods are introduced to solve some of these problems. Among these methods, Short-Time Fourier Transform (STFT) is considered to be the simplest technique of analysis. The first part of this work proposes the application of STFT as a time-frequency method which can provide more information about a signal both in time and in frequency and demonstrate a better representation of the signal than that of the conventional methods in machinery diagnosis.

In the second part of this thesis, some of the time-frequency methods such as Wigner distribution, Choi-Williams distribution, and RID distribution are briefly reviewed and

advantages and disadvantages of different methods are examined. Then the capacity of each method is examined in a practical application by an in-house program developed for all of time-frequency methods. Primarily, computer generated signals are used to perform a preliminary test to evaluate the efficiency of the methods. Then, the signal recorded from an experimental set up is applied to verify the performance of these methods. Finally, the different methods are evaluated by using realistic signal recorded from a defective gearbox and a defective dryer machine.

The third part of this research deals with the development of new techniques such as wavelet analysis, by which it is possible to compensate for weaknesses in other time-frequency methods. Wavelet analysis has a special characteristic of time-frequency localization, which is very effective in the analysis of transient or time-varying signals. Also, a brief study of the wavelet transform, wavelet functions, the discrete wavelet transform, the wavelet packet transform and adaptive wavelet transforms is presented. Then, the advantages and disadvantages of different wavelet transforms are shown by using appropriate examples. Finally, the effectiveness of wavelet analysis in condition monitoring and diagnostics of machines is illustrated by experimental results obtained from a defective bearing and a faulty gearbox.

The fourth part of this thesis presents a user-friendly software designed to be a bridge between theoretical research in time-frequency/time-scale methods and the practical

applications of these methods in different domains. The software is able to calculate and display different time-frequency transforms from time signal data file. The software contains a number of time-frequency algorithms, such as: the Short-Time Fourier transform, the Wigner-Ville distribution, the smoothed Wigner-Ville distribution, the Choi-Williams distribution, the Born-Jordan-Cohen distribution, the Rihaczek-Marginau distribution, the Wavelet transform, the Wavelet packet transform, and the Adaptive Wavelet transforms. A graphical interface with color display and window environment of this program make the software a powerful and professional tool for time-frequency analysis.

TABLE DES MATIÈRES

LISTE DES TABLEAUX

LISTE DES FIGURES

INTRODUCTION

L'analyse du signal vibratoire d'une machine est l'une des principales méthodes de surveillance et de diagnostic des machines. Au début, l'objectif de surveillance d'une machine était d'assurer la sécurité et d'éviter les dégradations importantes. Si l'amplitude de la vibration (déplacement ou vitesse) dépassait des valeurs proposées pour le bon fonctionnement de la machine, le système de surveillance déclenchait une alarme ou l'arrêt de la machine. Ce mode de surveillance est connu sous le nom de maintenance préventive conditionnelle. Aujourd'hui, le concept de maintenance préventive conditionnelle a évolué vers celui de maintenance prévisionnelle. Ce nouveau concept non seulement comprend la fonction initiale de surveillance mais surtout permet de détecter d'une manière précoce les défauts d'une machine et d'en suivre l'évolution dans le temps. La détection des défauts au stade initial donne le temps nécessaire pour planifier, préparer et effectuer des réparations tout en provoquant des arrêts programmés à des moments opportuns.

En effet, pour un ingénieur de maintenance, il est très important de connaître la nature du défaut et sa gravité pour prendre une décision. Donc, les fonctions clés de la maintenance prévisionnelle sont la surveillance et le diagnostic. Cependant, les fondements du diagnostic et la surveillance reposent sur le traitement des signaux délivrés par les capteurs. Choisir une méthode du traitement du signal dans le domaine temporel, dans le domaine fréquentiel ou

dans le domaine du temps-fréquence peut considérablement affecter le résultat et la fiabilité d'une surveillance. Donc il n'est pas déraisonnable d'étudier l'efficacité et l'évolution des méthodes de traitement du signal afin de connaître laquelle ou lesquelles on doit choisir pour détecter l'origine exacte d'une anomalie dans le fonctionnement de la machine.

Les méthodes traditionnelles de surveillance

Surveiller une machine nécessite la détermination d'un certain nombre d'indicateurs avec un seuil associé à chacun. Tout dépassement de seuil signifie l'apparition ou l'aggravation d'un défaut ou d'un ensemble de défauts. Il faut noter que les indicateurs de surveillance peuvent être classés en deux groupes :

- Les indicateurs scalaires qui permettent de suivre l'évolution d'une grandeur dérivant de la puissance ou (et) de l'amplitude crête du signal vibratoire ;

- Les indicateurs de forme qui permettent de suivre à la fois l'évolution de la forme et de la puissance du signal.

Parmi les techniques d'analyse de vibration qui sont basées sur un indicateur de surveillance dans le domaine temporel, on peut signaler les suivantes :

1- La mesure de la valeur efficace du signal (Archambault, 1983; Barkov, Barkova et Mitchell, 1995; Ulieru, 1993).

2- La détection du niveau crête (Collacott, 1979; Swarup, 1990).

3- Le facteur crête (Archambault, 1983; Barkov, Barkova et Mitchell, 1995).

4- L'impulsion de choc (shock pulse) (Collacott, 1979; Lipovszky, Solyomvari et Varga, 1990; Mcfadden et Smith, 1983).

5- "Spike energy" (Julien Le Bleu et Ming 1995; Lipovszky, Solyomvari et Varga, 1990).

6- La méthode de Kurtosis (Brennan, Chen et Reynolds, 1997).

7- La méthode de démodulation (Barkov, Barkova et Mitchell, 1995; Enrico et Paolo, 1989; Jones, 1996; Brennan, Chen et Reynolds, 1997; Reynolds, 1995).

8- La forme d'onde dans le domaine du temps (Eshleman, 1983).

9- La méthode des orbites (Bently, Zimmer, Palmattier et Muszynska, 1986; Liangsheng, Yaodong et Jiyao, 1989; Liangsheng, Yaodong et Xiong, 1989; Lipovszky, Solyomvari et Varga, 1990).

10- La ligne centrale d'arbre (Bently, Zimmer, Palmattier et Muszynska, 1986).

D'autre part, la transformée de Fourier est un outil traditionnel, qui nous permet de passer d'une représentation temporelle à une représentation fréquentielle et d'évaluer le spectre ou la distribution d'énergie des signaux dans le domaine fréquentiel.

Parmi les techniques d'analyse de vibration dans le domaine des fréquences notons :

1- L'analyse spectrale (Angelo, 1987; James, 1986; Robert, 1994; Robert, 1985).

2- L'Holospectrum (Liangsheng, Yaodong et Jiyao, 1989).

3- Le diagramme en cascade (Leuridan, Auweraer et Vold, 1994; Trevillion, Parge, Carle, Good, 1989; Sculthorpe et Johnson, 1987).

4- Le cascade-Holospectrum (Liangsheng, Yaodong et Jiyao, 1989).

5- Le diagramme de Nyquist et Bode (Bently, Zimmer, Palmattier et Muszynska, 1986; Trevillion, Parge, Carle, Good, 1989; Majovsky et Salamone, 1988; Smith et Woodward, 1988).

6- L'analyse cepstrale (Archambault, 1989; Debao, Hongcheng, Yuanyun et Bo, 1989).

Les méthodes temps-fréquence

L'information utile est souvent véhiculée à la fois par les fréquences émises et par la structure temporelle du signal (l'exemple de la musique est caractéristique). La représentation d'un signal comme fonction du temps montre mal le spectre des fréquences en jeu, alors qu'au contraire son analyse de Fourier masque l'instant d'émission et la durée de chacun des

éléments du signal. Une représentation adéquate devrait combiner les avantages de ces deux descriptions complémentaires.

Or, dans le cas des machines tournantes, les défauts sont caractérisés par un écho en fréquence localisé dans le temps. Nous nous sommes donc tourné vers des méthodes mettant en valeur des perturbations fortement localisées en temps et en fréquence, ce qui nous a amené à considérer les transformées temps-fréquence.

La première méthode en temps-fréquence qui a été utilisée dès 1940 par Gabor pour la transmission de données était le spectrogramme ou la transformée de Fourier à fenêtre glissante (TFFG). C'est une méthode simple et efficace qui s'utilise surtout pour analyser des signaux non stationnaires.

Les principaux avantages de cette méthode sont les suivants :

a) elle donne toujours une distribution positive.

b) elle présente l'énergie totale du signal.

Les inconvénients de cette méthode sont les suivants:

a) elle dépend complètement de la longueur temporelle de la fenêtre.

b) elle donne les fréquences existantes dans chaque intervalle de temps mais elle ne donne pas le temps exact de chaque fréquence ni sa durée.

c) elle ne peut pas donner l'énergie instantanée ni le spectre instantané.

D.Gabor (1946) et J.Ville (1947) se sont attaqués au problème de la représentation mixte du signal. Une première idée, qui a été présentée par Gabor, est une méthode mathématique qui s'appelle "coherent states" en mécanique quantique. Ville a dérivé la distribution que Wigner avait élaborée en 1932 pour étudier la statistique de la mécanique quantique (quantum statistical mechanics). Ville, à la recherche du spectre instantané, voulait déployer l'énergie du signal dans le plan temps-fréquence et obtenir une densité d'énergie ayant au moins les propriétés suivantes :

- La somme des énergies pour toutes les fréquences à un temps particulier donne l'énergie instantanée.

- La somme des énergies pour tous les temps à une fréquence particulière donne le spectre instantané.

Ces deux propriétés s'appellent les conditions marginales en temps et en fréquence. On peut tout de suite constater que contrairement au spectrogramme, la transformée de Wigner-Ville donne la fréquence instantanée. Mais la distribution Wigner-Ville présente aussi des désavantages :

a) elle ne donne pas toujours une distribution positive.

b) pour un signal à composantes multiples, elle induit les termes rectangulaires (cross terms) qui sont des artefacts dont la localisation dans le plan temps-fréquence est à mi-

chemin de celle des termes carrés (self terms) correspondants.

Un an après Wigner, Kirkwood (1933) développait une autre distribution et il soutenait que celle-ci était plus simple à appliquer, dans certains cas, que la distribution de Wigner. Cette distribution est identifiée comme le spectre d'énergie complexe. Elle satisfait les conditions marginales mais elle ne donne pas la fréquence instantanée.

Une nouvelle formulation de cette distribution considérant le point de vue physique fut donnée par Rihaczek en 1968. Margenau et Hill (1961) ont obtenu cette même distribution par la méthode de la fonction caractéristique.

En 1952, Page a obtenu une nouvelle distribution qui s'appelle la puissance instantanée du spectre. La distribution de Page satisfait les conditions marginales mais elle ne retourne pas à zéro à la fin du signal.

En 1980, Classen et Mecklenbrauker ont donné une formulation générale englobant les distributions temps-fréquence engendrées à ce jour. Cette formule a une fonction arbitraire appelée noyau. En choisissant des noyaux différents, on peut avoir des distributions différentes. Cette méthode simple qui produit toutes les distributions a l'avantage de permettre la prévoyance de résultats généraux. De plus, en ajoutant des contraintes sur le noyau, on peut obtenir une distribution avec des propriétés particulières (Cohen, 1966). Dans une importante série d'articles, Classen et Mecklenbrauker (1980) ont développé une

approche complète et ils ont présenté des idées et procédures nouvelles pour étudier les distributions mixtes.

En 1989. Choi et Williams ont présenté une nouvelle approche où ils se sont attaqués à l'inconvénient principal de la distribution de Wigner-Ville, soit les termes rectangulaires. Le noyau de leur distribution a une constante telle qu'en ajustant cette constante, on peut minimiser les termes rectangulaires qui sont des artefacts dont la localisation dans le plan temps-fréquence est à mi-chemin de celle des termes carrés correspondants. En augmentant la constante, on va vers la distribution de Wigner-Ville et en diminuant le paramètre, on élimine les termes rectangulaires mais en même temps on perd de la résolution dans le temps et dans la fréquence.

En 1966, Born et Jordan ont utilisé le noyau "sinc". Mais les propriétés intéressantes de ce noyau, qui font diminuer l'amplitude des termes rectangulaires, étaient découvertes après le travail de Jeang et Williams (1992). Une revue bibliographique complète sur les méthodes temps-fréquence a été donnée par Cohen (1989).

En 1990, une nouvelle distribution était développée par Zhao, Atlas et Marks. Leur distribution non seulement diminue les termes rectangulaires mais elle les transfère à l'endroit des termes carrés.

En 1993, Louglin, Pitton et Atlas ont élaboré une méthode générale pour transférer les termes

rectangulaires à l'endroit des termes carrés. Ils ont utilisé un noyau en forme de fonction générale. Ce choix d'une fonction générale amènera à perdre quelques propriétés désirables de la distribution.

En 1994, Zhang et Sato ont présenté un noyau composé qui a été produit en combinant le noyau de Choi-Williams et celui de Margenau-Hill. Cette distribution aussi transfère les termes rectangulaires à l'endroit des termes carrés.

Mais le problème de toutes ces distributions est que le transfert des termes rectangulaires donne une modulation des termes carrés, ce qui nous empêche de trouver la vraie modulation sur les termes carrés.

Diethorn (1994) a étudié une généralisation du noyau de type Choi-Williams. Il a exprimé le noyau en forme exponentielle avec trois paramètres. En manipulant adéquatement les trois paramètres, on peut obtenir une meilleure résolution que celle de Choi-Willams avec une diminution des termes rectangulaires.

Zhengu Guo, Daurand et Haward C. Lee (1994) ont présenté un noyau basé sur la fonction de Bessel de premier type. Cette distribution élimine les termes rectangulaires et donne une bonne résolution dans le domaine temps-fréquence.

On peut dire que Boashash (1978) fut le premier à utiliser la technique temps-fréquence pour des problèmes réels et à développer de nouvelles méthodes et à les appliquer à des problèmes

d'exploration géophysique. Bazelaire et Viallix (1987) ont utilisé la distribution de Wigner pour étudier les tremblements de terre. Dans le domaine du diagnostic de machine, Forrester (1989) a utilisé la distribution de Wigner pour trouver des défauts dans le système de transmission d'un hélicoptère. Il a montré que la distribution Wigner-Ville peut révéler le défaut avec plus précision que les méthodes conventionnelles.

Dans une série d'articles, Mcfaden et Wang (1990; 1991; 1992) ont expliqué comment ils ont appliqué les méthodes temps-fréquence au diagnostic des machines. Ils ont présenté la complexité de la représentation temps-fréquence produit par la méthode de Wigner-Ville et ont suggéré une fenêtre temporelle qui peut améliorer les résultats de Wigner-Ville (Boudreaux-Bartels et Hlawatsch, 1992).

Rohrbaugh (1993) a utilisé l'analyse temps-fréquence pour des machines marines. Il a comparé la STFT avec la représentation temps-fréquence de Cohen ayant un noyau cône (cone-kernel). Rohrbaugh et Cohen (1995) ont appliqué une nouvelle méthode de temps-fréquence qui est développée par Louhlin, Pitton et Atlas (1994) au diagnostic de pompes. Cette méthode est appelée "positive time-frequency distribution" et elle est plus efficace que la méthode de STFT pour le diagnostic de machines alternatives.

Quelques applications des méthodes temps-fréquence à la surveillance de processus d'usinage comme le perçage et le broyage ont été présentées par Loughlin, Atlas, Bernard et Pitton (1995). Ils ont montré que les nouvelles méthodes peuvent fournir plus de détails,

sur signal que la méthode STFT. Atlas, Bernard et Narayanan (1996) ont offert un résumé des applications de l'analyse temps-fréquence dans différents domaines de diagnostic des machines. Ils ont souligné l'importance d'applications des méthodes temps-fréquence dans le secteur industriel et la surveillance des machines.

Dans un travail récent, Loughlin et Bernard (1997) ont présenté quelques applications de la méthode "positive time-frequency distribution" aux signaux vibratoires de différentes machines.

Les méthodes de temps-échelle (ondelettes)

Tout comme les techniques "temps-fréquence", ces techniques appartiennent à un ensemble plus général d'algorithmes qu'on retrouve aussi bien chez les mathématiciens que chez les spécialistes du traitement de signal.

Les premières publications sur les ondelettes remontent à 1984 avec l'article d'Alex Grossmann et Jean Morlet. L'essentiel de leurs idées s'inspire de travaux théoriques déjà anciens (notamment le théorème des fonctions élémentaires introduit vers 1960), d'idées plus récentes exploitées dans le traitement numérique de certains signaux sismiques et d'outils mathématiques utilisés en physique théorique (Gasquet et Witmoski, 1992).

En 1982, J. Morlet a proposé une ondelette prototype ainsi que son spectre d'amplitude. Cette ondelette montre que, comme dans le cas de temps-fréquence, les fonctions élémentaires de la transformée en ondelettes sont des filtres à bande passante avec l'avantage que procurent des bandes variables, soit d'obtenir une analyse multi-résolution.

En 1989, Stephane Mallat a utilisé les filtres miroirs en quadratures (FMQ) pour construire à l'aide d'une organisation hiérarchique des algorithmes temps-échelle qui permettent de calculer rapidement les coefficients d'ondelettes orthogonales. Cet algorithme est appelé la transformée en ondelettes rapides (TOR) et la transformée correspondante est appelée la transformée discrète en ondelettes (TDO) (Rioul et Vetterli, 1991). La division logarithmique de la bande fréquentielle dans la TDO est appelée le "splitting algorithm" (Meyer, 1992) ou algorithme de décomposition. Une série des conditions suffisantes pour la régularité de ces filtres a été donnée par Daubechies (1988, 1992). Une revue de la transformée discrète en ondelettes et le lien entre la transformée en ondelettes et la banque de filtres ont été donnés par Shensa (1992), Vetterli (1992)et Ramchandram et Vetterli (1996).

L'inconvénient majeur d'une TDO est qu'elle présente une échelle logarithmique de fréquence, ce qui ne permet pas une analyse fréquentielle plus fine aux fréquences élevées. L'algorithme ayant une échelle fréquentielle plus fine est la transformée en paquets d'ondelettes (TPO) (Hess-Nielsen et Wickerhauser, 1996; Ramchandram et Vetterli, 1996). Dans la transformée en paquets d'ondelettes, on applique le "splitting algorithm"

simultanément aux deux canaux fréquentiels. Ceci nous donne une échelle linéaire de fréquence. Pour rendre la transformée encore plus flexible et plus précise, on doit aller vers la transformée adaptative au signal (Mallat, 1993).

L'utilisation des méthodes d'ondelettes pour le diagnostic des machines est très récente. L'identification des défauts dans les roulements à billes (Li et Ma, 1992; Hongbin, 1995) et dans les boîtes d'engrenage (Mcfadden et Wang, 1993; Mcfadden et Wang, 1995; Lopez, Tenney et Deckert, 1994) sont des exemples d'application de cette méthode aux éléments essentiels des machines tournantes. Dans le cas des machines réciproques, la méthode des ondelettes est une méthode satisfaisante pour fournir les caractéristiques des signaux vibratoires (Grivelet, 1990). Zhongxing et Liangsheng ont appliqué la méthode du paquet d'ondelettes au diagnostic d'un compresseur (Zhongxing et Liangsheng, 1994). Dans une autre approche, Dalpiaz et Rivola (1995, 1997) ont utilisé la transformée en ondelettes pour la surveillance et le diagnostic dans les mécanismes contenant des cames.

Objectifs du présent travail

Comme le montre l'étude de la bibliographie, le diagnostic des machines a fait l'objet de quelques travaux dans les domaines du temps et de la fréquence. La méthode usuelle de traitement du signal présente de nombreux inconvénients dans ce type de problème.

L'utilisation de la transformée de Fourier (FFT) a ses limites. D'une part, il faut respecter le théorème d'échantillonnage. D'autre part, les signaux concernés doivent être stationnaires, ce qui limite l'utilisation de la transformée dans les applications.

Dans notre cas, les défauts sont caractérisés par des phénomènes transitoires, non stationnaires ou cyclo-stationnaires. Vu la difficulté de trouver les défauts dans la représentation temporelle ou fréquentielle, il est nécessaire d'aller vers la représentation mixte ou la représentation temps-fréquence-énergie, qui nous permet :

- de détecter et de suivre l'évolution de défauts qui induisent une puissance vibratoire fiable, qui cependant peut modifier considérablement la forme du signal. C'est notamment le cas des défauts qui induisent une modulation de l'amplitude ou de la fréquence de certaines composantes caractéristiques de la chaîne cinématique complexe (roulement des paliers des lignes d'arbre à faible et très faible vitesse de rotation : broyeurs à boulets, fours rotatifs, laminoirs, cylindres sécheurs et sections "presses" de machine à papier, etc);

- de surveiller les installations dont le processus de fonctionnement normal génère des chocs périodiques d'amplitudes élevées (compresseurs à vis, à pistons, machines alternatives, etc) susceptibles de masquer l'apparition de défauts induisant des forces impulsionnelles (dégradation de roulement, écaillage de denture, jeux de palier, d'accouplement, de clavette, etc).

Dans cette thèse nous prenons en charge les points suivants:

a) Un problème que pose la représentation temps-fréquence est le manque de précision et de résolution dans des méthodes temps-fréquence et temps-échelle telle que la méthode en ondelettes et STFT. Pour résoudre ce problème, nous développons une nouvelle méthode appelée "*Zoom in wavelet transform*"qui permet à l'utilisateur d'aller chercher une précision désirable dans une bande de fréquence choisie. Ainsi, nous proposons une méthode de STFT qui utilise un indicateur courant du diagnostic de machine pour ajuster la résolution dans le plan temps-fréquence.

b) Un autre problème de représentation temps-fréquence est le bruit qui nous empêche de voir le signal. Malgré le fait que la représentation temps-fréquence disperse le bruit sur le plan temps-fréquence donc garde le niveau du bruit bas, il reste que le niveau du bruit complique parfois l'identification des défauts.

Pour résoudre ce problème, deux méthodes de "de-noising" sont utilisées :

1- "De-noising" par la méthode en ondelettes.

2- "De-noising" par l'algorithme de "Matching Pursuit".

Il faut noter qu'on ne peut pas appliquer la méthode courante de "de-noising", qui est de faire la moyenne, parce que les signaux captés sur une machine peuvent être non stationnaires.

c) Un autre problème de représentation temps-fréquence est le manque d'un logiciel facile à utiliser. Pour résoudre le problème, un logiciel de traitement de signal utilisant les différentes méthodes du type "temps-fréquence" et du type "temps-échelle" ainsi que la méthode FFT, et en tenant compte des améliorations décrites en ***a)*** et en ***b)*** est développé dans le cadre de cette thèse. Ce logiciel permet aux ingénieurs ou aux techniciens en surveillance de machine de faire le traitement de signal vibratoire de machines et de structures même s'ils n'ont pas d'expérience spécifique en analyse de signal.

d) Un autre problème de représentation temps-fréquence est le choix de la méthode d'analyse. Pour examiner la fiabilité des techniques d'investigation temps-fréquence sur lesquelles repose le logiciel, nous procédons à des analyses de signaux dotés de caractéristiques différentes créés par l'ordinateur.

Ensuite, nous effectuons quelques essais expérimentaux dans le laboratoire de diagnostic des machines afin de passer au diagnostic industriel des machines. À cette étape, les difficultés posées par les signaux réels et la nécessité de développer des techniques encore plus complémentaires pour résoudre ces problèmes sont apparus.

Après avoir surmonté les problèmes pratiques, nous exécutons quelques essais industriels sur les signaux captés sur une boîte d'engrenages et sur un séchoir de machine à papier.

Organisation de la thèse

Cette thèse est constituée d'articles qui forment le corps principal du travail. Comme on vient de voir, l'introduction comporte une brève revue historique suivie par une bibliographie des méthodes traditionnelles de surveillance de machine, des méthodes temps-fréquence et des méthodes temps-échelle. Les objectifs du travail et l'organisation de cette thèse sont également définis dans ces pages. Le premier chapitre présente l'application de la méthode de la transformée de Fourier à fenêtre glissante au diagnostic de machines. Dans ce chapitre les avantages et les inconvénients des méthodes traditionnelles de diagnostic de machines sont étudiés et la nécessité d'appliquer des méthodes temps-fréquence est discutée par quelques exemples. Cet article a été soumis à l'International Journal of Condition Monitoring and Diagnostic Engineering Management (COMADEM). Le deuxième chapitre présente les distributions temps-fréquence et les applications de ces distributions à la détection des défauts. La classe générale des méthodes temps-fréquence et une étude approfondie des méthodes temps-fréquence sont également présentées dans ce chapitre. Ainsi, les différentes méthodes temps-fréquence sont comparées au moyen de plusieurs exemples. L'article a été soumis au Journal of Sound and Vibration.

Le chapitre trois présente l'application de la transformée en ondelettes dans le domaine du diagnostic des machines. Dans ce chapitre une autre représentation temps-fréquence par des méthodes temps-échelle est présentée et les avantages et désavantages de cette méthode sont

montrés par quelques exemples. De plus les nouvelles méthodes du *"Zoom in Wavelet Transform"* et du "de-noising" sont décrites. Cet article a été soumis au Journal of Mechanical Systems and Signal Processing.

Le quatrième chapitre porte sur les algorithmes temps-fréquence et sur leurs applications. Ce chapitre décrit le logiciel général qui a été développé dans le cadre de cette recherche et les options qu'on peut obtenir par ce logiciel. Cet article a été soumis à l'International Journal of Computers and Their Applications.

Enfin, la conclusion de cette thèse suivie par quelques perspectives de travaux futurs sont présentées.

CHAPITRE I

USING SHORT-TIME FOURIER TRANSFORM IN MACHINERY FAULT DIAGNOSIS*

[1]M.S. Safizadeh, [1]A.A. Lakis and [2]M. Thomas

1: Département de Génie Mécanique, École Polytechnique de Montréal

Case Postale 6079, Succ. Centre-ville, Montréal, Canada H3C 3A7

2: Département de Génie Mécanique, École de Technologie Supérieure

1100, rue Notre-Dame Ouest, Montréal, Canada H3C 1K3

1.1 Abstract

The detection of faults in machinery is based on the verification of classical vibration parameters, including both time domain and frequency domain parameters. There are several methods by which one can estimate these parameters and each of the methods has advantages and disadvantages. In certain cases, such as transient events in machinery or varying speed rotating machinery, traditional methods of vibration analysis either in time or in frequency are incapable of reflecting changes in the operating conditions. The use of time-frequency

★: Soumis pour publication dans "International Journal of Condition Monitoring and Diagnostic Engineering Management (COMADEM)"

methods is one step towards a solution of some of the problems and the Short-Time Fourier Transform (STFT) is the simplest method of time-frequency analysis.

This paper proposes the application of the STFT as a time-frequency method which can provide more information about a signal both in time and in frequency, and give a better representation of the signal than the conventional methods used in machinery diagnosis.

In this paper, we review the traditional vibration analysis techniques which are widely used in practice. Secondly, we discuss the necessity of time-frequency analysis in the field of machinery diagnostics. Thirdly, the theory of the Short-Time Fourier Transform is briefly explained. Some practical examples of defective bearings and defective gearboxes are analyzed by the STFT method and, in conclusion, the effectiveness and advantages of the STFT are demonstrated.

1.2 Introduction

With increased competition in the production and greater pressure on the price of industrial rotating machinery, the necessity for efficient methods of the condition monitoring and detecting faults in machinery has become apparent. It is necessary to find, on the one hand, ways to protect the productivity of critical equipment and, on the other hand, ways to reduce operating and maintenance costs. The most efficient method will be one which recognize that

a problem exists before damage has occurred in machine, so that ample time is available to schedule repairs with minimum disruption to operations and production [1].

The wave forms of vibration signals from rotating machinery are often recorded and analyzed by processing the data using analysis techniques. Each different technique gives some information about the condition of the machinery but the need exists for a technique which gives all the necessary information.

In practice, after deciding on the type of sensor, its location and the parameter to be monitored [2], the processing technique to be chosen will depend upon the precise condition we wish to monitor. If *fault detection* is our objective, then the speed and reliability of the processing technique are important but, if *fault diagnosis* is our objective, the accuracy of the method is critical.

There are several conventional methods for the detection and identification of faults. Some of these methods provide a representation of signals in the time domain and others in the frequency domain. In all of the methods, it is assumed that signals are stationary. This assumption, however, is not always accurate. In certain machines, in the early stages of defects, vibrational signals become non-stationary; in this case, conventional methods are not applicable.

In recent years, a number of new analytical methods have been developed in the field of

signal processing: these are called "joint time-frequency analysis methods". However, they are not generally used in the field of machinery diagnostics. There has been considerable progress in research into the development of the theory of joint time-frequency methods and other non-stationary signal processing methods, but more work must be carried out to prove to industry that these new methods are effective in the condition-monitoring of mechanical systems.

The objective of this work is, firstly, to outline the limitations of conventional methods and, secondly, to demonstrate the speed and accuracy which can be obtained by using joint time-frequency analysis methods in the field of machinery diagnostics. In this paper we first present a review of traditional methods with their advantages and disadvantages. Secondly, we discuss the necessity for using time-frequency methods, and present a brief theory of the Short-Time Fourier Transform as the fastest and the easiest method among other time-frequency methods. Thirdly, a technique of adaptively adjusting the window length used in the Short-Time Fourier Transform is presented. Finally, some examples of fault detection and the identification of real problems are given, using the Short-Time Fourier Transform.

1.3 Time-based and frequency-based vibration analysis techniques

There are a large number of vibration analysis techniques which may be applied to the

processing of a vibrational signal. These techniques can highlight different characteristics of the signal which may be used in the detection and diagnosis of faults in machinery. Many studies have been carried out to find the most effective technique for the analysis, monitoring and diagnostics of machines. Unfortunately, none of these techniques has been proven to be efficient. In the following section, the advantages and disadvantages of conventional methods are described in order to understand why time-frequency methods are needed.

Conventional vibration analysis methods fall into two categories:

a) Time-domain vibration analysis techniques

b) Frequency-domain vibration analysis techniques

1.3.1 Time-domain vibration analysis techniques

***I*) Time wave form:**

Using an instrument as simple as an oscilloscope or FFT analyzer, it is possible to view the wave form of the vibration. It may be possible to identify the period of events existing in a machine and any amplitude modulation in the vibration signal [3]. However, although the time domain often shows the nature of the mechanical problem better than the frequency domain, there are several reasons which lead us to avoid the use of the time domain display

in machine monitoring. For instance, in the case of a complex machine, the vibration signature may combine several signals with different frequencies, amplitudes and phases, and it would be virtually impossible to decompose the signature into its separate components. However, used in conjunction with other methods, it could prove helpful.

***II*) Overall level (R.M.S.) measurements:**

Overall level measurements [4-6] are the most common vibration measurement in use. It is a simple and inexpensive type of measurement, which is calculated by estimating the root mean square (RMS) level of the time record. It has been found that, in rotating machinery, velocity is the best indicator of general condition. Charts are available which indicate acceptable levels, for example VDI 2056 (table 1.1). The greatest limitation is the lack of precise information to be extracted from the data. These charts are extremely generalized in conception, and have little regard to mobility. The mobility relationship is defined as:

$$Vibration = Force \times Mobility$$

where the mobility is the ability of a structure to move under force. Since the mobility changes from machine to machine, vibration level changes accordingly. For example, the measurement of a damaged bearing must be made on the outside of the bearing housing support. The signal detecting procedure is affected by the transmission path to the sensor.

Unless a problem is severe, the overall level measurements may not change significantly. Unfortunately, people have relied too heavily on these measurements alone, and have been surprised to see machines fail, apparently without warning.

***III*) Peak level detection:**

As an alternative to RMS, the peak level of the signal can be used [7, 8]. A baseline "peak" level is defined for a new machine, and any variations from this norm would be indicative of a change in machine condition. Operational standards have been developed which recommend vibration boundary levels for satisfactory or unsatisfactory running conditions. For example standard API 610 [API standard 610, 7th edition, Centrifugal Pumps for General Refinery Services] defines vibration limits for centrifugal pumps. This is particularly useful for monitoring the change in the amount of impulsion, possibly due to the occurrence of impacts. However, this method is not reliable, since resonant behavior often dominates the vibration signal, and therefore only a very severe transient impact will bring about any change in the peak level.

IV) Crest factor:

The crest factor [4, 6] (sometimes called the impact index) is the ratio of the peak level to the RMS level of the vibrational signal. The time waveform of a machine in good health is mostly random. When a localized fault appears, a periodic peak is seen to occur in the signal. As the fault increases, the waveform becomes far more impulsive, with higher peak levels, but the RMS value is not affected significantly. In work carried out by the General Electric Company [9], it was shown that the crest factor could be used as an indicator of bearing condition. The crest factor limits are as follows: 2 to 3 indicates a normal bearing, 3 to 8 indicates fault initiation and 8 to 10 indicates fault growth. However, this method has certain limitations. The RMS level is significantly increased in bearings with multiple or spreading defects, resulting in the reduction of the crest factor. Background noise is also a problem because it increases the RMS level and consequently decreases the crest factor.

V) Shock pulse:

The shock pulse method [7, 10] detects the development of a mechanical shock wave caused by increasing damage. For example, impacts produced by small defects in a bearing may excite resonances in the bearing and the machine. The periodic signals with characteristic frequencies from a bearing may indicate deformations or defects in the bearing, but they are

not always visible and frequently follow the rhythm in higher frequencies (higher of 2kHz). To observe the shock pulses, first the vibration is measured by a transducer mounted on the casing of the machine. Then, the signal from the transducer is passed through a bandpass filter to isolate one of the resonances. Finally, the filtered signal is transformed into a train of impulses by passing it through a pulse converter (Figure 1.1).

By observing the increase of the level and the rhythm, it is possible to determine which of the bearing elements is damaged (Figure 1.2). It is also useful to calculate the amplitude spectrum of the train of impulses; the complete procedure is also known as the high frequency resonance technique or high frequency shock pulse [11]. This approach is efficient but has certain disadvantages. When there is more than one fault in a machine, the pulse repetition will not correspond to one single fault. For example, if there are simultaneous cavities on the inner and outer races of a bearing, the frequency of the shock pulses will correspond to neither BPFI (*ball-pass frequency on the inner race*) nor BPFO (*ball-pass frequency on the outer race*) but with their sum: BPFI+BPFO.

***VI*) Spike energy:**

This method was developed in 1970 to measure the condition of rolling bearings [10]. It is based on the high frequency peak value of the acceleration. Spike Energy shows the intensity

of impact energy caused by mechanical faults. To measure Spike Energy, as with the Shock Pulse method, the output signal of the accelerometer is filtered through a bandpass filter, and the time variation of the signal is measured by a peak-to-peak detector as an indicator of the severity of the impact measurements. Spike Energy is expressed in "gSE" units. Spike Energy Spectrum may also be obtained by using FFT analysis. This technique is often used in high frequency vibration such as metal-to-metal contact and cavitation. Details of an application of this technique to vibration monitoring of seal-less pumps are given in [12].

This method has proven satisfactory in fault detection, but it has problems similar to those of the Shock Pulse method and may be misleading in the case of simultaneous faults.

VII) Demodulation:

An alternative way to monitor rotating machines is demodulation or the enveloping method. This method is based on the properties of amplitude-modulated signals which are often encountered in machine monitoring. The type of fault is indicated by the impact rates. The envelope of a wave modulated in amplitude reveals the repetition frequency of the impacts (Figure 1.3). The potential applications of these properties hinge on the availability of mathematical tools that enable assessment of the envelope function characteristics. Demodulation analysis of a bandpass filtered signal is based on the Hilbert Transform which

generates the envelope of the time signal. The Hilbert Transform (H) of the signal in time $s(t)$ is defined as

$$H[s(t)] = \frac{1}{\pi} \int_{-\infty}^{\infty} \frac{s(t)}{t-\tau} d\tau = \bar{s}(t) \tag{1.1}$$

This constitutes the imaginary part of the analytical signal defined as

$$z(t) = s(t) + j\bar{s}(t) = |s(t)|e^{i\theta(t)} \tag{1.2}$$

where $\theta(t) = arctg\left[\frac{\bar{s}(t)}{s(t)}\right]$ and the module of the analytical signal, $|z(t)| = \sqrt{s^2(t) + \bar{s}^2(t)}$, represents the envelope of the time signal $s(t)$. The time envelope calculated by the Hilbert Transform can be useful in bearing defect detection [6, 13, 14] or gearbox defect detection [15]. The problem with the demodulation method [16] is that the Hilbert Transform cannot be used to demodulate the whole vibration signal. The signal first has to be filtered by passing it through a bandpass filter in order to separate one of the dominant harmonics and all of its sidebands. If a narrow bandpass filter is chosen, it is likely to miss some of the higher order sidebands of the chosen harmonic. And if a broad bandpass filter is used, it is likely to pass some of the sidebands from adjacent harmonics.

In both cases, the modulation calculated by the Hilbert Transform will not represent the amplitude modulation of the signal. As a solution to this problem, the rectification process in the demodulation method is replaced by peak value waveform [17].

VIII) Kurtosis:

The technique of Kurtosis analysis is another method used to indicate the "peakedness" of the signal. Kurtosis (Ku) is a statistical parameter, derived from the statistical moments of the probability density function of the vibrational signal. " Ku " is defined as

$$Ku = \frac{\int_{-\infty}^{\infty} s^4 P(s)ds}{[\int_{-\infty}^{\infty} s^2 P(s)ds]^2} \tag{1.3}$$

where s is the magnitude of the vibration signal with zero mean and $P(s)$ is the distribution of s.

To give a simple explanation of this parameter, knowing that the first moment about zero gives the mean value of distribution:

$$\mu = \int_{-\infty}^{\infty} sp(s)ds \tag{1.4}$$

The second moment called variance gives the standard deviation and is defined as:

$$\mu_2 = \sigma^2 = \int_{-\infty}^{\infty} s^2 p(s) ds \tag{1.5}$$

Higher order moments are defined by the general integral.

$$\mu_n = \int_{-\infty}^{\infty} s^n p(s) ds \tag{1.6}$$

Then, Kurtosis is just the fourth moment , μ_4 , normalized with respect to the square of the variance.

$$Kurtosis = \frac{\mu_4}{\sigma^4} \tag{1.7}$$

A bearing in good condition has a Gaussian distribution function and the Kurtosis value of its signal is equal to three, but a damaged bearing has a Kurtosis value which will be greater than three. Advantages of this methods are: a) Kurtosis value is independent of load and speed conditions, b) it has been found that the amplitude distributions, and therefore the *Ku* value, are relatively unaffected by variations in the transmission paths of vibrational signals. But for modulated signals this technique may lead to inaccurate predictions [15].

IX) Orbits:

Orbits display or Lissajous curves [10, 18] are obtained by displaying time base waveforms from two transducers whose outputs are phase shifted by 90 degrees (Figure 1.4). Orbits are particularly useful in the analysis of the vibration of a shaft during rotation. The shaft orbit can provide basic amplitude, frequency and phase lag angle information. It is able to indicate wear in a journal bearing, shaft misalignment, shaft imbalance and shaft rub. Since the orbits are directly constructed in the time domain, they are deformed by noise, surface quality and self-excited low frequency vibration of the rotating shaft [19]. Consequently, the detection of faults in rotating machinery by this method is often unsuccessful. Nevertheless, Orbits display is used to complement other methods [20].

X) Shaft centerline:

The shaft centerline position is used to estimate the shaft centerline relative to the geometric centerline and clearance of the bearing. From these data, the shaft attitude or position, its angle and eccentricity ratio can be calculated and may be used as an indication of bearing wear and misalignment generated by heavy loads [20]. The Shaft centerline position method has the same limitations as the Orbits method.

1.3.2 Frequency domain vibration analysis techniques

I) Spectrum analysis:

A spectrum is derived from the vibration waveform by performing a "Fast Fourier Transform" [3]. The benefit of the spectrum is that each rotating element in a machine generates identifiable frequencies; the peaks in frequencies define the type of fault and the amplitude of the peaks indicates the severity of the fault [21, 22]. Spectrum analysis information may be used in different ways to recognize defects in machines. The spectral indices such as R.M.S. levels [23] can show the difference between the current spectrum and the baseline or the previous spectrum. These indices are good indicators of the overall performance of machinery. An alternative way is to define an allowable tolerance limit on the baseline spectrum such that, if there is a fault in the machinery, the spectrum will exceed the limit. The narrow bandwidth spectrum may be replaced by a constant percentage bandwidth spectrum in order to simplify its application.

Although spectrum analysis is one of the best vibration indicators of machine condition, it must be pointed out that the defect frequency may be close to frequencies excited by other components in machines; therefore, by a small change in speed, the position of the peaks may change and give incorrect results. To prevent this problem, a new spectrum called the Synthesized Spectrum may be used [24]. However, these fault frequencies and fault conditions are not always easily identifiable. A discussion on how spectrum analysis may

provide erroneous results and therefore false warnings is presented in [25] and a number of conditions which are necessary in order to obtain correct results with different types of spectrum are given.

***II*) Waterfall plot:**

A Waterfall plot (also known as a cascade plot) is composed of FFT magnitude spectrums displayed at different machine speeds (Figure 1.5). This method is used to examine sub-synchronous and super-synchronous components during run-up or run-down stages of a machine [26]. The advantage of this format over single or overlaid spectrum displays is that changes in the spectrum versus changes of speed may be identified visually. This method is specially applied to certain types of fault such as oil whirl/whip, cracked shaft [27] and rubs. Although Waterfall display is useful, it has some limitations. When the characteristics of the signal are changing rapidly in time, the spectral representation of the signal at each speed is degraded. If the speed varies relatively slowly (1000-4000 RPM over 60 sec) the Waterfall technique may give data of an acceptable order of magnitude [28]. If the speed varies more rapidly, this technique may provide inaccurate results.

III) Holospectrum:

This method [19] provides information not only about peak frequency and amplitude, but also about phase relationships In general, vibrations of a rotor are measured by two accelerometers, as in the Orbits method. Holospectrum is formed by a simple vector in each frequency (Figure 1.6). It is composed of a circle, line and ellipse placed on the frequency axis. A circle is obtained if the amplitudes of two components are equal and their phases are 90 or 270. A circle is obtained in the rotating frequency of a shaft if there is imbalance in the shaft. A line is obtained if the phase lag between two elements of a machine is 0° or 180° and the slope of the line depends on their amplitude proportion. This method has the same limitations as the Orbits method.

IV) Cascade Holospectrum:

Following the Cascade spectrum diagram principle, the 2-dimensional Holospectrum can be used to construct the Cascade Holospectrum diagram (Figure 1.7). The Cascade Holospectrum diagrams [19] may provide us with more information about the transient events of a machine during run-up and run-down, and may intuitively demonstrate the change in the Holospectrum components of different orders. In contrast to the Cascade diagram, the Cascade Holospectrum gives the phase relations between the two

accelerometers. This method has the disadvantages of Waterfall diagram and Holospectrum technique.

V) Bode and polar plot:

The Bode plot is a log-log diagram of the amplitude of a complex signal (often transfer function) versus the frequency accompanied by a semi-log diagram of the phase of the signal. The Polar plot, also known as the Nyquist plot, is another representation of the signal in polar coordinates with the radius of the curve corresponding to the amplitude of the signal, and the phase signal corresponding to the value of the phase to the horizontal axis. Frequency or running speed is changed along different points (Figure 1.8). Although these plots are useful in the field of balancing problems, mode shape of the rotor, cracked shaft detection and rubs [20, 26, 29, 30], they are of little use in the case of machine monitoring. In this case, spectrum representation is preferred to the Bode plot. The Polar plot is also of little help in finding the natural frequencies of a system because it needs curve-fitting algorithms. These plots are a different way of displaying results, but do not offer a new method of analysis.

***VI*) Cepstrum analysis:**

If the inverse Fourier Transform of the logarithm of the correlation function is taken, we obtain what is termed as the Cepstrum which is a function of the independent variable "Quefrency" in milliseconds [24].

$$C(\tau) = FFT^{-1}[\log G_{xx}(f)] \tag{1.8}$$

It is used to highlight periodicities in the spectrum, in the same way that the spectrum is used to highlight periodicities in the time waveform. Thus, the harmonics in the spectrum are summed into one peak in the cepstrum, making it easier to identify, and observe trends in, specific fault frequencies. Quefrency shows frequency spacing in the spectrum but it shows nothing about absolute frequency. On the other hand, it is possible to edit out the effect of the transmission path because both this and the excitation, which are multiplicative in the spectrum, become additive in the Cepstrum. It has been found to be useful in bearing and gear-box analysis [4, 31]. However, this method has some disadvantages. Firstly, the spectrum sometimes has several harmonics and sidebands in the low and middle frequencies; these appear in the Cepstrum and distort the harmonics and sidebands in the higher frequencies. In such a case, it may be hard to identify the type of defect by the Cepstral method. Secondly, there is no relationship between the magnitude of the Cepstrum and the severity of the defect.

1.4 Time-frequency analysis

1.4.1 Is time-frequency analysis really necessary?

As mentioned in the last section, each of the conventional vibrational methods used in fault detection and identification for steady speed machines has several limitations. The assumption of constant speed in the above methods results in stationary and pseudo-stationary vibration signals. However, even if we take this assumption into account, the limitations of the above methods reduce their performance. On the other hand, there are presently several types of varying speed rotating machinery for which the stationary or pseudo-stationary vibration signals cannot be assumed to be accurate. These types of rotating machinery include gear drives, rolling element bearings, internal combustion engines, cam-driven mechanisms and reciprocating machinery. Rapidly varying speed in this group of rotating machinery generates non-stationary vibrational signals. The application of conventional techniques to the analysis of non-stationary vibrational signals may yield incorrect results.

The most common traditional techniques of vibration analysis are based on frequency domain analysis and, among these, spectral analysis plays a major role. The use of spectral analysis techniques with machines of rapidly varying speed often results in a smeared spectrum because the frequency components are changed over time, and averaging over

several blocks of analysis may result in an obscured spectral representation. Although the presentation of the signal in the time domain may indicate some modulations, it will be very difficult to identify the sources of these modulations. It appears, therefore, that it is necessary to employ a new technique which would combine frequency information with amplitude changes in time. Furthermore, the initial appearance of a defect in a machine can produce transient phenomena in the vibrational signal. Passage of a ball over a localized defect in a bearing, contact of a damaged tooth with other teeth in the gearbox, and piston slap in the engine are examples of well-known industrial problems generating transient events. Frequency domain vibration analysis methods, such as the power spectrum, average the transient events so that they do not appear clearly in the spectral lines. Time domain methods, which are also used to analyse transitory signals, can loose the frequency information of different machine components. Finally, if both methods are used, it will be difficult to relate the frequency information to the forces causing the amplitude variation of the signal in the time domain. Therefore, rather than separate observation of the time from observation of the frequency characteristics of a signal, it is necessary to use a joint time-frequency technique.

In 1946, time-frequency (TF) analysis was applied to speech communication [32] for the first time, but application of this method to the field of mechanical signature analysis started only in the early 1990's. The earliest time-frequency method is known as the Spectrogram or Short-Time Fourier Transform (STFT). In recent years, various TF techniques, such as the

Wigner-Ville Distribution and Wavelet transforms, have been developed in the signal processing field.

Only the STFT method will be discussed in the following sections, as being a technique which is very fast and very easy to interpret. This technique will be applied to fault detection and identification in two well-known industrial elements, the ball-bearing and gearbox. The suitability of this method in the field of machinery diagnostics will be demonstrated.

1.4.2 The short-time Fourier transform

The STFT may be considered a method that breaks down the non-stationary signal into many small segments which can be assumed to be locally stationary, and applies the conventional FFT to these segments.

The STFT of a signal $s_t(\tau)$ is achieved by multiplying the signal by a window function, $h(\tau)$, centered at "t", to produce a modified signal. Since the modified signal emphasises the signal around time "t", Fourier Transforms will reflect the distribution of frequency around that time.

$$S_t(\omega) = \frac{1}{2\pi}\int_{-\infty}^{\infty} e^{-j\omega\tau} s(\tau) h(\tau - t) d\tau \qquad (1.9)$$

We may consider $S_t(\omega)$ as the sum of the Fourier base functions but the base functions are a modulated version of the window function (Figure 1.9).

The energy density spectrum at time "t" may be written as follows:

$$P(t,\omega) = |S_t(\omega)|^2 = \left| \frac{1}{2\pi} \int_{-\infty}^{\infty} e^{-j\omega\tau} s(\tau) h(\tau - t) d\tau \right|^2 \qquad (1.10)$$

For each different time we get a different spectrum and the ensemble of these spectra provide the time-frequency distribution $P(t,\omega)$.

Resolutions in time and frequency will be determined by the width of window h(τ). A large window width is chosen when we need greater accuracy in frequency and a small window width when we want to have greater accuracy in time. However, the STFT depends greatly on the width of the window and by varying the window used, one can exchange resolution in time for resolution in frequency. Figure 1.10 shows a signal composed of a constant frequency and an impulse. A great difference in the STFT representation of the signal is apparent if the width of the window is changed.

1.4.3 Adapting the short-time Fourier transform

To solve the problem of the "trade-off" in resolution between the time and frequency domains in the Short-Time Fourier Transform, we must consider the origin of the problem. Use of a single fixed window during the analysis of the signal is the origin of the STFT problem.

We compute the adaptive STFT using a window of variable length. The criterion for adjusting the window length is the Kurtosis parameter. As mentioned in 2.1.8 of this article, this parameter is an indicator of the signal's "peakedness" as a consequence of the presence of defects in the machine.

The window length is determined by considering an initial T length for the window, thus computing the Kurtosis parameter for this slice of the signal. If it is greater than 3, the window length is divided into two. This work is repeated until the Kurtosis parameter for the signal segment in the window is less than or equal to 3. During this time, the spectrum of the signal segment is calculated. Then we move the window and repeat the same steps for the whole of the signal.

By this technique, the window length is adjusted depending on the characteristics of the signal. The benefits of this technique are:

- obtaining a performance surpassing that of the fixed window length STFT.

- providing a technique that is better suited to the diagnosis of mechanical signals than other methods.

1.5 Applications of time-frequency analysis to machinery diagnosis

1.5.1 Some industrial applications of time-frequency analysis in mechanical systems

In the last few decades, many methods of time-frequency analysis have been applied to various areas of physics and engineering, such as speech processing and image processing. In the field of machinery diagnostics, Forrester [33] has used time-frequency methods in the detection of damaged gears in helicopter gearboxes. He has shown that, with the signal enhancement techniques (conventional methods) offered by Stewart and McFadden, it is difficult to distinguish one type of fault, e.g. tooth-cracking or pitting, from another but the Wigner-Ville Distribution (one of the time-frequency methods) can more accurately reveal the type of defect. Wang and McFadden [34-37] have also studied the application of time-frequency analysis to the detection of gear damage. They have demonstrated that direct use of the Wigner-Ville Distribution can produce a complicated time-frequency representation of the signal and, furthermore, it has been suggested that the application of an appropriate window function in the time domain can improve the results of Wigner-Ville [38]. On the other hand, they have shown that the complexity of the Wigner-Ville representation,

although reduced, still remains and still makes it difficult to detect mechanical failure in gear systems. They have proven that application of the Spectrogram (STFT) for the early detection of damage in gears has some advantages over the application of Wigner-Ville Distribution [39].

In another work, Rohrbaugh [40] has applied time-frequency analysis to several sets of marine machinery. He compared the Spectrogram (STFT) with cone-kernel time-frequency representation from Cohen class distributions. He showed that, while the Spectrogram can reveal the general time-varying characteristics of a vibrational signal, for more information about the signal we must consider other time-frequency methods.

Rohrbaugh and Cohen [41] outlined another new time-frequency method developed by Loughlin, Pitton and Atlas [42] for the detection of faults in pumps, and found it to have several advantages over the Spectrogram when dealing with reciprocating machinery. This method is known as "positive time-frequency distribution" and is based on a minimum cross-entropy scheme (MCE). Some applications of time-frequency analysis to the monitoring of machining processes, such as drilling and grinding operations, have been presented by Loughlin, Atlas, Bernard and Pitton [43]. They showed that, although the Spectrogram (STFT) is an efficient method for the demonstration of the time-varying characteristics of a process, sometimes newer time-frequency methods can provide more detail on the signal. They concluded that the newer methods of time-frequency analysis may assist in the early

detection of problems. Atlas, Bernard and Narayanan [44] summarized some applications of time-frequency analysis in different domains of machinery diagnostics. They emphasised the importance of using time-frequency analysis in manufacturing and monitoring applications. In a recent work, Loughlin and Bernard [45] presented some applications of MCE time-frequency methods to different machine vibrational signals.

The papers cited above give some examples of the application of different time-frequency methods, including the STFT, to condition monitoring of mechanical systems. Each of these papers shows the way in which a new time-frequency method can reveal certain information about the signal that can not be obtained by traditional methods.

Today, one of the most important factors limiting the progress of machine diagnostic techniques is the lack of familiarity of mechanical engineers with new signal processing methods. The complicated theory of time-frequency analysis and the absence of an operational software for time-frequency analysis restrict engineers from using these methods in machine diagnosis.

Among the various time-frequency methods, the Short-Term Fourier Transform is the easiest and the fastest method.

This work is an attempt to present the limitations of conventional methods of vibration analysis in machine diagnosis and to emphasise the application of the STFT to fault detection

and identification.

A user-friendly software has also been developed to facilitate the use of time-frequency methods by engineers whether or not they are familiar with time-frequency analysis.

1.5.2 Software for time-frequency analysis of signals

The software is designed to be run interactively; it produces and represents results in the energy-time-frequency plane for sampled time signals. Firstly, we choose the required signal from the list of available signals in the principal window, by mouse. Secondly, we select the method of analysing the signal: the FFT, the STFT, or the adaptive-window STFT, and provide information about the signal and options relating to the chosen method, such as the length and type of window for the STFT. Finally, the program represents the results in the form of the time-frequency plane projection of the signal and a three dimensional representation of the signal in the energy-time-frequency space. The energy intensity is conveyed by different colors. The three dimensional representation can be rotated in order to obtain the best point of view.

The working and accuracy of the program can be verified by a theoretical signal. The first example is a sum of sines (Figure 1.11). The signal is composed of the sum of three sines: 100 Hz, 300 Hz and 1000 Hz. As predicted, the time-frequency plane of the STFT shows

three lines at 100 Hz, 300 Hz and 1000 Hz parallel with the time axis and the time-frequency-energy space shows three peaks constant in time (Figure 1.12).

The next examples are an amplitude-modulated sine at 1000 Hz (Figures 1.13 to 1.14) and a frequency-modulated sine at 1000 Hz (Figures 1.15 to 1.16). The modulation may easily be seen in the time domain and it appears to be unnecessary to use the STFT; however, in real cases we never have a signal without noise and it is often impossible to find a modulation in time. A frequency modulation is particularly difficult to identify by its spectrum. In the time-frequency domain, the modulations are very clearly displayed. The importance of the STFT is more apparent when applied to industrial signals. It is noted that signals with different modulations in time and frequency are very usual in machinery diagnosis and the time-frequency representation gives a good interpretation of these signals.

1.5.3 Experimental application of short-time Fourier transform

After verifying the program by computer-simulated signals, we can investigate the data obtained from an experimental case: the application of the STFT method to pin-point a defect, the characteristics of which are known, located on a rolling bearing. The test was conducted on a bearing having a simple defect on the inner raceway. This test was performed in a laboratory using the test setup shown in Figure 1. 17. An interchangeable rotating shaft

was supported by two journal bearings (SKF 1210 EKTN9 self-aligning double row) labelled 2 and 3. An electric motor provided 12.2Hz rotation for the bearing shaft. Load was imposed by the break which was installed on the gearbox output. The defective bearing was mounted on support A.

The defect was created by scratching the bearing raceway with an electric pen. Figure 1.18 shows the signal measured on bearing A and its spectrum. The results for the defective bearings were also verified by calculating the frequency at which the rolling elements passed over the defects [1]. The geometric characteristics of the system are as follows:

pitch diameter D=69 mm

Diameter of the rolling body d=10.32 mm

Contact angle α =7.87 deg

Number of rolling elements N =17

Bearing frequency of rotation F_r=12.2 Hz

On the inner raceway, the frequency of rolling body defect impact is:

$$F_i = \frac{F_r N}{2}\left[1 + \frac{d}{D}\cos(\alpha)\right] \tag{1.11}$$

The pass frequency on a point of the inner raceway computed by using equation (1.11) is at

approximately 238 Hz. We can find the default frequency among other frequencies by the spectrum in Figure 1.18 but we cannot be certain that this is indeed the default frequency because the default frequency must have a special characteristic. In this case, the default frequency must be an amplitude-modulated wave at approximately 238 Hz with the frequency of modulation being equal to the rotating frequency.

The time-frequency representation of the signal provided by the STFT shows the amplitude-modulated signal at the default frequency and its harmonics (Figure 1.19). We can easily calculate the frequency of modulation and verify that it is correct and equals the rotating frequency.

1.5.4 Industrial application of short-time Fourier transform

The second case of data obtained from a real case concerns the defective gear train of a hoist drum in a large shovel operating at an open pit iron mine. The data are measured by International Measurement Solutions company in order to find the problem in the machine.

Gears generate a mesh frequency equal to the number of teeth on the gear multiplied by the rotational speed of the shaft driving it. A high vibration level at the mesh frequency is often caused by tooth error, wear of the meshing surfaces, or any other problem that would cause the profiles of meshing teeth to deviate from their ideal geometry. Sidebands at the mesh

frequency, on the other hand, are typically due to a failure of mating teeth. Imagine a cracked tooth which is not yet broken, and will consequently not be noticed by the operating personnel. However, it will, due to its weakened mechanical condition, deflect more under load than the other (healthy) teeth when it goes into mesh. This results in a signal with amplitude modulation. Thus, an increasing level in the sidebands spaced with rotation speed in the frequency spectrum results from the cracked tooth.

A minimum length of time is required to perform an FFT analysis of each process. The time resolution required will depend on the period of each tooth mesh and the desired level of accuracy. Sometimes, it is not possible to measure the signal for a time long enough to provide the periodicity of shock in the FFT spectrum.

In this particular case, the process did not even last one revolution of the driven gear. The case was investigated by time-frequency distribution precisely because it is known that time-frequency methods do not need as much time signal as the FFT spectrum.

Figure 1.20 shows respectively the signal and its spectrum. The spectrum of the signal indicates some large peaks around 200 Hz and some other smaller peaks in the vicinity of 400 Hz, 800 Hz and 1200 Hz. However, it is very difficult to assume or confirm any defects at this point. On the other hand, the amplitude-modulated characteristic of the signal is clearly displayed in the representation of the signal in the time-frequency domain, as shown in Figure 1.21. It is very simple to read the gear-meshing frequency at approximately 200Hz

and three large impacts due to three partially broken teeth at a frequency of approximately 400 Hz and obtain the frequency of the modulation. In addition, the time and frequency of each peak are easily identified.

1.6 Conclusion

It has been shown that, although the majority of conventional methods may give good results when detecting a single fault in various simple elements of machines, no single technique can provide all the answers for all cases. It is difficult to decide which method gives the best result, in particular when the precise type of fault is not known.

The Short-Term Fourier Transform is an effective method of time-frequency analysis and a powerful tool in machine condition monitoring. The short-time spectrum gives a clear representation of the time-frequency plane and a simple interpretation of the energy variation due to damage. There is, unfortunately, a fundamental problem with this approach: high resolution cannot be obtained simultaneously in the time domain and the frequency domain. Although this method gives the time-frequency information with limited precision, in order to achieve greater precision we must turn to advanced time-frequency methods such as the adaptive Short-Term Fourier Transform. This method produces reasonable and useful window lengths for the Short-Term Fourier Transform.

The development of a user-friendly software package facilitates the use of time-frequency techniques in machine diagnosis. The time-frequency methods, including the short-time spectrum, have been implemented on a computer and used, along with conventional methods, in the analysis of vibrational signals. The advantages of the short-time spectrum have been demonstrated by using this method, not only on measured signals from bearings installed in an experimental set-up, but also on vibrational signals from an industrial gearbox.

1.7 References

[1] R.G. Smiley, *Rotating Machinery: Monitoring and Fault Diagnosis*, Sound and Vibration, 17(9) (1983) 26.

[2] A. Lifshits, H.R. Simmons and A.J. Smalley, *More Comprehensive Vibration Limits for Rotating Machinery*, Journal of Engineering for Gas Turbines and Power, 108(10) (1986) 583.

[3] R. L. Eshleman, *Machinery Diagnostics and your FFT*, Sound and Vibration, 17(4) (1983) 12.

[4] R. Archambault, *Getting More Out of Vibration Signals: Using the Logarithmic Scale*, Proceedings of the 1st International Machinery Monitoring & Diagnostic Conference & Exhibit, (1989) 567.

[5] D. Ulieru, *Diagnosis by Measurement of Internal Vibration and Vibration Analysis on Maintenance of Rotating Machinery such as Turbo Chillers*, Proceedings, Annual Technical Meeting - Institute of Environmental Sciences, 2 (1993) 525.

[6] A. Barkov, N. Barkova and J.S. Mitchell, *Condition Assessment and Life Prediction of Rolling Element Bearing - Part 1*, Sound And Vibration, 29(6) (1995) 10.

[7] A.R. Collacott, *Vibration Monitoring Diagnosis*, John Wiley & sons, 1979.

[8] J. Swarup, *Vibration Analysis of Centrifugal Pumps*, Sound and Vibration, 24(5) (1990) 12.

[9] B. Weichbordt and F.J. Bowden, *Instrumentation for Predicting Bearing Damage*, G.E.C. Technical Report RADC-TR-69-437, 1970

[10] G. Lipovszky, K. Solyomvari and G. Varga, *Vibration Testing of Machines and their Maintenance*, Elsevier, 1990.

[11] P.D. Mcfadden and J.D. Smith, *Vibration Monitoring of Rolling Element Bearings by the High-Frequency Resonance Technique*, C-Mech TR 30, 1983.

[12] J. Le Bleu and Xu Ming, *Vibration Monitoring of Seal-less Pumps Using Spike Energy*, Sound and Vibration, 29(12) (1995) 10.

[13] E. D'Amato and P. Rissone, *Using the Envelope Method to Monitor Rolling Bearings*, Proceedings of the 1st International Machinery Monitoring & Diagnostic Conference & Exhibit, (1989) 560.

[14] R.M. Jones, *Enveloping for Bearing Analysis*, Sound and Vibration, 30(2) (1996) 10.

[15] M.J. Brennan, M.H. Chen and A.G. Reynolds, *Use of Vibration Measurements to Detect Local Tooth Defects in Gears*, Sound and Vibration, 31(11) (1997) 12.

[16] A.G. Reynolds, *The Detection of Local Tooth Defects in Gearing by Vibration Analysis*, M. Sc. Dissertation, Royal Naval Engineering College. Manadon. 1995.

[17] J.C. Robinson, R.G. Canada and K.R. Piety, PeakVue Analysis - New Methodology for Bearing Fault Detection, Sound and Vibration, 30(11) (1996) 22.

[18] Qu Liangsheng, C. Yaodong and Liu Xiong, *A New Approach to Computer Aided Vibration Surveillance of Rotating Machinery*, International Journal of Computer Applications in Technology, 2(2) (1989) 108.

[19] Qu Liangsheng, C. Yaodong and Liu Jiyao, *The HOLOSPECTRUM: A New FFT Based Rotor Diagnostic Method*, Proceedings of the 1st International Machinery Monitoring & Diagnostic Conference & Exhibit, (1989) 196.

[20] D.E. Bently, S. Zimmer, G.E. Palmatier and A. Muszynska, *Interpreting Vibration*

Information From Rotating Machinery, Sound and Vibration, 20(2) (1986) 14.

[21] R.M. Jones, *A Guide to the Interpretation of Machinery Vibration Measurements - Part I*, Sound and Vibration, 28(5) (1994) 24

[22] R.M. Jones, *A Guide to the Interpretation of Machinery Vibration Measurements - Part II*, Sound and Vibration, 28(9) (1994) 12.

[23] J.E. Berry, *Diagnostic Evaluation of Machinery Using Vibration Signature Analysis*, Sound and Vibration, 20(6) (1986) 10.

[24] Angelo Martin, *Vibration Monitoring of Machines*, Brüel & Kjaer Technical Review, No. 1, PP 1-36, 1987

[25] R.L. Leon, *Is Your Periodic Machinery Monitoring Program Telling You the Truth, the Whole Truth, and Nothing But ...?*, Sound and Vibration, 19(6) (1985) 24.

[26] B. Trevillion, P. Parge, P. Carle and M. Good, *Machinery Interactive Display and Analysis System Description and Applications*, Proceedings of the 1st International Machinery Monitoring & Diagnostic Conference & Exhibit, (1989) 176.

[27] B.R. Sculthorpe and K.M. Johnson, *Vibration Monitoring Techniques on Reactor Coolant Pumps*, Sound and Vibration, 21(9) (1987) 18.

[28] J. Leuridan, H. Var der Auweraer and H. Vold, *The Analysis of Nonstationary Dynamic Signals*, Sound and Vibration, 28(8) (1994) 10.

[29] B. Majovsky and D.J. Salamone. *Dynamic Analysis of a Steam Turbine Vibration Problem*, Sound and Vibration, 22(9) (1988) 18.

[30] D.R. Smith and G.M. Woodward, *Vibration Analysis of Vertical Pumps*, Sound and Vibration, 22(6) (1988) 24.

[31] Li Debao, Z. Hongcheng, Z. Yuanyun and Wang Bo, *Cepstrum Analysis and the Fault Diagnosis of Rotating Machine*, Proceedings of the 1st International Machinery Monitoring & Diagnostic Conference & Exhibit, (1989) 596.

[32] D. Gabor, *Theory of Communication*, J. IEEE (London), 93 (1946) 429.

[33] B.D. Forrester, *Use of Wigner-Ville Distribution in Helicopter Fault Detection*, Proceeding of Australian Symposium on Signal Processing and Applications - ASSPA 89, Adelaide, PP. 78-82, April 1989.

[34] P.D. Mcfadden and W. Wang, *Time-Frequency Domain Analysis of Vibration Signals for Machinery Diagnostics. 1: Introduction to the Wigner-Ville Distribution*, Report No. : OUEL-1859/90; ETN-91-98957, Department of Engineering Science, Oxford University, 1990.

[35] P.D. Mcfadden and W. Wang, *Time-Frequency Domain Analysis of Vibration Signals for Machinery Diagnostics. 2: The Weighted Wigner-Ville Distribution*, Report No. : OUEL-1891/91; ETN-92-91087, Department of Engineering Science, Oxford University, 1991.

[36] P.D. Mcfadden and W. Wang, *Time-Frequency Domain Analysis of Vibration Signals for Machinery Diagnostics. 3: The Present Power Spectral Density*, Report No. : OUEL-1911/92; ETN-92-92063, Department of Engineering Science, Oxford University, 1992.

[37] P.D. Mcfadden and W. Wang, *Time-Frequency Domain Analysis of Vibration Signals for Machinery Diagnostics. 4: Interpretation Using Image Processing Techniques*, Report No. : OUEL-1953/92; ETN-94-95148, Department of Engineering Science, Oxford University, 1992.

[38] F. Hlawatsch and G.F. Boudreaux-Bartels, *Linear and Quadratic Time-Frequency Signal Representations*, IEEE Signal Processing Magazine, 9(4) (1992) 21.

[39] W.J. Wang and P.D. McFadden, *Early Detection of Gear Failure by Vibration Analysis - I. Calculation of the Time-Frequency Distribution*, Mechanical Systems and Signal Processing, 7(3) (1993) 193.

[40] R. Rohrbaugh, *Application of Time-Frequency Analysis to Machinery Condition*

Assessment, Soc. Proceedings of the 27th Asilomar Conference on Signal, Systems & Computer, 2 (1993) 1455.

[41] R.A. Rohrbaugh and L. Cohen, *Time-Frequency Analysis of a Cam Operated Pump*. Life Extension of Aging Machinery and Structures: Proc. Of the 49th Meet. of MFPT Soc., Vibration Inst.: Virginia Beach, 49 (1995) 349.

[42] P. Loughlin, J. Pitton and E. Atlas, *Construction of Positive Time-Frequency Distributions*, IEEE Trans. Sig. Proc., 42 (1994) 2697.

[43] P. Loughlin, L. Atlas, G. Bernard and J. Pitton, *Application of Time-Frequency Analysis to the Monitoring of Machining*, Life Extension of Aging Machinery and Structures: Proc. of 49th Mtg. of MFPT Soc., Vibration Inst.: Virginia Beach, 49(4) (1995) 305.

[44] L. Atlas, G. Bernard and S.B. Narayanan, *Applications of Time-Frequency Analysis to Signal From Manufacturing and Machine Monitoring Sensors*, Proceedings of the IEEE, 84(9) (1996) 1319.

[45] P.J. Loughlin and G.D. Bernard, *Cohen-Posch (Positive) Time-Frequency Distributions and Their Application to Machine Vibration Analysis*, Mechanical Systems and Signal Processing, 11(4) (1997) 561.

1.8 Nomenclature

$s(t)$	The magnitude of the vibration signal with zero mean
$P(x)$	The distribution of the signal $s(t)$
μ_n	The n^{th} moment of the signal $s(t)$
$C(\tau)$	The Cepstrum of a signal
FFT	Fast Fourier transform
$G_{xx}(f)$	The complex spectrum of the signal $s(t)$
$P(t,\omega)$	The joint distribution function of time and frequency
$S(\omega)$	The spectrum of the signal $s(t)$
$s_t(\tau)$	The short-time Fourier transform of the signal $s(t)$
$h(\tau)$	Window function
$S_t(\omega)$	The spectrum of the short-time Fourier transform of the signal $s(t)$
$STFT$	Short-time Fourier transform

Table 1.1

18145		Not Permissible	Not Permissible	Not Permissible	Just Tolerable
11.2	141			Just Tolerable	
7.1	137		Just Tolerable		Allowable
4.5	133	Just Tolerable		Allowable	
2.8	129		Allowable		Good Turbo-machines
1.8	125	Allowable		Good Large machines > 75 KW	
1.12	121		Good Medium machines 15-75 KW		
0.71	117	Good Small machines < 15 KW			
0.45	114				
0.28	109				
RMS Velocity (mm/s)	V dB (Ref 10E-6 mm/s)	Group L	Group M	Group G	Group T

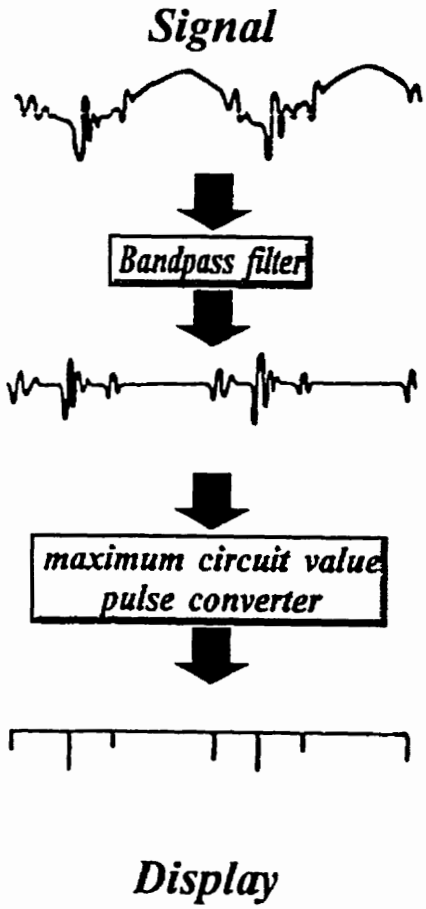

Figure 1.1: The stages in the conversion of shock pulse waves to high frequency pulses

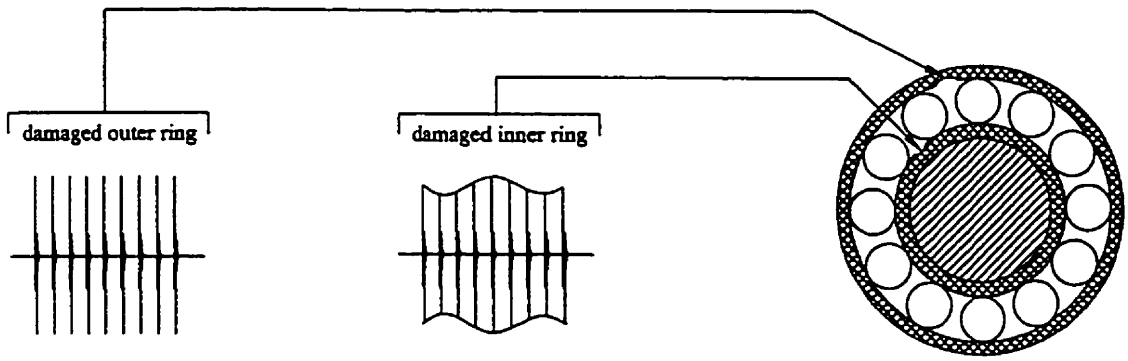

Figure 1.2: Pulse shocks from damaged inner race and damaged outer race of a bearing

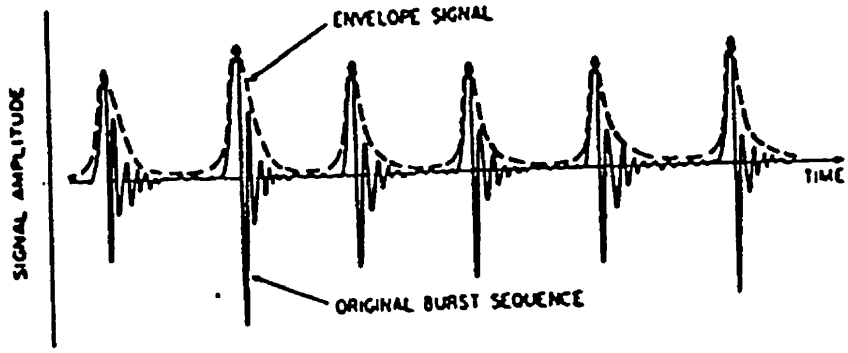

Figure 1.3: The envelope method shows the behavior of a signal

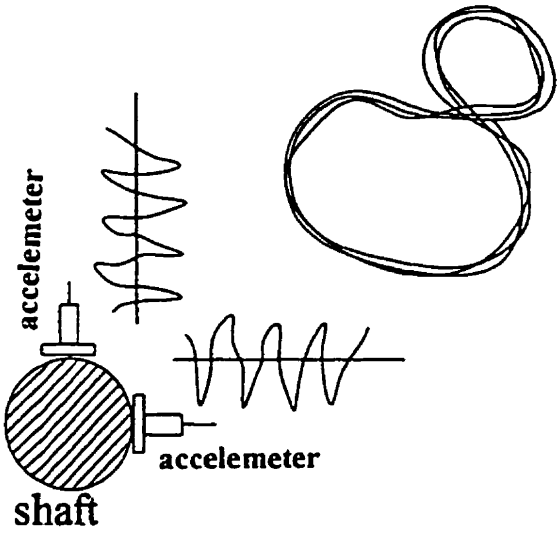

Figure 1.4: Typical shaft orbital motion (Lissajous' figure)

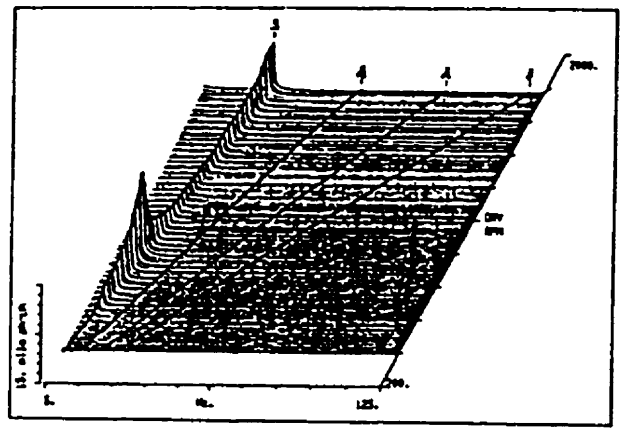

Figure 1.5: Waterfall plot of a turbine coast down (Trevillion, Page, Carle et Good, 1989)

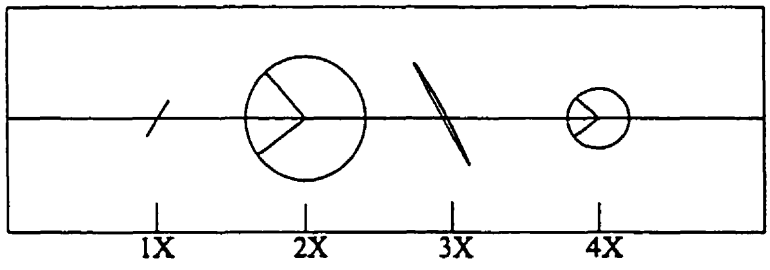

R.P.M.	MAX	DEG.
3816.02	4.14	49.5
5381.20	22.61	145.0
18759.51	10.9	43.5

Figure 1.6: The Holospectrum showing the radial vibration of a rotor

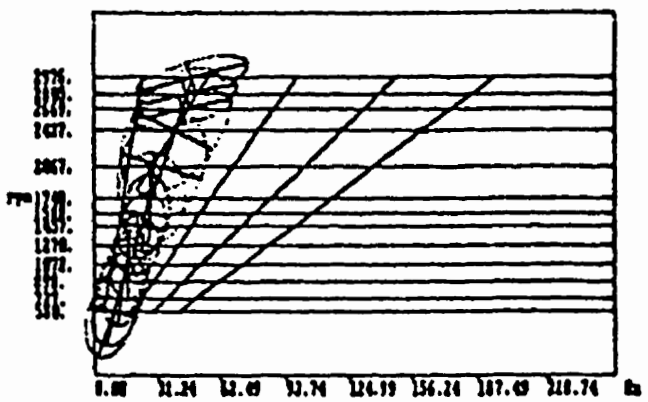

a)

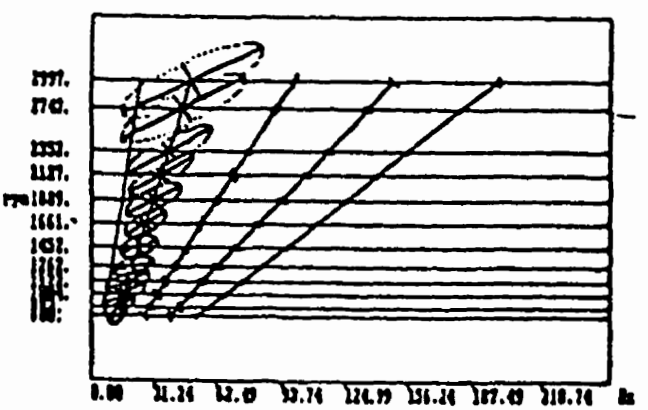

b)

Figure 1.7: The cascade Holospectrum diagrams of a turbine (Liangsheng, Yaodong et Jiyao, 1989)
a) run-up stages.
b) run-down stages

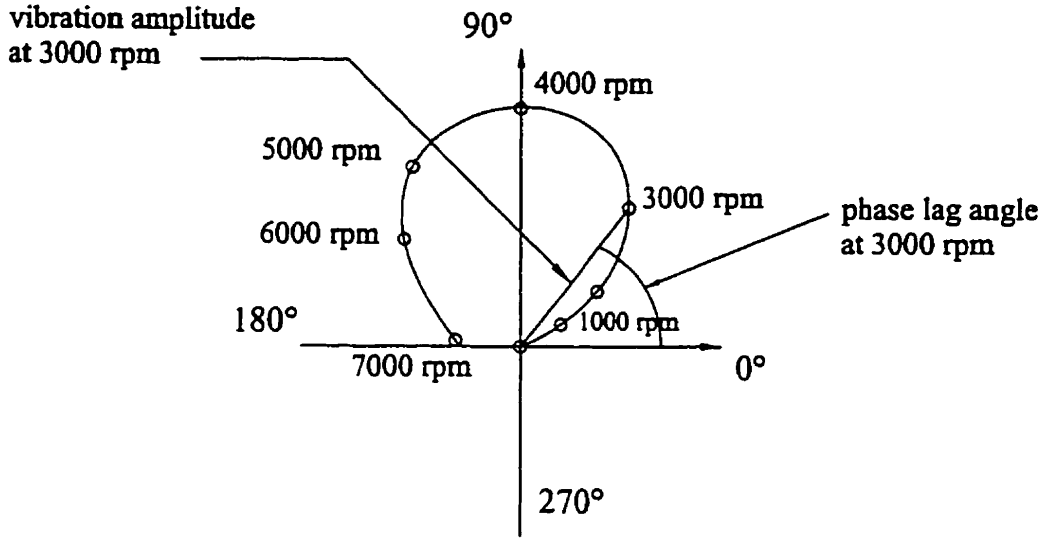

Figure 1.8: Nyquist plot

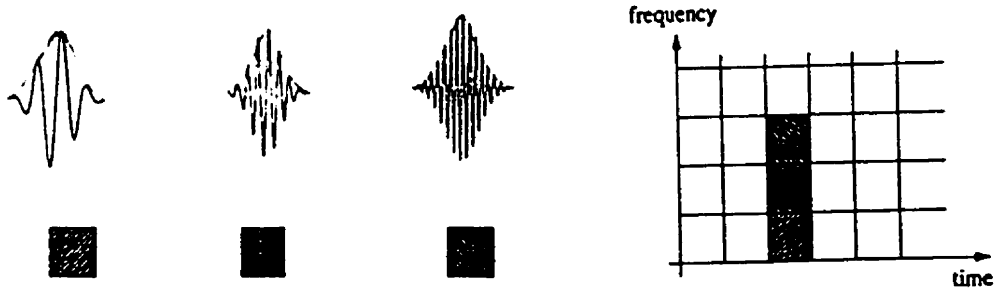

Figure 1.9: Basis functions and time frequency resolution of the short-time Fourier transform (STFT)

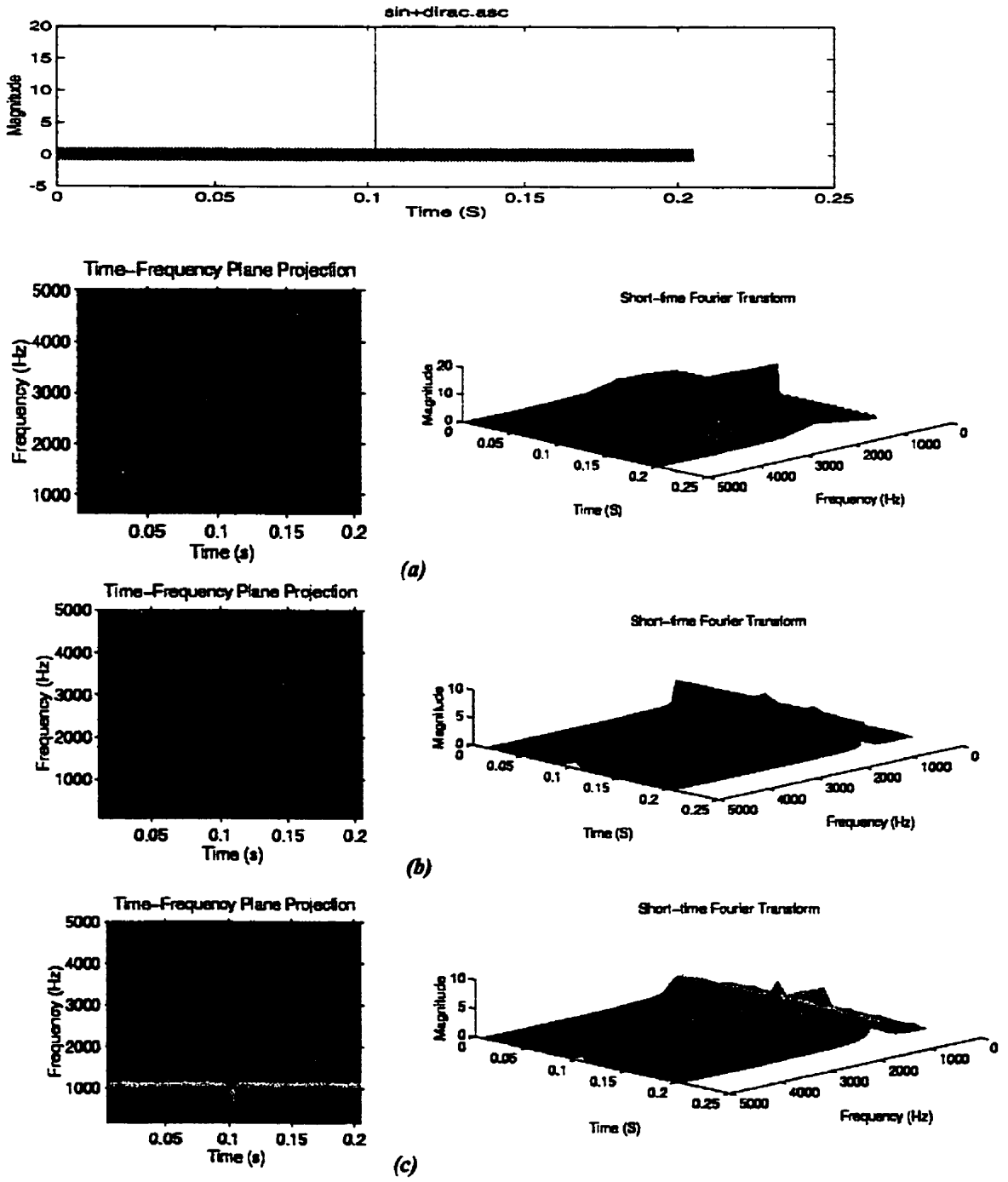

Figure 1.10: The STFT of a signal composed of a constant frequency plus an impluse.
(a) we use a short window, which gives a good indication of when the impluse occurred but gives abroad localization for the frequency.
(b) we use a long duration window, which gives the opposite effect.
(c) a compromise window is used.

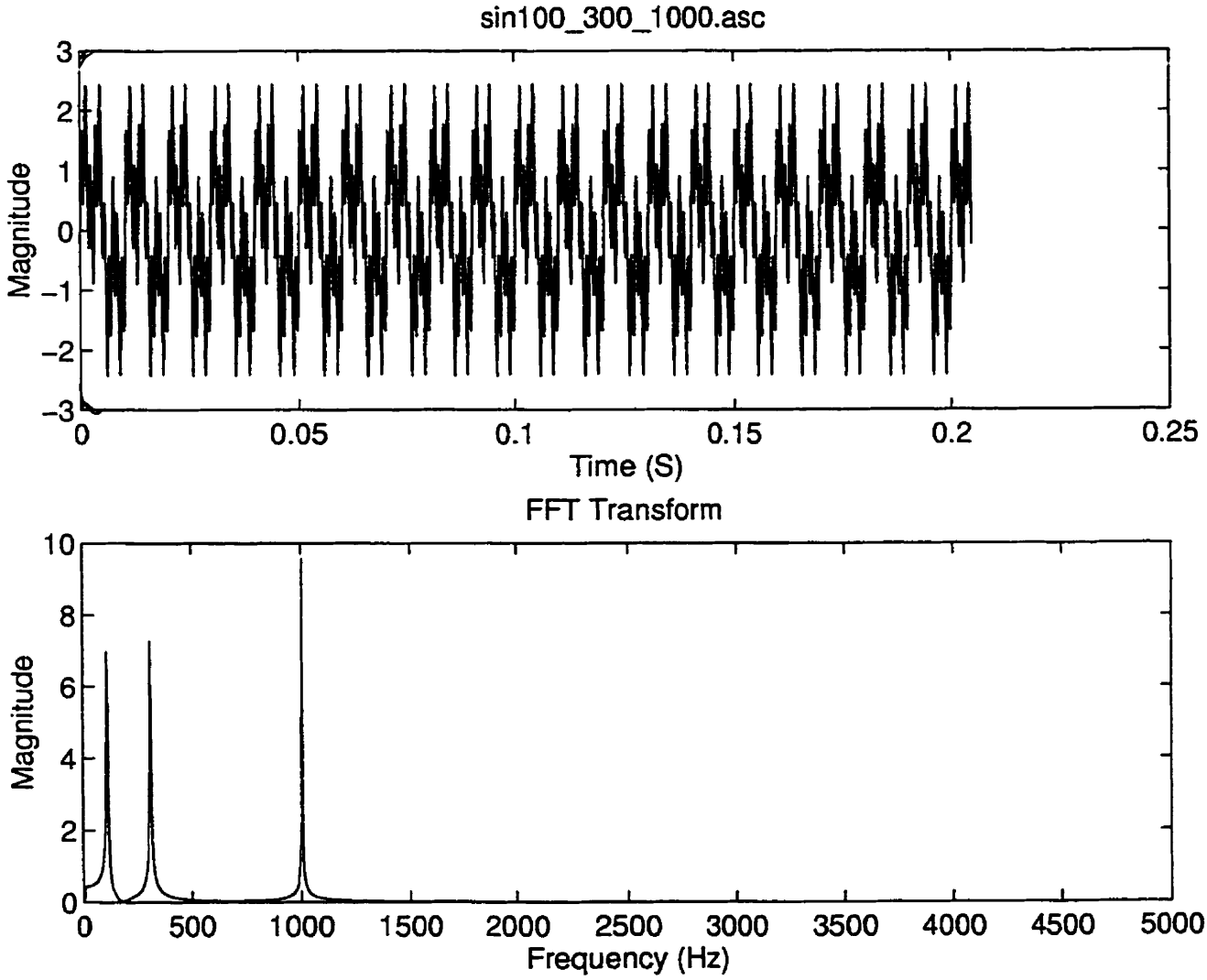

Figure 1.11: Sum of sines signal and its spectrum

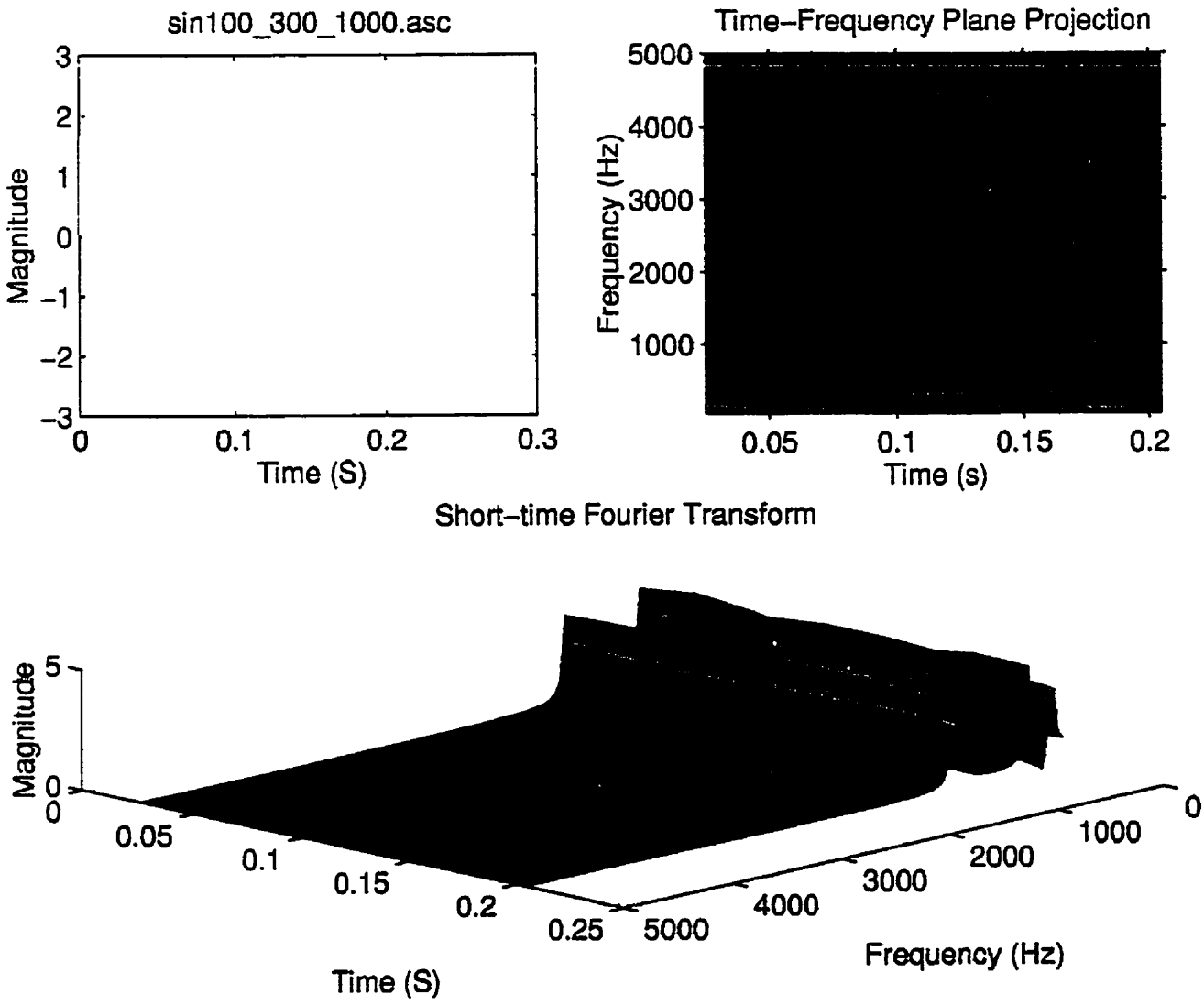

Figure 1.12: Short-time Fourier transform of the sum of sines signal

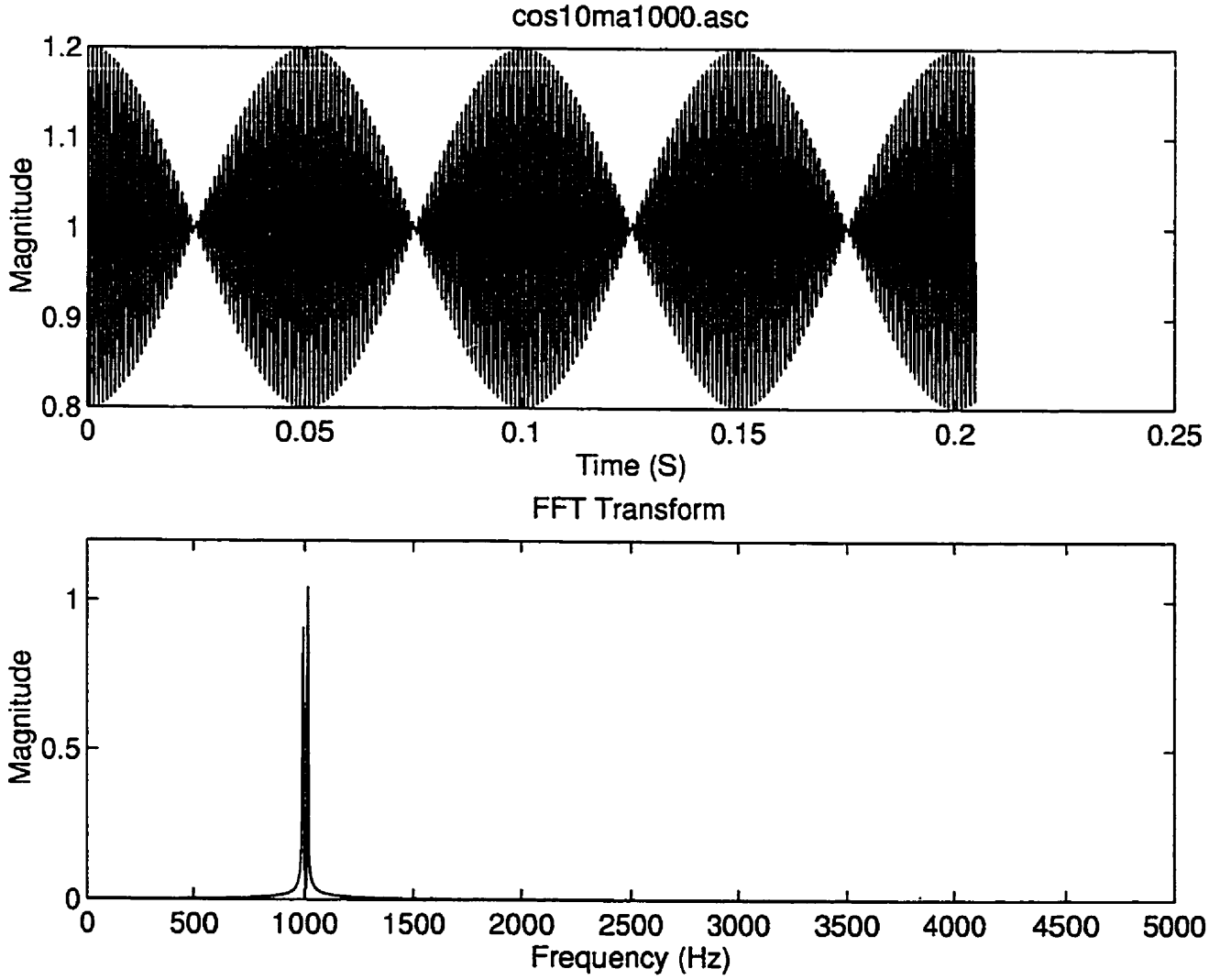

Figure 1.13: Amplitude-modulated signal and its spectrum.

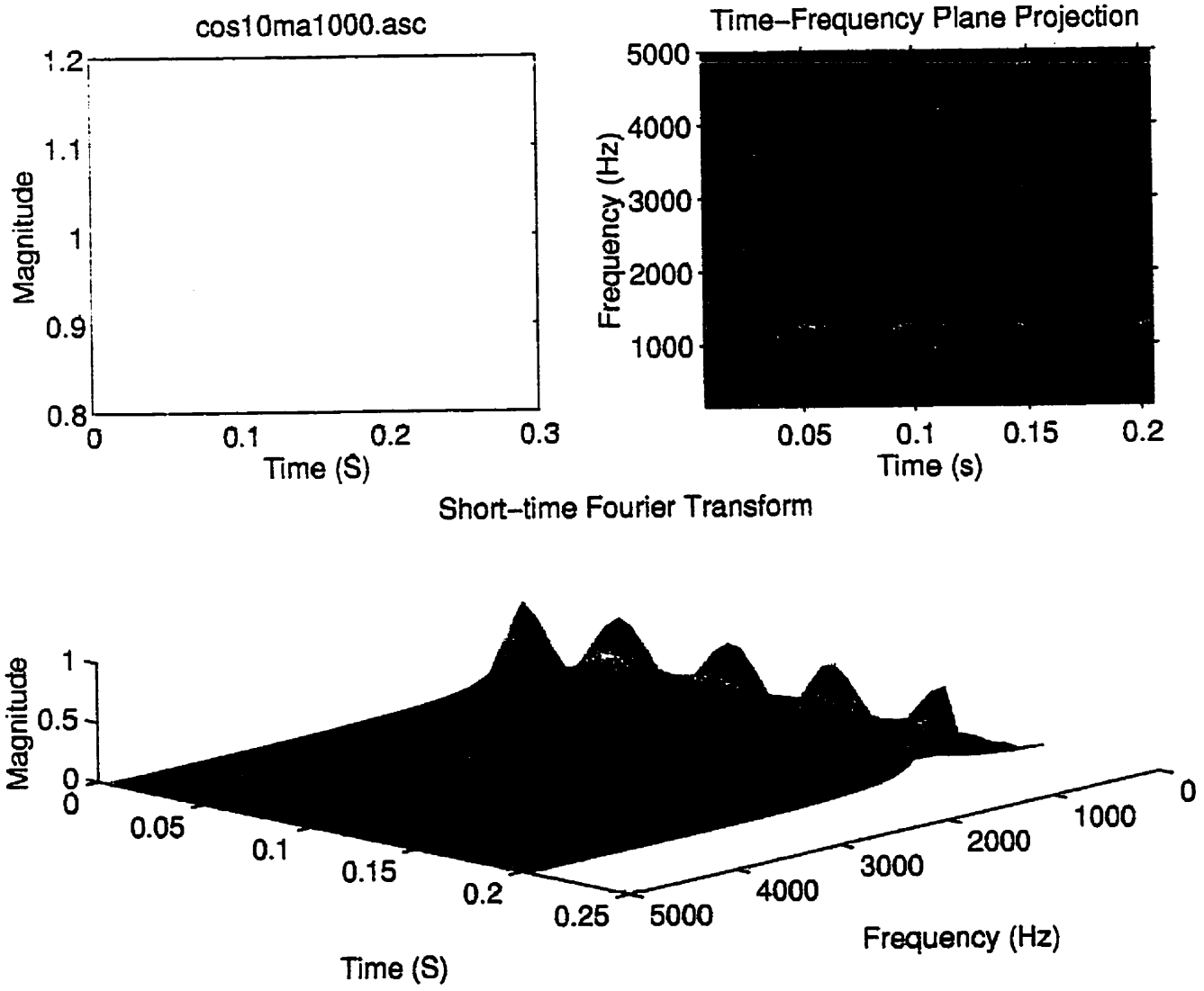

Figure 1.14: Short-time Fourier transform of the amplitude modulated signal.

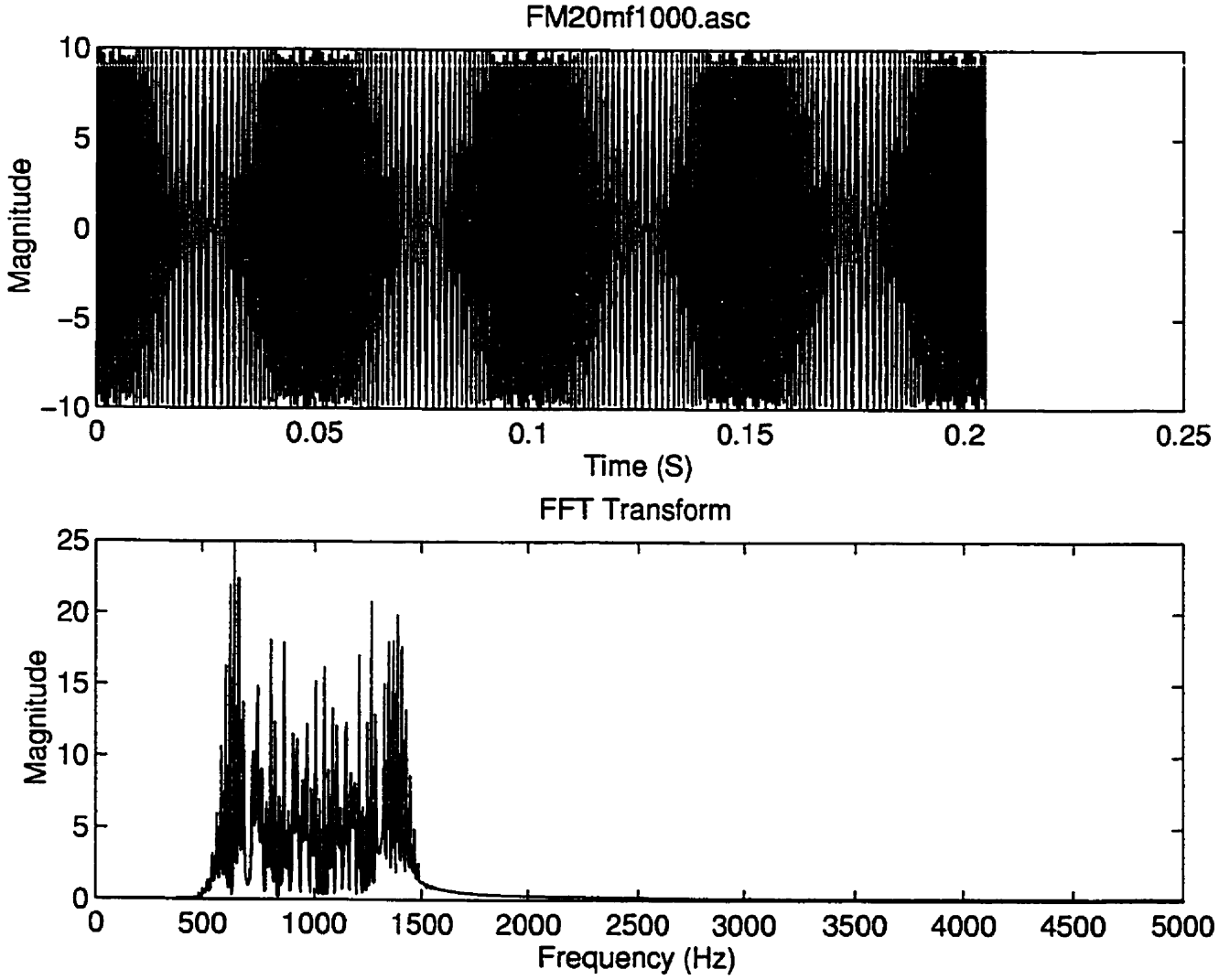

Figure 1.15: Frequency-modulated signal and its spectrum.

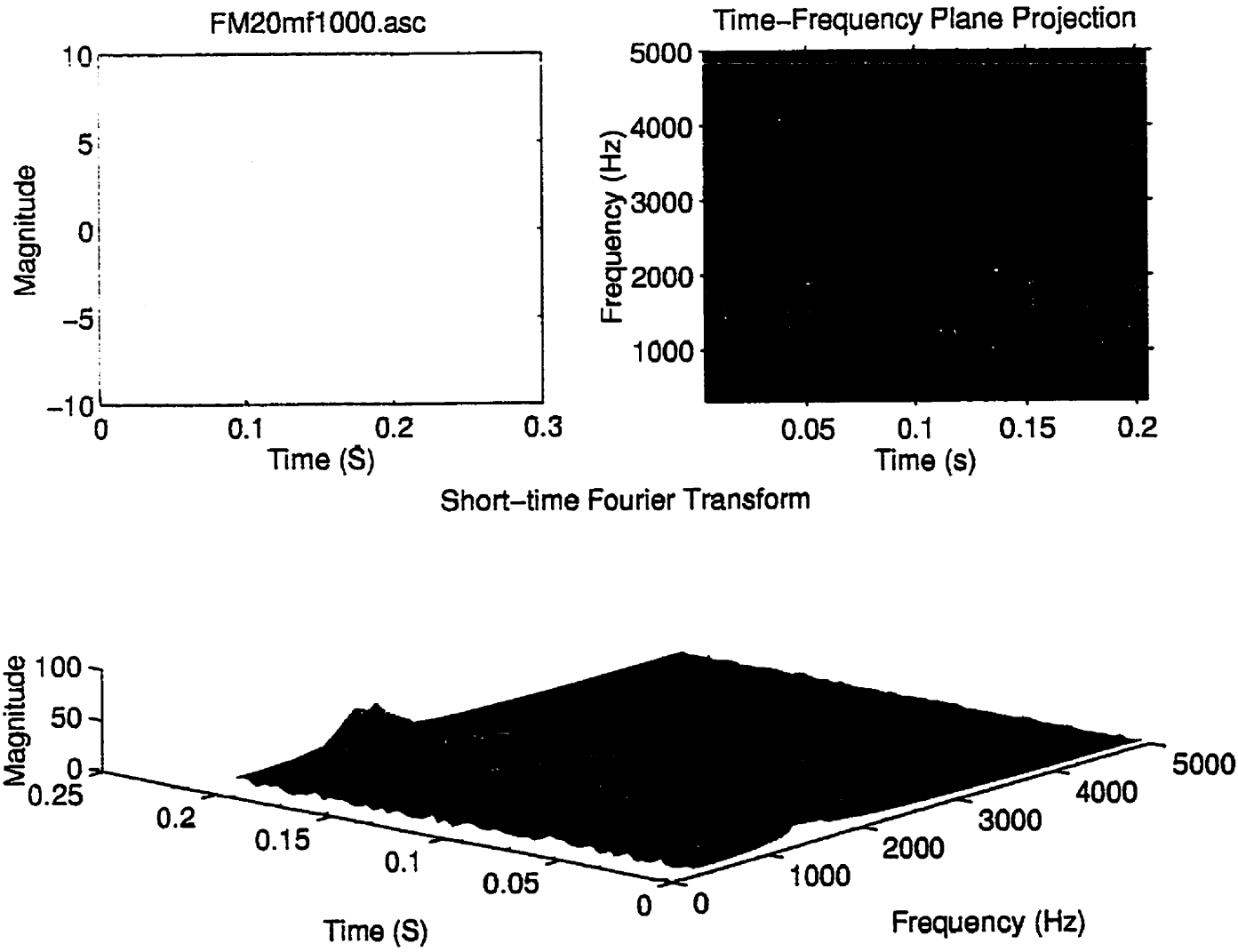

Figure 1.16: Short-time Fourier transform of the frequency-modulated signal

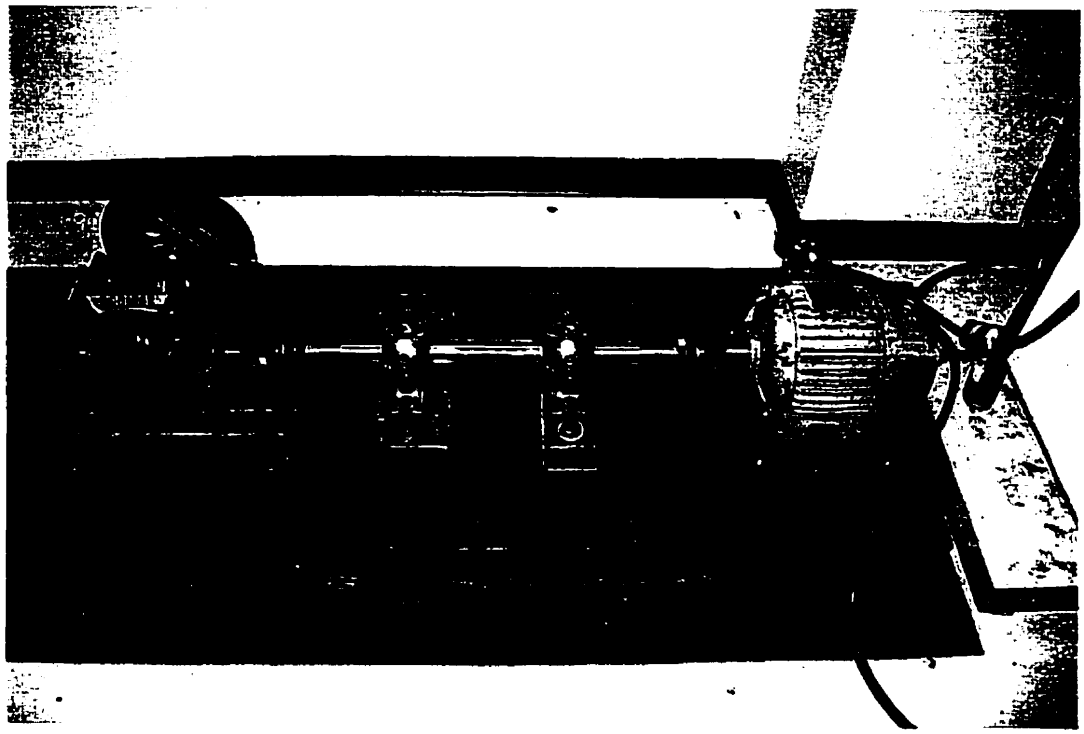

Figure 1.17: Test setup.

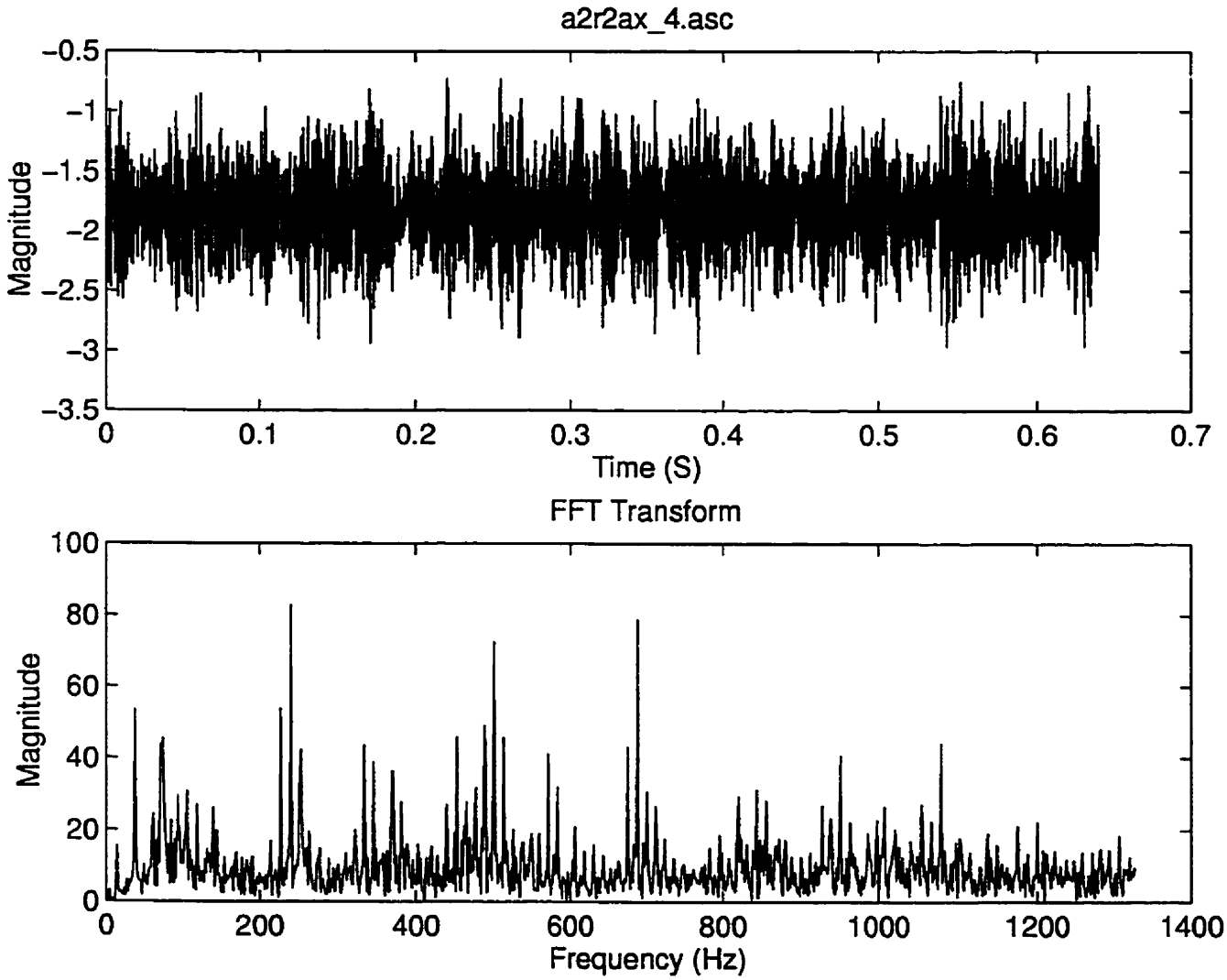

Figure 1.18: The signal measured on a defective bearing and its spectrum.

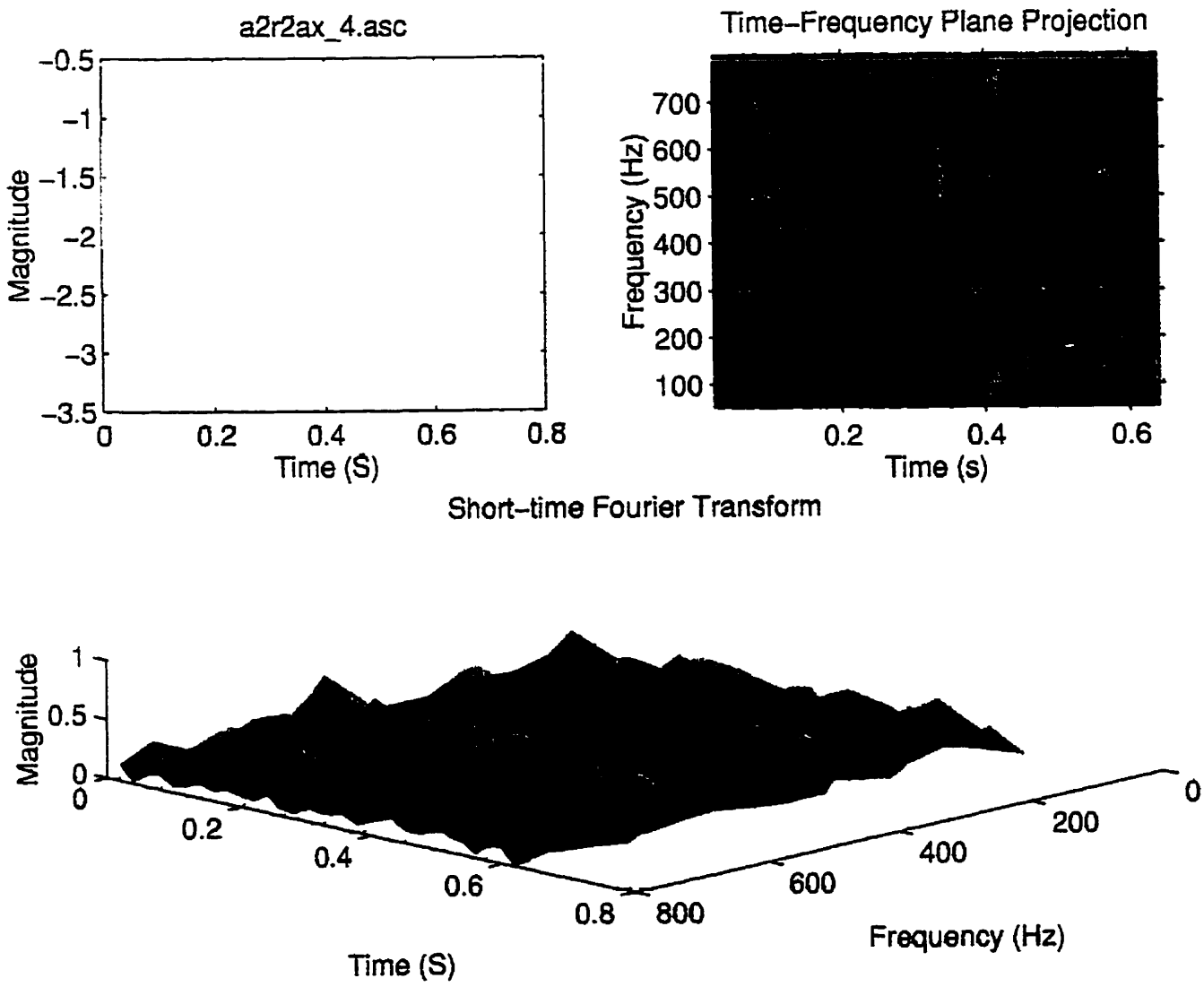

Figure 1.19: Short-time Fourier transform of the defective bearing signal.

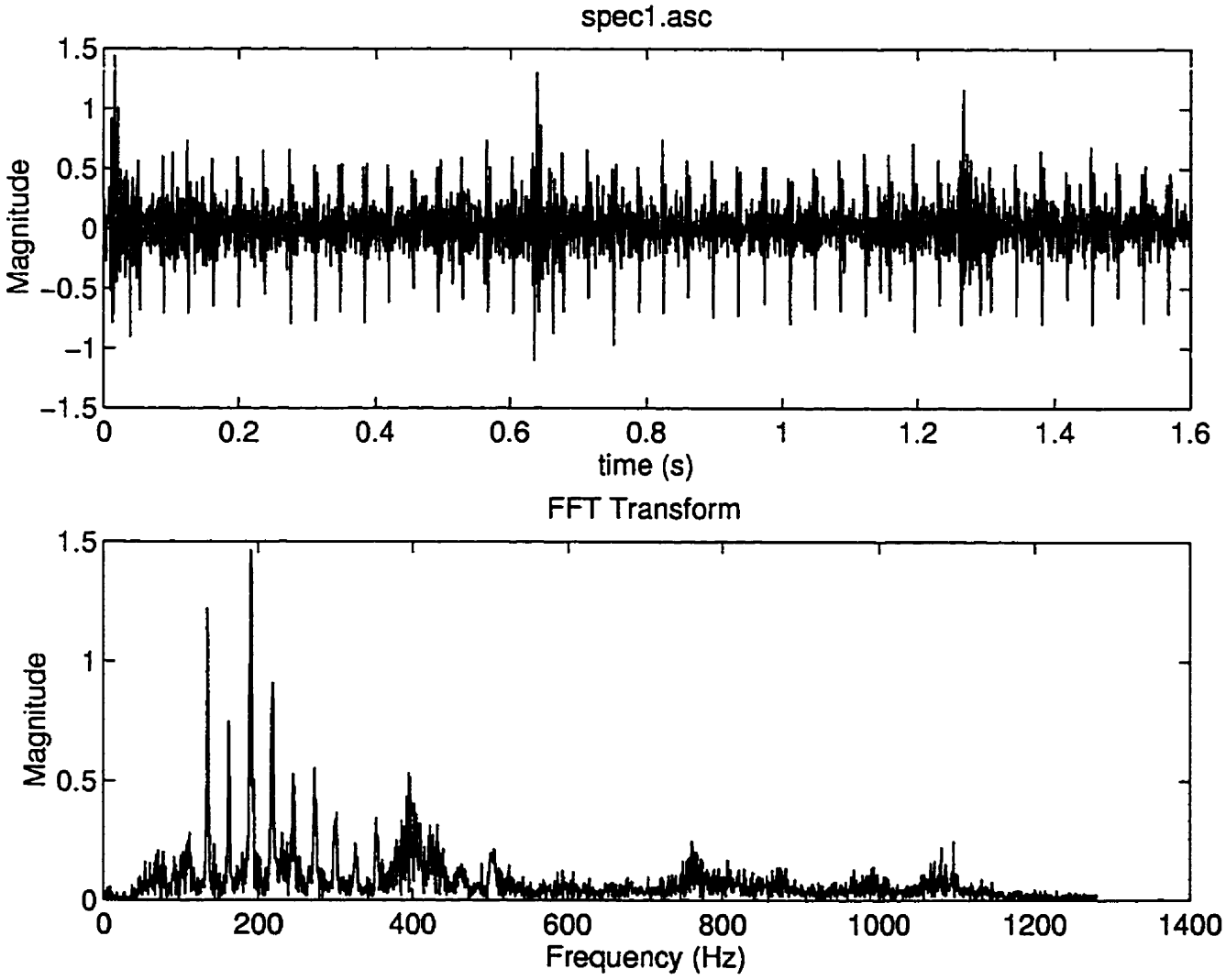

Figure 1.20: The signal measured on a defective gearbox and its spectrum.

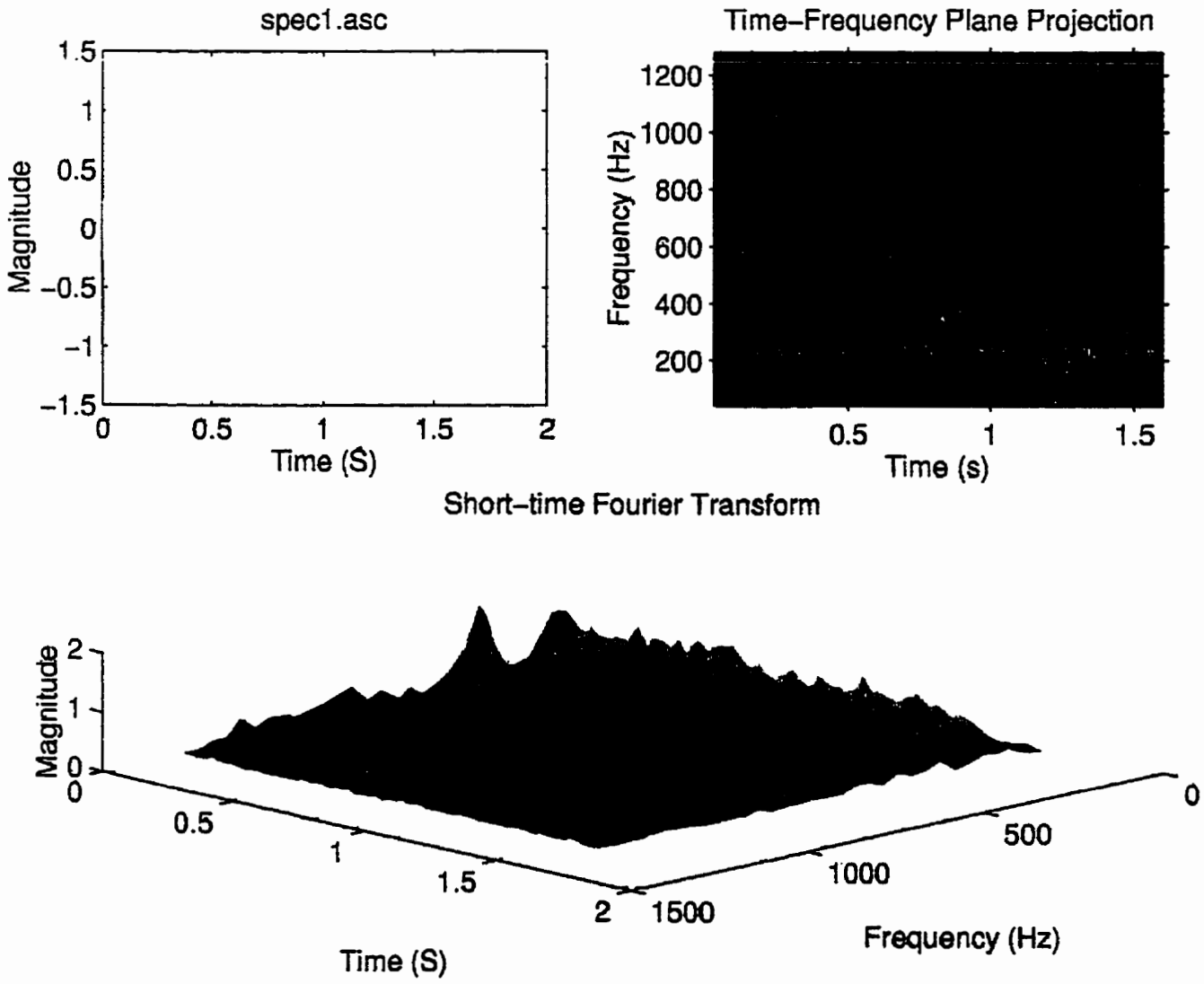

Figure 1.21: Short-time Fourier transform of the defective gearbox signal.

CHAPITRE II

TIME-FREQUENCY DISTRIBUTIONS AND THEIR APPLICATION TO MACHINERY FAULT DETECTION*

[1]M.S. Safizadeh, [1]A.A. Lakis and [2]M. Thomas

1: Département de Génie Mécanique, École Polytechnique de Montréal

Case Postale 6079, Succ. Centre-ville, Montréal, Canada H3C 3A7

2: Département de Génie Mécanique, École de Technologie Supérieure

1100, rue Notre-Dame Ouest, Montréal, Canada H3C 1K3

2.1 Abstract

Time-frequency analysis is relatively new in the field of mechanical signal processing and has yet to be applied to its full potential. This method of analysis is effective in the detection of faults in machinery and, in certain instances, is the most efficient method available. In this paper, some of the methods of time-frequency analysis such as the Wigner Distribution, the Choi-Williams Distribution, and the RID Distribution, are briefly reviewed and the advantages and disadvantages of each are considered. The efficacy of each method is tested by the practical application of an in-house software program developed for all time-

★: Soumis pour publication dans "Journal of Sound and Vibration"

frequency methods. Firstly, computer-generated signals are used to determine the effectiveness of a method. Secondly, the signal recorded from an experimental set-up is applied in order to verify performance. Finally, the various methods are evaluated using real-life signals recorded from a defective gearbox and a defective dryer machine. This paper demonstrates the effectiveness of time-frequency analysis in presenting a clear and exact representation of a signal, and compares the results with those obtained using the Short-Time Fourier Transform and traditional methods of analyzing signals measured on a rotating machine.

2.2 Introduction

The primary objective of all research into signal processing has been to find an efficient method which would generate results rapidly and clearly and in a manner which could be relatively easily interpreted.

The Short-Time Fourier Transform (STFT), used as a time-frequency representation of the signal energy, was one of the first attempts to see a signal in three dimensions and obtain rapid calculation and clear interpretation. The STFT is obtained by applying a fixed-length moving window to the non-stationary data sequence prior to computing the spectrum. The result is a time average of the signal spectrum over the window width. However, although

this method provides a time-frequency representation of the signal, both the time and the frequency resolution are completely dependent upon the choice of the window length and the method does not satisfy certain prerequisites for a joint time-frequency distribution.

Use of the STFT in the solution of problems in signal processing was followed by the development of time-frequency methods. Researchers tried to find a way to show the distribution of signal energy as a joint function of time and frequency which, on the one hand, satisfy certain conditions and, on the other hand, reduce the time-frequency resolution dependence on the window.

The Wigner Distribution (WD), first used in quantum mechanics [1], has been used to overcome the problem of the STFT. It was employed in signal processing by Ville in 1948 [2]. The WD has very desirable properties which have been extensively investigated by Classen and Mecklenbrauker [3]. The major draw-back of the WD is the presence of cross terms between frequency components in the time-frequency plane. Cross terms and their properties have been studied by Hlawatsch and Flandrin [4-5].

Some smoothing of the Wigner Distribution is needed to suppress the cross terms. A windowed- Wigner Distribution by a function that is peaked around τ, $h(\tau)$, will be called a pseudo-Wigner Distribution (PWD) [3]. If the smoothing is carried out in both the time and frequency domains, the distribution will be called a smoothed Wigner Distribution (SWD)

[6]. In addition to the Wigner Distribution, several others have been developed but all had the problem of cross terms [7-8]. In 1966, Cohen provided a general formula for generating different distributions [9]. Other distributions are obtained by changing an arbitrary function called the kernel. In his recent work, he gave a complete review of the time-frequency distributions [10].

Instead of smoothing the Wigner Distribution to eliminate the cross terms, Choi-Williams introduced a new kernel which can reduce the cross terms [11]. Unfortunately, the Choi-Williams Distribution does not completely satisfy the support properties in time and frequency. Recently, Jeong and Williams [12] defined the conditions which a kernel must satisfy to suppress the cross terms. This class of distribution is called the Reduced Interference Distributions (RID), and is an improved version of the exponential distribution.

It can be seen that each distribution has both advantages and disadvantages; the choice of distribution for a given practical application depends on the problem concerned. In Section 2, the necessary properties of a time-frequency distribution are summarized, time-frequency distributions are compared, and their advantages and disadvantages are given.

In Section 3, the history of time-frequency applications is presented; an in-house software developed for time-frequency distribution is discussed; and the effectiveness of the time-frequency distribution is shown by analyzing signals measured from experimental and on-site tests.

2.3 Time-frequency distributions

2.3.1 Time-frequency distribution property requirements

An ideal joint time-frequency function of signal $s(t)$ possesses a number of important properties, which form the basis for interpreting the function as a time-frequency distribution of the signal energy.

These properties discussed in [3] are summarized as follows:

a) the instantaneous signal power at a certain time is equal to the projection of the $P(t,\omega)$ on the time axis: $$\frac{1}{2\pi}\int_{-\infty}^{\infty} P(t,\omega)d\omega = |s(t)|^2$$

b) the energy density spectrum of $s(t)$ at a certain frequency is equal to the projection of the $P(t,\omega)$ on the frequency axis: $$\int_{-\infty}^{\infty} P(t,\omega)dt = |S(\omega)|^2$$

The *a)* and *b)* definitions are called time and frequency marginal conditions.

c) the first-order moment of the $P(t,\omega)$ with respect to frequency may be expressed as follows

$$\Omega(t) = \frac{1}{P(t)} \int_{-\infty}^{\infty} \omega P(t,\omega) d\omega \quad \text{where} \quad P(t) = \int_{-\infty}^{\infty} P(t,\omega) d\omega$$

The $\Omega(t)$ can be interpreted as the average frequency of the $P(t,\omega)$ at time t.

For real signals the average frequency provides no information. Let us therefore assume that $s(t)$ is complex-valued in the form $s(t) = v(t)e^{j\varphi(t)}$ where $v(t)$ and $\varphi(t)$ are real functions, $v(t)$ is the envelope of $s(t)$, and $\varphi(t)$ is the phase of $s(t)$. Using this representation of $s(t)$, we find that $\Omega(t) = \varphi'(t)$. Therefore it can be concluded that the instantaneous frequency is an average frequency at a particular time.

d) the first moment of the $P(t,\omega)$ with respect to time at a particular frequency is

$$T(\omega) = \frac{1}{P(\omega)} \int_{-\infty}^{\infty} tP(t,\omega) dt \qquad \text{where} \quad P(\omega) = \int_{-\infty}^{\infty} P(t,\omega) dt$$

If we consider the complex spectrum $F(\omega) = A(\omega)e^{j\psi(\omega)}$ where $A(\omega)$ is its amplitude and $\psi(\omega)$ is its phase angle, we can prove that $T(\omega) = -\psi'(\omega)$.

Thus, the average time of the $P(t,\omega)$ at a particular frequency is equal to the negative of the derivative of the spectral phase of the signal.

e) the time shift: If $s(t) \rightarrow s(t-\tau)$ then $P(t,\omega) \rightarrow P(t-\tau,\omega)$

f) the frequency shift: If $s(t) \rightarrow s(t)e^{j\Omega t}$ then $P(t,\omega) \rightarrow P(t,\omega-\Omega)$

g) the time limited signal property.

If $s(t)$ is restricted to a finite time interval only and $s(t) = 0$ for $t \prec t_a$ or $t \succ t_b$

then the $P(t,\omega)$ is restricted to the same time interval $P(t,\omega) = 0$ for $t \prec t_a$ or $t \succ t_b$

h) the frequency limited signal property.

If $S(\omega) = 0$ for $\omega \prec \omega_a$ or $\omega \succ \omega_b$ then $P(t,\omega) = 0$ for $\omega \prec \omega_a$ or $\omega \succ \omega_b$

From a mathematical point of view, there is an infinite number of joint functions which satisfy these conditions since the conditions do not define the problem uniquely. Several distributions have been proposed over the last fifty years but in this section only certain distributions with desirable properties will be studied.

2.3.2 Time-frequency methods

The Wigner Distribution (WD) is one of the joint time-frequency distributions that is fundamentally different from the STFT The original formulation was proposed by Wigner in 1932 and used in quantum mechanics. The Wigner Distribution of signal $s(t)$ is defined as

$$WD_s(t,\omega) = \int_{-\infty}^{\infty} s(t+\tau/2)s^*(t-\tau/2)e^{-j\omega\tau}d\tau \tag{2.1}$$

where $s(t)$ is a continuous complex signal and "*" denotes the complex conjugate (unless otherwise indicated, the ranges of integrals are from $-\infty$ to ∞ throughout this paper.)

This representation may be interpreted as the Fourier Transform of

$$R_s(t,\tau) = s(t+\tau/2)s^*(t-\tau/2) \tag{2.2}$$

with respect to the lag variable τ where $R_s(t,\tau)$ is defined as the instantaneous auto correlation of a complex signal $s(t)$, Therefore :

$$WD_s(t,\omega) = \int R_s(t,\tau)e^{-j\omega\tau}d\tau \tag{2.3}$$

The Wigner Distribution possesses very high resolution in both time and frequency, and it has the properties ***a)*** to ***h)***. Despite the desirable properties of the Wigner Distribution, it has two major draw-backs: it is not necessarily non-negative and it is a bilinear function producing interferences or cross terms for multi-component signals. The Wigner Distribution of the sum of two signals $s_1(t) + s_2(t)$ is

$$WD_{s_1+s_2}(t,\omega) = WD_{s_1}(t,\omega) + 2Re\left[WD_{s_1 s_2}(t,\omega)\right] + WD_{s_2}(t,\omega) \tag{2.4}$$

which has a cross term " $2Re\left[WD_{s_1 s_2}(t,\omega)\right]$ ", in addition to the two auto terms. Cross terms lie between signal components in different regions in the time-frequency plane and are oscillatory. They can have a peak value as high as the auto terms and make the interpretation of the time-frequency representation of signals very difficult. Ville used the Wigner Distribution in signal analysis in 1948 when he replaced the continuous complex signal with the analytical signal. $s(t)$ is an analytical signal if the imaginary part of $s(t)$ is equal to the Hilbert transform of the real part of $s(t)$, so that

$$s_I(t) = \frac{1}{\pi}\int \frac{s_R(t)}{t-\tau} d\tau \tag{2.5}$$

In the case where $s(t)$ is an analytical signal, the Wigner Distribution is termed the Wigner-Ville Distribution (WVD). By using the analytical signal in the Wigner Distribution firstly, the negative frequencies which have no physical significance for a real signal are eliminated and, consequently, the cross terms between the negative and positive parts of the spectrum are eliminated; secondly, the Nyquist frequency can be applied to the sampling frequency of the signal. However, although the analytical signal eliminates some cross terms, there are still cross terms between multiple components which make interpretation difficult.

In practical applications, the Wigner Distribution requires some smoothing in order to suppress the cross terms. The pseudo-Wigner Distribution (PWD) is defined by:

$$PWD_s(t,\omega) = \int s(t+\tau/2)s^*(t-\tau/2)h(\tau)e^{-j\omega\tau}d\tau \qquad (2.6)$$

where $h(\tau)$ is a window function or a low pass filter in order to reduce cross terms which have oscillations of relatively high frequencies. The pseudo-Wigner Distribution can be considered as a frequency-domain variation of the Wigner Distribution.

$$PWD_s(t,\omega) = WD_s(t,\omega) *_{\omega} H(\omega) \qquad (2.7)$$

where $H(\omega)$ is the Fourier Transform of $h(\tau)$.

Filtering broadens the representations in the frequency domain and, as a result, the pseudo-Wigner Distribution gives a modest time resolution at the expense of sacrificing the frequency resolution. Such smoothing is desirable when time-domain filtering is not needed and the sacrifice of frequency resolution for time resolution is acceptable.

If, in order to suppress cross terms in the Wigner Distribution, smoothing in both the time and frequency domains is needed, a smoothed Wigner Distribution (SWD) is appropriate. The smoothed Wigner Distribution is defined as

$$SWD_s(t,\omega) = \iint WD_s(u,\xi)\Phi(t-u,\omega-\xi)du d\xi \tag{2.8}$$

where $\Phi(t,\omega)$ is a two-dimensional smoothing function. The smoothed Wigner Distribution reduces cross terms with oscillations in the time and frequency domains at the expense of resolution in both domains.

The Short-Time Fourier Transform (STFT), which is the most widely used time-frequency representation in practical application, is defined as

$$STFT_s(t,\omega) = \int s(\tau)h(\tau-t)e^{-j\omega\tau}d\tau \tag{2.9}$$

where $h(t)$ is a window function. The modulus squared of the STFT is called a spectrogram.

$$S_s(t,\omega) = \left|STFT_s(t,\omega)\right|^2 \tag{2.10}$$

By two-dimensional convolution theorem, we have

$$\left|STFT_s(t,\omega)\right|^2 = \frac{1}{2\pi} WD_s(t,\omega) * WD_w(-t,\omega) \tag{2.11}$$

The spectrogram is a special case of the smoothed Wigner Distribution in which the smoothing filter is $\Phi(t,\omega) = \frac{1}{2\pi} WD_w(-t,\omega)$.

The spectrogram has the non-negativity property which facilitates the interpretation of the spectrogram as the signal energy distribution, but does not preserve the time and frequency energy marginals of a signal. In general, the non-negativity property often conflicts with other desirable properties. However, a major drawback of the STFT is that it requires a trade-off between the time and frequency resolutions. Although, the Short-Time Fourier Transform with a window that conforms to the signal components provides maximum resolution in the smoothed Wigner Distribution, the STFT has less concentration than the Wigner Distribution. Moreover, for unknown signals, how can appropriate windows be found without *a priori* knowledge of the signal components?

Apart from the Wigner Distribution, several other distributions have been proposed. These

are similar to the Wigner Distribution in that they satisfy the marginal, the instantaneous frequency condition, and various other properties. The Rihaczek [7] and the Page [8] Distributions are two of those proposed.

The Rihaczek distribution, which gives a complex energy spectrum, is defined as

$$e(t,\omega) = \frac{1}{\sqrt{2\pi}} s(t) S^*(\omega) e^{-j\omega t} \tag{2.12}$$

The real part of the Rihaczek distribution, which is called Margenau-Hill distribution, lacks many desirable properties such as instantaneous frequency, but does satisfy the marginal conditions.

Page considered only the signal up to the present time t and abandoned the future because it is unknown. A new signal is defined as follows :

$$\begin{cases} s_t(t') = s(t') & for \quad t' \le t \\ s_t(t') = 0 & for \quad t' \succ t \end{cases}$$

The Page Distribution for the above signal definition may be written as follows :

$$P^-(t,\omega) = 2Re \frac{1}{\sqrt{2\pi}} s^*(t) S_t^-(\omega) e^{j\omega t} \tag{2.13}$$

where $S_t^-(\omega) = \frac{1}{2\pi}\int_{-\infty}^{t} s(t')e^{-j\omega t'}dt'$

The Page Distribution satisfies the marginal conditions but is unable to show correctly a multi- components signal in the time-frequency plane. Figure 2.1 shows a representation of a multi- components signal by the Wigner, Rihaczek and Page distributions. The signal is a sine with frequency ω_1 started at $t = 0$ and stopped at $t = t_1$, restarted again at $t = t_2$ with another frequency ω_2 , and ended at $t = t_3$. Each of the three distributions displays energy density where one does not expect to find it.

In 1966, a method was derived that could generate an infinite number of new distributions in a very simple way. This general distribution formula is obtained by replacing $\phi(\theta,\tau)$ with $\Phi(t,\omega)$ in the formula (2.8):

$$WD_s(t,\omega) = \iiint e^{j(-\theta t-\tau\omega+\theta u)}\varphi(\theta,\tau)s(u+\tau/2)s^*(u-\tau/2)du\,d\tau\,d\theta \qquad (2.14)$$

where $\varphi(\theta,\tau)$ is the two dimensional inverse Fourier transform of $\Phi(t,\omega)$ and θ and τ

are respectively the frequency lag and the time lag. Formula (2.14) is referred to as Cohen's class of time-frequency distributions and characterizes time-frequency distributions by an auxiliary function, called the kernel function $\varphi(\theta,\tau)$. The properties of a distribution are reflected by simple constraints on the kernel, and by examining the kernel one can readily be assured of the properties of the distribution. This allows one to pick and choose those kernels that produce distributions with prescribed, desirable properties. By using this general formula we can find the kernel function for each of the distributions which have been defined, such as the Wigner, Rihacezk, Margenau-Hill and Page. The kernel function for the Wigner, Rihacezk, Margenau-Hill and Page distributions are respectively 1, $e^{j\theta\tau/2}$, $\cos\frac{\theta\tau}{2}$ and $e^{j\theta|\tau|/2}$.

In 1980, Choi and Williams presented a new kernel for reducing cross terms in the Wigner Distribution. Their kernel is defined as

$$\varphi(\theta,\tau) = e^{-\theta^2\tau^2/\sigma} \tag{2.15}$$

where σ is a parameter which trades off auto-term resolution for cross term suppression or vice versa. By increasing σ, we achieve a distribution similar to the Wigner Distribution and by decreasing σ, we eliminate the cross terms but we loose resolution in the time and

frequency domains. The Choi-Williams distribution may be written as follows :

$$CWD_{\sigma}(t,\omega)=\frac{1}{4\pi^{3/2}}\iint\frac{1}{\sqrt{\tau^2/\sigma}}\exp\left(-\frac{(u-t)^2}{4\tau^2/\sigma}\right)s^*(u-\tau/2)s(u+\tau/2)e^{-j\omega\tau}dud\tau \quad (2.16)$$

Figure 2.2 shows the Choi-Williams representation with a different value of σ for a sinusoidal signal with two constant frequencies. Although, the Choi-Williams Distribution satisfies the marginal conditions, it violates the support properties ***g)*** and ***h)***. It attenuates the cross terms equally in the time and the frequency domains and provides a higher resolution than the smoothed Wigner Distribution. Although the Choi-Williams Distribution is the best choice for analyzing mutli-component signals in which the components have a constant frequency content, its resolution for signal components with significant frequency modulation or time-varying signals is very poor. However, the Choi-Williams Distribution is insensitive to the time-scale of the components, due to the shape of its kernel.

By generalizing from Choi-Williams' work, a broader class of exponential distribution (ED) defined by Diethorn [13] induces a kernel of the following form:

$$\varphi(\theta,\tau)=e^{\frac{-|\theta|^p|\tau|^q}{\sigma}} \quad (2.17)$$

By carefully selecting parameters p,q and σ, we may obtain the desired properties.

To reduce the cross terms and preserve simultaneously the properties ***a)*** to ***h)***, Jeang and

Williams [12] introduced a new class of time-frequency distribution, called the Reduced Interference Distributions (RID). The RID satisfies properties ***a)*** to ***h)***, as does the WD. The RID kernel should be not only a low-pass filter but also a function of $\theta\tau$ which satisfies

$$|\varphi(\theta,\tau)| \prec\prec 1 \qquad \text{for} \quad |\theta\tau| \succ\succ 0$$

where θ and τ are respectively the frequency lag and the time lag.

The kernel of the RID is defined as follows :

$$\varphi_{RID}(\theta,\tau) = H(\theta\tau) \tag{2.18}$$

where H is a two dimensional low-pass filter type. The WD is not a member of the RID because its kernel does not have the reduced interference property. Although the RID satisfies many properties, it has many disadvantages. First, the RID may or may not satisfy the regularity property and it does not have the unitary property. Secondly, the RID only reduced the height of the cross terms and spread them over a larger time-frequency area. In particular, the RID is not able to suppress the cross term which is located on the θ or the τ axis.

In 1966, Born and Jordan [14] used a sinc kernel which is defined as

$$\varphi(\theta,\tau) = \frac{\sin(a\theta\tau)}{a\theta\tau} \tag{2.19}$$

with $a = 1/2$. But its property of reducing interference distributions was derived from the work of Jeang and Williams in 1992.

In 1990, a new time-frequency distribution with very interesting features, called the cone-shaped kernel, was developed by Zhoa, Atlas and Marks (ZAM) [15]. This distribution not only suppresses the cross terms, but also produces good resolution in both time and frequency. Their kernel is defined as

$$\varphi_{ZAM}(\theta,\tau) = g(\tau)|\tau|\frac{\sin(a\theta\tau)}{a\theta\tau} \tag{2.20}$$

where $g(\tau) = 1,\ a = 1/2$.

Figure 2.3 shows the comparison between the Spectrogram and the ZAM Distribution. This distribution hides the cross terms by placing them under the auto terms.

In 1993, Louglin et al. [16] studied a general method for placing cross terms under auto terms. They used a kernel in the form of

$$\varphi(\theta,\tau) = f(\theta,\tau)\sin(a\theta\tau) \tag{2.21}$$

Depending on the choice of $f(\theta,\tau)$ these kernels may or may not satisfy other desirable properties. In 1994, a new kernel function called the "compound kernel" was presented by Zhang and Sato [17]. This kernel is the product of the Choi-Williams and Margenau-Hill kernels.

$$\varphi_{zz} = \exp(-2\pi^2\theta^2\tau^2/\sigma^2)\cos(2\pi\beta\theta\tau) \tag{2.22}$$

where σ and β are two parameters which may be identified as follows:

when $\sigma \to \infty$, $\beta \to 1/2$, we obtain the Margenau-Hill Distribution;

when $\beta \to 0$, we have the Choi-Williams Distribution, and

when $\sigma \to \infty$, $\beta \to 0$, we get the Wigner-Ville Distribution.

In this distribution, the cross terms are transposed with the auto terms. Consequently, the correct value of the auto terms is slightly modulated due to cross terms. Figure 2.4 illustrates the cross- sectional features of both distributions for various values of the parameter σ.

The last three types of kernel are of little interest because they change the forms of auto terms which are very important in fault detection in machinery.

Zhenyu Guo et al. [18] presented a new kernel based on the first order Bessel function. The kernel is given by

$$\varphi_{zdh} = \frac{J_1(2\pi\alpha\theta\tau)}{\pi\alpha\theta\tau} \tag{2.23}$$

where α is a scaling factor and J_1 is the first order Bessel function. For $\alpha \leq 0.5$, this distribution can be considered as a member of the RID, and when $\alpha \succ 0.5$, it behaves like the Choi-Williams distribution but is not identical to it. Although the Bessel distribution does not have the non-negativity property, by adjusting α, it is possible to analyse the time-frequency behaviors of transient deterministic and random signals.

It has been shown that the different distributions perform better for some signals than others, and that the choice of kernel is very important and may be dependent on the signal. A general method for constructing the distributions of which the kernel is dependent on the signal, and which possess certain desirable properties of the distribution, has been developed by Baraniuk and Jones [19]. It is noted that distributions with signal-independent kernels are called bilinear distributions, but distributions with signal-dependent kernels where the kernel is adjusted according to the signal at hand, are called adaptive optimal kernel distributions.

In this method, an optimization procedure is applied to a case where the kernel is adjusted

in accordance with the signal at hand.

2.4 The application of time-frequency analysis to machinery diagnostics

2.4.1 Brief historical perspective

From an application point of view, Boashash [20] was the first to use the time-frequency technique for real problems. He applied it to geophysical exploration. The Wigner Distribution was used by Bazelaire and Viallix [21] to obtain data to measure the absorption and dispersion coefficients of the ground and to formulate a new understanding of seismic noise. Forrester [22] has made a great contribution to machinery diagnostics by using the WVD in the vibration analysis of defective helicopter gearboxes. He showed that signal enhancement techniques are not capable of distinguishing tooth cracking from spalling and can be misleading in their indications of the extent of damage, but WVD can detect both the type and extent of faults. Meng and Qu [23] presented the effectiveness of using WVD in rotating machinery fault diagnosis.

In a series of reports, McFadden and Wang [24-27] reviewed several definitions of the continuous and the discrete WVD, implemented WVD for the detection of gear damage, and compared the results with those from existing narrow band enhancement techniques. In another application of time-frequency analysis, Rohrbaugh [28] used the time-frequency

method to find defects in different elements of several sets of marine machinery, such as fans and motor-generators. Rao, Taylor and Harrison [29] used the Wigner Distribution in the diagnosis of faults in a high-power gas turbine. They described the advantages of WD in providing high-resolution estimates of non-stationary, narrow-band signals in the time-frequency domain. Another application of time-frequency analysis to the detection of faults in a gearbox is described by Oehlmann et al. [30].

Williams [31] used the Reduced Interference Distributions (RID) time-frequency technique in the analysis of signals measured from bearings. He showed that the spectrogram and Waterfall Plot do not adequately represent time-varying signals.

The detection of faults in reciprocating machines such as internal combustion engines and pumps is particularly difficult. Rohrbaugh and Cohen [32] applied time-frequency methods to the analysis of a cam-operated pump. They showed that time-frequency methods can provide more detail about the signal, thus facilitating the detection of faults. In comparing time-frequency analysis with the STFT and traditional methods, they found time-frequency methods to be superior. In another work, Samimy and Rizzoni [33] presented the application of time-frequency analysis to the detection of internal combustion engine knock. The transient nature and time-varying characteristics of the signal mean that only time-frequency methods will give a satisfactory result.

Another application of time-frequency methods is in machine tool monitoring. Zheng and

Whitehouse [34] described the potential of the Wigner Distribution for the detection of incipient chatter. Loughlin et al. [35] discussed the application of time-frequency analysis to drilling and grinding operations. They demonstrated how a new technique can reveal features that do not appear in the Short-Time Fourier Transform.

The Wigner-Ville Distribution has been applied in various fields : as an indicator of drill attrition in industry or surface-fault in a diesel engine. Changes in the dynamic characteristics of ground using seismic analysis were presented by Bigret et al. [36]. Atlas, Bernard and Narayanan [37] gave a review of the application of time-frequency analysis to different elements of rotating machine monitoring and machine tool monitoring.

In 1992, Boashash [38] published a book about time-frequency analysis and its application. In this book, he reviewed several articles on different methods of time-frequency analysis and applications of the analysis in several different domains.

All of the above papers show the potential of time-frequency analysis in different fields of mechanical engineering. They demonstrate the applicability of time-frequency analysis to the solution of problems in machine monitoring. In the next section we will compare some of the time-frequency analyses by applying these methods in experimental and real cases.

2.4.2 Software for time-frequency analysis of signals

An in-house user-friendly software program has been developed for time-frequency analysis. This program is capable of calculating and demonstrating the different time-frequency transforms in two and three dimensions. The program includes the Fourier spectrum analysis, the Short-Time Fourier Transform, the Wigner-Ville Distribution, the smoothed Wigner-Ville Distribution, the Choi-Williams Distribution, the Rihaczek-Margenau Distribution, the Born-Jordan-Cohen Distribution, and many other time-frequency methods. In this section, the performance of each method is illustrated by a test signal generated by computer. The test signals are similar to those which are often observed in machine diagnosis.

The first example, which is called a sum of sines, is a multi-component signal with constant frequencies. This kind of signal is generated by faults such as imbalance, misalignment, looseness, and resonance which cause the constant frequencies at $N \times RPM$. The signal consists of three sines with frequencies 100 Hz, 300 Hz and 1000 Hz. In the time-frequency plane, one sees three lines at 100 Hz, 300 Hz and 1000 Hz parallel with the axis of time and, in time-frequency-energy, the three sines are shown in the form of three peaks constant in time. Figure 2.5 shows the signal and its Fourier spectrum. As shown in Fig. 2.6, the STFT of the signal presents exactly what we expected. Figure 2.7 shows the Wigner-Ville distribution of the signal, and we can see that the autoterms are contaminated by the interference terms. It is very difficult to identify the three frequencies without advance

knowledge of the signal.

The SWV (smoothed Wigner-Ville) shows the three peaks clearly in Figure 2.8. In the Choi-Williams Distribution of the signal, by changing the value of σ, we can obtain a good representation of the three frequencies, as shown in Figure 2.9. In the Born-Jordan-Cohen Distribution of the signal, shown in Figure 2.10, resolution is lost due to the elimination of the cross-terms.

The second example is an amplitude-modulated cosine at 1000 Hz with frequency modulation equal to 15 Hz, as shown in Figure 2.11. Cases such as a damaged gearbox and a defective bearing usually generate amplitude-modulated signals. Whilst it is not always possible to identify these by the Fourier spectrum or time waveform, with time-frequency analysis it is relatively simple. Figures 2.12 to 2.17 show the different time-frequency representations of the signal, and all these methods give a clear representation of the signal with varying resolution. It must be noted that the STFT requires an adjustment of the window and the Choi-Williams method requires an appropriate value of σ in order to provide satisfactory resolution. Among these representations, the Wigner-Ville Distribution provides the best result.

Certain types of gearbox problem may result in a frequency-modulated signal that is extremely difficult to identify. Such a signal is represented by a frequency-modulated cosine at 1000 Hz with frequency modulation equal to 20 Hz, as shown in Figure 2.18. As shown

in Figure 2.18, it is not possible to determine the characteristics of the signal using its Fourier spectrum. On the other hand, time-frequency methods clearly demonstrate the time-varying characteristic of the signal, as shown in Figures 2.19 to 2.24 . The Wigner-Ville, the smoothed Wigner-Ville, and the Choi-Williams Distributions give better representations of the signal than the others.

The last example is a frequency and amplitude modulated cosine at 1000 Hz, as shown in Figure 2.25. This case is more complicated than the others but time-frequency methods provide clear representations of the signal, as shown in Figures 2.26 to 2.31. In this case, the Wigner-Ville, the smoothed Wigner-Ville, and the Choi-Williams Distributions again give better representations of the signal than do the others.

2.4.3 Experimental study of time-frequency methods

2.4.3.1 Experimental apparatus

In this section, an experimental installation which enables us to simulate different defect configurations in rotating machinery is presented. The experimental prototype (see Figure 2.32) consists of three distinct parts: part I, motor; part II, journal, and part III, receptor.

Part I is a three-phase asynchronous motor (550-575 V, power 2 HP). The rotating speed can

vary from 0-1725 r.p.m. Part II consists of an interchangeable rotating shaft which is supported by two journal bearings (SKF 1210 EKTN9 self aligning double row) labeled A and B. There are three shafts on which bearings with different defects are mounted. And Part III consists of a reducing gearbox with a ratio of 40:1 and a brake that can produce a variable resistance torque. Parts I, II, and III are connected by two couplings. An accelerometer is mounted on the experimental installation and is connected to an analyser.

2.4.3.2 Tests and results

We examined the time-frequency methods to pin-point defects of known characteristics and location on the rolling bearing. There was a small defect on the inner raceway of the bearing. The defect was created by scratching the bearing raceway with an electric pen. Figures 2.32 to 39 show the signal measured on bearing A, its spectrum and all other distributions. The results for the defective bearing were also verified by calculating the frequency at which the rolling elements passed over the defects [39]. The geometric characteristics of the bearing are as follows:

pitch diameter D=69 mm

Diameter of the rolling body d=10.32 mm

Contact angle α =7.87 deg

Number of rolling elements N =17 (per row)

Bearing frequency of rotation F_r=12.2 Hz

On the inner raceway, the frequency of rolling body defect impact is:

$$F_i = \frac{F_r N}{2}\left[1+\frac{d}{D}\cos(\alpha)\right] \tag{2.24}$$

The pass frequency on a point of the inner raceway is calculated and is equal to 238 Hz. The spectrum in Figure 2.33 shows the default frequency, along with other frequencies. However, the spectrum can be misleading [23]: we cannot be certain which is the default frequency unless we know its special characteristics. In this case, the default frequency should be an amplitude-modulated wave at approximately 238 Hz with the frequency of modulation being equal to the rotating frequency.

The amplitude-modulated signal at the default frequency and at $2\times$ default frequency in the STFT is shown, and we calculate the frequency of modulation and verify that it is correct and equal to the rotating frequency.

Among time-frequency methods, the Wigner-Ville cannot provide a good representation of the signal due to the cross terms which are generated between the signal components. The smoothed Wigner-Ville shows the signal even better than the STFT and we can clearly see the amplitude modulation and easily calculate the frequency of the modulation. The Choi-

Williams gives a representation which is not as satisfactory as that produced by the smoothed Wigner-Ville as it is necessary to choose an appropriate value of σ. The Born-Jordan-Cohen gives a good appearance of the signal but, again, the resolution in time and frequency is not as satisfactory as that produced by the smoothed Wigner-Ville or the Choi-Williams. The Rihaczek-Margenau cannot even give a good appearance of the signal.

Therefore, after comparing the different time-frequency transforms of this signal we conclude that the SWV gives the best representation of the signal in this case.

2.4.4 Application of time-frequency methods to industrial problems

2.4.4.1 Gearbox test

The first set of data is obtained from a defective gear train of a hoist drum in a large shovel operating at an open pit iron mine. The data are measured by International Measurement Solutions company in order to find the problem in the machine.

Gears generate a mesh frequency equal to the number of teeth on the gear multiplied by the rotational speed of the shaft driving it. A high vibration level at the mesh frequency is often caused by tooth error, wear of the meshing surfaces, or any other problem that would cause the profiles of meshing teeth to deviate from their ideal geometry. Sidebands at the mesh

frequency, on the other hand, are typically due to a failure of mating teeth. Imagine a cracked tooth which is not yet broken, and will consequently not be noticed by the operating personnel. However, it will, due to its weakened mechanical condition, deflect more under load than the other (healthy) teeth when it goes into mesh. This results in a signal with amplitude modulation. Thus, an increasing level in the sidebands spaced with rotation speed in the frequency spectrum results from the cracked tooth.

A minimum length of time is required to perform an FFT analysis of each process. Here, the time resolution required will depend on the period of each tooth mesh and the desired level of accuracy. Sometimes, it is not possible to measure the signal for long enough to provide the periodicity of shock in FFT spectrum. In our case, the process does not even last one revolution of the driven gear.

Figures 2.40 to 2.46 show respectively the spectrum, the STFT, the Wigner-Ville, the smoothed Wigner-Ville, the Choi-Williams, the Born-Jordan-Cohen and the Rihaczek-Margenau representation of the signal (SPEC1). The FFT spectrum of the signal shows some peaks around 200 Hz and other smaller peaks at 400 Hz, 800 Hz and 1200 Hz. However, it is very difficult to find the problem without more information, and we are unable to visualize the pattern of the signal in the time-frequency plane. It is possible to see the amplitude-modulated signal in the STFT of the signal. The gear-meshing frequency is seen to be at approximately 200Hz and three large impacts due to three partially broken teeth at

approximately 400 Hz. It is possible to find the frequency of the periodicity of the peaks on the STFT. However, the smoothed Wigner-Ville gives a better representation than the STFT. The frequency of the periodicity is found with more precision in the smoothed Wigner-Ville representation than in the STFT representation. The Choi-Williams, with an appropriate value of σ, gives a representation of the signal in which a part of the energy of the second peak is dispersed between the first peak and the third peak. In the Born-Jordan-Cohen, the second peak is almost invisible and it is difficult to obtain satisfactory information about the signal. The Rihaczek-Margenau does not give a clear representation of the signal and the second peak has completely vanished. Here, again the SWV gives the best representation of the signal.

2.4.4.2. Bearing test

The second test was carried out on the dryer of a paper machine at the Abitibi-Consolidated Company in Quebec. A typical dryer section consists of about 60 paper-drying cylinders which are divided into five top and five bottom sections, as shown in Fig. 2.47. The standard paper dryer is a four- or five-foot diameter hollow cylinder of cast iron. The dryer journals must support the dryer which is extremely heavy and rugged. The drive of the dryer section has a critical function and any undesirable vibration in one of the cylinders can affect the passage of the paper over this section. Therefore, a precise and periodic diagnosis of the

dryer bearing is essential. An efficient diagnostic method can recognize the problem before damage has occurred. For this reason, time-frequency methods are used in this particular case to show their capacity, potential and credibility.

Figure 2.48 shows the measured signal on dryer # 27 and its spectrum. From the individual impacts which appear at regular intervals in the spectrum, one can conclude that there is a problem in the dryer. The low-level intense noise in the spectrum makes it impossible to see the amplitude modulations associated with the impacts. Time-frequency analysis makes the detection of this fault a straight-forward matter. Figures 2.49 to 2.52 show the different time-frequency representations of the signal. The constant impacts in time lead us to the defects which cause frequency constants components such as the defect on the outer race of a bearing. In this machine, bearings play an important role and it is to be expected that we first verify the bearing defaults. From the characteristics of the bearings, it is possible to calculate the different frequency of the bearing defaults. The frequency of the first impact corresponds to the BPFO (*ball-pass frequency on the outer race*) of the bearing and the other impacts are $2 \times BPFO, 3 \times BPFO, \ldots$. After replacing the bearing by a new one, this diagnosis is confirmed by an inspection of the old bearing.

In this case, there is not a great difference between the time-frequency distributions, and the STFT with an appropriate window may provide a clear representation. Thus, it is not possible, in this instance, to choose one method as being superior to the others, because the

choice of method depends on the signal and the resolution requirement in the analysis.

2.5 Discussion and conclusion

By comparing the results obtained from time-frequency analysis of different mechanical signals, we can conclude that :

1- Time-frequency analysis has definite advantages over time-based vibration analysis or frequency-based vibration analysis and these advantages make it a powerful tool in machine monitoring.

2- The STFT can give a satisfactory representation of a signal in the time-frequency plane provided that an appropriate length of window for cutting the signal is chosen. The resolution in time or frequency is always dependent on the length of window.

3- The Wigner-Ville is not able to produce a satisfactory representation of multi-component signals due to the presence of cross terms. It is valid only for mono-frequency signals.

4- The smoothed Wigner-Ville is the most appropriate among the transforms which we have studied in this paper. It gives not only a clear representation of the signal but also satisfactory resolution in time and in frequency.

5- The Choi-Williams may give a representation of the signal which is as satisfactory as that of the SWV but it is necessary to find a suitable value of σ.

6- By the Born-Jordan-Cohen, we can obtain an image of the signal in the time-frequency plane; however, the resolution in time and in frequency are not always accurate and it is not possible to calculate exactly the frequency of modulation or the frequency and the time of a transient peak in a time-frequency plane.

7- The Rihaczek-Margenau may not provide a satisfactory representation of the signal when the signal comes from a real case, but for theoretical signals it gives a good representation.

In summary, the choice of a distribution in a practical application depends on the problem concerned, and none of these distributions provides us with complete and conclusive results, thus we cannot rank one above the others. For this reason, we recommend that researchers consider all distributions and compare the results in each case studied.

2.6 References

1. E.P. Wigner 1932 Phys. Rev. 40, 749-759, On the Quantum Correction for Thermodynamic Equilibrium.

2. J. Ville 1948 Cables et Transmission 2A, 61-74, Théorie et Applications de la Notion de Signal Analytique.

3. T.A.C.M. Classen and W.F.G. Mecklenbrauker 1980 Philips J. Res. 35, 217-250, The Wigner Distribution - A Tool for Time-Frequency Signal Analysis Part I: Continuous Time Signals.

4. F. Hlawatsch 1984 Proc. Int. Conf. Signal Processing (Florence, Italy), 363-367, Interference terms in the Wigner distribution.

5. P. Flandrin Mar. 1984 Proc. IEEE 1984 Int. Conf. Acoust., Speech, Signal Processing (San Diego, CA), 41.B.4.1-4.4, Some Features of Time-Frequency Representation of Multicomponent Signals.

6. L.Jacobson and H. Wechsler 1983 Proc. IEEE ICASSP-83 (Boston, MA), 254-256, The Composite Pseudo Wigner Distribution (CPWD): A Computable and Verstaile approximation to the Wigner distribution (WD).

7. W. Rihaczek 1986 IEEE Trans. Informat. Theory IT-14, 369-374, Signal Energy Distribution in Time and Frequency.

8. C.H. Page 1952 J. Appl. Phys. 23, 103-106, Instantaneous Power Spectra.

9. T.A.C.M. Classen and W.F.G. Mecklenbrauker 1980 Philips J. Res. 35, 276-300, The Wigner Distribution - A Tool for Time-Frequency Signal Analysis Part II: Discrete Time Signals.

10. L. Cohen 1989 Proc. IEEE 77(7), 941-981, Time-Frequency Distribution - A Review.

11. H.I. Choi and W.J. Williams 1989 IEEE Trans. Acoust., Speech, Signal Processing 37(6), 862-871, Improved Time-Frequency Representation of Multicomponent Signals Using Exponential Kernels.

12. J. Jeong and W. Williams IEEE Trans. Sig. Proc. 40, 402-412, Kernel Design for Reduced Interference Distributions.

13. E.J. Diethorn 1994 IEEE Trans. Signal Processing 42(5), The Generalized Exponential Time-Frequency Distribution.

14. L. Cohen 1966 J. Math. Phys. 7, 781-786, Generalized Phase-Space Distribution Functions.

15. Y. Zhao, L.E. Atlas and R.J. Marks 1990 IEEE Trans. Acoust., Speech, Signal Process. 38(7), 1084-1091, The Use of Cone Shaped Kernels for Generalized Time-Frequency Representations of Non stationary Signals.

16. P. Loughlin, E.L. Atlas and J. Pitton 1993 Advanced Time-Frequency Representations for Speech Processing, Visual Representations of Speech Signals, M. Cooke, S. Beete and M. Crawford (eds.), John Wiley & Sons.

17. B. Zhang and S. Sato 1994 IEEE Trans. Signal Processing 42(1), A Time-Frequency Distribution of Cohen's Class With a Compound Kernel and Its Application to Speech Signal Processing.

18. G. Zhonyu, L. Daurand and C.L. Howard 1994 IEEE Transactions on Signal Processing 42(7), 1700-1706, The Time-Frequency Distributions of Non stationary Signals Based on a Bessel Kernel.

19. R.G. Baraniuk and D.L. Jones 1993 IEEE Trans. Signal Processing 41(4), 1589-1602, A Signal-dependent Time-Frequency Representation: Optimal Kernel Design.

20. B. Bouachache 1978 Représentation Temps-Fréquence, Soc. Nat. ELF Aquitaine,

Pau, France, Publ. Recherches, No. 373-378.

21. E. Bazelaire and J.R. Viallix 1987 Proc. 49th Eur. Ass. Explor. Geophys. Mtg. (Belgrade, Yugoslavia), 1-2, Theory of Seismic Noise.

22. B.D. Forrester 1989 Proc. ASSPA89, 78-82, Use of the Wigner-Ville Distribution in Helicopter Fault Detection.

23. Meng Qingfeng and Qu Liangsheng 1991 Mechanical Systems and Signal Processing 5(3), 155-166, Rotating Machinery Fault Diagnosis Using Wigner Distribution.

24. P.D. Mcfadden and W. Wang 1990 Report No. : OUEL-1859/90; ETN-91-98957, Department of Engineering Science, Oxford University, Time-Frequency Domain Analysis of Vibration Signals for Machinery Diagnostics. 1: Introduction to the Wigner-Ville Distribution.

25. P.D. Mcfadden and W. Wang 1991 Report No. : OUEL-1891/91; ETN-92-91087, Department of Engineering Science, Oxford University, Time-Frequency Domain Analysis of Vibration Signals for Machinery Diagnostics. 2: The Weighted Wigner-Ville Distribution.

26. P.D. Mcfadden and W. Wang 1992 Report No. : OUEL-1911/92; ETN-92-92063, Department of Engineering Science, Oxford University, Time-Frequency Domain Analysis of Vibration Signals for Machinery Diagnostics. 3: The Present Power Spectral Density.

27. P.D. Mcfadden and W. Wang 1992 Report No. : OUEL-1953/92; ETN-94-95148, Department of Engineering Science, Oxford University, Time-Frequency Domain Analysis of Vibration Signals for Machinery Diagnostics. 4: Interpretation Using Image Processing Techniques.

28. R. Rohrbaugh 1993 Soc. Proceedings of the 27th Asilomar Conference on Signal, Systems & Computer 2, 1455-1458, Application of Time-Frequency Analysis to Machinery Condition Assessment.

29. P. Rao, T. Fred and G. Harrison 1990 Sound and Vibration 24(5), 22-25, Real-Time Monitoring of Vibration Using the Wigner Distribution.

30. H. Oehlmann, D. Brie, V. Begotto and M. Tomczak 1995 2nd International Symposium Acoustical and Vibratory Surveillance Methods and Diagnostic Techniques 1(10), 243-253, Analyse Temps-Fréquence de l'Ecaillage d'Engrenage

de Boîtes de Vitesses.

31. W.J. Williams, C.K.H. Koh and J. Ni 1995 Life Extension of Aging Machinery and Structures: Proc. Of the 49th Meet. of MFPT Soc. 49(4), Vibration Inst.: Virginia Beach, 315-326, Bearing Monitoring Using Reduced Interference Distributions.

32. R.A. Rohrbaugh and L. Cohen 1995 Life Extension of Aging Machinery and Structures: Proc. Of the 49th Meet. of MFPT Soc. 49(4), Vibration Inst.: Virginia Beach, 349-361, Time-Frequency Analysis of a Cam Operated Pump.

33. B. Samimy and G. Rizzoni 1996 Proceeding of the IEEE 84(9), 1330-13343, Mechanical Signature Analysis Using Time-Frequency Signal Processing: Application to Internal Combustion Engine Knock Detection.

34. K. Zheng and D.J. Whitehouse 1992 Proceedings of the Mechanical Engineers. Part C, Journal of Mechanical Engineering Science 206(C4), 249-264, The Application of the Wigner Distribution Function to Machine Tool Monitoring.

35. P. Loughlin, L. Atlas, G. Bernard and J. Pitton 1995 Life Extension of Aging Machinery and Structures: Proc. Of the 49th Meet. of MFPT Soc., 49(4), Vibration

Inst.: Virginia Beach, 305-314, Application of Time-Frequency Analysis to the Monitoring of Machining.

36. R. Bigret, P. De Sloovere, G. Hays and M. Lassoued 1995 2nd International Symposium Acoustical and Vibratory Surveillance Methods and Diagnostic Techniques 1(10), 315-326, Application Industrielles de la Transformée de Wigner-Ville.

37. L. Atlas, G. Bernard and S.B. Narayanan 1996 Proceedings of the IEEE 84(9), 1319-1329, Applications of Time-Frequency Analysis to Signal From Manufacturing and Machine Monitoring Sensors.

38. B. Boashash 1992 Time-Frequency Signal Analysis, John Wiley & Sons.

39. J.E. Berry 1991 Sound and Vibration 25(11), 24-35, How to Track Rolling Element Bearing Health with Vibration Signature Analysis.

2.7 Nomenclature

$s(t)$	Magnitude of the vibration signal with zero mean
$S(\omega)$	Spectrum of the signal $s(t)$
$P(t,\omega)$	The joint distribution function of time and frequency
$\Omega(t)$	The first order moment of the $P(t,\omega)$ with respect to frequency
$T(\omega)$	The first order moment of the $P(t,\omega)$ with respect to time
$v(t)$	Amplitude of the signal $s(t)$
$\varphi(t)$	Phase of the signal $s(t)$
$A(\omega)$	Spectral amplitude of the signal $S(\omega)$
$\psi(\omega)$	Spectral phase of the signal $S(\omega)$
$WD(t,\omega)$	Wigner distribution
$R(t,\tau)$	Instantaneous auto correlation function
$s_I(t)$	Imaginary part of the signal

$s_R(t)$ Real part of the signal

$WVD(t,\omega)$ Wigner-Ville distribution

$PWD(t,\omega)$ Pseudo-Wigner distribution

$SWD(t,\omega)$ Smoothed Wigner distribution

$e(t,\omega)$ Energy density in time and frequency

$\varphi(\theta,\tau)$ Kernel function

$CWD(t,\omega)$ Choi-Williams distribution

$RID(t,\omega)$ Reduced interference distribution

$BJC(t,\omega)$ Born-Jordan-Cohen distribution

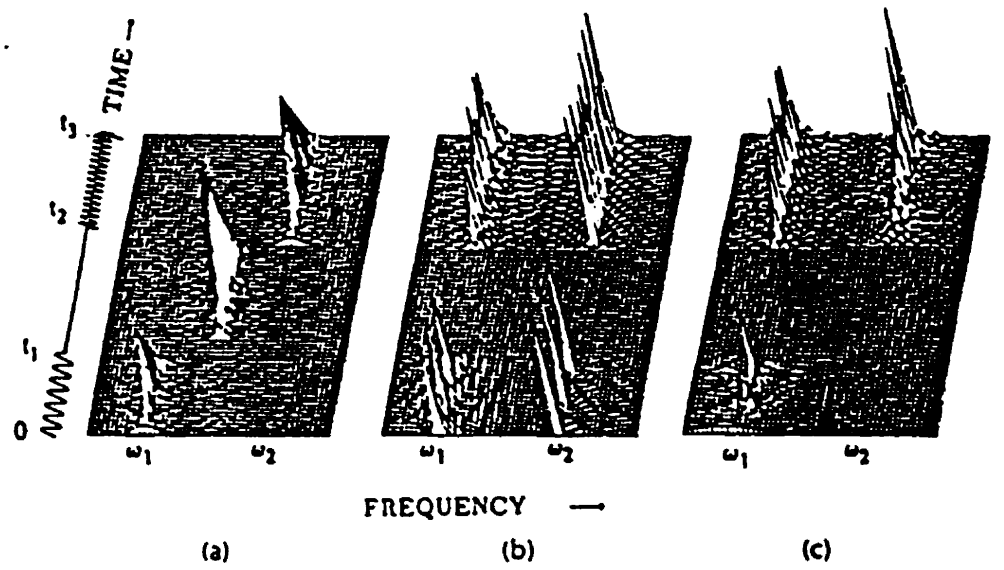

Figure 2.1: Representation of a multi components signal by (a) Wigner, (b) Rihaczek and (c) Page distribution (Cohen, 1966)

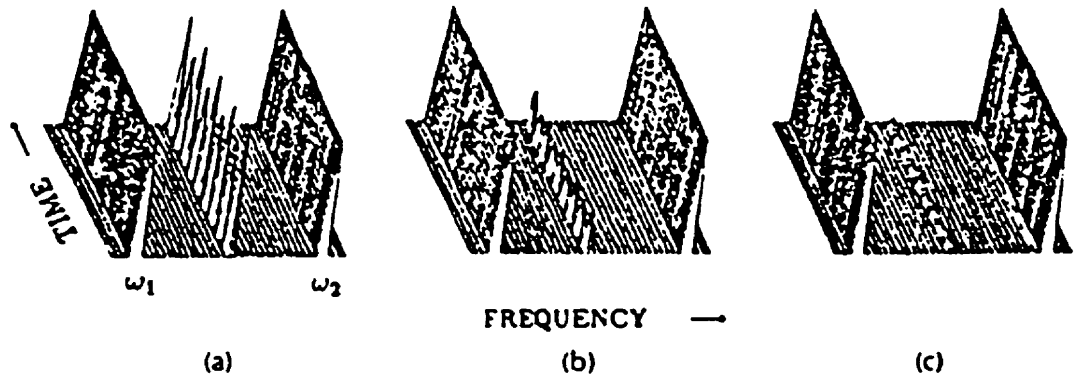

Figure 2.2: (a) Wigner and (b), (c) Choi-Williams distributions for the sum of two sine waves with (b) $\sigma = 10^6$ and (c) $\sigma = 10^5$ (Zhao, Atlas et Marks, 1990)

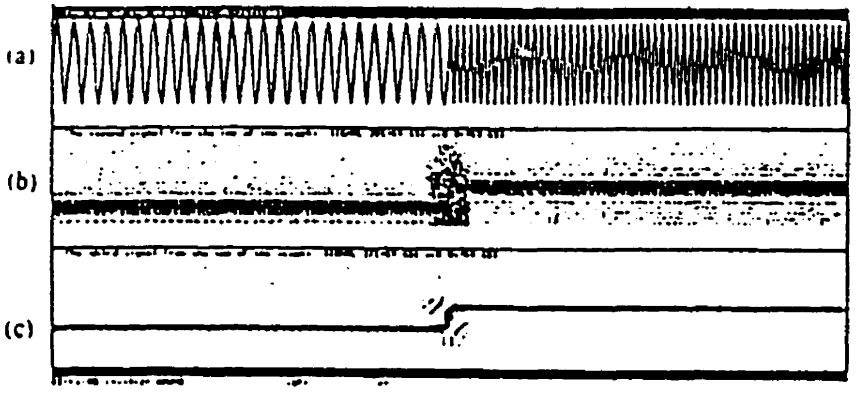

Figure 2.3: The comparison between (b) the STFT and (c) the ZAM distribution of a signal with a rapid frequency change (Loughlin, Atlas et Pitton, 1993)

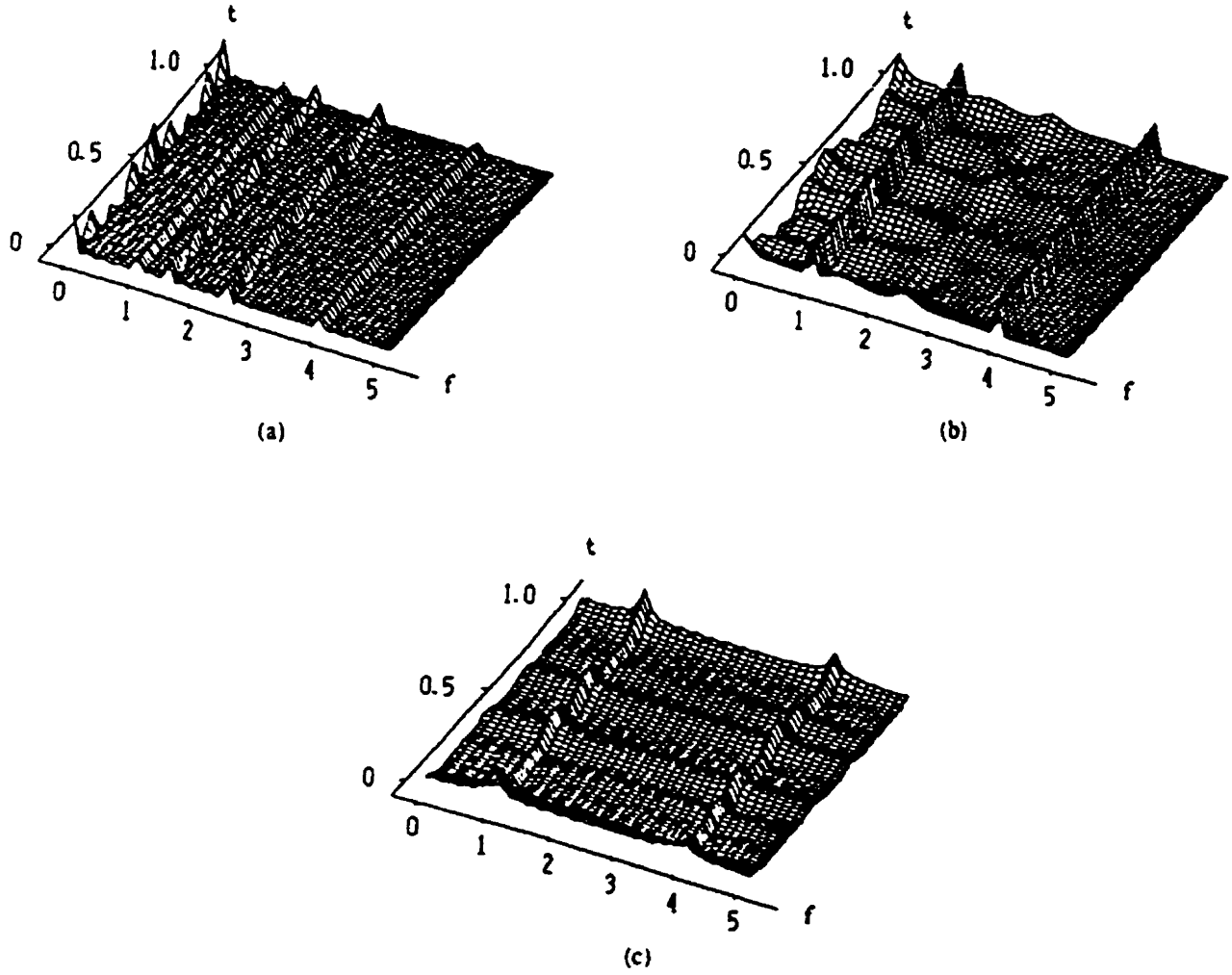

Figure 2.4: A comparison among (a) the Wigner-Ville (b) the Choi-Williams with σ =10 and (c) the Zhang-Sato with σ =10 for a sinusoidal signal with two and three components (Zhonyu, Daurand et Howard, 1994)

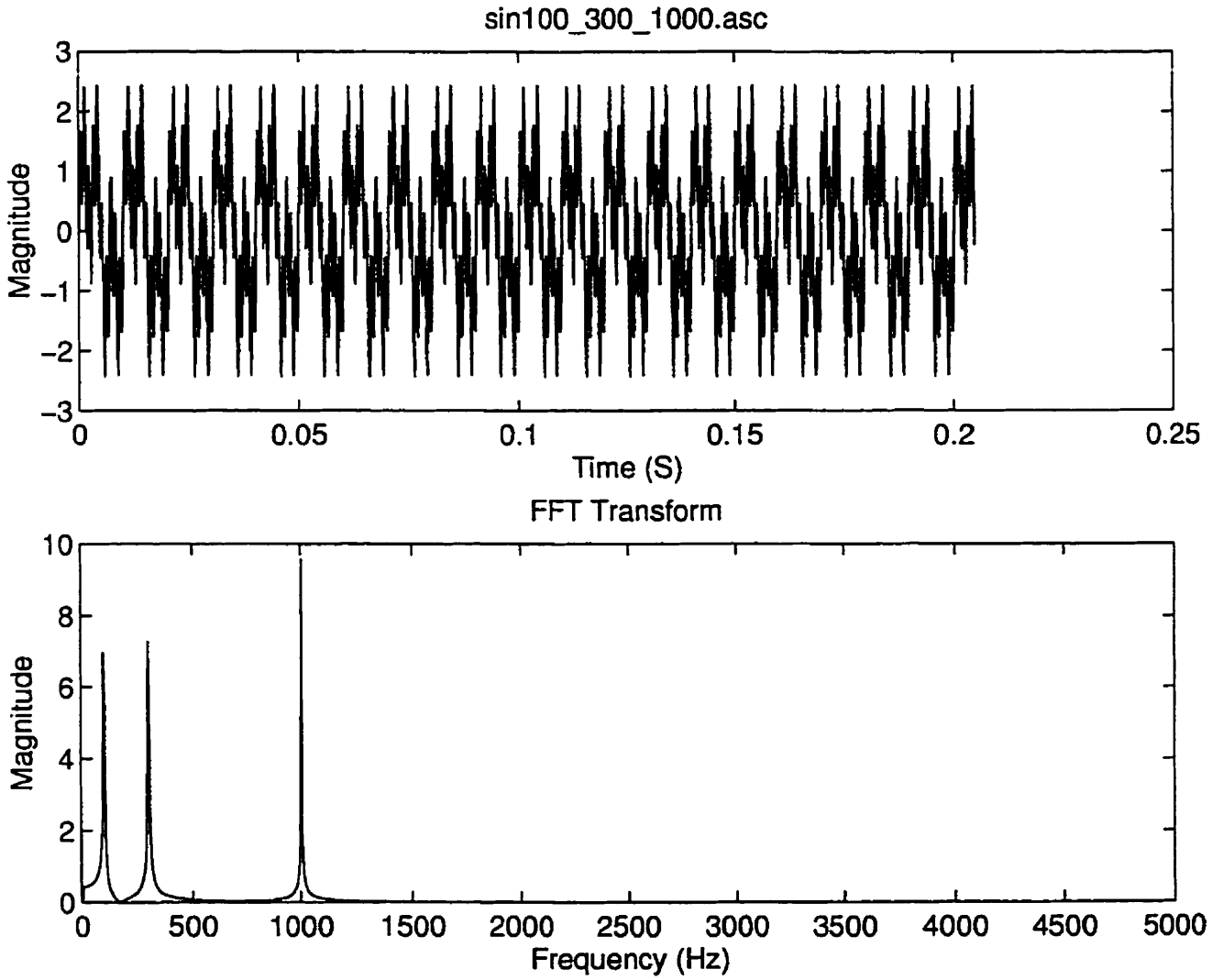

Figure 2.5: Time and spectrum representation of a sum of sines.

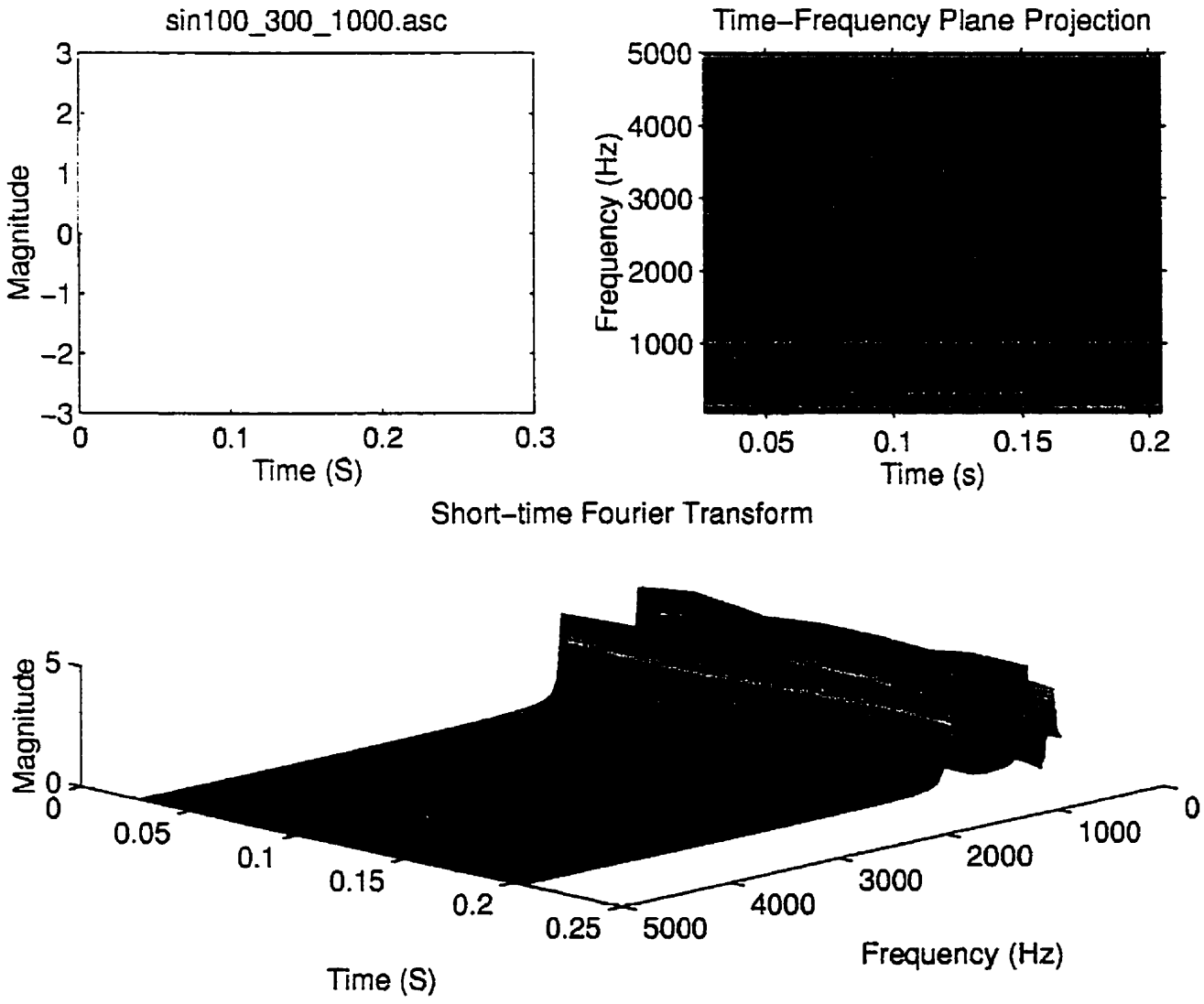

Figure 2.6: Spectrogram representation of a sum of sines.

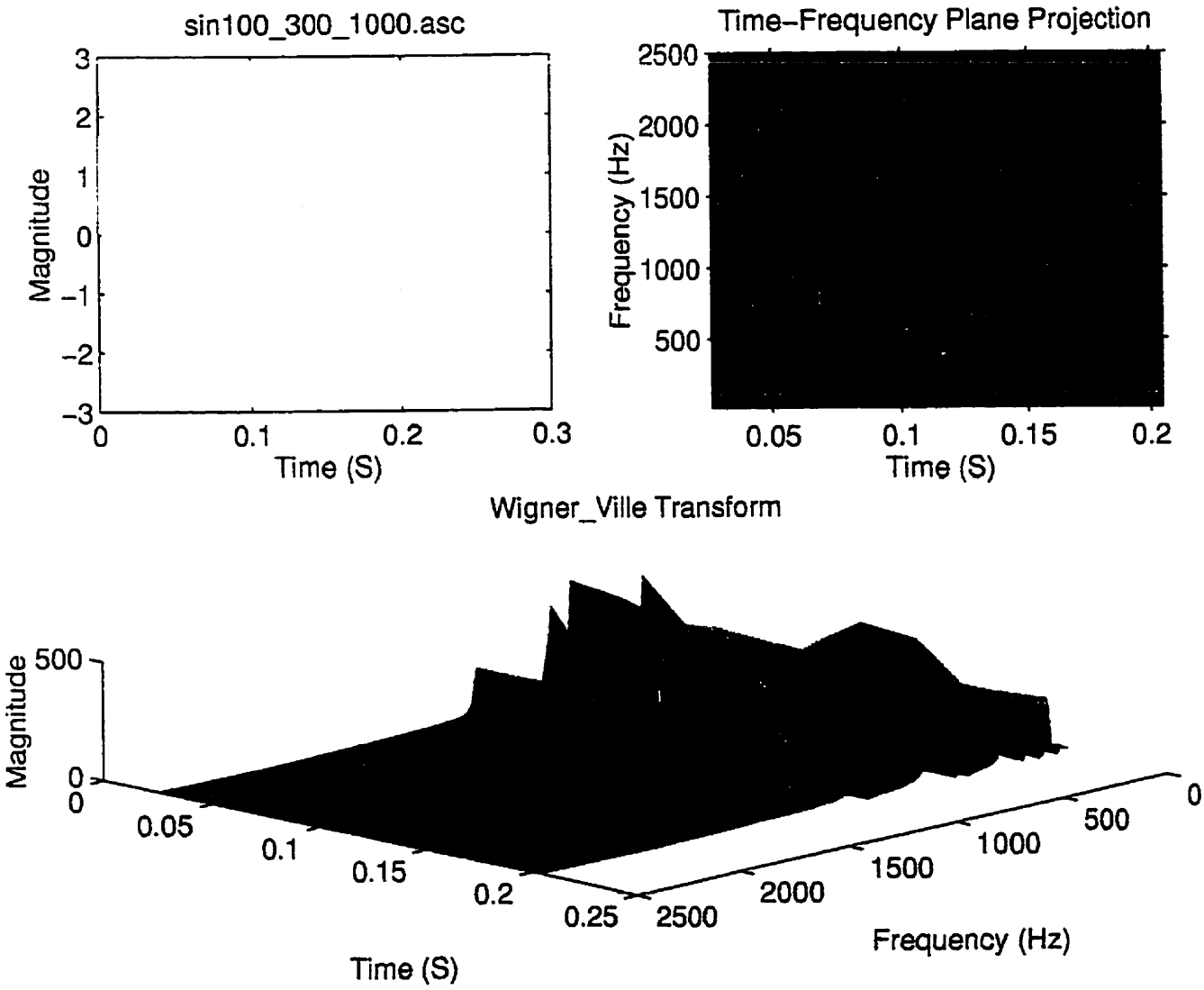

Figure 2.7: Wigner-Ville representation of a sum of sines.

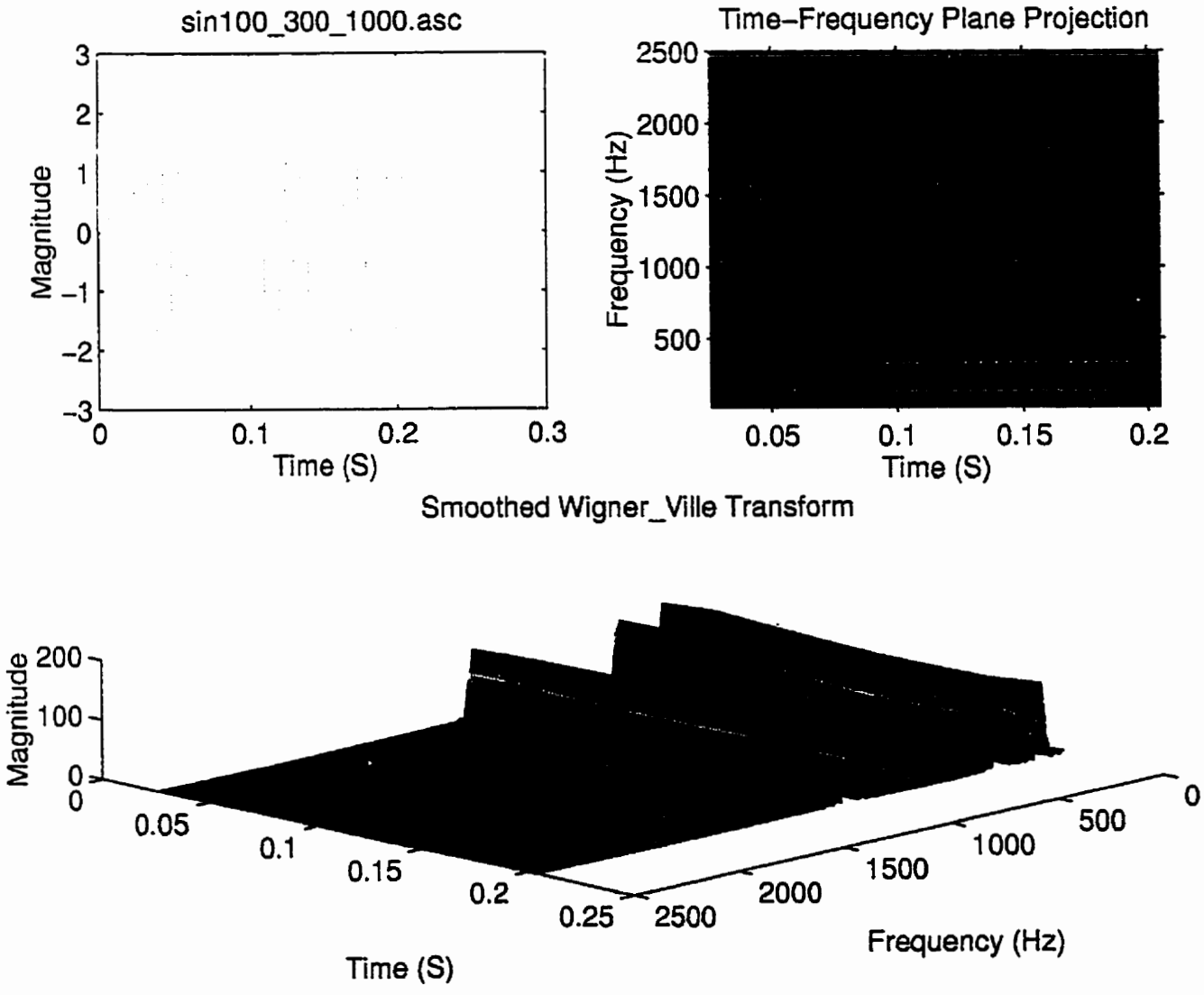

Figure 2.8: Smoothed Wigner-Ville representation of a sum of sines.

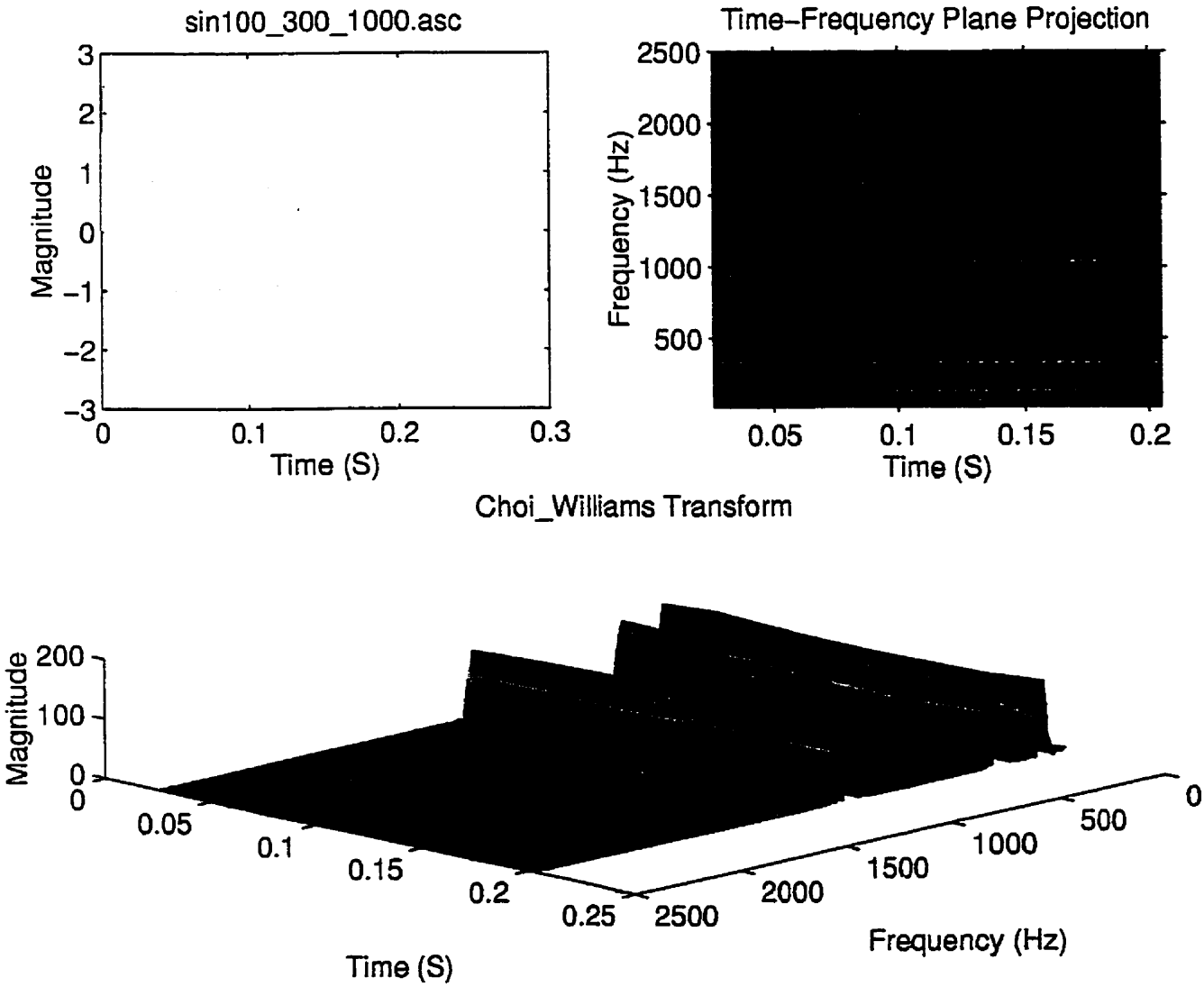

Figure 2.9: Choi-Williams representation of a sum of sines.

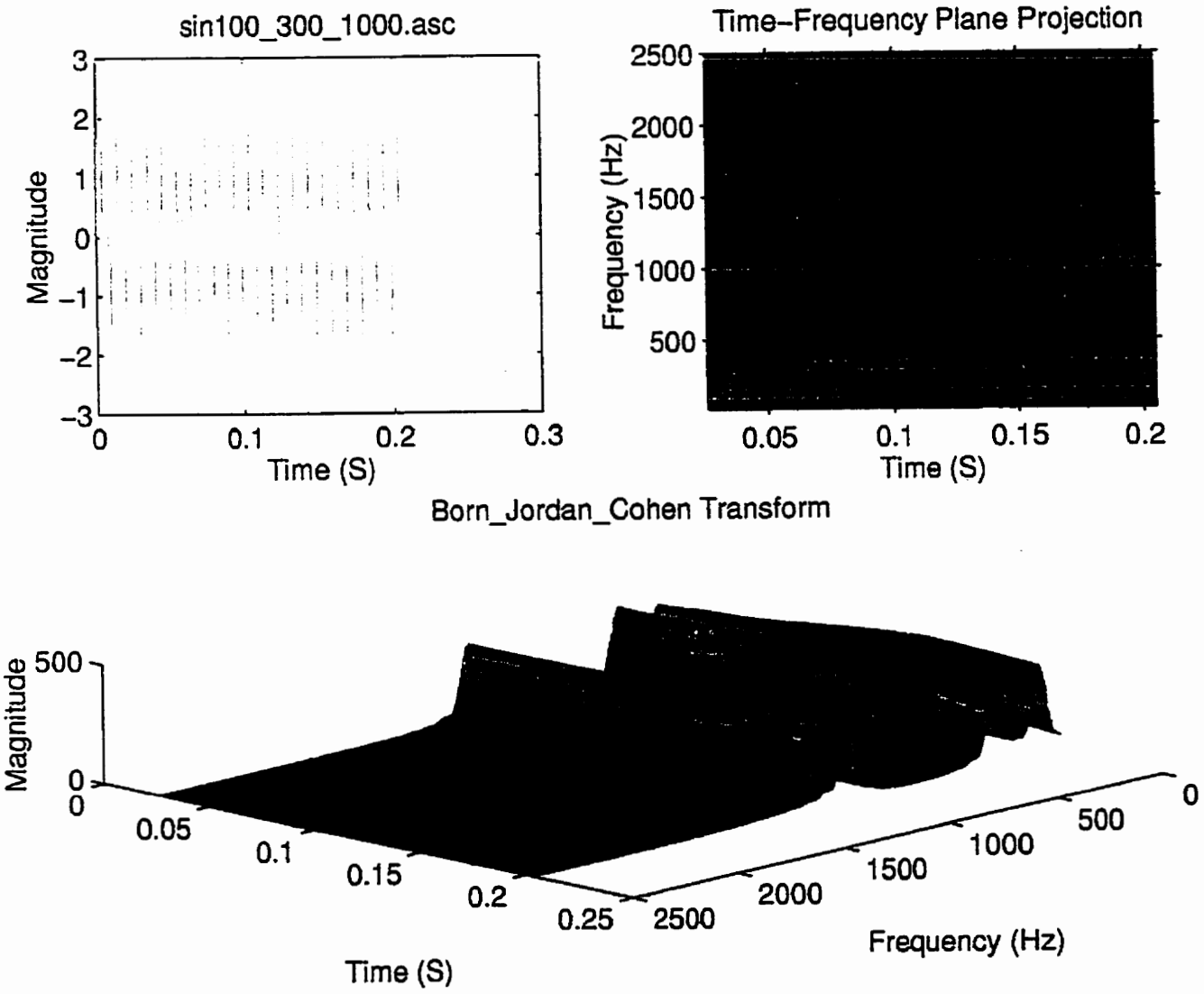

Figure 2.10: Born-Jordan-Cohen representation of a sum of sines.

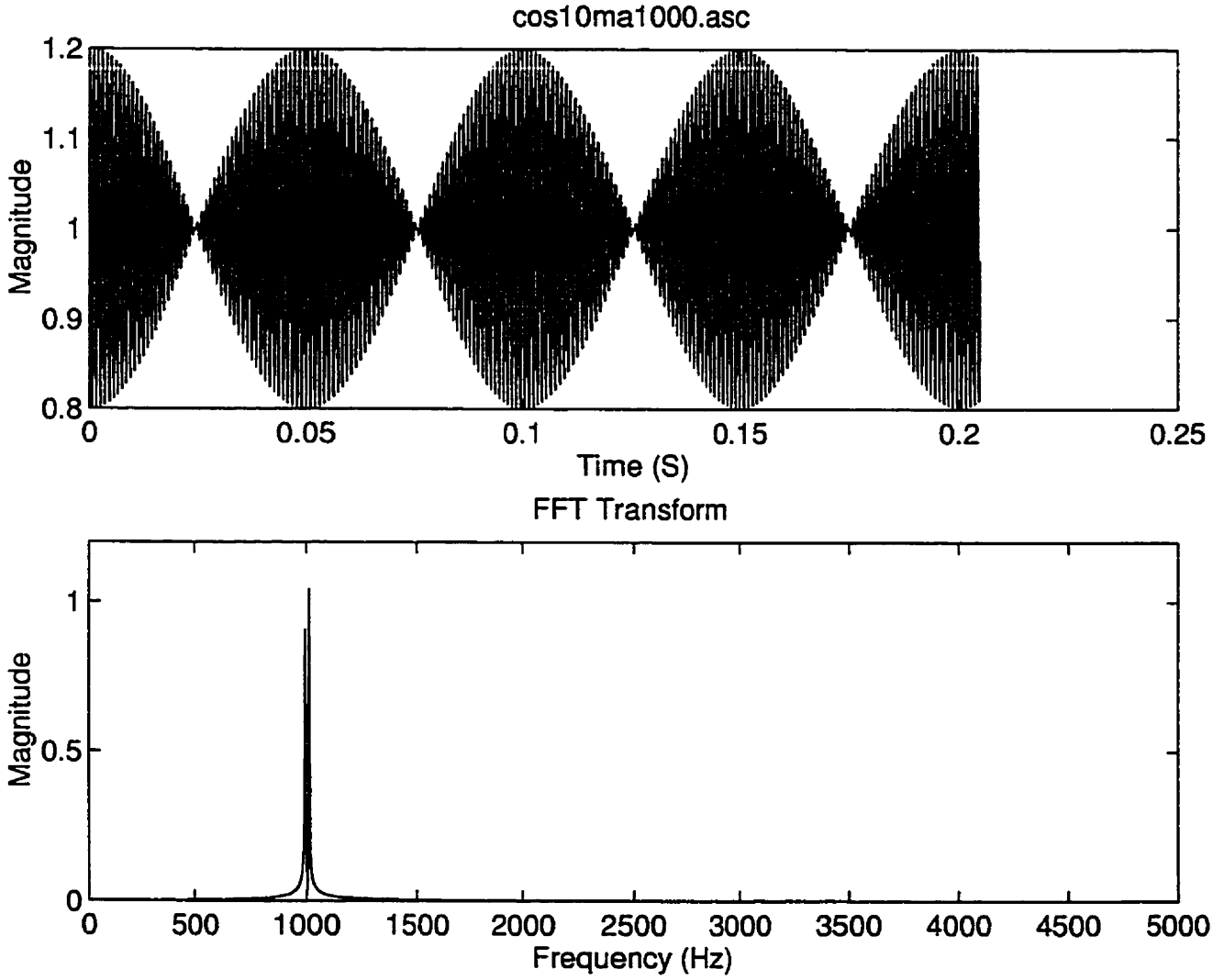

Figure 2.11: Time and spectrum representation of an amplitude-modulated wave.

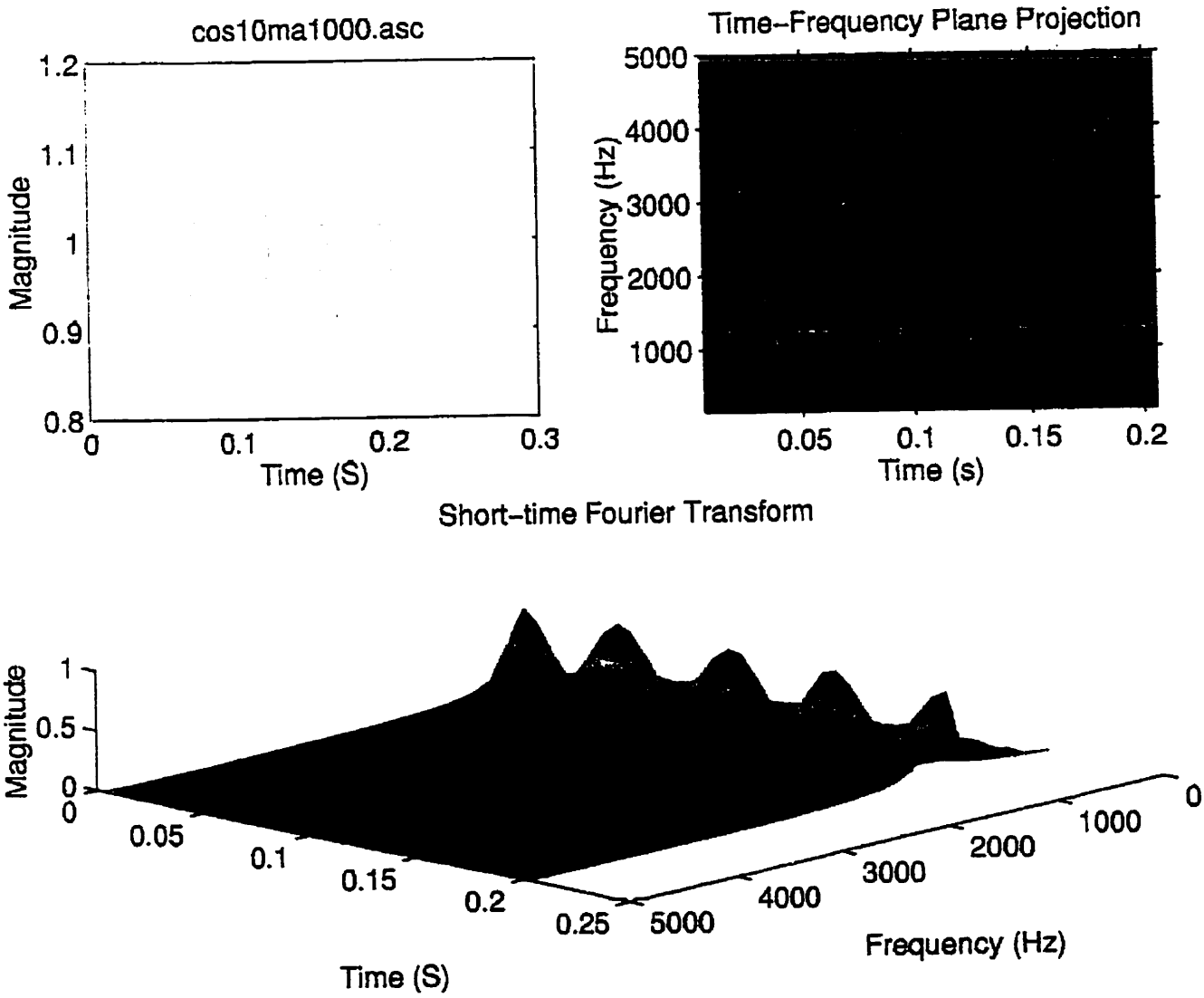

Figure 2.12: Spectrogram representation of an amplitude-modulated wave.

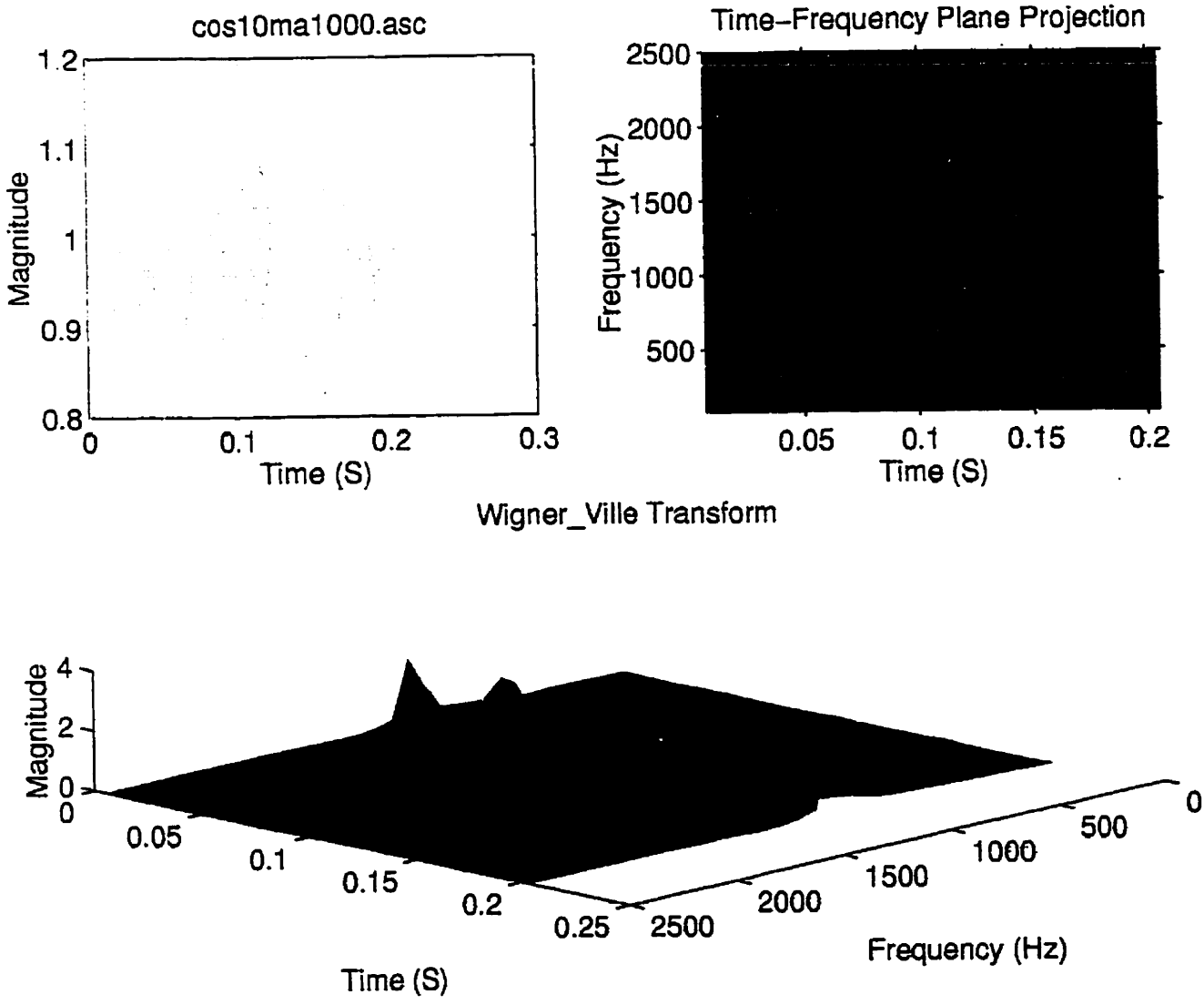

Figure 2.13: Wigner-Ville representation of an amplitude-modulated wave.

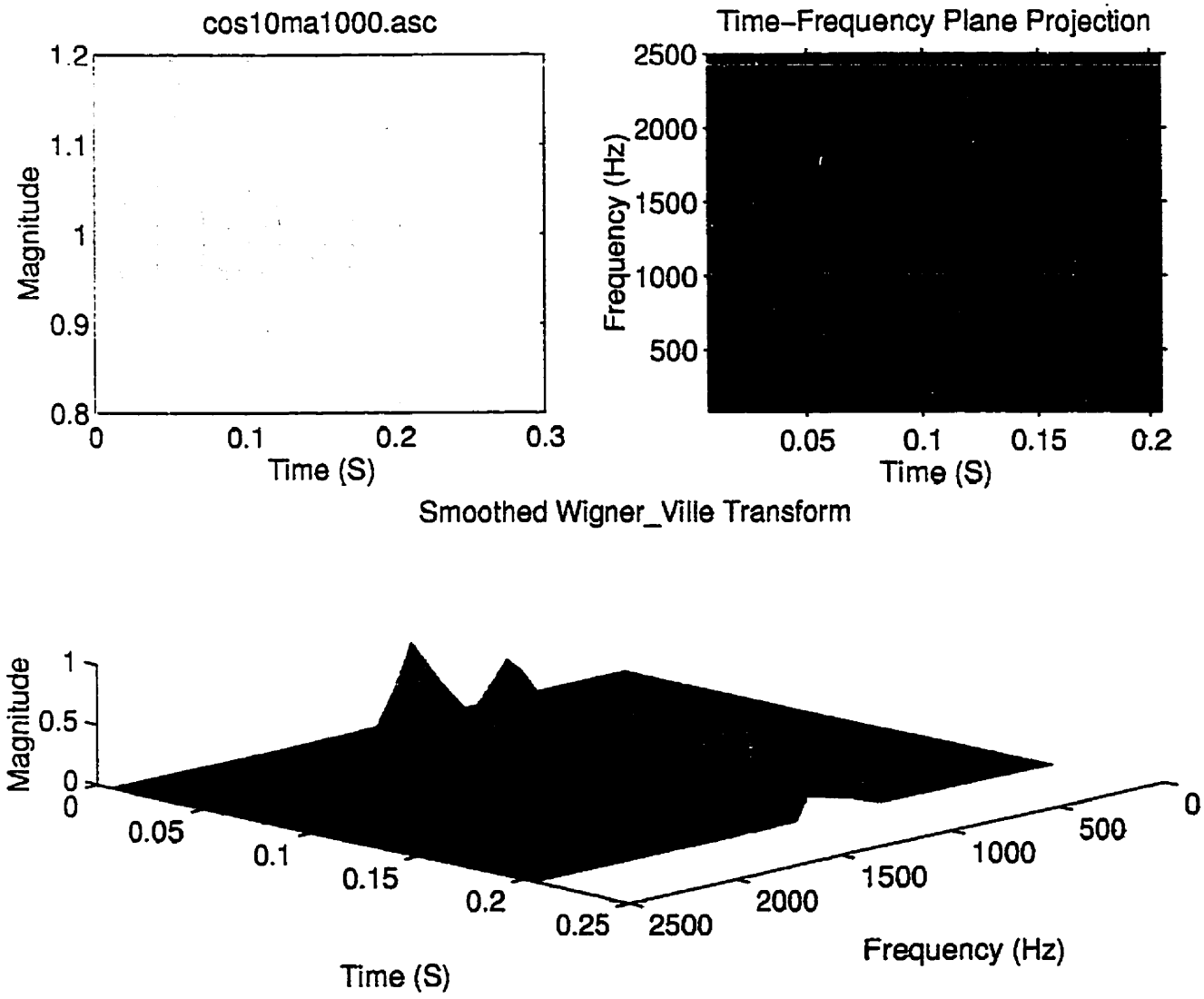

Figure 2.14: Smoothed Wigner-Ville representation of an amplitude-modulated wave.

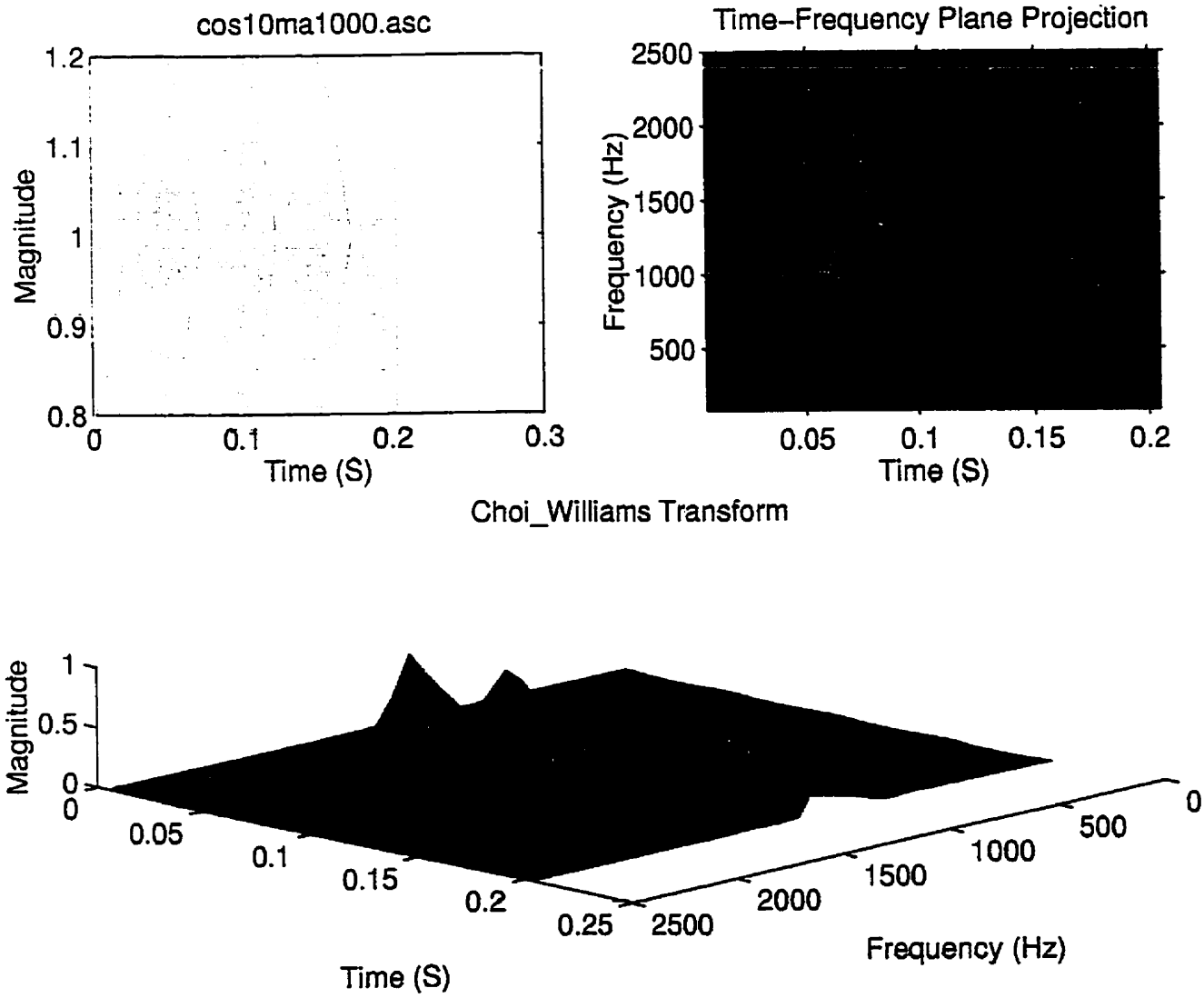

Figure 2.15: Choi-Williams representation of an amplitude-modulated wave.

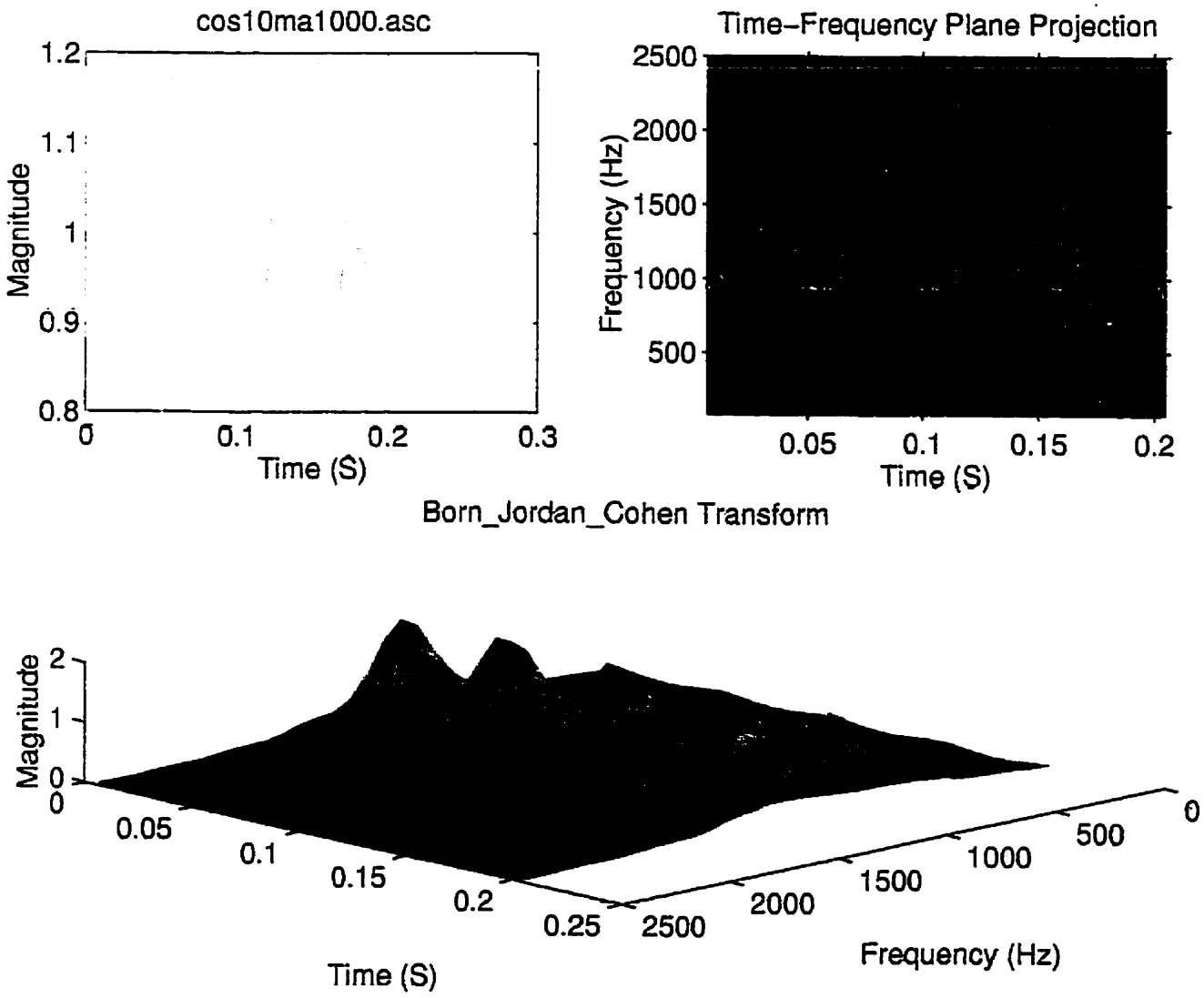

Figure 2.16: Born-Jordan-Cohen representation of an amplitude-modulated wave.

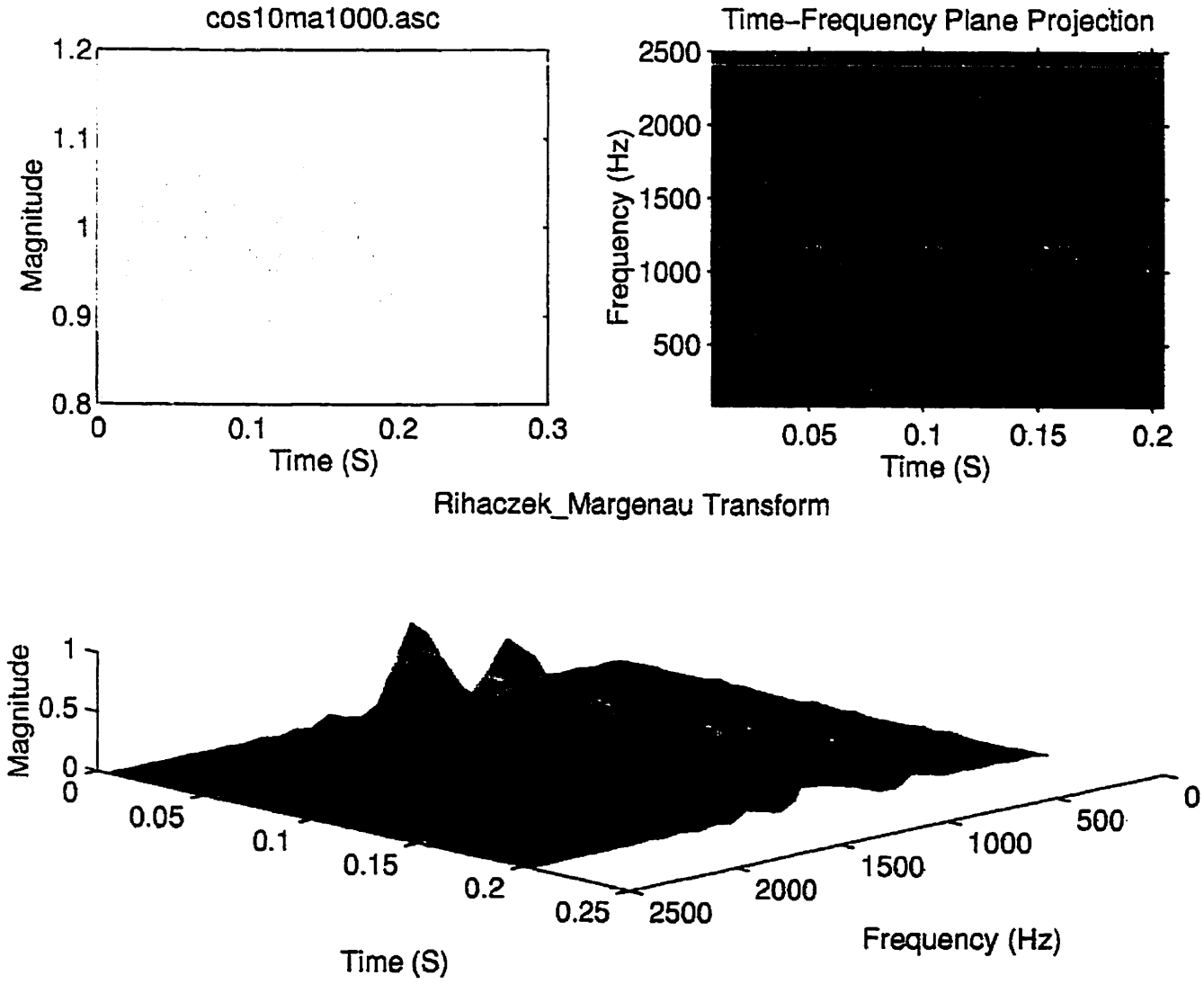

Figure 2.17: Rihacezk-Margenau representation of an amplitude-modulated wave.

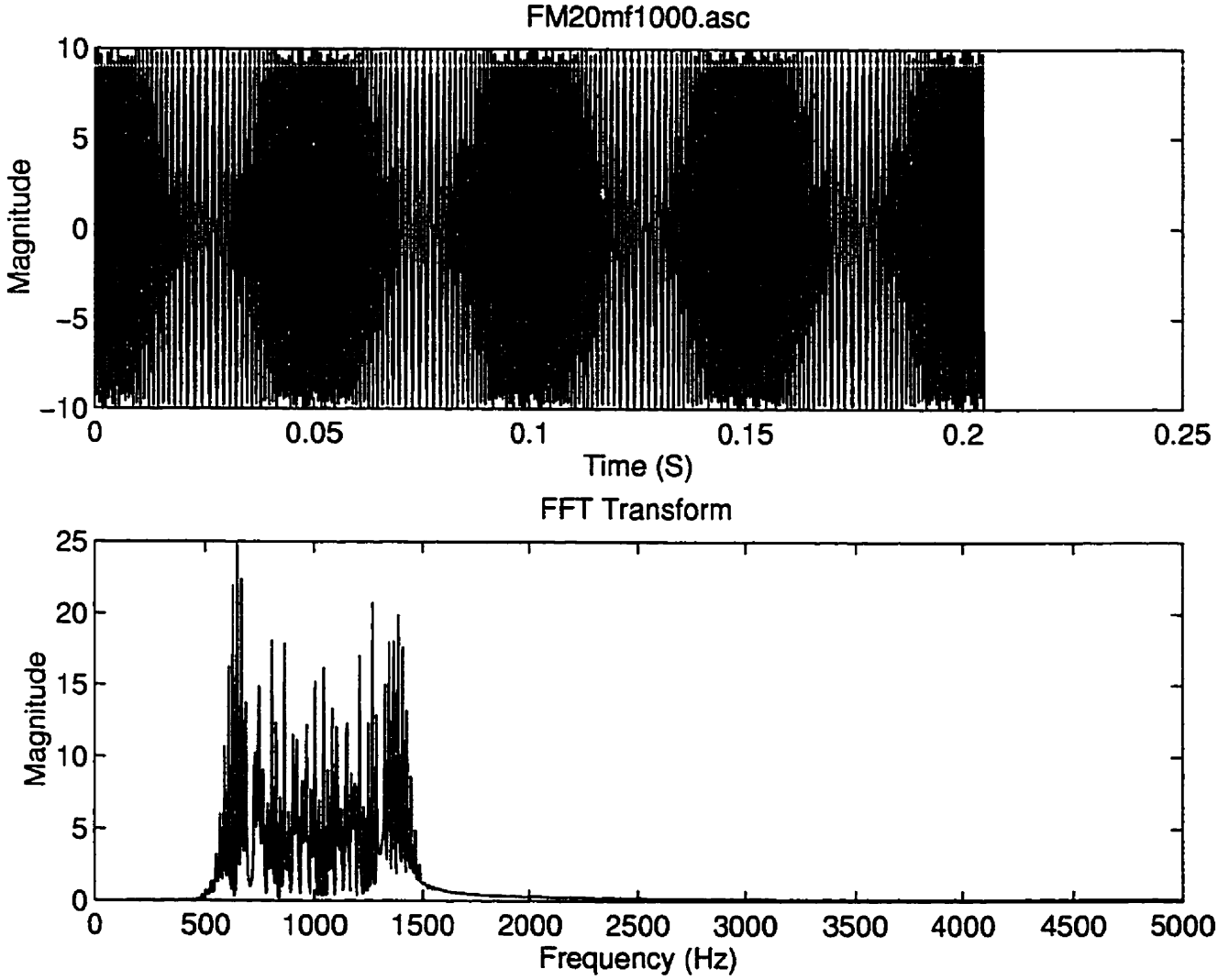

Figure 2.18: Time and spectrum representation of a frequency-modulated wave.

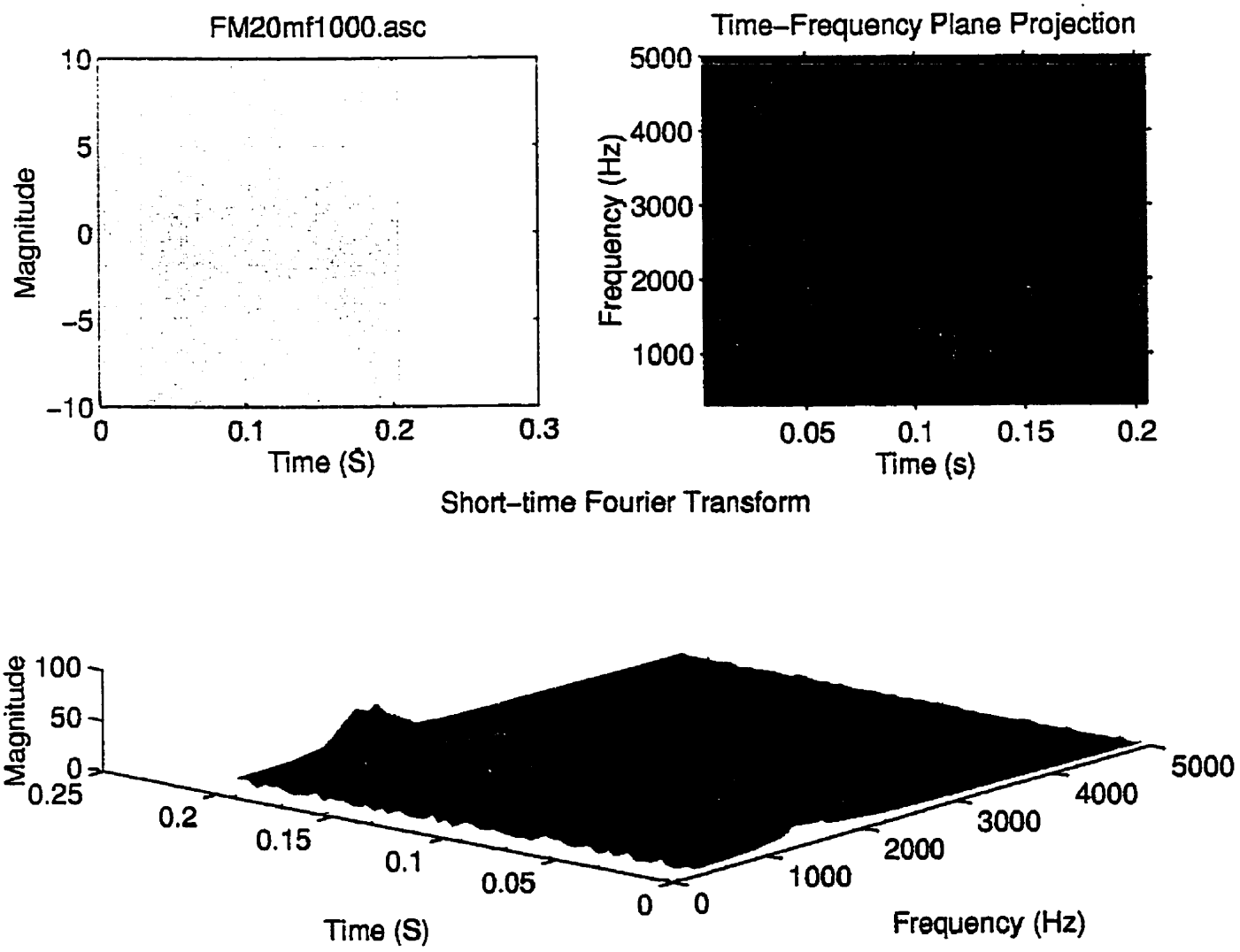

Figure 2.19: Spectrogram representation of a frequency-modulated wave.

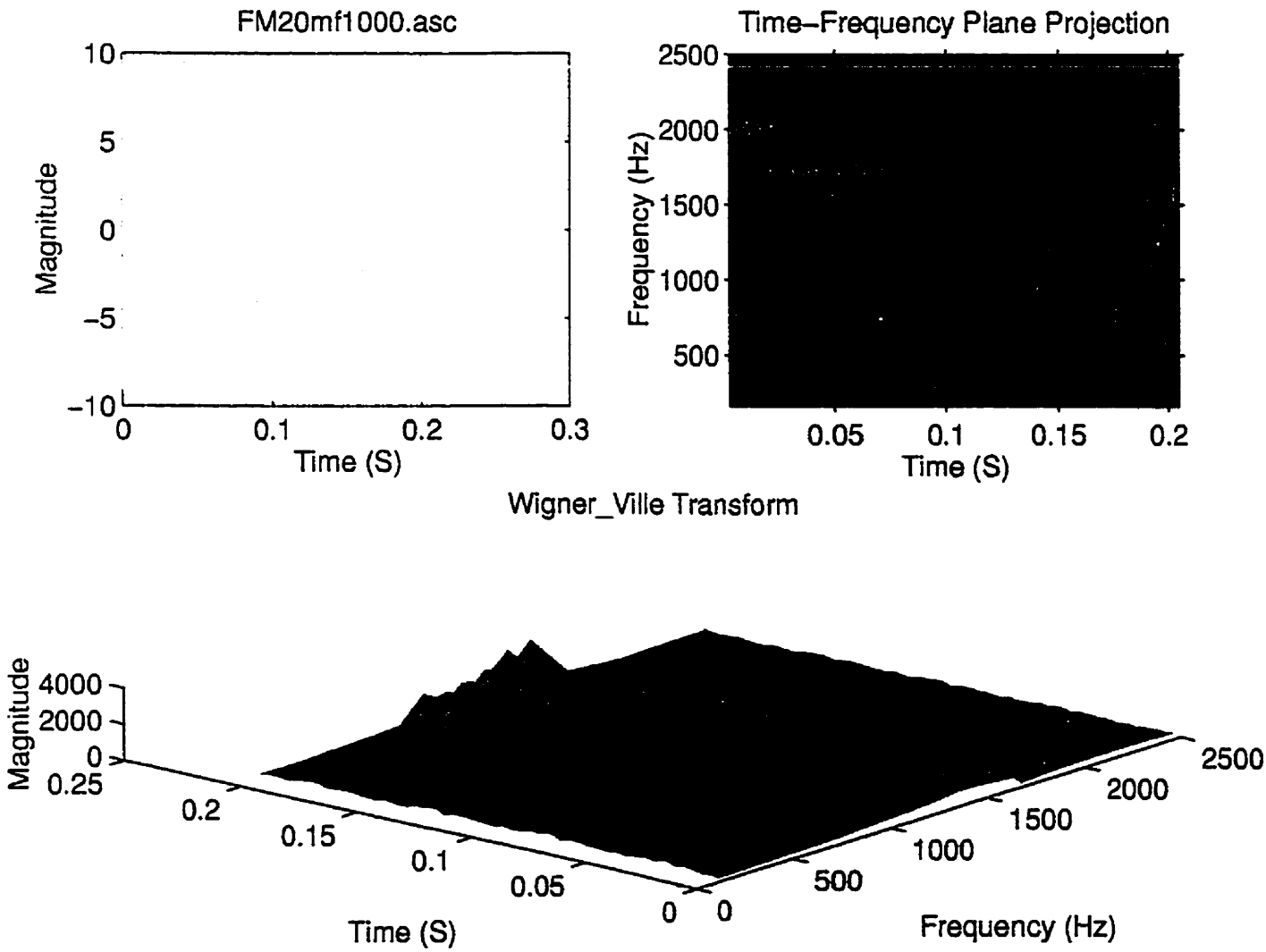

Figure 2.20: Wigner-Ville representation of a frequency-modulated wave.

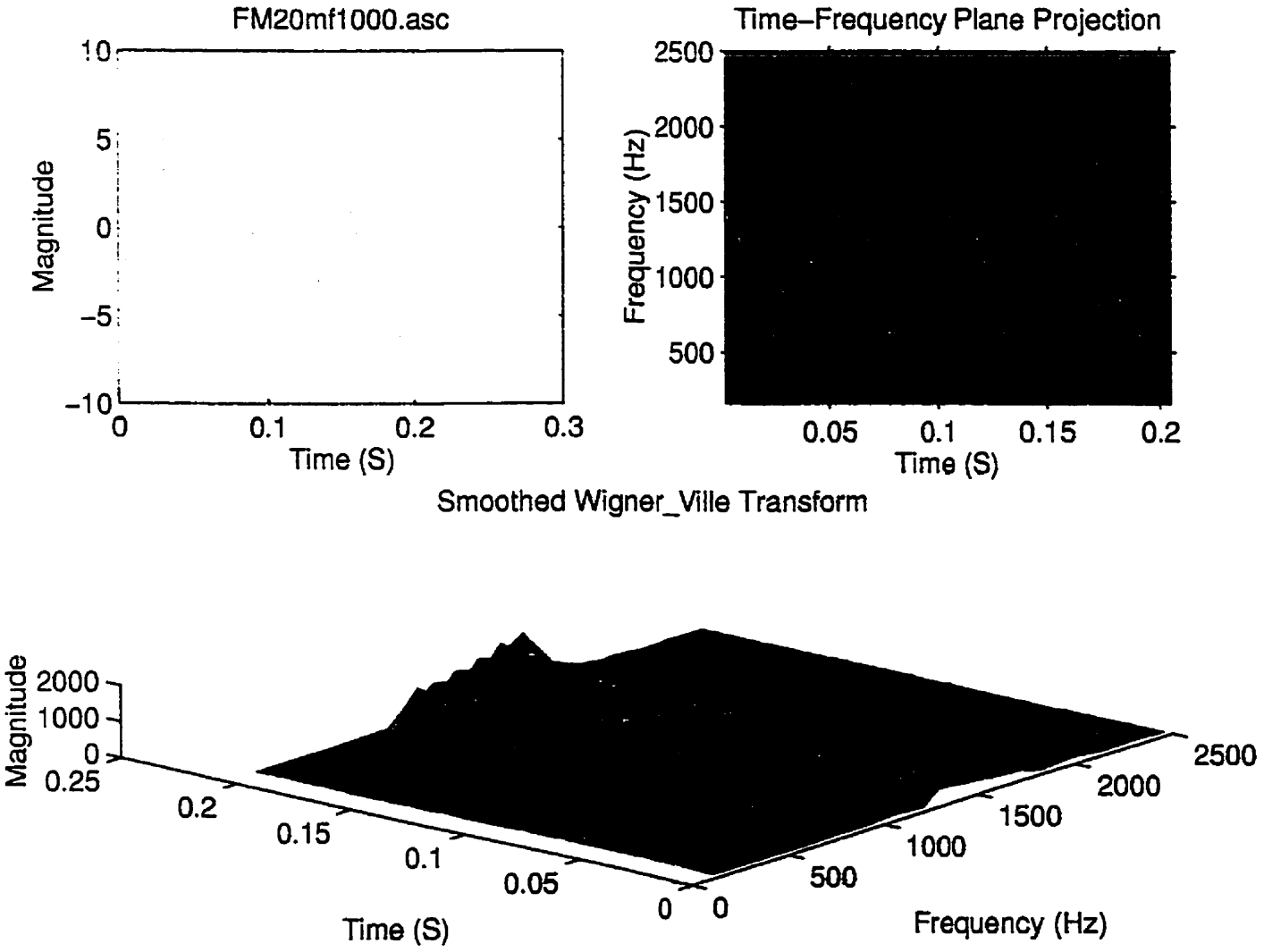

Figure 2.21: Smoothed Wigner-Ville representation of a frequency-modulated wave.

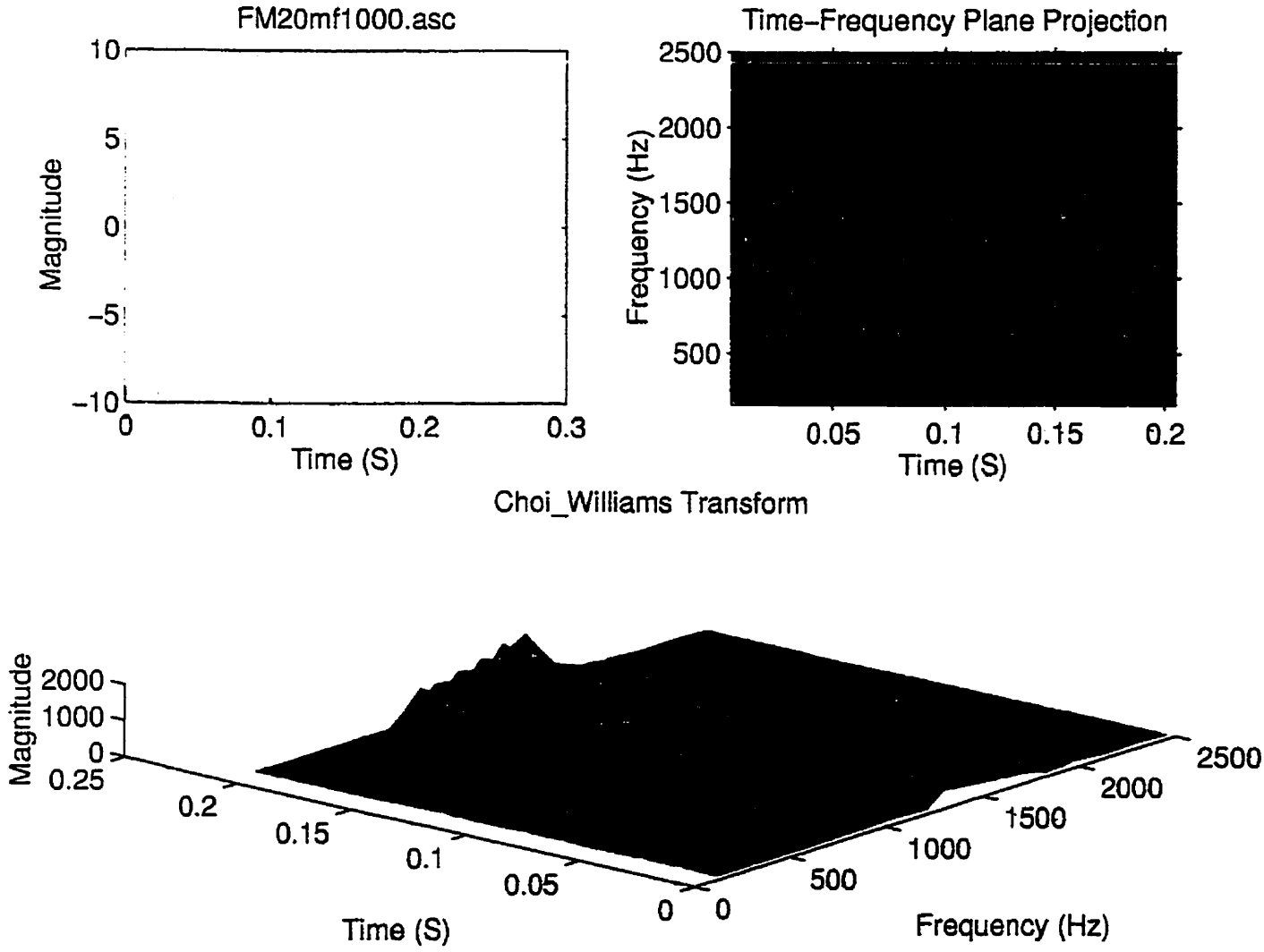

Figure 2.22: Choi-Williams representation of a frequency-modulated wave.

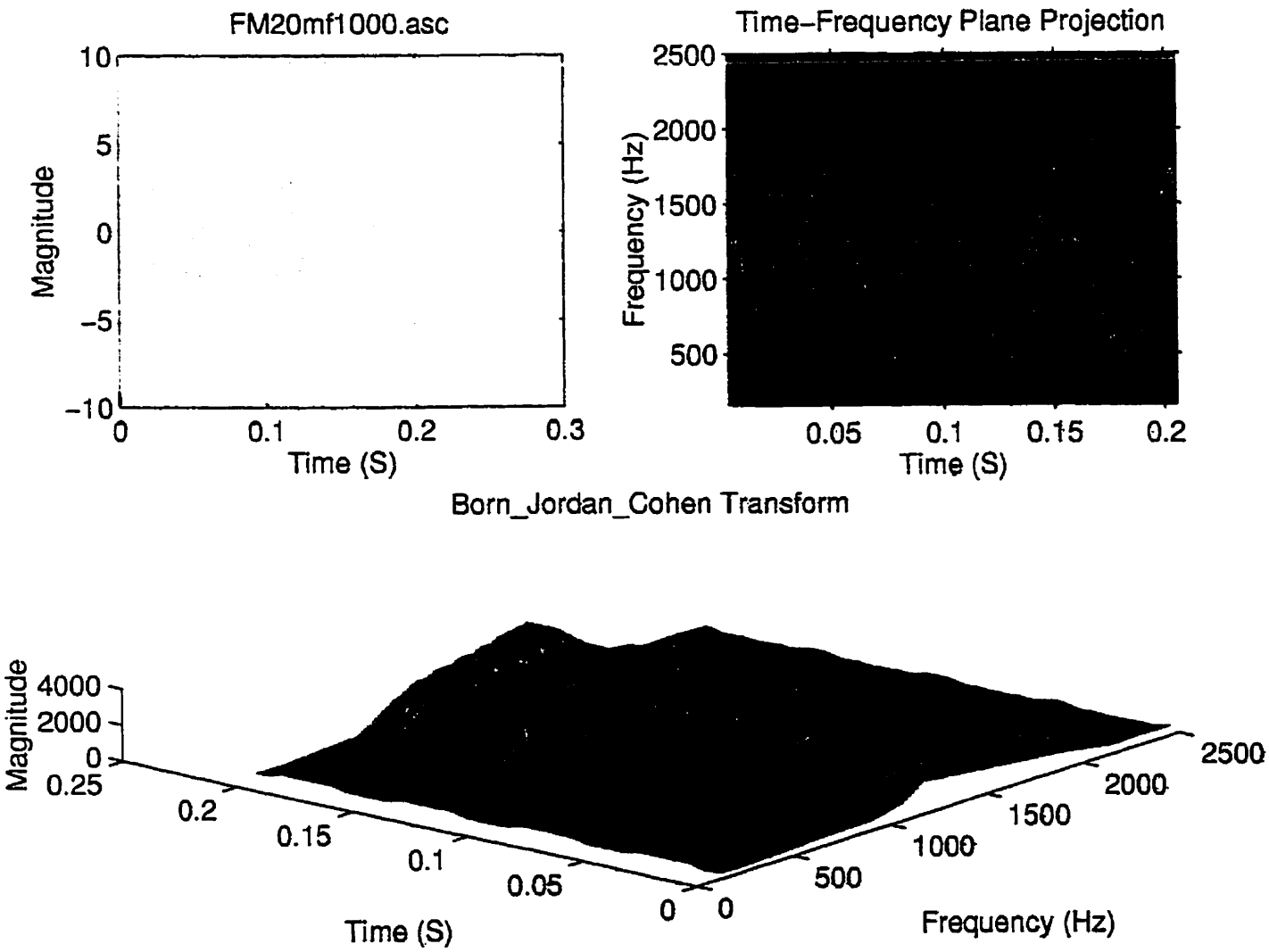

Figure 2.23: Born-Jordan-Cohen representation of a frequency-modulated wave.

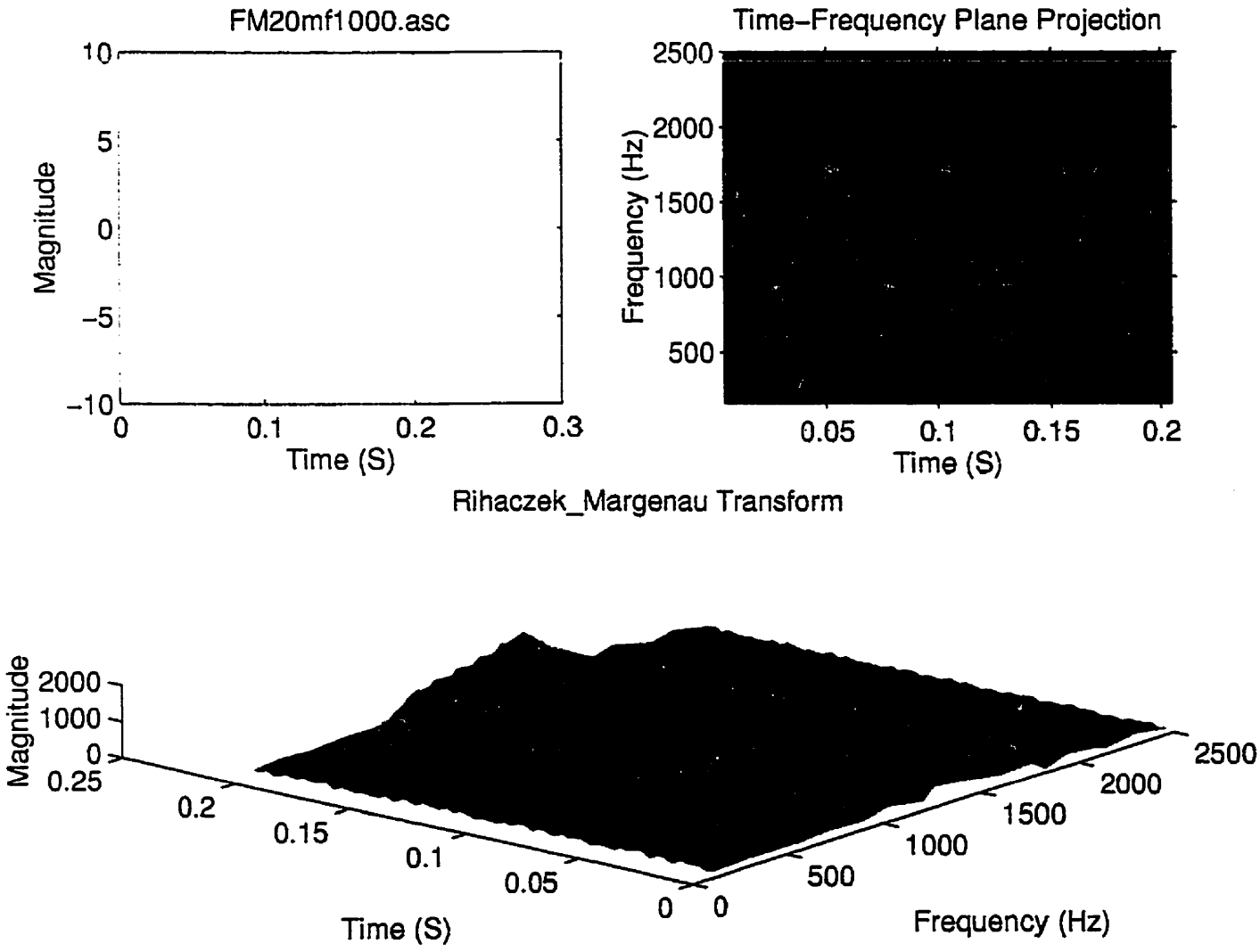

Figure 2.24: Rihacezk-Margenau representation of a frequency-modulated wave.

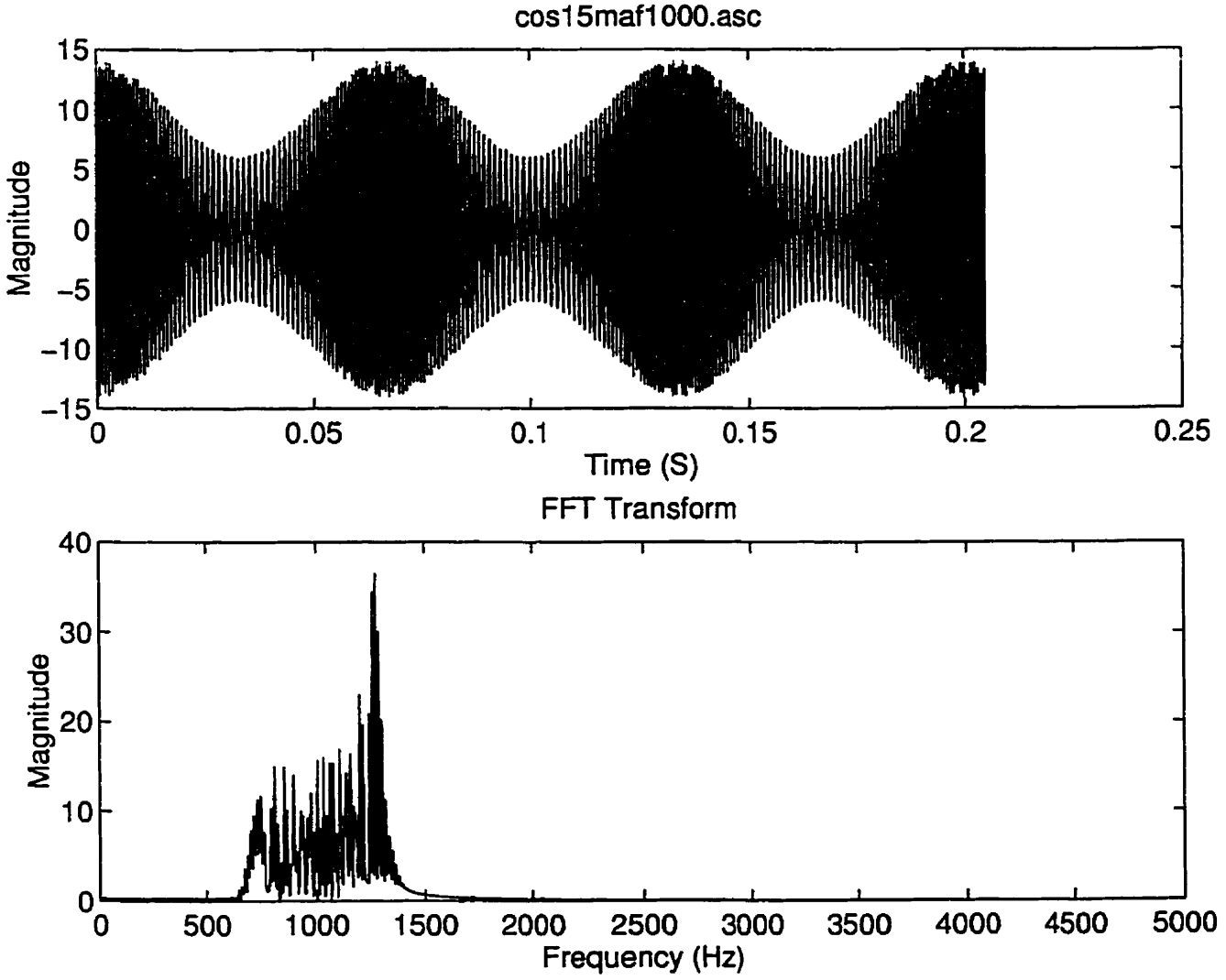

Figure 2.25: Time and spectrum representation of a frequency and amplitude modulated wave.

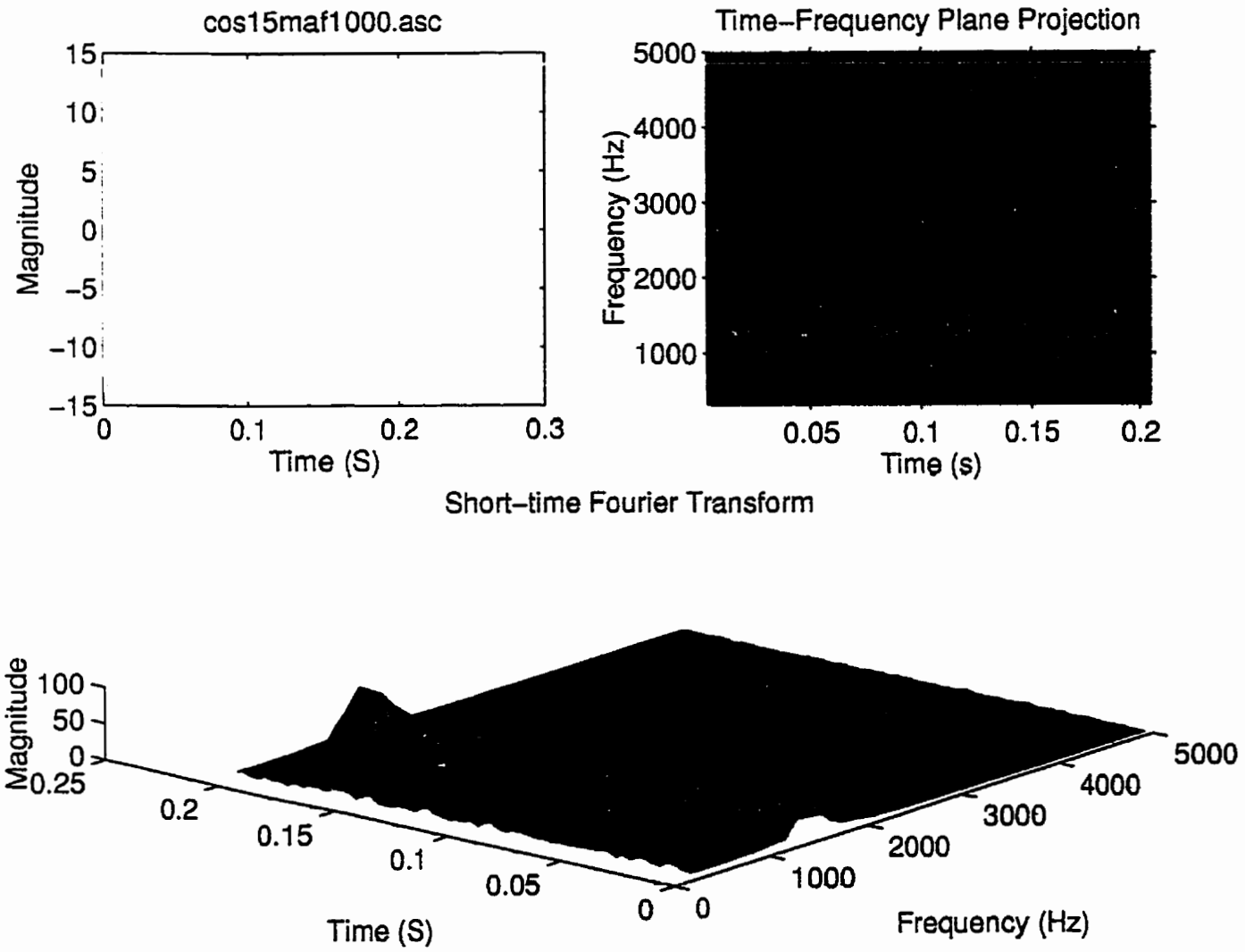

Figure 2.26: Spectrogram representation of a frequency and amplitude modulated wave.

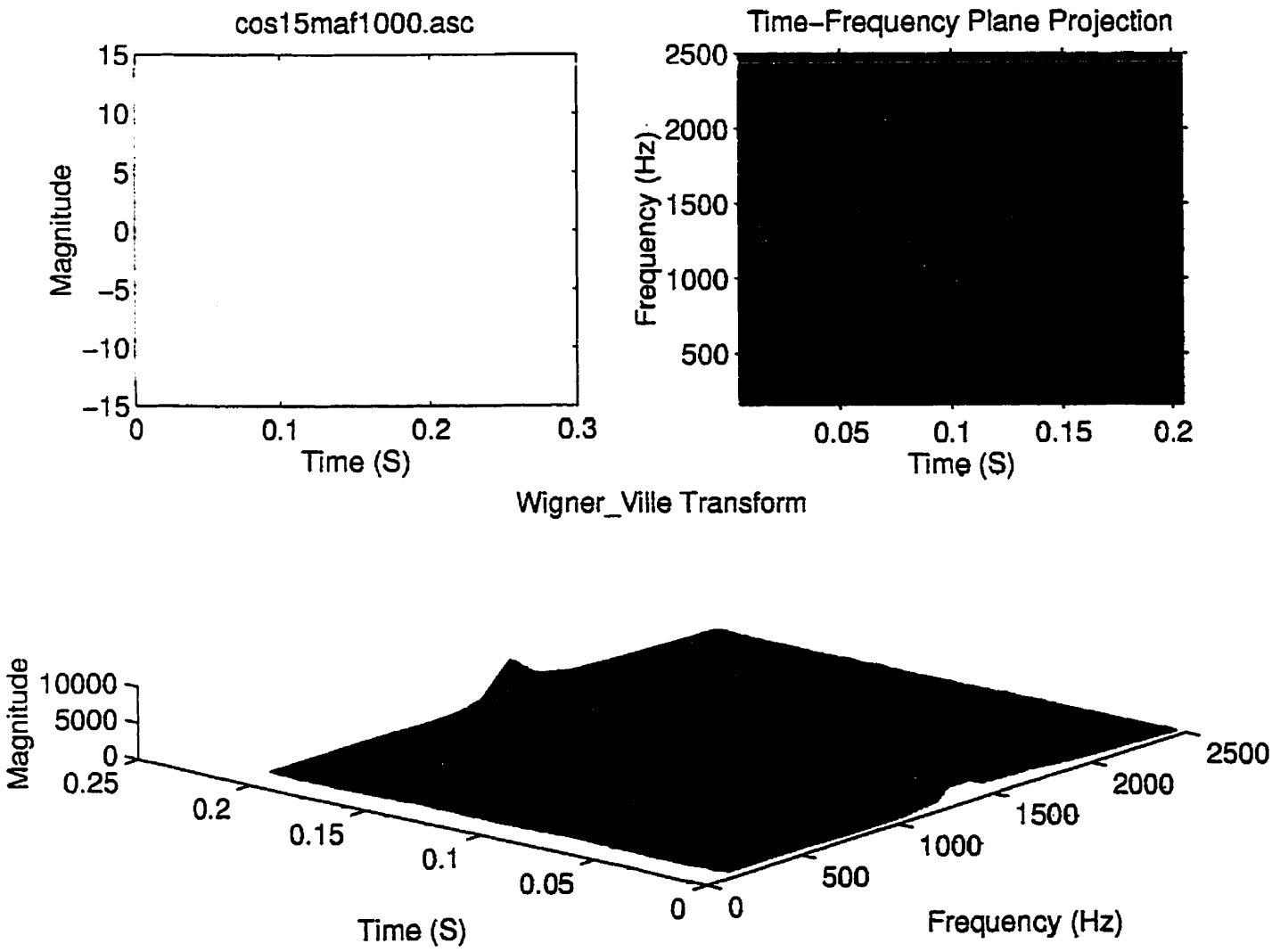

Figure 2.27: Wigner-Ville representation of a frequency and amplitude modulated wave.

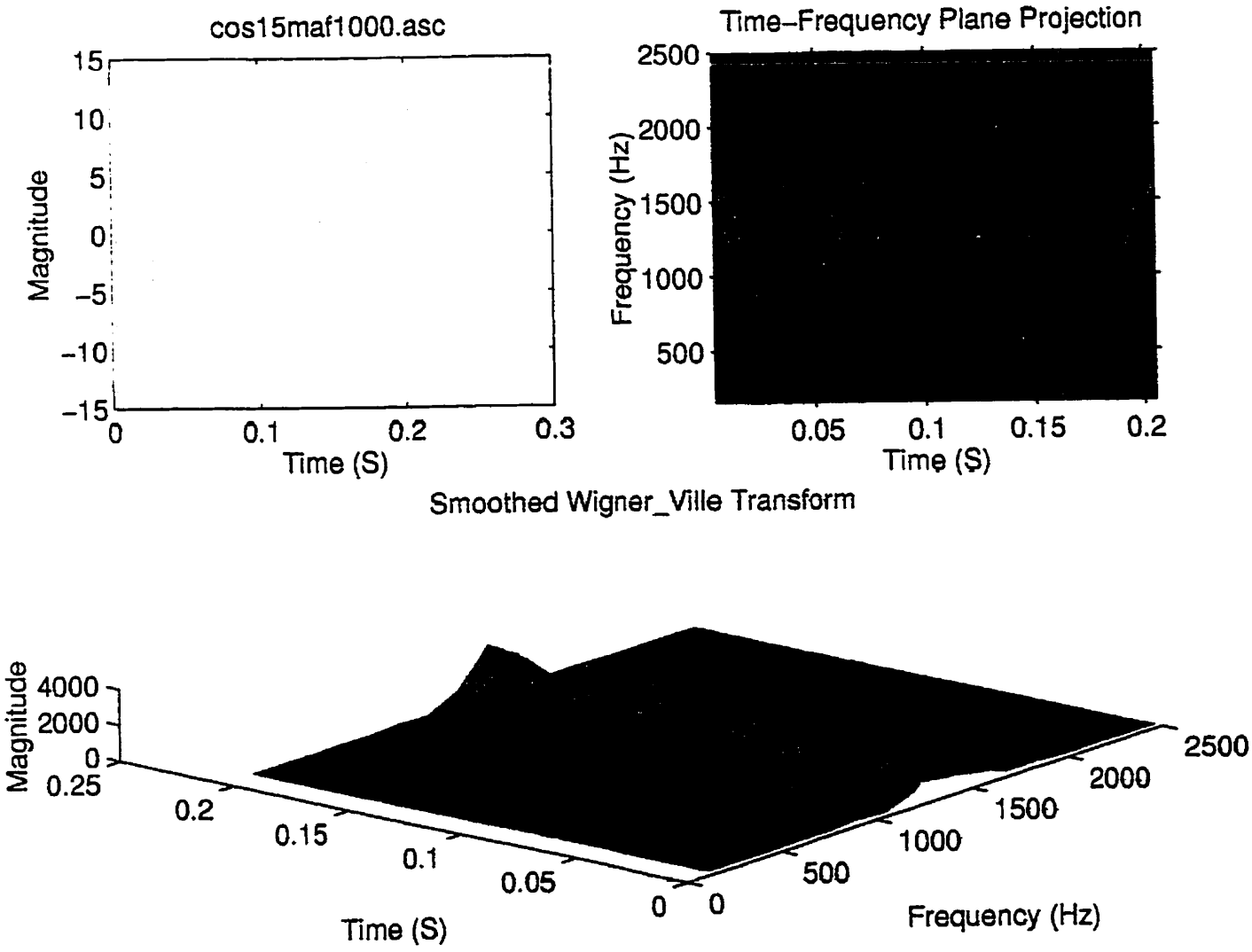

Figure 2.28: Smoothed Wigner-Ville representation of a frequency and amplitude modulated wave.

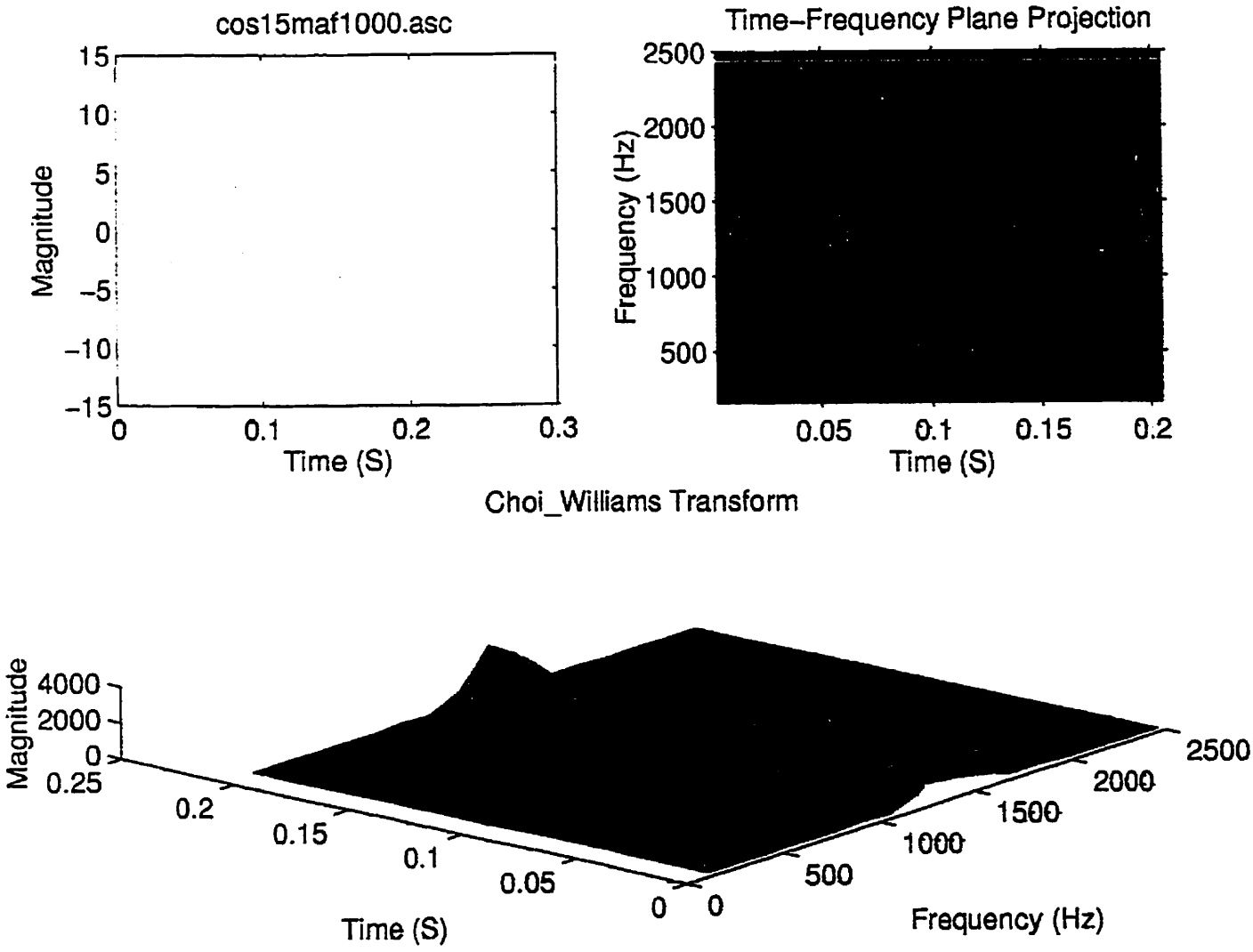

Figure 2.29: Choi-Williams representation of a frequency and amplitude modulated wave.

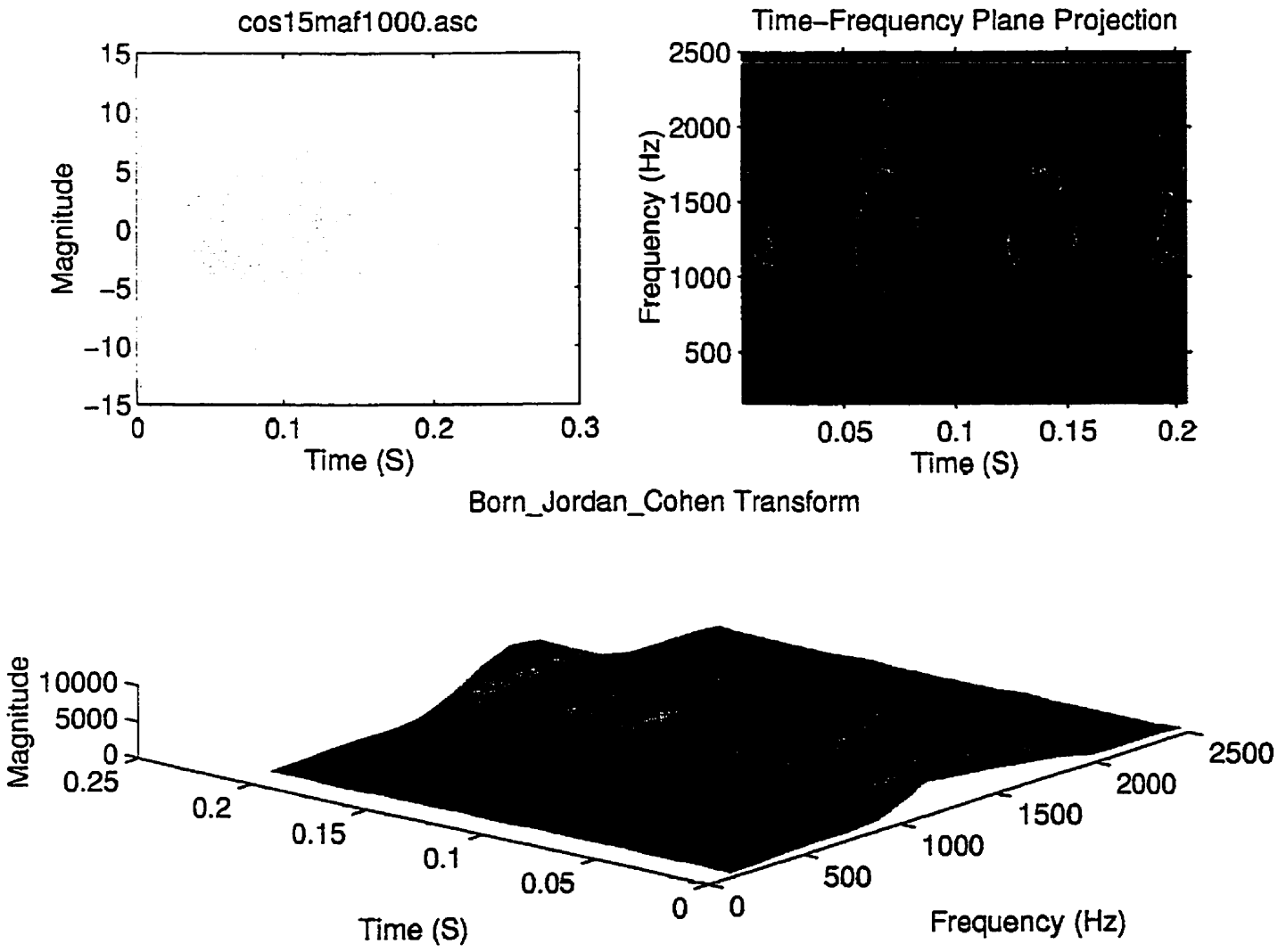

Figure 2.30: Born-Jordan-Cohen representation of a frequency and amplitude modulated wave.

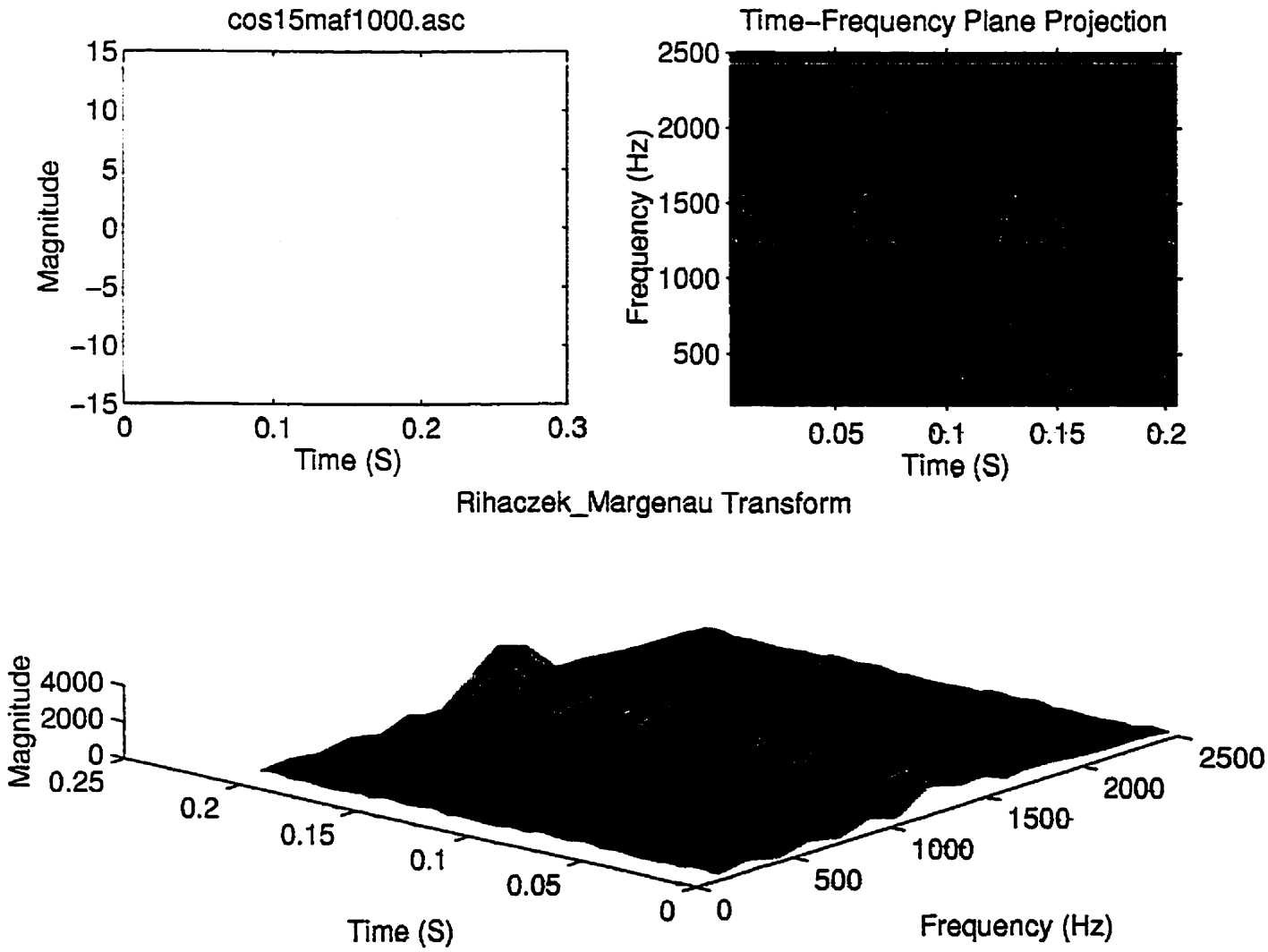

Figure 2.31: Rihacezk-Margenau representation of a frequency and amplitude modulated wave.

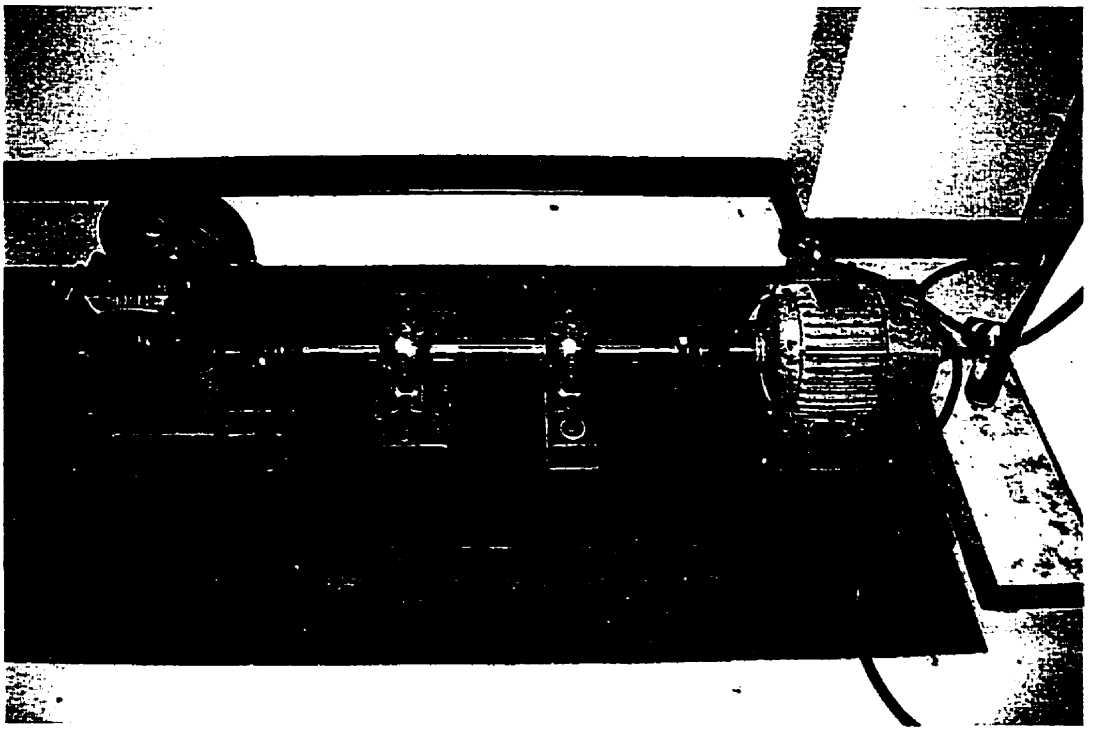

Figure 2.32: Test setup.

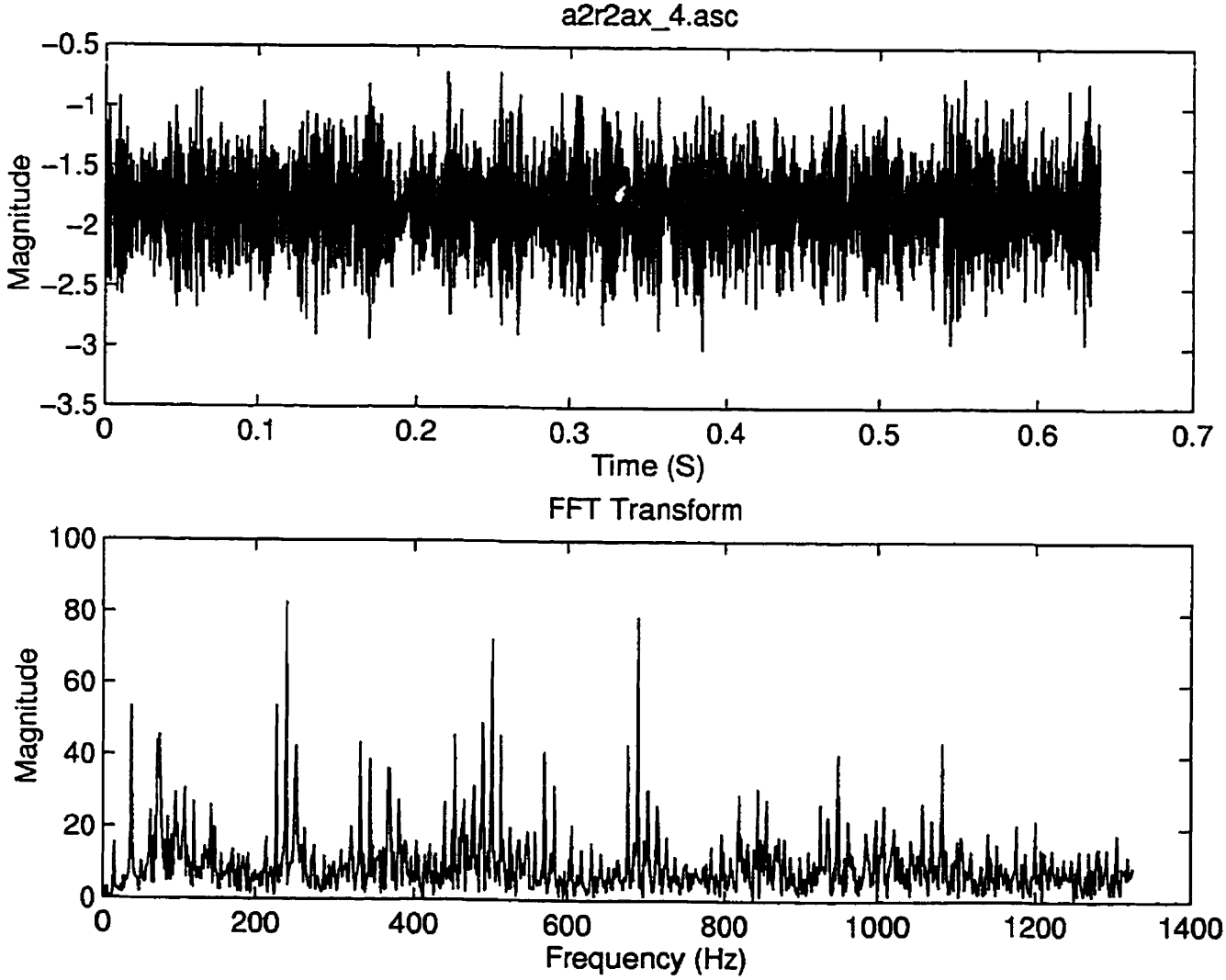

Figure 2.33: Time and spectrum representation of the signal measured on a defective bearing.

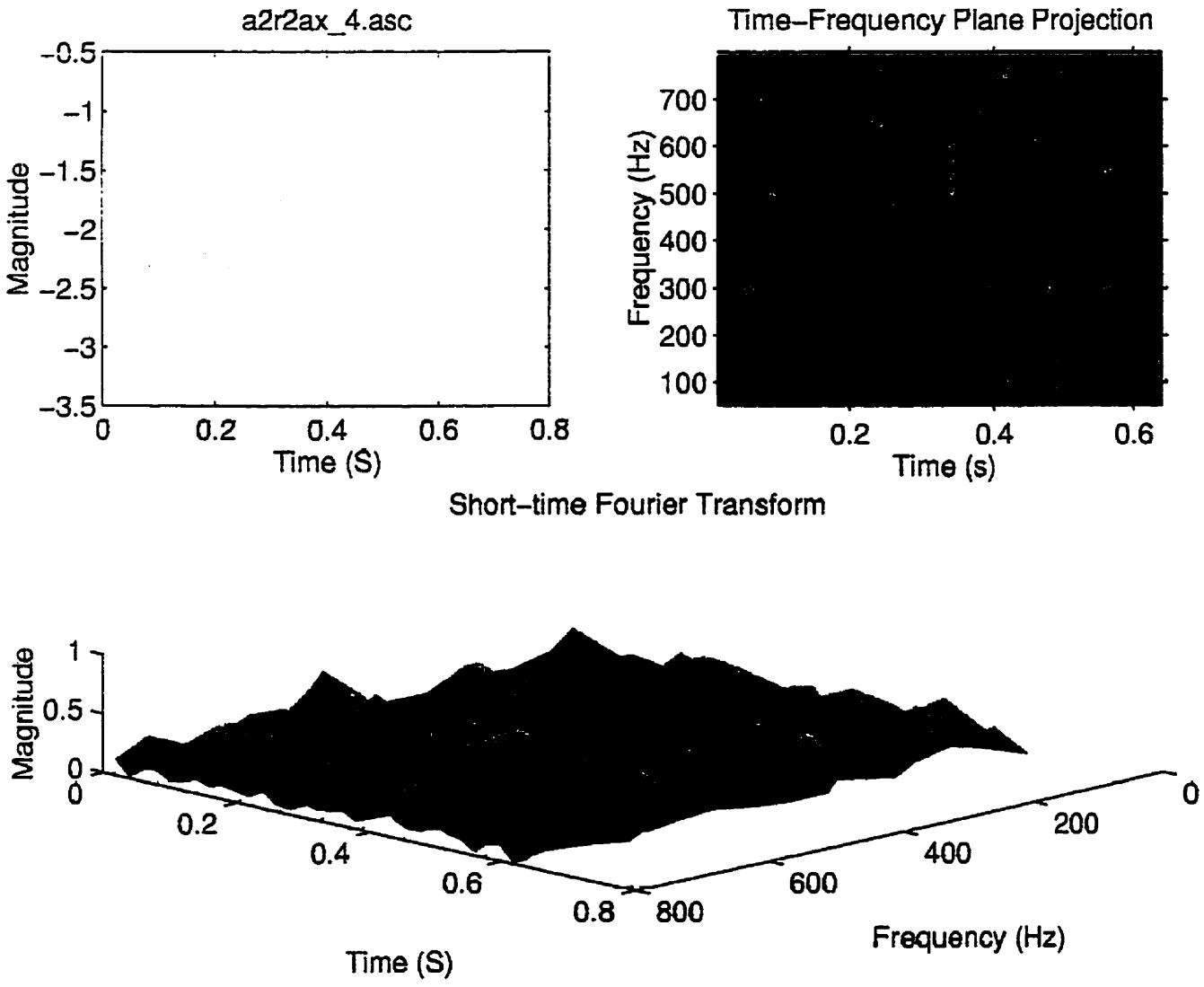

Figure 2.34: Spectrogram representation of the signal measured on a defective bearing.

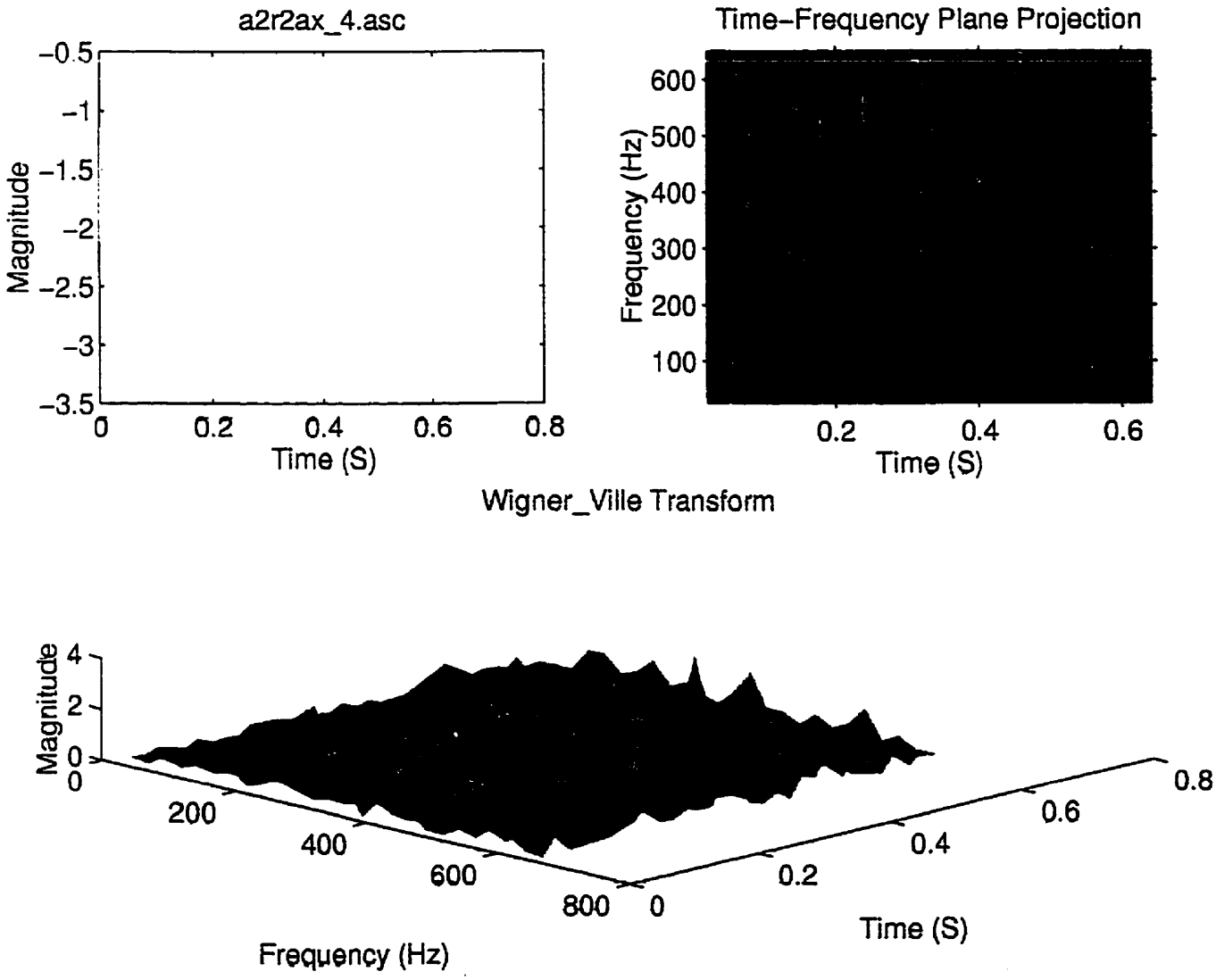

Figure 2.35: Wigner-Ville representation of the signal measured on a defective bearing.

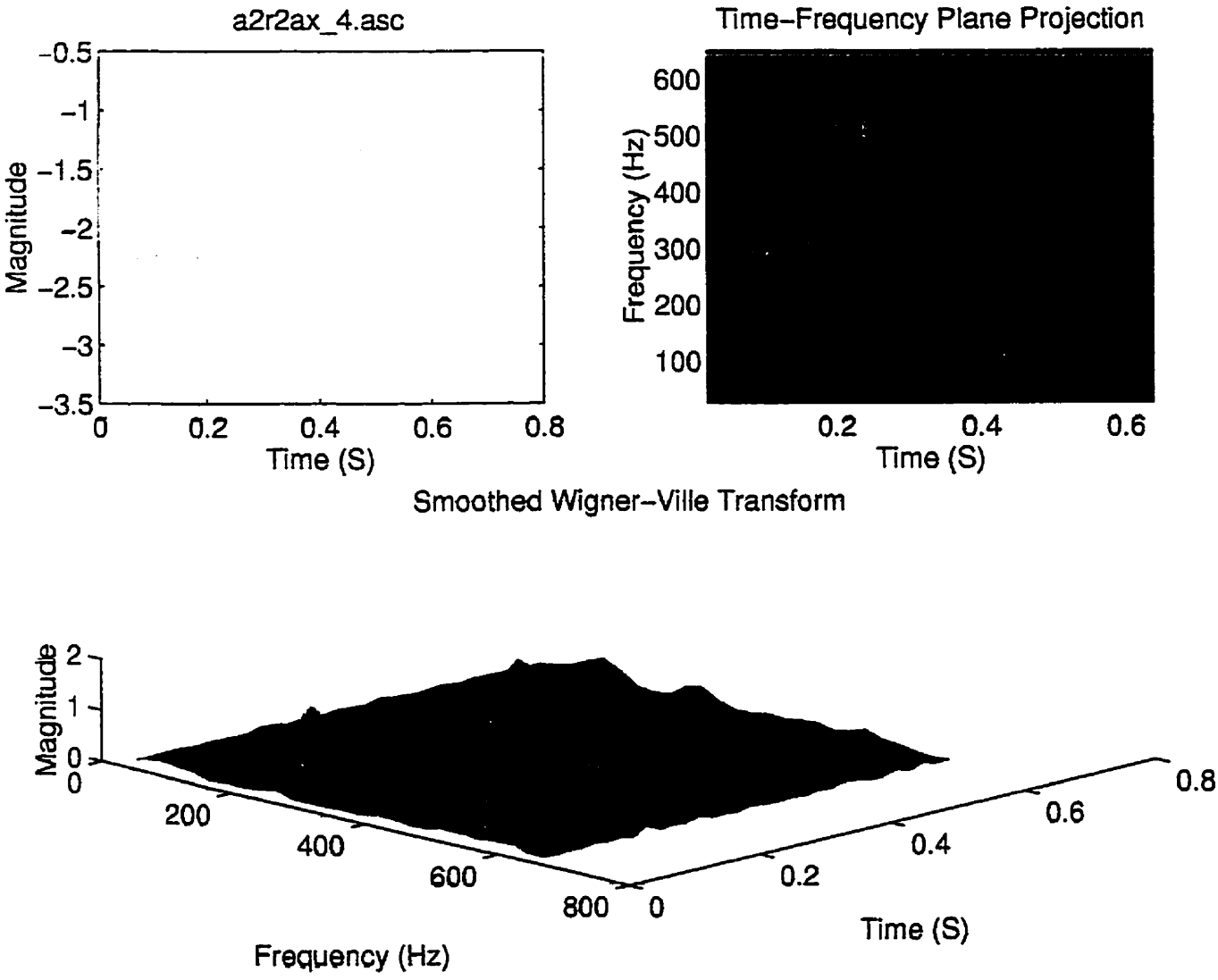

Figure 2.36: Smoothed Wigner-Ville representation of the signal measured on a defective bearing.

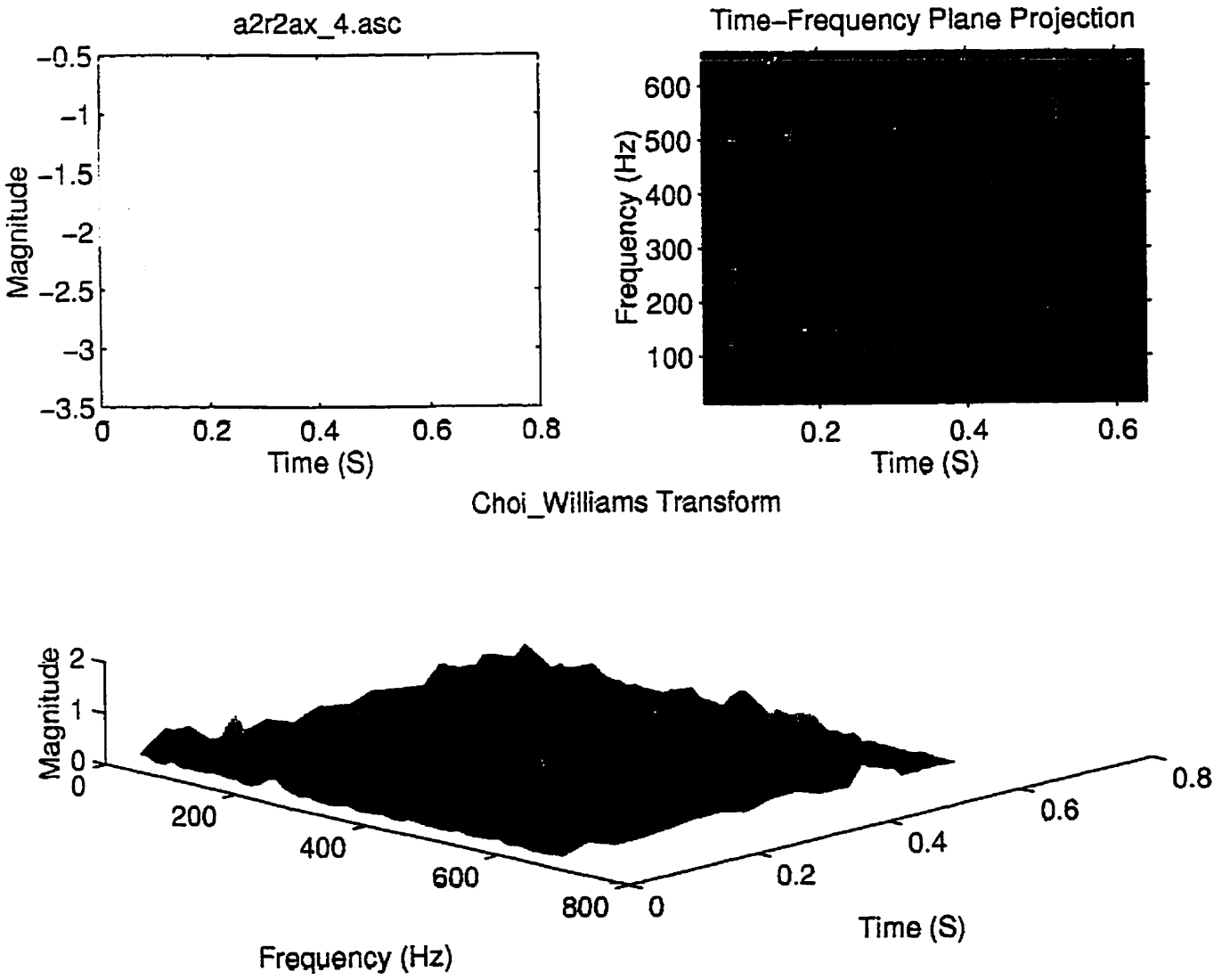

Figure 2.37: Choi-Williams representation of the signal measured on a defective bearing.

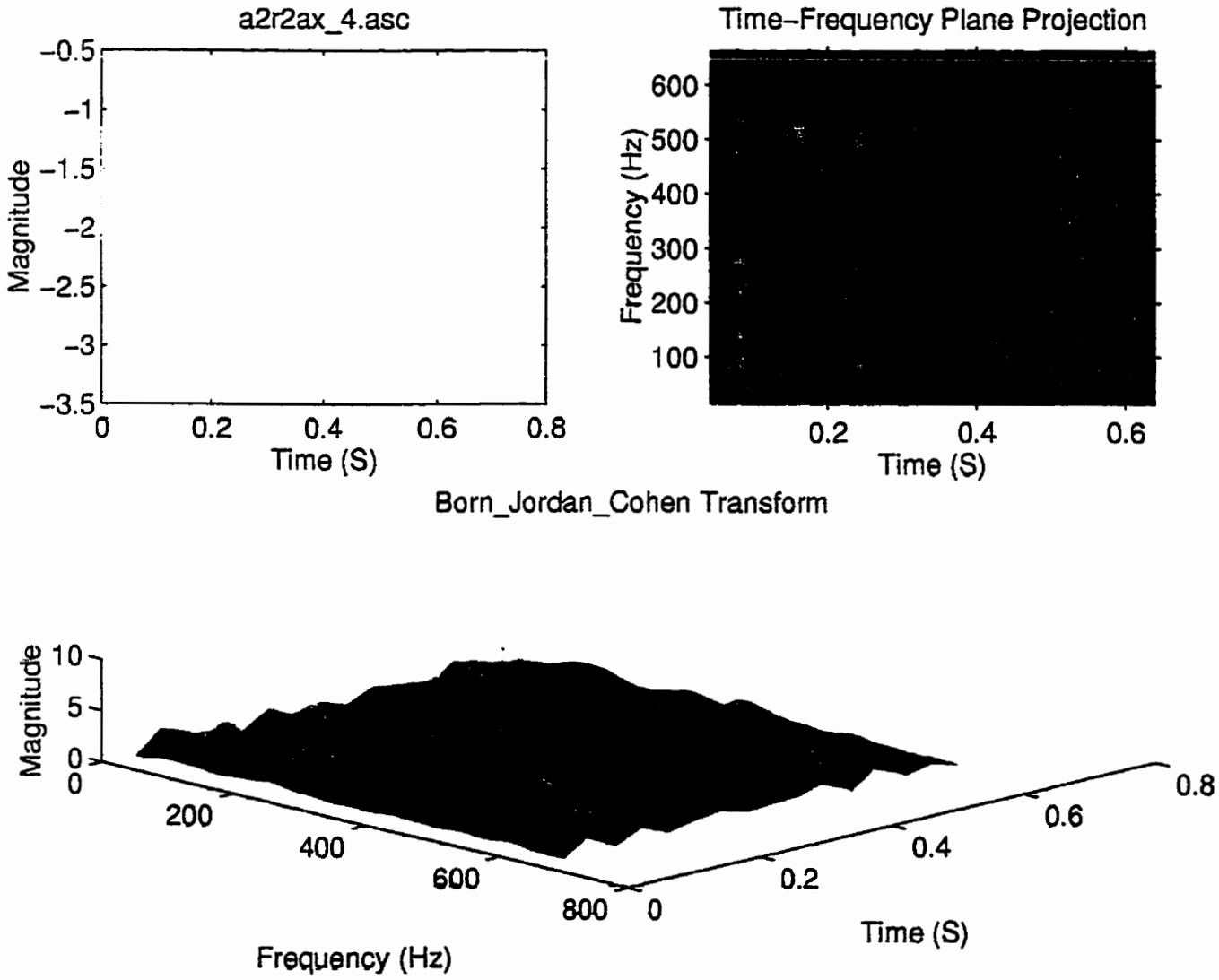

Figure 2.38: Born-Jordan-Cohen representation of the signal measured on a defective bearing.

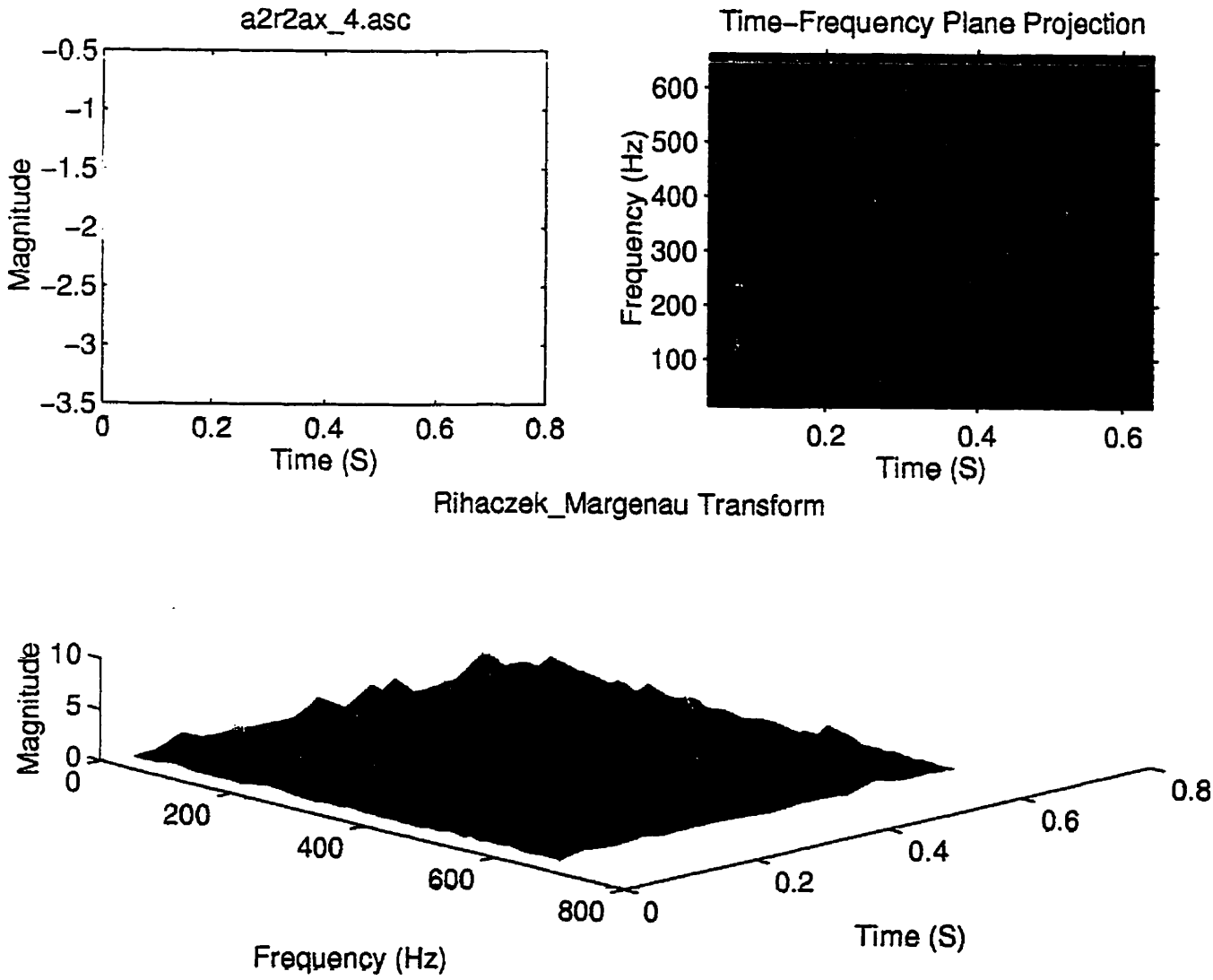

Figure 2.39: Rihacezk-Margenau representation of the signal measured on a defective bearing.

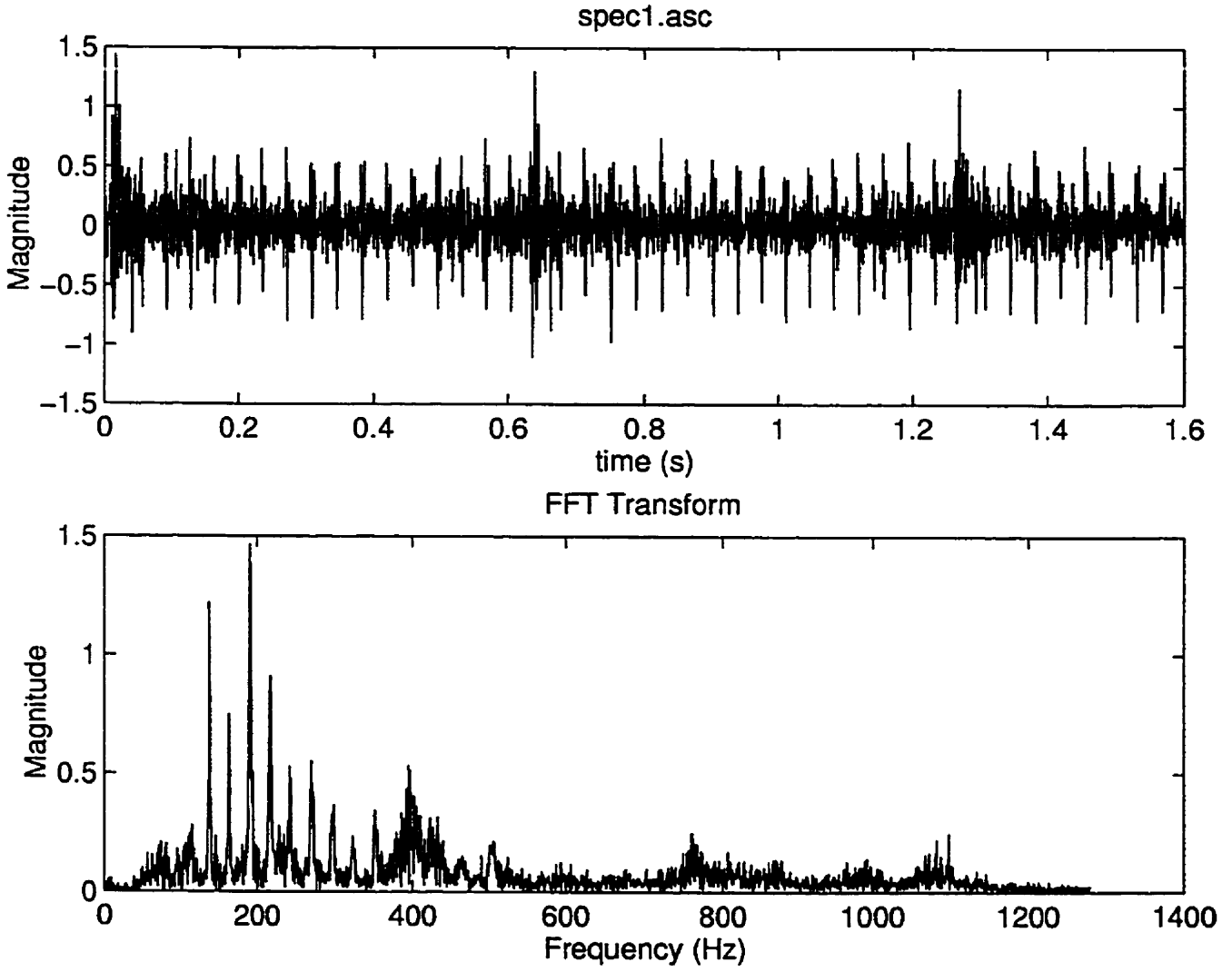

Figure 2.40: Time and spectrum representation of the signal measured on a defective gearbox.

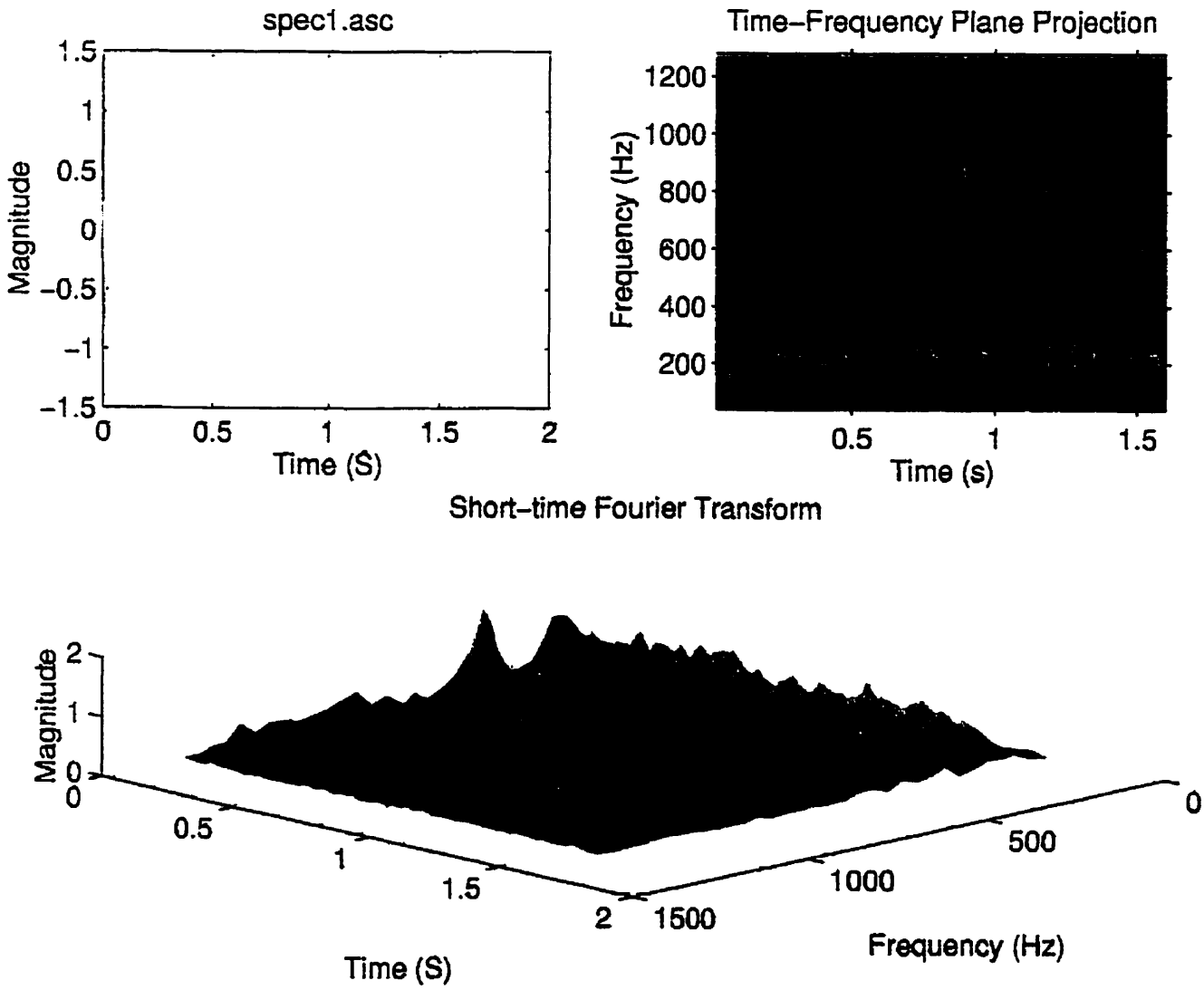

Figure 2.41: Spectrogram representation of the signal measured on a defective gearbox.

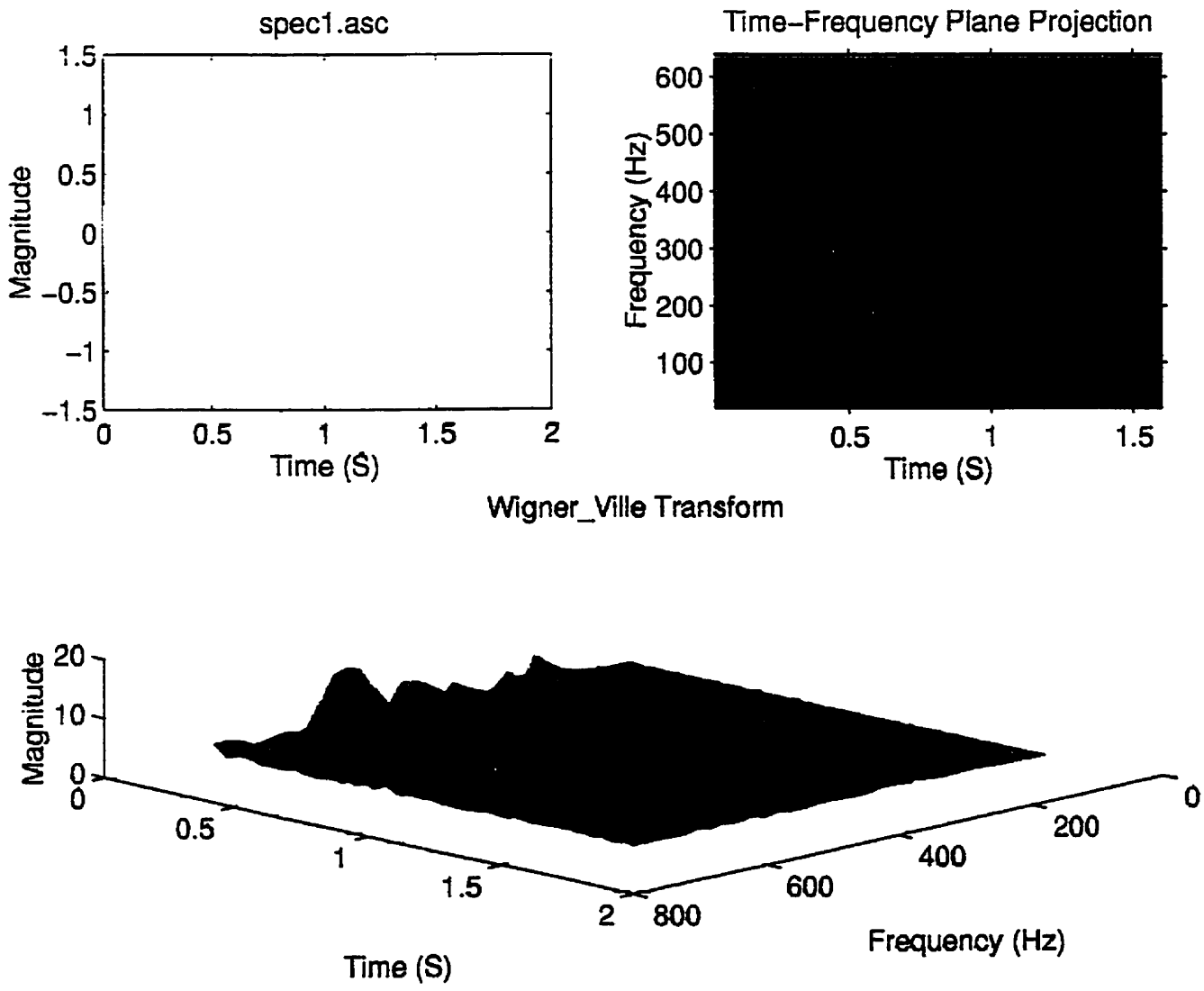

Figure 2.42: Wigner-Ville representation of the signal measured on a defective gearbox.

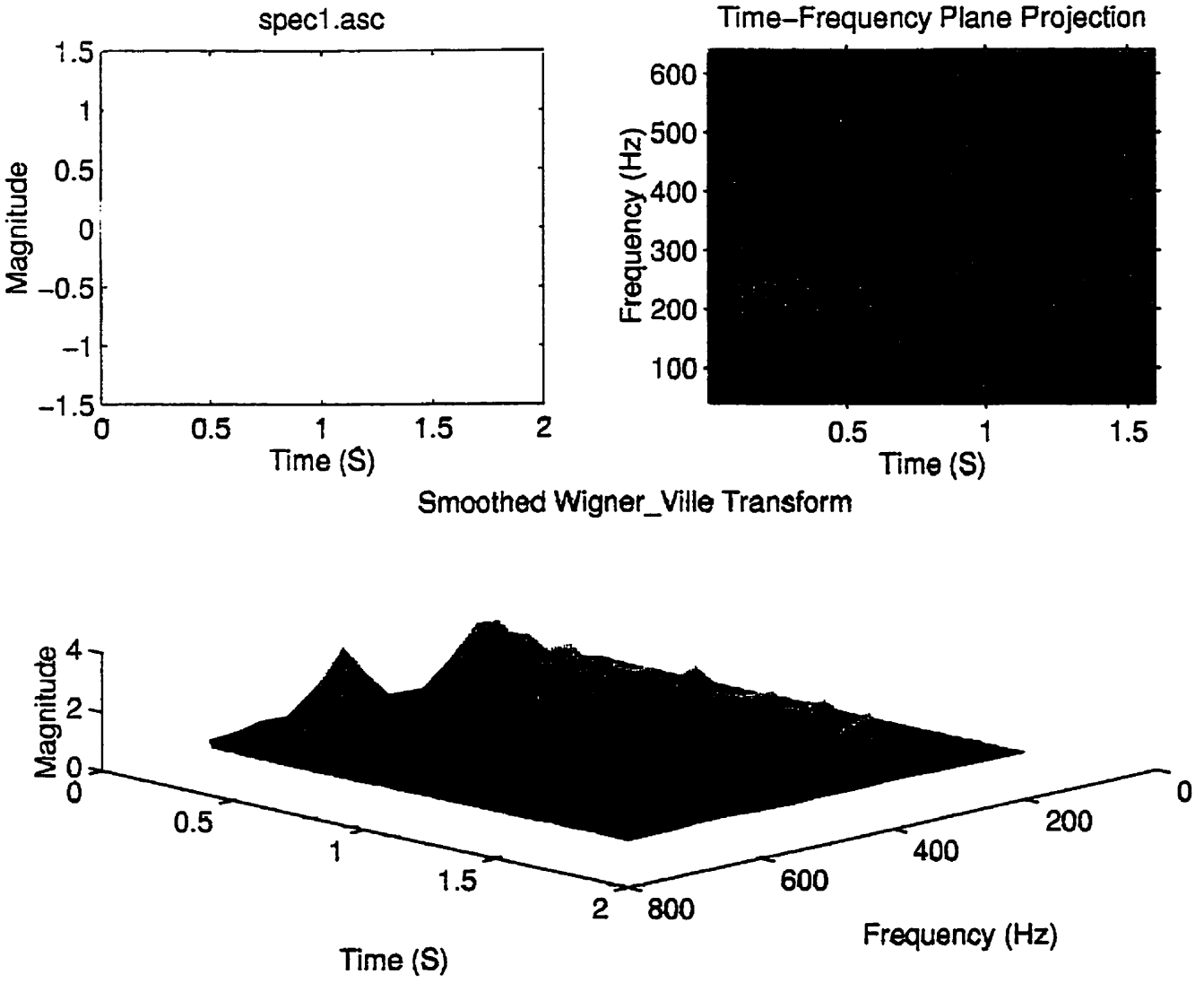

Figure 2.43: Smoothed Wigner-Ville representation of the signal measured on a defective gearbox.

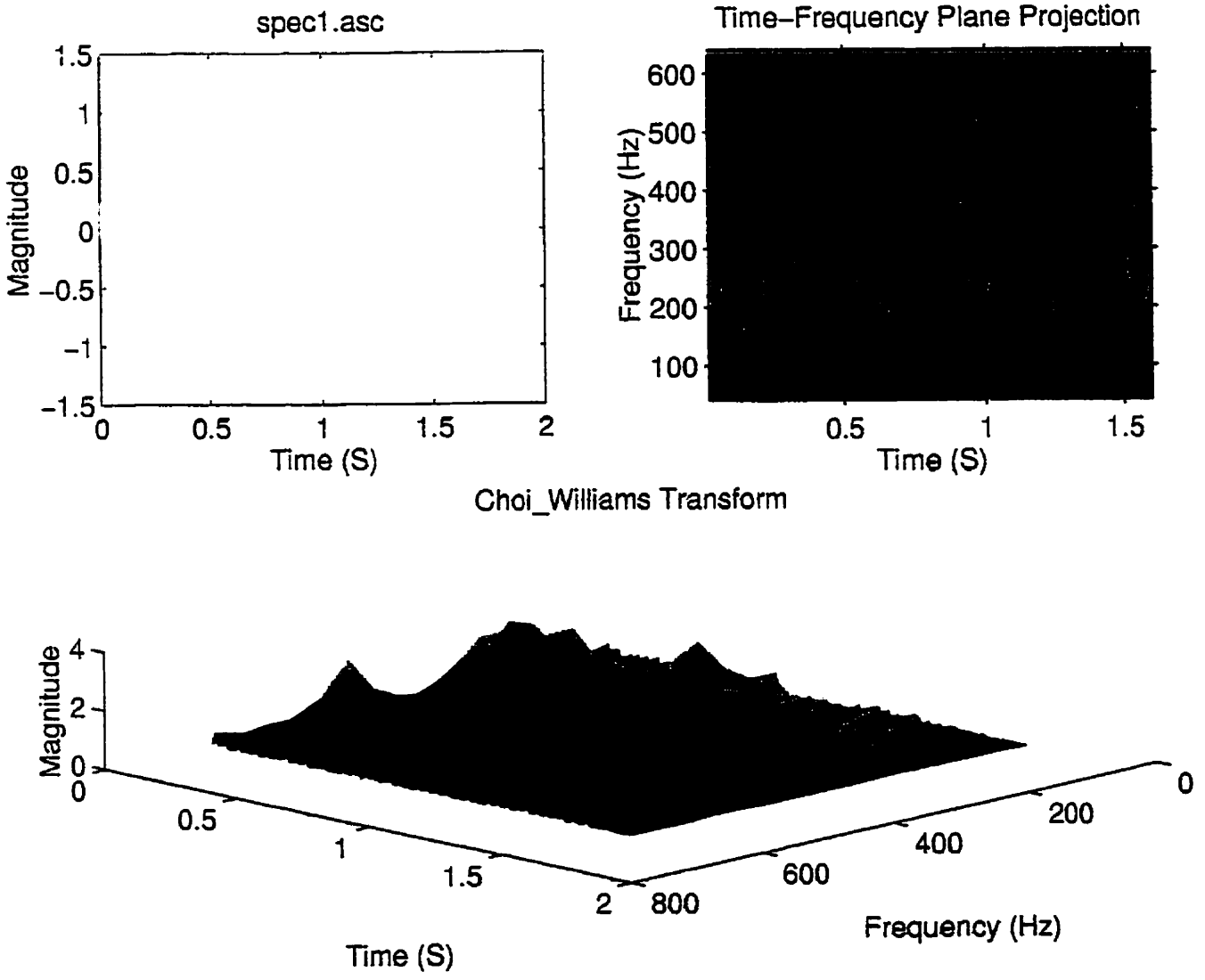

Figure 2.44: Choi-Williams representation of the signal measured on a defective gearbox.

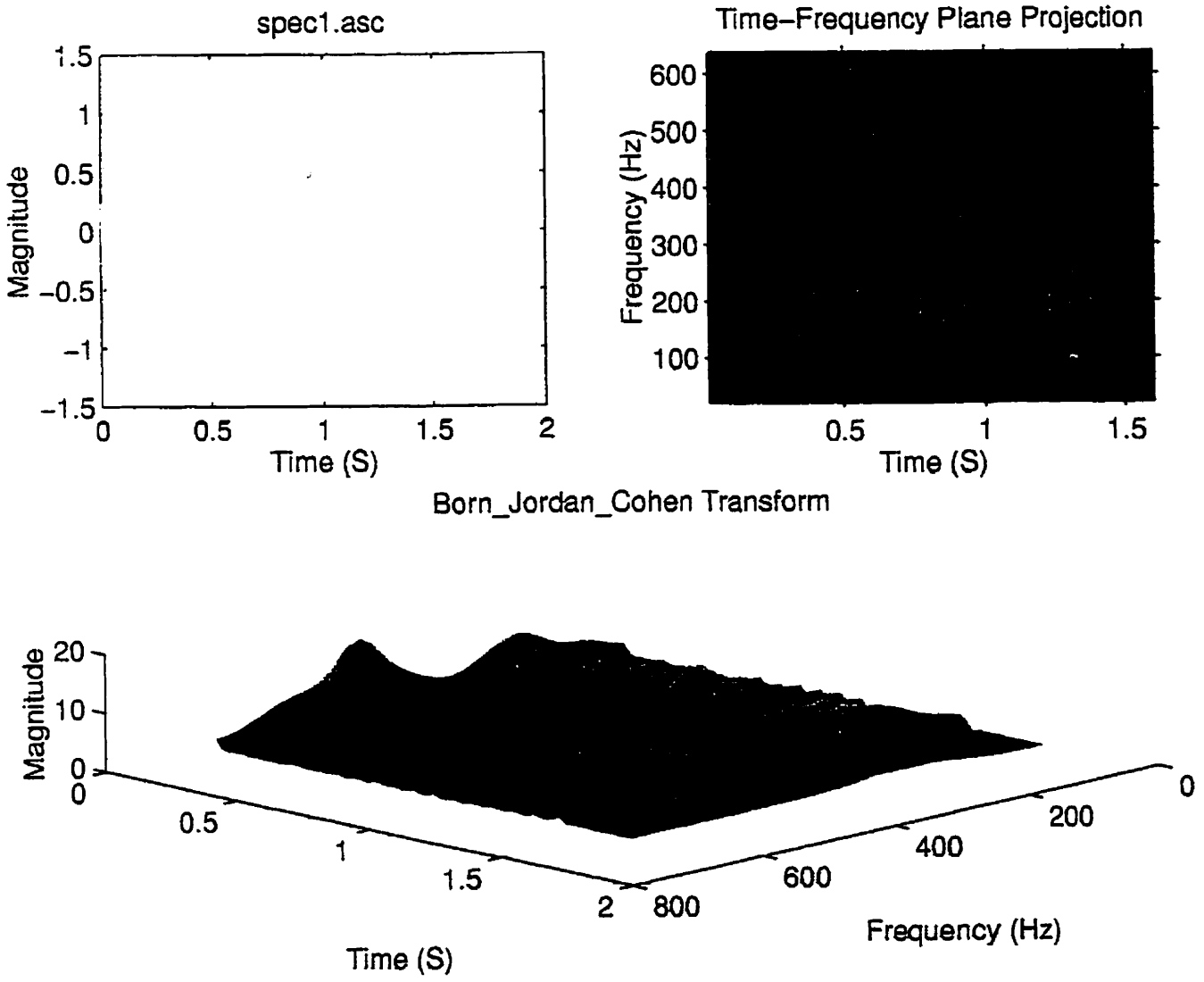

Figure 2.45: Born-Jordan-Cohen representation of the signal measured on a defective gearbox.

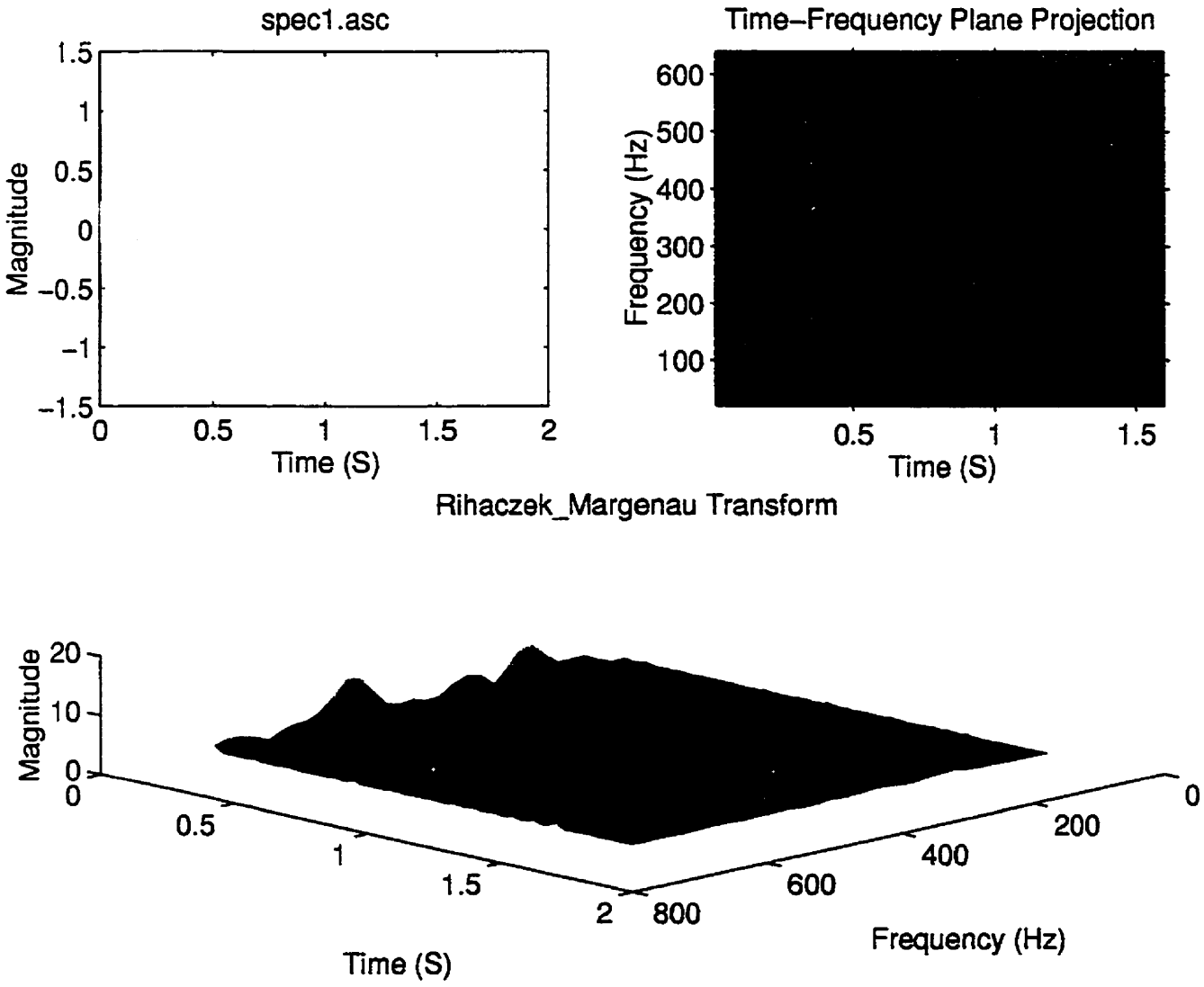

Figure 2.46: Rihacezk-Margenau representation of the signal measured on a defective gearbox.

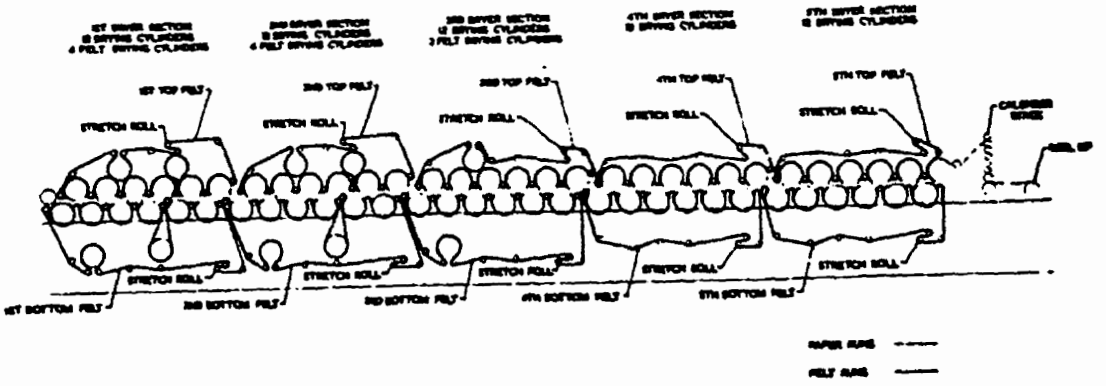

Figure 2.47: Paper machine dryer part

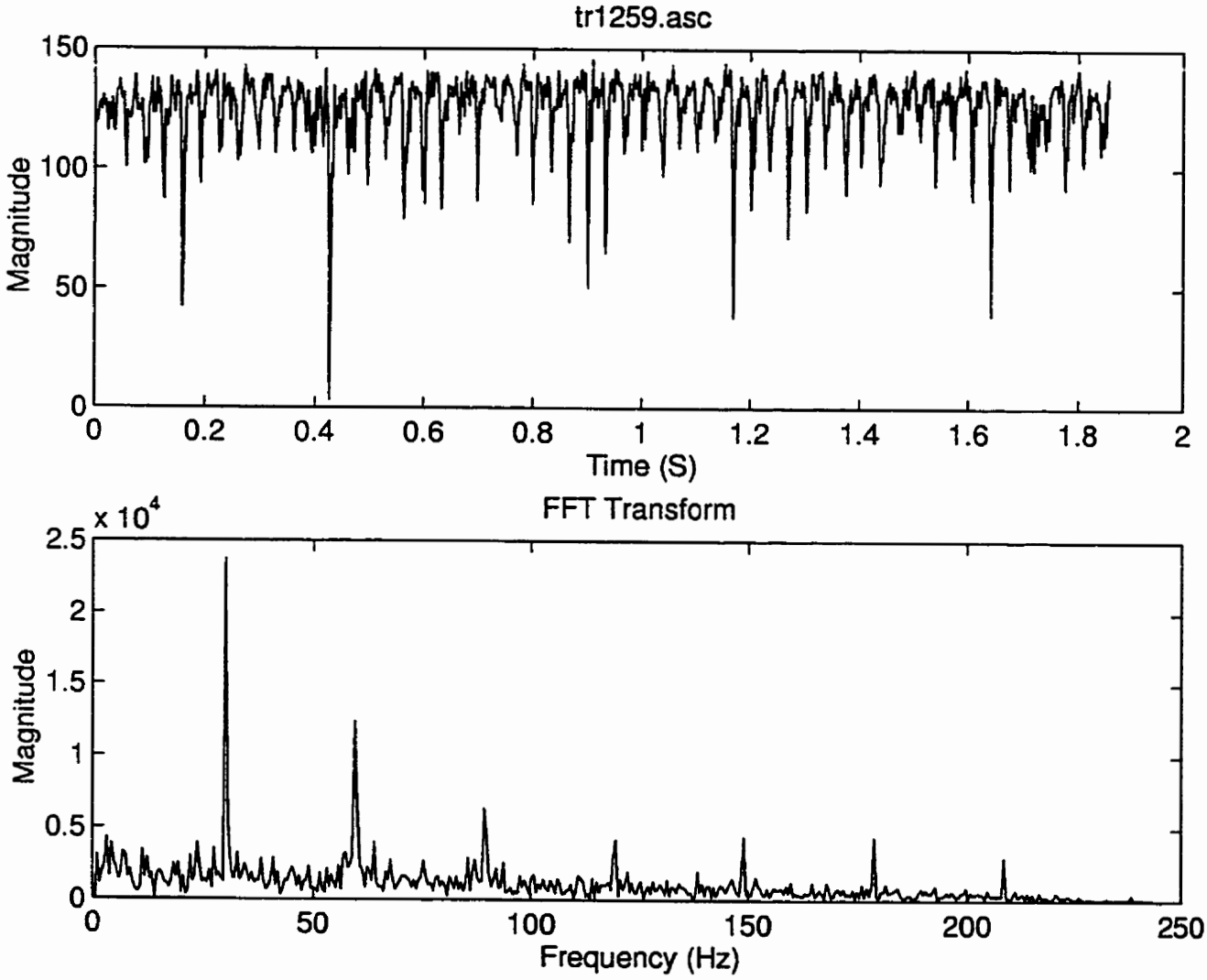

Figure 2.48: Time and spectrum representation of the signal measured on a defective dryer machine.

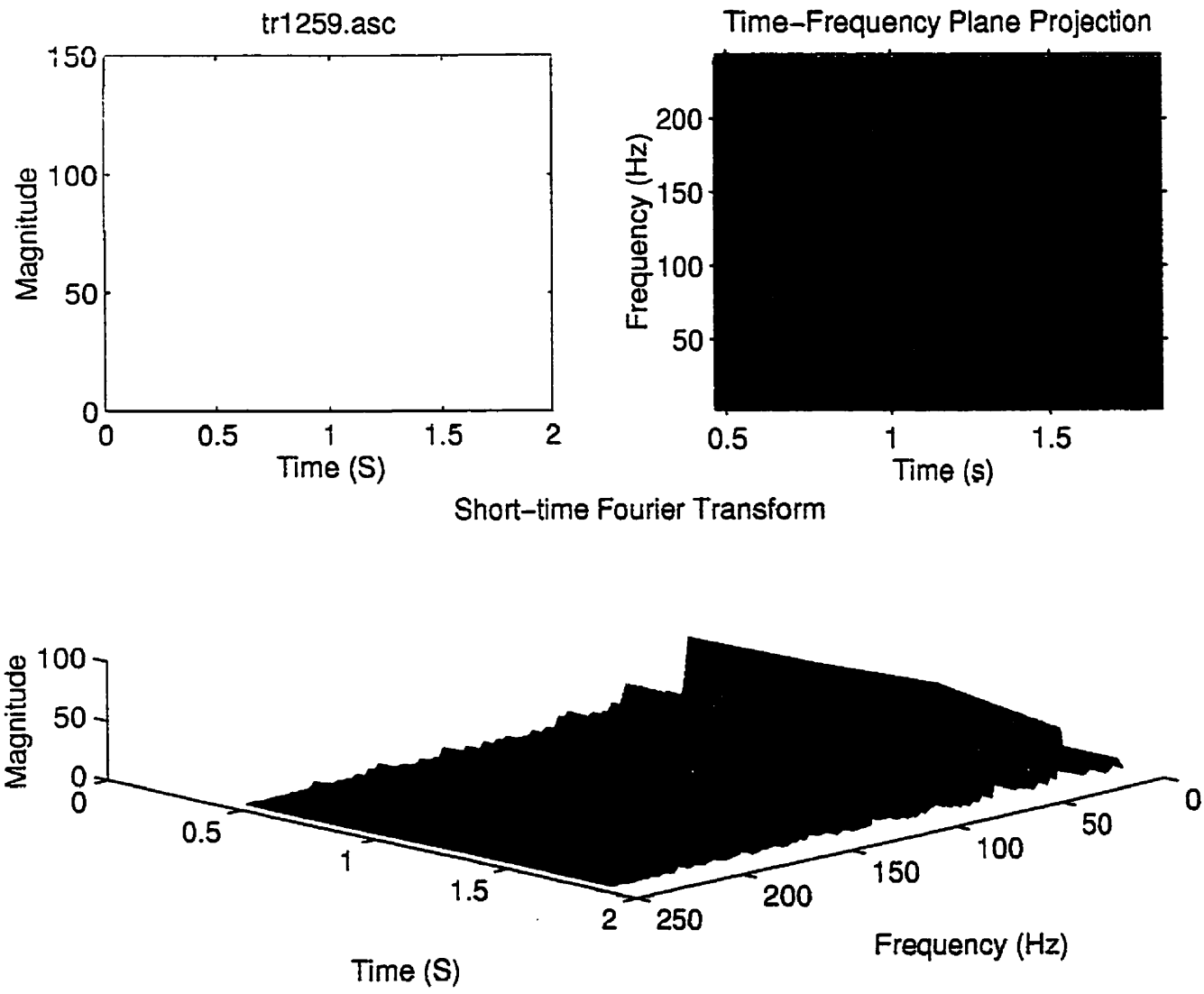

Figure 2.49: Spectrogram representation of the signal measured on a defective dryer machine.

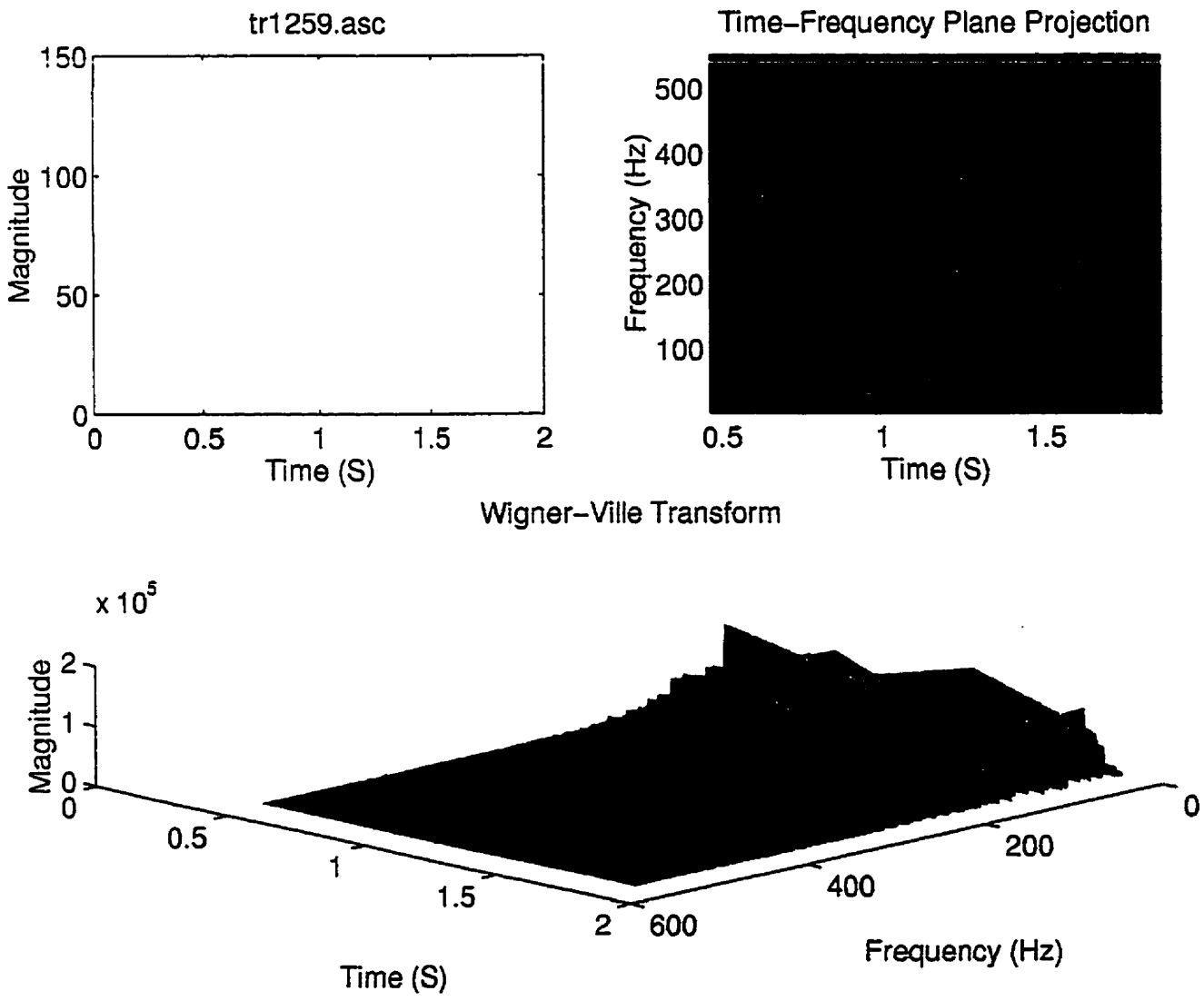

Figure 2.50: Wigner-Ville representation of the signal measured on a defective dryer machine.

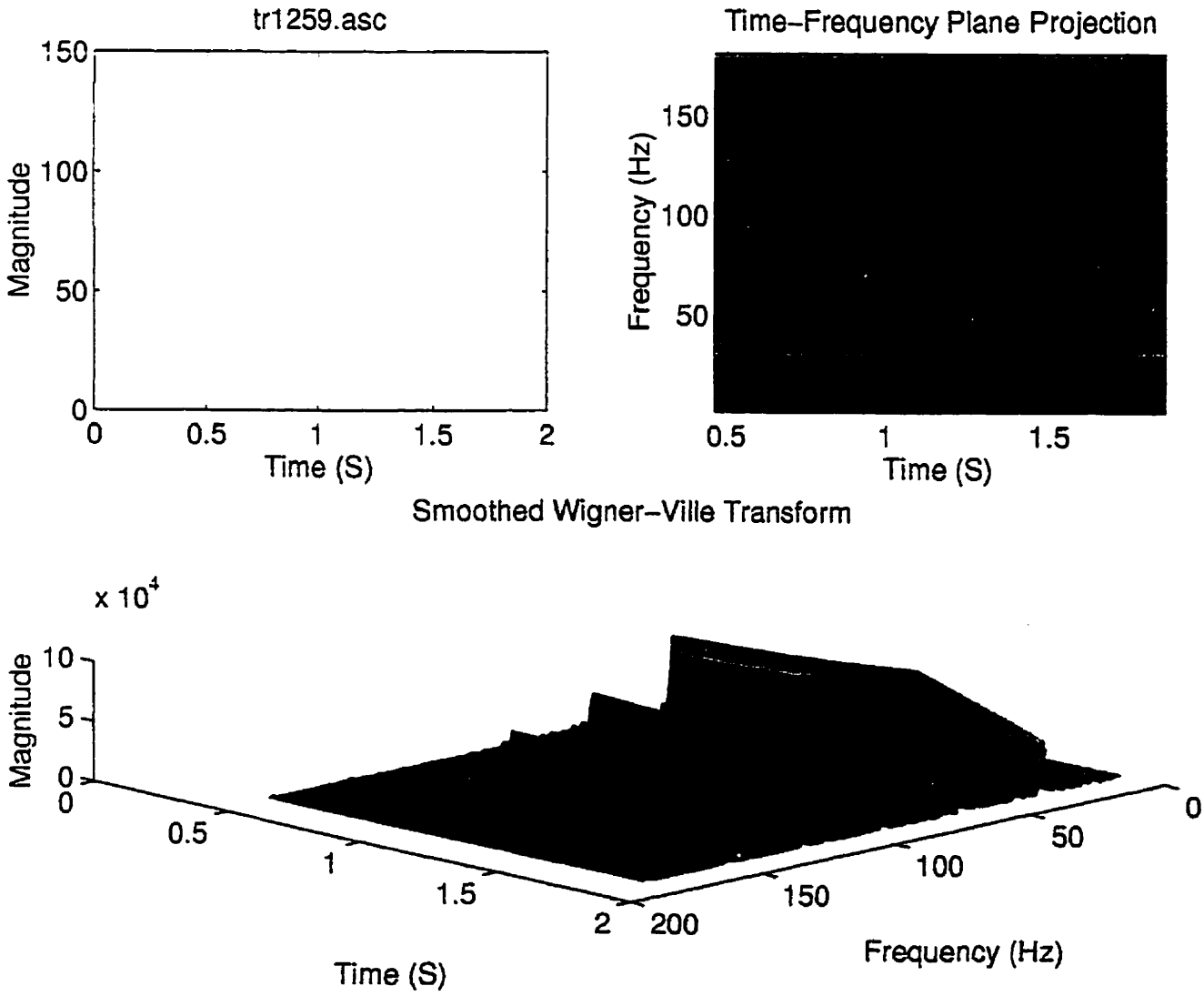

Figure 2.51: Smoothed Wigner-Ville representation of the signal measured on a defective dryer machine.

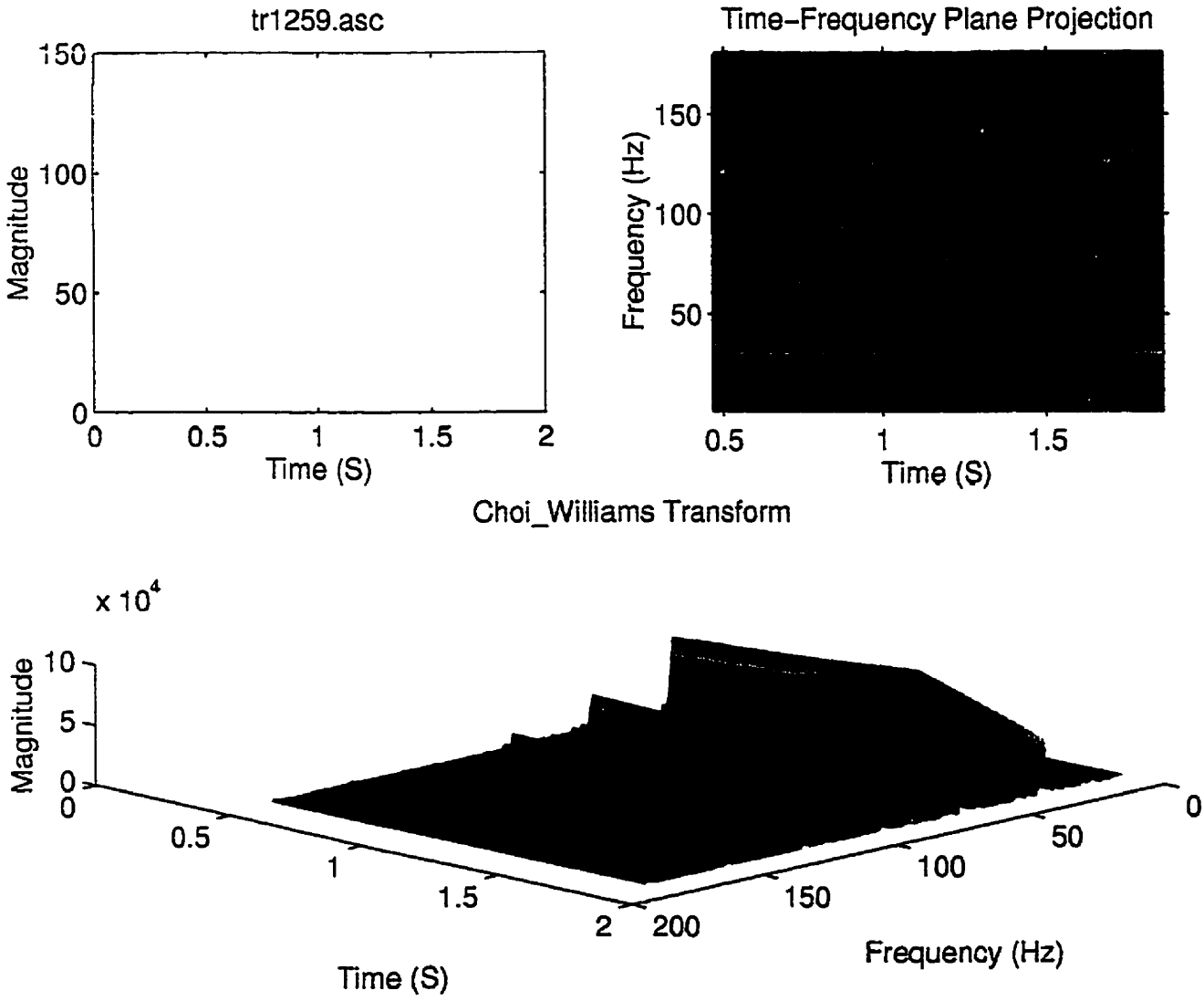

Figure 2.52: Choi-Williams representation of the signal measured on a defective dryer machine.

CHAPTIRE III

APPLICATION OF WAVELET TRANSFORM IN MACHINE FAULT DETECTION

[1]M.S. Safizadeh, [1]A.A. Lakis and [2]M. Thomas

1: Département de Génie Mécanique, École Polytechnique de Montréal

Case Postale 6079, Succ. Centre-ville, Montréal, Canada H3C 3A7

2: Département de Génie Mécanique, École de Technologie Supérieure

1100, rue Notre-Dame Ouest, Montréal, Canada H3C 1K3

3.1 Abstract

Time-frequency analysis has been found to be effective in monitoring the transient or time-varying characteristics of machinery vibration signals, and therefore its use in machine condition monitoring is increasing. While the short-time Fourier transform and the Wigner-Ville distributions are generally considered satisfactory in the field of time-frequency analysis, the development of such new techniques as wavelet analysis, by which it is possible to compensate for weaknesses in other time-frequency methods, may lead to new solutions

★: Soumis pour publication dans "Journal of Mechanical Systems and Signal Processing"

to unsolved problems. Wavelet analysis has a special characteristic of time-frequency localization, which is very effective in the analysis of transient or time-varying signals.

In this paper, we present a brief study of the wavelet transform, wavelet functions, the discrete wavelet transform, the wavelet packet transform and adaptive wavelet transforms. Examples are given to show the advantages and disadvantages of different wavelet transforms. Finally, the effectiveness of wavelet analysis in condition monitoring and diagnostics of machines is illustrated by experimental results from a defective bearing, followed by the application of this technique to the detection of a broken tooth in a gearbox.

3.2 Introduction

A diagnosis is not an assumption, it is a conclusion reached after a logical evaluation of the observed symptoms. The diagnostic process includes the following steps:

a) Observation of the different symptoms and determination of the various defects in the machinery which may have caused them;

b) A systematic search for possible defects in the measured signals;

c) Evaluation of various hypotheses and determination of the one which is compatible with all apparent symptoms.

The diagnosis, therefore, is based on the systematic analysis of the symptoms found in the measured signals. The key factor is the signal analysis. A great many indicators have been developed for machine condition monitoring and fault detection, such as the crest factor and Kurtosis. Comparing new reading against published severity chart such as VDI 2056 shows the existence of defaults.

Machine monitoring and/or diagnosis on the basis of variations in the indicator values of the signal spectrum in "large bands" and in "narrow bands" is very unreliable. One reason for this is that it is necessary to define a large number of indicators corresponding to a small number of defects.

In addition, we need to take into consideration not only the increase in the power of the signal, but also the development of its form. Analysis of this development is carried out in the frequency domain (diagnosis by comparison of the spectrums).

On the other hand, the identification of tooth comb parts in high frequency by traditional spectrum analysis is often impossible, since the frequencies of these components correspond to very high orders of the rotation frequency, and all fluctuations in the rotation frequency produce important frequency variations in each of the components by sweeping across several spectral lines. The spectrum obtained in this way is very noisy and it is difficult to determine the repetitive frequencies of the shocks.

Modifications to the form of representation of the signal, such as Cepstrum (the inverse Fourier transform of the logarithmic spectrum of the signal) and the Hilbert transform of the narrow band of the signal, reveal further information. Here, we are dealing with non-stationary or cyclo-stationary events in the time domain. Advanced signal processing techniques are required to enable us to represent the signal in three dimensions (time-frequency-amplitude). These techniques permit us:

a) To detect and follow the development of the defects which generate weak vibrational power. However, the weak vibrational power can modify the form of the signal to a considerable extent, as happens when defects produce the amplitude modulation or frequency modulation of certain characteristic components. Examples of this are the journal bearing of a shaft with a slow or very slow rotational velocity, a rotating oven, dryer cylinders, the press sections of a paper machine, etc.;

b) To supervise the installations in which the normal functional process produces high amplitude periodic shocks (piston or screw compressor, reciprocating machinery [1] and cam mechanisms [2], ...) which may mask the faulty frequency producing the impulsive forces. (fault in a bearing, coupling, ...).

The time-frequency methods are regarded as advanced diagnostic techniques which offer high sensitivity to faults and a good diagnostic capability.

The Short-Time Fourier Transform (STFT) is one method of time-frequency analysis which we have studied [3]. In the STFT, signal is cut by a window with length T and centered at time t; the spectrum coefficients are calculated for this portion of the signal. The window is then moved to a new position and so on. The major drawback of the STFT is the fixed-length of the window (T) during the analysis of the signal. This limitation of the STFT creates the fundamental problem of the STFT, namely that high resolution can not be obtained simultaneously in the time and frequency domains. If the window length is T, then its frequency bandwidth is of the order $1/T$ (because of $BT=1$). Thus, the two conditions of a narrow window and a narrow bandwidth are irreconcilable.

Another time-frequency method which we have studied [4] are the Wigner-Ville distributions. In this case, it is postulated that a series of sampled data is available for analysis. The instantaneous correlation, $R_f(\tau, t_1)$, at time (t_1) with a time lag τ, is defined as

$$R_f(\tau, t_1) = \lim_{T \to \infty} \int_{t_1}^{t_1+\tau} f(t - \tau/2) f(t + \tau/2) dt \tag{3.1}$$

and its Fourier transform may be written as follows:

$$S_f(\omega, t_1) = \int_{-\infty}^{\infty} R_f(\tau, t_1) e^{-j\omega\tau} d\tau \tag{3.2}$$

Where $S_f(\omega, t_1)$ is the instantaneous spectrum density function according to frequency ω and time t_1. Theoretically, $S_f(\omega, t_1)$ is the frequency content measurement of a non-stationary random process at time t_1.

In practice, it is impossible to calculate the correlation function $R_f(\tau, t_1)$ on a series of samples from $-\infty$ to $+\infty$, because this type of sample is never available.

Therefore, if we replace:

$$\int_{t_1}^{t_1+\tau} f(t-\tau/2) f(t+\tau/2) d\tau$$

in the equation (3.2), by the instantaneous value: $f(t-\tau/2) f(t+\tau/2)$ we will obtain

$$W_f(\omega, t) = \int_{-\infty}^{\infty} f(t-\tau/2) f(t+\tau/2) e^{-j\omega\tau} d\tau \qquad (3.3)$$

$W_f(\omega, t)$ is a function of ω and t for a sampled single x and is called the Wigner Distribution of *f(t)*.

In the case of deterministic signals, we use the analytical signal *z(t)* instead of the real signal *f(t)*, and the distribution is called the Wigner-Ville Distribution. The analytical signal *z(t)* is

defined as

$$z(t) = f(t) + j\bar{f}(t) \tag{3.4}$$

Where $\bar{f}(t)$, the imaginary part of the signal *z(t)*, is the Hilbert transform of the real signal *f(t)*.

In this way, the negative frequencies are eliminated and the signal is represented only by the real part of a rotary phaser with positive frequencies.

The analytical signal is very useful when we study the amplitude and modulation of the phase since this signal introduces the concept of instantaneous frequency and instantaneous power. The sampling frequency may also be used, followed by the Nyquist criteria because the spectrum of an analytical signal is a one-sided spectrum with only positive frequencies.

The Wigner-Ville Distribution is a distribution of energy in the time and frequency domains, where:

$$E_s = \iint WVD_f(\omega,t)dtd\omega \tag{3.5}$$

Unfortunately, the Wigner-Ville transform presents several anomalies:

a) This transform is a bilinear transform i.e. the cross terms generate a certain non-linearity;

b) The random noise in the original signal has a tendency to spread to other regions in

the time domain. Since the integral of equation (3.3) is centered at time t, the integral covers an infinite period of τ (time delay). Therefore, it depends on the characteristics of x as distinct from the local time t;

c) These transforms often give negative values, which makes the interpretation of the distribution difficult.

Furthermore, the Wigner-Ville method presents another difficulty: it is almost impossible to obtain a local spectrum density because of the continuity nature of the harmonic waves. To overcome this limitation attributable to harmonic analysis, an alternative method of signal analysis has, at a theoretical level, been developed.

Instead of using sines and cosines as base functions to decompose a signal, a set of orthogonal functions, called wavelets, has been used. Whilst, by definition, harmonic functions go to infinity, the wavelets are, in contrast, local functions. Gathering these wavelets and using different scales, it is possible to assemble a set of base functions in order to examine the local character of non-stationary signals.

The theory of wavelets is a mathematical method in which a series of special signals is used to construct a model for a signal, a system or a process. These special signals are small waves or wavelets. They must be oscillatory and possess an amplitude which decreases rapidly to zero in both positive and negative directions.

The first classical wavelet was derived by J. Morlet [5], a geophysical engineer at a French oil company, in 1982. He wanted to analyse some signals which had shorter-time transient components in high frequency than in low frequency. He needed both satisfactory frequency resolution in low frequency and satisfactory time resolution in high frequency. The usual method of time-frequency analysis at that time was the Short-Time Fourier Transform (STFT). As previously mentioned, the major disadvantage of the STFT is that it is impossible to obtain high resolution simultaneously in time and in frequency. Morlet's idea was to use a smooth window with some oscillations, as $\psi(t)$, and generate a label family from $\psi(t)$ by translation and dilation. As a basis for the wavelet transform, he chose a windowed cosine wave which was compressed in time for a higher frequency function and spread out for a low frequency function. He finally characterized his signal by inner products of the signal with these transform functions. A few years later, Alex Grossmann, a theoretical physicist, presented an exact inversion of Morlet's formula and helped him to find several applications for the wavelet transform [6]. In 1985, Y. Meyer, a pure mathematician, recognized that the wavelet transform had been already introduced as a mathematical tool in harmonic analysis by Calderon in the 1960s. He correlated the work of Grossmann and Morlet with Calderon's formula in harmonic analysis and also constructed the basis of an orthonormal wavelet with excellent time-frequency localization properties. In 1986, S. Mallat, a specialist in computer vision and image processing, used the multi-resolution approaches in computer vision and its application to a method of image coding called

"Pyramid", in order to define a similar structure for wavelet expansions. Mallat and Meyer succeeded in developing the mathematical structure for wavelet construction on the basis of multi-resolution signal representation [7, 8]. Meyer's work on the mathematical structure of the wavelet is documented in his book [9]. Using multi-resolution analysis, S. Mallat proposed that the wavelet coefficients may be computed using an efficient algorithm produced by a filter bank. To use filters in wavelet decomposition instead of deriving the filters from a wavelet basis, we can first construct a pair of appropriate FIR (finite impulse response) filters and then investigate whether they correspond to an orthonormal wavelet basis. The characteristics of such a pair of filters were discovered in 1970 and given the name "quadrature mirror filters" (QMF). By using QMF, exact construction of orthonormal wavelet bases has been possible. A sufficient condition for regularity of these filters has been given by Daubechies [10, 11]. This work resulted in a discrete-time wavelet transform [12, 13]. One of the important disadvantages of the wavelet transform is the logarithmic scale of the frequency axis in the time-frequency plane. As an alternative, an interesting generalization of the filter bank trees of the wavelet transform is the wavelet packets transform, which provides a linear scale frequency axis in the time-frequency plane [14, 15].

This paper presents the wavelet analysis as a newly-developed technique with important properties which make it a powerful tool in machine condition monitoring and fault detection. In section 2, the theory of wavelet transform is briefly described, followed by a discussion of the properties of different wavelet functions. Then, the discrete wavelet

transform and the fast wavelet transform based on multi-resolution analysis are studied and the wavelet packet transform and adaptive wavelet transforms are presented as variations of wavelet analysis. In this section, we also present a new method, called the "zoom in wavelet transform", by means of which the wavelet transform is used to obtain a finer resolution in the frequency domain. This method is a variation of the adaptive wavelet transform. In section 3, a computer program to implement the different methods of wavelet analysis is described and the different ways of using the wavelet transform to determine time-frequency localization are compared. Finally, wavelet analysis is applied to experimental vibration signals received from a damaged bearing and a broken tooth in a gearbox.

3.3 Wavelet transforms

It is known that discrete-time signal decompositions are methods of expressing an energy-limited signal as a linear combination of transform bases. The linear integral transforms can be considered as an inner product of a signal $f(t)$ with a transformation function. The standard example is the Fourier transform $F_f(\omega)$ of signal $f(t)$ which is defined as:

$$F_f(\omega) = < f, h > = \int_{-\infty}^{\infty} f(t)\,\overline{h}(t)\,dt \tag{3.6}$$

where the transformation kernel is $h(t) = e^{i\omega t}$.

From a mathematical point view, equation (3.6) decomposes $f(t)$ into a family of pure frequency signals $e^{i\omega t}$ which play the role of the Fourier transform bases. The sine-cosine functions are highly localized in frequency but widely spread in time. Therefore, the time domain information of the spectral components is hidden in the phase of the Fourier transform. Consequently, the Fourier transform is not well suited for time-place analysis.

For non-stationary signals, the Short-Time Fourier Transform (STFT) is the first and simplest method which is defined as

$$STFT_f(t,\omega) =< f, h_\tau >= \int_{-\infty}^{\infty} f(t)\,\overline{h}_\tau(t)\,dt \tag{3.7}$$

where $h_\tau(t) = g(t-\tau)\,e^{i\omega t}$ and τ define the translation of the window function $g(t)$. As the window is shifted in time, a new spectrum is obtained at each position, producing a time-frequency representation of the signal. The efficiency of the localization in the time-frequency plane depends on the width of the window function. The uncertainty factor, $\Delta t\,\Delta\omega \geq 1/2$, sets a limit on the product of time and frequency. This means that we cannot simultaneously obtain high resolution in both the time and frequency domains. However, by changing the width of the window, we can trade resolution in time for resolution in

frequency.

In a similar way, the wavelet transform can be defined if the Fourier transform bases are replaced by the wavelet transform bases, $h_{st}(t)$, as shown in Figure 3.1.

The wavelet transform is defined as:

$$W_f(s,\tau) =< f, h_{s,\tau} >= \int_{-\infty}^{\infty} f(t)\,\bar{h}(s,\tau)\,dt \tag{3.8}$$

The wavelet transform bases are a family of functions which are obtained from a single prototype wavelet by translation and dilation/contraction :

$$h_{s\tau}(t) = \frac{1}{\sqrt{s}} h\left(\frac{t-\tau}{s}\right) \tag{3.9}$$

where " s " is a real variable, known as the scale of wavelet transform and $h(.)$ is a fixed function, called "mother wavelet function". From equation (3.9), we can say that the wavelet transform extracts spectral information from the signal around time τ by means of inner links between the signal and scaled versions of the wavelet.

In the case of the wavelet transform, the selection of the basis functions is more flexible than the case with the STFT. The choice of short basis functions for low frequencies and long

basis functions for high frequencies makes the wavelet transform sharper in time in the higher frequencies and sharper in frequency at low frequencies.

3.3.1 Wavelet functions

The mother wavelet function may be any function satisfying the necessary condition that warrants the existence of the inverse wavelet transform. This admissible condition is defined as

$$\int_{-\infty}^{\infty} h(t)dt = 0 \tag{3.10}$$

which means that the wavelet must be oscillated and have a zero mean. Different families of wavelets can be generated by taking different admissible wavelet functions. The choice of the wavelet function is important and rather critical. The selection of the wavelet depends on the characteristics of the signal and on the acceptability of other effects in the representation due to the wavelet function. In the following we review some popular wavelets:

a) Haar wavelet

The Haar wavelet is the first and the simplest wavelet function which was constructed by

Haar in 1910.

He was a mathematician who looked for an orthonormal system with the functions $h_0(x), h_1(x), \cdots, h_n(x), \cdots$ defined between interval $[0,1]$, such that the series

$$< f, h_0 > h_0(x) + < f, h_1 > h_1(x) + \cdots + < f, h_n > h_n(x) + \cdots \qquad (3.11)$$

where $< u, v >= \int_0^1 u(x)v^*(x)dx$

Haar chose the step function $h(x)$, called Haar's wavelet function, which is defined as:

$$h(x) = \text{rectangle}\left[2(x - 1/4)\right] - \text{rectangle}\left[2(x - 3/4)\right] \qquad (3.12)$$

which is real and antisymmetric about $t = 1/2$, as shown in Figure 3.2. For $n \geq 1$, we have $n = 2^j + k,\ j \geq 0,\ 0 \leq k \leq 2^j$, and $h_n(x) = 2^{j/2} h(2^j x - k)$. In this case, the series $h_0(x), h_1(x), \cdots, h_n(x), \cdots$ is called an orthonormal base or Hilbertian base of $L^2[0,1]$.

It is easy to show that the functions of the series are orthonormal with respect to the scalar product and they are normalized by the factor $2^{j/2}$. Several years later, it was shown that

the Haar base has the multiscale structure which is a prerequisite for wavelet function.

A major disadvantage of Haar's wavelets is the discontinuity of this wavelet which cannot provide a good approximation for smooth functions. The Fourier transform of Haar's wavelet may be written as

$$H(f) = 2i \exp(-i\pi f)\frac{1-\cos \pi f}{\pi f} \tag{3.13}$$

The decay of the Haar wavelet is very slow. Figure 3.2 shows Haar's wavelet and its Fourier spectrum.

b) Morlet wavelet

This wavelet is in essence a Gaussian modulated harmonic function which was used by J. Morlet for the analysis of sound patterns:

$$h(t) = \exp(i2\pi f_0 t)\ \exp\left(-\frac{t^2}{2}\right) \tag{3.14}$$

Its real part is an even cos-Gaussian function. The Fourier transform of the Morlet wavelet

$$H(f) = 2\pi\left\{\exp[-2\pi^2(f-f_0)^2] + \exp[-2\pi^2(f+f_0)^2]\right\} \tag{3.15}$$

is the Gaussian functions shifted to f_0 and $-f_0$:

which is even and real positive valued. This wavelet does not satisfy the admissible condition, because $H(0) \geq 0$. In practice, one often chooses f_0 so that the ratio of the highest and the second highest maximum of $h(t)$ is approximately 1:2, i.e. $2\pi f_0 \approx 5$. In this case, the value of $H(0)$ is very close to zero, i.e. $H(0) = 3.7 \times 10^{-6}$. Here, it can be considered as zero with a good approximation.

By this wavelet , the analysis is not orthogonal. The real part of the $h(t)$ and its Fourier spectrum are shown in Figure 3.3.

c) Mexican-hat wavelet

This wavelet is in fact the second derivative of the Gaussian function which is introduced by Gabor.

$$h(t) = (1 - |t|^2) \exp\left(-\frac{|t|^2}{2}\right) \tag{3.16}$$

It is even and real valued. The Fourier transform of the Mexican-hat wavelet is

$$H(f) = 4\pi^2 f^2 \exp(-2\pi f^2) \tag{3.17}$$

which is even and real valued, as shown in Figure 3.4. The decay of the wavelet coefficient is fast. This wavelet has been applied in vision analysis.

d) Meyer wavelet

Y. Meyer is a pure mathematician who constructed an orthonormal wavelet basis with excellent time-frequency localization properties in 1985. The Meyer wavelet is defined in

$$H(f) = \exp(-i\pi f)\sin[v(f)] \tag{3.18}$$

the frequency domain as

which $v(f)$ is a symmetric function defined by

$$\begin{cases} v(1-f) = \dfrac{\pi}{2} - v(f) & for \quad 1/3 \le f \le 2/3 \\ v(2f) = \dfrac{\pi}{2} - v(f) & for \quad 1/3 \le f \le 2/3 \end{cases} \tag{3.19}$$

The Meyer wavelets in the time domain can be written as follows:

One can easily check that it is a real symmetric function at $t = 1/2$. By changing the auxiliary function $v(f)$,we obtain a different family of wavelets. Although the Meyer wavelet shows rapid polynomial decay, it has wide support. This wavelet is also infinitely

$$h(t) = 2\int_0^{\infty} \sin[v(f)]\cos[2\pi(t-1/2)f]df \tag{3.20}$$

differentiable.

The Meyer wavelet for $v(x) = x^4(35 - 84x + 70x^2 - 20x^3)$ is shown in Figure 3.5.

e) Lemarie-Battle's wavelets

Lemarie was a student of Meyer who worked in harmonic analysis and Battle was a mathematical physicist who was interested in quantum field theory. Independently of one another, they developed wavelet bases consisting of spline functions. An explicit expression for this wavelet family does not exist and the properties of each member of the family can be different and depend on the choice of the spline function. For a constant spline, the wavelets become similar to Haar wavelets. More detail for constructing filters using this wavelet family may be found in [11].

Although the wavelets have exponential decay which is an improvement over the decay of the Meyer wavelet, they loose regularity and are not compactly supported. One of the wavelets is shown in Figure 3.6.

f) Daubechies wavelets

Apart from the Haar wavelet function, almost all the orthonormal wavelet functions listed above consist of infinitely supported functions. One desirable property is to have a wavelet with compact support in the time domain, i.e., it is time limited in that it is non-zero only over a given interval. Such a wavelet gives a true sense of time locality. Daubechies constructed a family of orthogonal wavelets which converge to continuous functions with compact support. These wavelets have no explicit expression except for $db1$, which is the Haar wavelet. The Daubechies family wavelets are real but neither symmetrical nor asymmetrical and their regularity increases as the order of Daubiechies' wavelet increases. One member of the Daubechies family ($D4$) is shown in Figure 3.7. Details of the procedure for constructing au orthonormal base of compactly supported wavelets may be found in Daubechies' original paper [10].

These wavelets have other desirable properties. It can be shown that they are bounded, continuous functions and they are continuously differentiable.

3.3.2 Discrete wavelet transform

In order to apply the wavelet transform for digital signals, the wavelet parameters s, τ must be discretized. If we consider $s = S_0^m$ and $\tau = nS_0^m T_0$, the corresponding wavelets become:

$$h_{mn}(t) = s_0^{-m/2} \cdot h\left(s_0^{-m} t - nT_0\right) \tag{3.21}$$

where $m, n \in Z, \quad S_0 \succ 1, \quad T_0 \neq 0$

This way of discretization may be modified to give a dyadic grid by considering $S_0 = 2, \quad T_0 = 1$; therefore

$$h_{mn} = 2^{-m/2} \cdot h\left(2^{-m} t - n\right) \qquad m, n = 1,2,\ldots \tag{3.22}$$

It is possible to obtain an orthonormal basis for special choices of $h(t)$. The dyadic sampling grid in the time-scale plane is shown in Figure 3.8(a). The scale axis is often expressed in terms of frequency under transformation $s \rightarrow k / f$ where k is a constant. In fact, it can be shown that the Short-Time Fourier Transform, time-frequency distributions and time-scale methods (wavelet transforms) are members of a common class of energy

representations [16, 8]. A comparison between the basis functions and the time-frequency plane of the Short-Time Fourier Transform (STFT) and those of the wavelet transform is shown in Figure 3.8(b) and 3.8(c); the self-adjusting window (zooming) property is the major difference between the wavelet transform and the STFT. The zooming property of the wavelet transform is similar to a microscope or a telescope, where the resolution is automatically adjusted to a different scale of magnification. As shown in Figure 3.8(c), the important properties of the wavelet transform, such as its localisability and changeable resolution in the time and frequency domains, make it both more suitable and more effective in the analysis of non-stationary vibration signals such as transients.

The implementation of the wavelet transform according to (3.22) may only be carried out with some difficulty because, as m increases, $h(t)$ must be sampled at progressively more points. This makes the computations very slow. In 1989, Stephane Mallat [17, 7] proposed an efficient discrete-time algorithm for the computation of the wavelet transform. Mallat, using quadrature mirror filters and multi-resolution analysis, constructed a new algorithm for the computation of the wavelet transform, which calculates the wavelet coefficients very rapidly. It is called the Fast Wavelet Transform and its idea comes from a method called subband coding, which has been used in speech compression. Subband coding, which consists of two branches with filtering followed by down sampling by two, can decompose a signal into two parts. The part that is passed through a low-pass filter gives an

approximation of the signal, and the part that is passed through a high-pass filter gives the detail. It is interesting to note that the original signal can be recovered from its two filtered and subsampled parts if the filters have the property of perfect reconstruction, as shown in Figure 3.9(a). Such filters are called quadrature mirror filters. As shown in equation (3.8), a wavelet transform can be interpreted as a decomposition of a signal into a set of frequency channels of different band widths. Mallat's algorithm is a cascade extension of this elementary two-channel filter bank in a binary tree structure, as shown in Figure 3.9(b).

A review of discrete-time wavelet transform and the relationship between wavelet transform and filter banks is given by Shensa [19], Vetterli et al. [15, 18].

2.3. Wavelet packet transform and adaptive wavelet transforms

In wavelet transform, the frequency axis has a logarithmic scale which gives good frequency resolution at lower frequencies and good time resolution in the higher frequencies. For this reason, it is suggested that the wavelet transform be used to analyse signals with long-duration events in the lower frequencies and short-duration events in the higher frequencies.

The generalisation of the discrete-time wavelet transform is called the wavelet packet transform and can be described as a full-tree-structured filter bank, as shown in Figure 3.10. An interesting advantage of the wavelet packet is that the frequency axis has linear scale

which gives better frequency resolution in the higher frequencies, at the price of some loss of time resolution.

It is clear that the wavelet transform is appropriate for signals with transient phenomena in the higher frequencies; however, it may perform less well over other time-frequency transforms. The resolution exchange between time and frequency in the wavelet transform is always fixed and independent of the signal being analysed. This may not be satisfactory in the analysis of an arbitrary class of signals with either unknown or time-varying characteristics. To improve the performance of the wavelet transform, it is necessary to use the signal-adaptive transform, which is more satisfactory than the original fixed transform although it is important to ensure that this flexibility does not come at too great a cost.

There are two way of achieving this objective:

a) By selecting filter banks to optimize the time and frequency resolutions:

we may select the binary trees in filter banks by taking the characteristics of the signal into account, instead of using the fixed tree of the wavelet transform or the wavelet packet transform, as shown in Figure 3.11. In this way, we can locally exchange resolution in time for resolution in frequency and vice versa.

b) By optimizing the wavelet function with respect to the signal structure:

the second way involves the construction of waveform libraries and the choice of those particular waveforms which are the best adapted for the decomposition of the signal structures. Such waveforms are called time-frequency atoms and the libraries of waveforms are called the dictionary of time-frequency atoms.

One method which follows the idea of searching for good representation from a dictionary of time-frequency atoms is the method of matching pursuit [21]. This method is a linear decomposition of any signal into waveforms that are selected from a dictionary of Gabor functions.

A general family of time-frequency atoms can be generated by scaling $(s > 0)$, translating (τ) and frequency modulating (ξ) a single window function $g(t)$.

$$g_\gamma(t) = \frac{1}{\sqrt{s}} g\left(\frac{t-\tau}{s}\right) e^{i\xi t} \tag{3.23}$$

where the index $\gamma = (s, \tau, \xi)$ denotes an element of this family of atoms. The $g(t)$ is the Gaussian window $g(t) = 2^{1/4} e^{-\pi t^2}$.

Then $f(t)$ can be written

$$f(t) = \sum_{n=-\infty}^{+\infty} a_n g_m(t) \tag{3.24}$$

where a_n are the expansion coefficients which provide some information on certain types of properties of $f(t)$, depending upon the choice of the atoms $g_m(t)$.

This method is particularly suitable for decomposing signals whose localizations in time and frequency vary widely.

3.3.4 De-noising

Removing noise from a signal by wavelet analysis is one of the most recent applications of wavelets [22].

The idea of de-noising by wavelet analysis consists of decomposing the signal by wavelet transform, removing noise from components, and reconstructing the signal.

Wavelet analysis is a linear method; therefore the wavelet coefficients of the linear combination of two signals are equal to the linear combination of their wavelet coefficients.

$$W_{(f_1+f_2)} = W_{f_1} + W_{f_2} \tag{3.25}$$

A noisy signal can be modeled in the following form:

$$f(t) = s(t) + e(t) \tag{3.26}$$

Where *f(t)* is a noisy signal, *s(t)* is the original signal, and *e(t)* is the noise. Eliminating the noise part of the signal may be done in three following steps:

a) Compute the wavelet decomposition of the signal *f(t)*

b) Determine a limit for optimal de-noising and suppress only the portion of the wavelet coefficients that exceeds this limit.

c) Reconstruct the signal with the help of modified wavelet coefficients *s(t)*.

In practice, the decomposition and reconstruction procedures are accomplished respectively by the fast wavelet transform and the inverse fast wavelet transform.

It is clear that the performance of the de-noising method depends mostly on the step *(b)*. Suppressing a part of a signal, called the thresholding procedure, is carried out using different optimization techniques, which give different threshold values [23]. In the next section, we will see how this application of the wavelets can improve the wavelet transform

representation of signals.

3.4 Application of the wavelet transform to machinery fault diagnosis

The wavelet transform is one of the newer methods of time-frequency analysis that have been used in various science and engineering fields in recent decades. Although the wavelet transform has been applied to image processing and speech recognition with great success, there have been only a few applications in machinery diagnostics, for example, the work of McFadden et al. in the application of the wavelet transform to fault detection in a gearbox [24, 27]. Damage in bearing elements is one of major problem in rotating machines that can be detected by the wavelet transform [28, 29]. Fault detection and identification in a helicopter gear-box was carried out by Lopez et al. [30].

It has been shown that, in the diagnosis of faults in reciprocating machines, the wavelet transform may be considered as a satisfactory technique for extracting the characteristics of vibration signals [31]. Zhongxing and Liangsheng [32] used the wavelet packet technique to analyse the vibration signals of a compressor. In another approach, Dalpiaz and Rivola [2, 33] applied the wavelet transform to the condition monitoring and diagnostics of cam mechanisms. We note that in most of the above applications the Gaussian wavelet function was chosen as a mother wavelet function.

3.4.1 Software for wavelets transforms

A user-friendly software has been developed to permit the use of different methods of time-frequency analysis such as the Short-Time Fourier Transform, the Wigner-Ville Distributions, and the Wavelet Transforms. The program allows the user to carry out different distributions of Cohen's class of time-frequency methods such as the Choi-Williams Distribution and the Born-Jordan-Cohen Distribution. In addition, it provides different kinds of wavelet transforms, for example: the wavelet transform, the wavelet packet transform, and the wavelet transform by the Gabor Dictionary. In addition, the new technique of the "zoom in wavelet transform" makes it possible to obtain very satisfactory frequency resolution.

This program has been developed especially for the diagnosis of defects in machinery, and includes most of the commonly-used methods of time-frequency analysis. We have tried to use those kernels and filters which are compatible with the current signals in machine diagnostics. The program has some interesting options which are of considerable practical value in such cases. For example, de-noising by wavelet transform, which is an important tool in the analysis of noisy signals, allows the user to obtain an improved time-frequency representation.

Some examples from simulated signals have been used to verify the function and accuracy of the program. The first example is the sum of three sines: 300Hz, 1000 Hz and 3000 Hz;

the time frequency plane shows three constant frequency bands. Although the wavelet transform of the signal, as shown in Figure 3.12(b), indicates a concentration of the signal's energy in the three bands, there is also the dispersion of this energy in the adjacent bands especially when an incorrect filter is chosen, as shown in Figure 3.12(c). On the other hand, it is impossible to determine the exact values of the frequencies by the logarithmic scale of the frequency axis.

The wavelet packet transform of this example gives better representation in the time-frequency plane than the wavelet transform of this signal (Figure 3.13). The linear scale of the frequency axis gives better frequency resolution. Filter selection plays an important role here also.

The matching pursuit algorithm gives the best representation of this signal, as shown in Figure 3.14. The resolution of frequencies in the time-frequency plane is very satisfactory.

The second example is a Dirac function in 0.1 sec. This function is an example of transitory signals. The wavelet transform of the example is shown in Figure 3.15. This time, the wavelet transform gives the best representation of the signal in the time-frequency plane. The peak appears exactly at 0.1 sec. The very good time resolution provided by the wavelet transform in the higher frequencies makes it a powerful tool for the detection of transitory phenomena in the signals.

The wavelet packet transform shows the Dirac function in approximately 0.1 sec (Figure 3.16). Its time resolution is not as satisfactory as that of the wavelet transform. There is a difference between the results obtained by the wavelet transform and those obtained by the wavelet packet transform (the wavelet packet transform has better frequency resolution in the higher frequencies than the wavelet transform, but at the expense of a loss of time resolution in these frequencies).

The matching pursuit algorithm gives a representation of the signal that is not as good as that given by the wavelet transform, but is better than that given by the wavelet packet transform, as shown in Figure 3.17.

The next example is an amplitude-modulated cosine at 1000 Hz. The wavelet transform representation of the signal in the time-frequency plane shows the modulation of the signal. To obtain a clear representation of this signal, it is preferable to see simultaneously the mean-square wavelet map (three-dimensional representation) of the signal, as shown in Figure 3.18. The wavelet packet transform of the signal accompanied with the mean-square wavelet packet map of the signal is shown in Figure 3.19. Here, we use Haar wavelet function which provides a good time resolution. To obtain clear representation of the signal in frequency, we can use a Daubechies 20 wavelet function which provides good frequency resolution at the expense of a loss of time resolution.

For this type of signal, the matching pursuit algorithm is not recommended because the

modulation is not displayed (Figure 3.20).

The final example is a frequency-modulated signal at 1000 Hz. The wavelet transform and the mean-square wavelet map of the signal are shown in Figure 3.21. In the time-frequency plane, the representation of the signal is once again unclear. If there are other components in the signal, it will be very difficult to identify the signal. The mean-square wavelet map of the signal is not clear, either.

The wavelet packet transform gives a better representation of the signal than the wavelet transform; in particular, the mean-square wavelet packet map of the signal is clear, as shown in Figure 3.22.

Again, the matching pursuit algorithm cannot be recommended because the frequency modulation cannot be identified (Figure 3.23).

3.4.2 Experimental application of the wavelet transforms

After comparing the theoretical behavior of several variations of the wavelet transform when applied to different signals, we now investigate signals obtained from experimental cases. A pin-point defect with known characteristics and location was created on a rolling bearing. The test set-up consisted of an electric motor, a shaft mounted on two journal bearings (SKF

1210 EKTN9 self-aligning, double row), labelled 2 and 3, a gear-box and a break to impose the load. The defect was created on support A by scratching the inner raceway of the bearing with an electric pen. Figure 3.24 shows the experimental set-up.

The vibration signal was measured on support A by an accelerometer and transferred to an analyser. The measured signal was converted into American National Standard Code for Information Interchange (ASCII) format and transferred to the in-house software program for analysis.

The frequencies of different types of bearing defect may be computed using the geometric characteristics of the bearing and the rotating frequency [34]. The geometric characteristics of the damaged bearing are as follows:

Pitch diameter D=69 mm

Diameter of the rolling body d=10.32 mm

Contact angle α =7.87 deg

Number of rolling elements N =17 (per row)

Bearing frequency of rotation F_r=12.2 Hz

The frequency defect caused by damage on the inner raceway of this bearing can be computed by the following formula:

$$F_i = \frac{F_r N}{2}\left[1 + \frac{d}{D}\cos(\alpha)\right] \tag{3.27}$$

Equation (3.25) gives us a value for the pass frequency on a point of the inner raceway which equals approximately 238 Hz. Note that the frequency of this type of defect has a special characteristic. The default frequency should be an amplitude-modulated wave at approximately 238 Hz with the frequency of modulation equal to the rotating frequency.

Figures 3.25-3.26 show respectively the wavelet transform and the wavelet packet transform of the vibrational signal of the defected bearing. It is almost impossible to identify the defect by theses figures because the original signal is very noisy. To obtain clear representation of the signal, it is necessary to remove at first the noise from the signal. To do this, there are two possibilities in the software: *De-noising by classical wavelet transform* and *De-noising by Matching Pursuit algorithm*. Here, we use the de-noising by matching pursuit algorithm and The de-noised signal is called *dn-bearing*. Figures 3.27-3.28 show respectively the wavelet transform and the wavelet packet transform of the de-noised signal. As shown, the wavelet transform of the de-noised signal clearly shows the repetitive peaks in frequency band 200-400 Hz. The frequency of amplitude modulation in this band is approximately 12.2

Hz which equals to the rotating frequency. Then, the default in bearing may be easily be identified by the wavelet transform of the de-noised signal. The wavelet packet transform of this signal provides more frequency resolution but it is not as clear as the wavelet transform of the signal. The default frequency is situated in frequency band 200-300 Hz.

3.4.3 Industrial application of the wavelet transform

In the last section, the performance of wavelet transforms for a defect created on the inner raceway of a bearing was described. In this section, the efficiency of wavelet transforms for an industrial case without any prediction of defects is demonstrated. This case comes from the defective gear-train of a hoist drum in a large shovel operating at an open-pit iron mine.

Gearbox faults may be classified into shaft (misalignment, imbalance) and tooth (wear, scuffing, cracking) related problems. Damage to a single tooth is called a local tooth fault, and will be investigated in this section. Vibration signals measured on a gearbox include the tooth-meshing frequency, transient events caused by defects, gearbox resonance vibrations and system and sensor transmission characteristics. These vibration signals are non-stationary signals which require specific techniques because application of the conventional methods, such as Fourier analysis, to gearbox fault detection are often difficult. Time-frequency methods provide new techniques for the analysis of non-stationary signals and

have advanced capabilities for the separation of different phenomena. The application of some time-frequency methods to the analysis of gearbox faults has been described in [3, 4], and here, the application of another group of time-frequency methods, called time-scale analysis, is presented.

The time signal of the damaged gearbox and its wavelet transform are shown in Figure 3.29. The repetitive pulses in the wavelet transform in the band between 320 Hz and 640 Hz are caused by a broken tooth. The mean square wavelet map of this signal gives representation of the wavelet transform in three dimensions. The wavelet packet transform of the signal in Figure 3.30 gives not only a better time-frequency representation of the signal but also better frequency resolution than the wavelet transform. The mean square wavelet packet of the signal clearly shows the pulses.

The time-frequency plane projection by the Gabor Dictionary of the signal is shown in Figure 3.31 but it is not easy to obtain the characteristics of the signal from this figure.

Although the mean square wavelet packet map of the signal gives the best representation of the signal, the frequency resolution of the signal may not be as fine as is needed. To obtain a finer frequency resolution , we can use the *zoom in wavelet transform* which is based on choosing the best trees in the filter bank. By this method, first, the desired frequency band is selected and, second, a suitable frequency resolution is achieved by wavelet packet transform of this frequency band. A *zoom in wavelet transform* in the frequency band

between 320 Hz and 640 Hz is shown in Figure 3.32.

3.5 Conclusion

The above study has shown the performance of a new method for the diagnosis of defects in machinery. We have demonstrated that the wavelet transform provides a high frequency resolution in the lower frequencies and a high time resolution in the higher frequencies. This characteristic of the wavelet transform may be advantageous in machinery fault detection. The wavelet functions play an important role in obtaining a good representation of a signal and they are chosen in accordance with the characteristics of the signal.

The wavelet packet transform is a full tree filter bank which gives a linear-scale frequency axis. It gives better frequency resolution than the wavelet transform but the latter gives superior time resolution. In machine monitoring and fault detection, it is sometimes necessary to have high frequency resolution in order to identify the type of defect and, in this case, one could recommend the use of the wavelet packet transform. However, this approach does result in a loss of information in the time domain and the time-frequency representation becomes complicated. For this reason, we have presented a new technique which is called the "zoom in wavelet transform". This technique permits us to obtain desirable frequency resolution with clear time-frequency representation.

This article has also presented an easy-to-use software package which includes the majority of methods of time-frequency analysis and compares the wavelet transforms with other methods. The software is equipped with several interesting options such as a new method of de-noising by wavelet transform. This method, which has been applied recently in signal processing, improves the time-frequency representation of noisy signals.

The transient and the time-varying signals in machine condition monitoring present different behavior in their time-duration. The adaptive wavelet transforms are powerful tools which are capable of decomposing the signal into those waveforms that are best adapted to the signal structure.

A computer program implementing the wavelet transforms has been used to compare the performance of different wavelet methods. It has been shown, by the numerically generated signals and two experimental tests on a damaged bearing and a broken gear tooth, that the wavelet analysis methods are effective in machine condition monitoring especially when a transient phenomenon exists in the signal. In the case where a defect in a machine generates amplitude-modulation signals or frequency-modulation signals, it is preferable to use other time-frequency methods such as the Wigner-Ville distributions or the STFT.

3.6 References

1. P. Grivelet 1990 Proceedings of the IMMDC Congress, Los Angeles, 393-399, Monitoring of Reciprocating Compressors Automatics Machines.

2. G. Dalpiza and A. Rivola 1995 2nd International Symposium Acoustical and Vibratory Surveillance Methods and Diagnostic Techniques, 327-338, Fault Detection and Diagnostics in Cam Mechanisms.

3. M. S. Safizadeh, A. A. Lakis and M. Thomas 1999 École Polytechnique de Montréal, Technical Report No. EPM/RT-99/05, Application of Short-Time Fourier Transform in Machine Fault Detection.

4. M. S. Safizadeh, A. A. Lakis and M. Thomas 1999 École Polytechnique de Montréal, Technical Report No. EPM/RT-99/06, Fault Detection and Identification using Wigner-Ville Distributions.

5. J. Morlet and Al 1982 Geophysics 47(2), 203, Wave Propagation and Sampling Theory-part II: Sampling Theory and Complex Waves.

6. A. Grossmann and J. Morlet 1984 SIAM J. Math. Anal. 15, 723-736, Decomposition of Hardy Functions into Square Integrable Wavelets of Constant Shap.

7. S. Mallat 1989 IEEE Transaction on Pattern Analysis and Machine Intelligence

11(7), 674-693, A Theory for Multi Resolution Signal Decomposition: The Wavelet Representation.

8. Y. Meyer 1990 Ondelettes et Opérateurs (two volumes). Paris: Hermann.

9. Y. Meyer 1992 Les Ondelettes Algorithmes et Applications, PP. 127-133, Paris: Armand Colin.

10. I. Daubechies 1988 Commun. Pure Appl. Math., Vol. XLI, 909-996, Orthonormal Based of Compactly Supported Wavelets.

11. I. Daubechies 1992 Ten Lectures on Wavelets, Philadelphia: SIAM.

12. ---- 1993 IEEE Trans. Signal Process. 41(8), 2591-2606, A Discrete-Time Multiresolution Theory.

13. M. Vetterli and J. Kovacevic 1995 Signal Processing in Wavelets and Subband Coding, Englewood Cliffs, NJ: Prentice-Hall.

14. N. Hess-Nielsen and M. V. Wickerhauser 1996 Proceedings of the IEEE 84(4), 523-539, Wavelets and Time-Frequency Analysis.

15. K. Ramchandran and M. Vetterli 1996 Proceeding of the IEEE 84(4), 541-560, Wavelets, Subband Coding and Best Bases.

16. O. Rioul and M. Vetterli 1991 IEEE SP Magazine, 14-38, Wavelet and Signal Processing.

17. S. Mallat 1987 Tech. Rep., Dep. Comput. Inform. Sci., Univ. Pennsylvania, Philadelphia, PA, Multi Resolution Approximation and Wavelets.

18. M. Vetterli 1992 IEEE Trans. Signal Processing 40(9), 2207-2232, Wavelets and Filter Banks : Theory and Design.

19. M. J. Shensa 1992 IEEE Trans. Signal Processing 40(10), 2464-2482, The Discrete Wavelet Transform: Wedding The À Trous and Mallat Algorithms.

20. R. R. Coifman and M. V. Wickerhauser 1992 IEEE Trans. Inform. Theory, Special Issue on Wavelet Transforms and Multires. Signal Anal. 38(3), 713-718, Entropy-Based Algorithms for Best Basis Selection.

21. S. Mallat 1993 IEEE Trans. Signal Processing 41(12), 3397-3415, Matching Pursuits with Time-Frequency Dictionaries.

22. D. L. Donoho and I. M. Johnstone 1994 CRAS Paris, t. 319, Ser I, 1317-1322, Idea De-noising in an Orthonormal Basis Chosen from a Library of Bases.

23. D. L. Donoho 1995 IEEE Trans. On Inf. Theory, 41(3), 613-627, De-noising by Soft-Thresholding.

24. W. J. Wang and P. D. McFadden 1993 American Society of Mechanical Engineers, Petroleum Division (Publication) PD Structural Dynamics and Vibrations Proceedings of the 16th Annual Energy - Sources Technology Conference and Exhibition 52, Application of the Wavelet Transform to Gearbox Vibration Analysis.

25. W. J. Staszewski and G. R. Tomlinson 1994 Mechanical Systems and Signal Proceesing 8, 289-307, Application of the Wavelet Transform to Fault Detection in a Spur Gear.

26. P. D. McFadden 1994 Proceedings of an International Conference on Condition Monitoring, Swansea UK, 172-183, Application of the Wavelet Transform to Early Detection of Gear Failure by Vibration Analysis.

27. W. J. Wang and P. D. McFadden 1995 Mechanical Systems and Signal Processing 9, 497-507, Application of Wavelets to Early Gear Damaged Detection.

28. C. J. Li and J. Ma 1992 Sensors and Signal Processing for Manufacturing, ASME Winter Annu. Meet., Bearing localized Defect Detection Through Wavelet Decomposition of Vibrations.

29. Mei Hongbin 1995 Proceedings of the International Conference on Structural Dynamics, Vibration, Noise and Control, 1334-1339, Application of Wavelet Analysis to Detection of Damages in Rolling Element Bearings.

30. J. E. Lopez, R. Tenney and J. Deckert 1994 Proc. IEEE-SP Int. Symp. on Time-Frequency and Time-Scale Analysis, 217-220, Fault Detection and Identification Using Real-Time Wavelet Feature Extraction.

31. P. Grivelet 1990 Proceedings of the IMMDC Congress, Los Angeles, Monitoring of Reciprocating Compressors by Vibration.

32. G. Zhongxing and Q. Liangsheng 1994 British Journal of Non-Destructive Testing 36(1), 11-15, Vibrational Diagnosis of Machine Parts Using the Wavelet Packet Technique.

33. G. Dalpiaz and A. Rivola 1997 Mechanical Systems and Signal Processing 11, 53-73, Condition Monitoring and Diagnostics in Automatic Machines: Comparison of Vibration Analysis Techniques.

34. R. G. Smiley 1983 Sound and Vibration 17(9), Rotating Machinery: Monitoring and Fault Diagnosis.

3.7 Nomenclature

$f(t)$	Magnitude of the vibration signal with zero mean
$R_f(\tau, t_1)$	Instantaneous correlation function
$S_f(\omega, t_1)$	Instantaneous spectrum density function
$F_f(\omega)$	Spectrum of the signal $f(t)$
$h(t)$	Transformation kernel
$STFT_f(t, \omega)$	Short-time Fourier transform of the signal $f(t)$
$W_f(s, \tau)$	Wavelet transform of the signal $f(t)$
$h_{s\tau}(t)$	Mother wavelet function
s	Scale of wavelet transform
τ	Time shift of wavelet transform

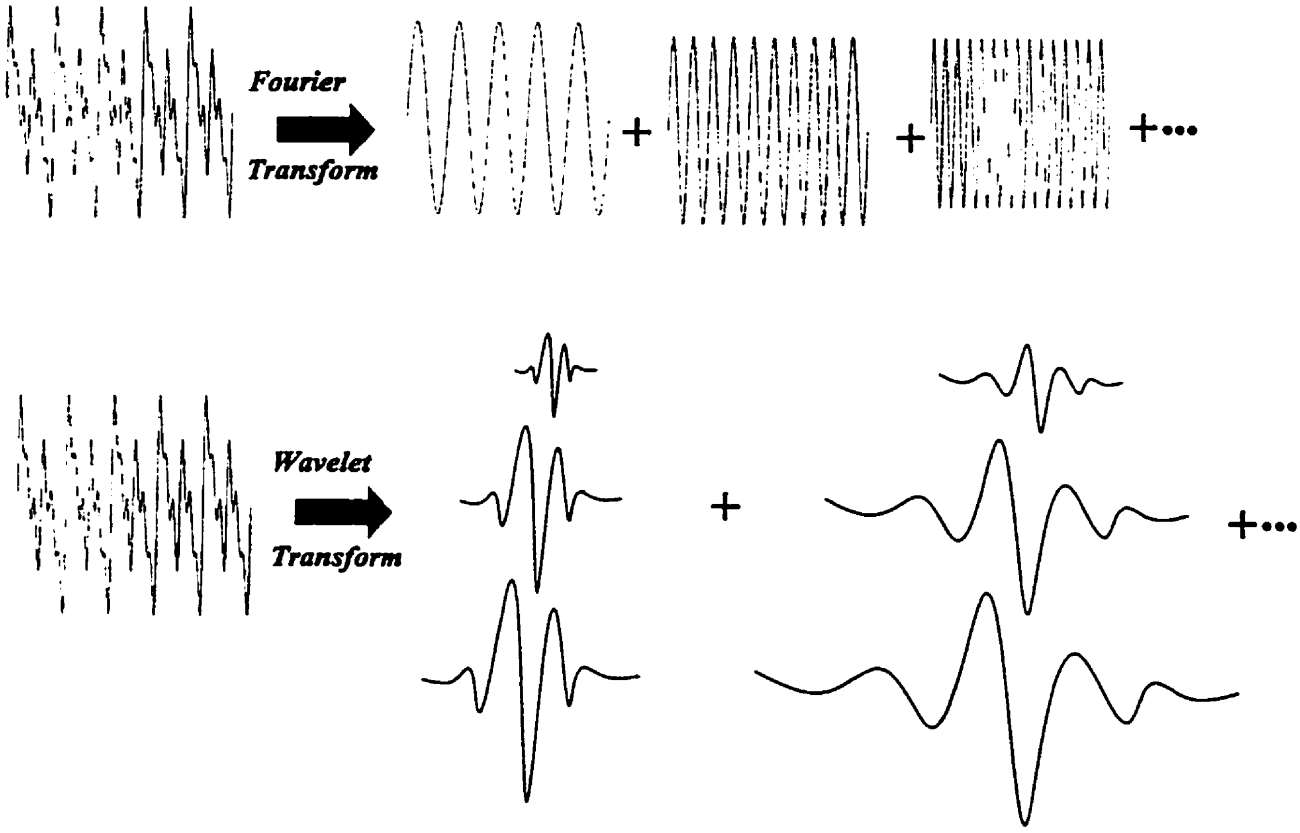

Figure 3.1: Comparison between Fourier transform and Wavelet transform

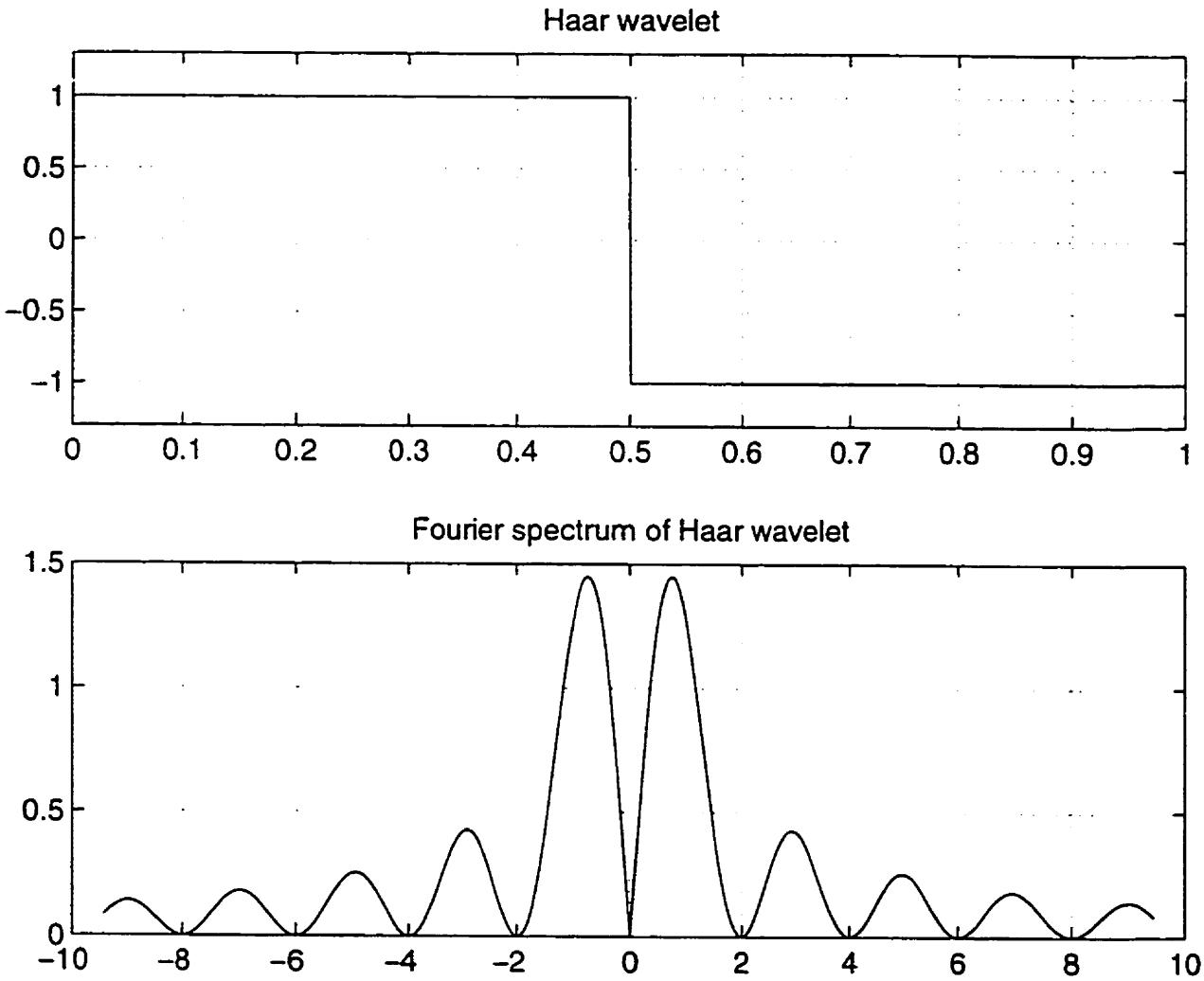

Figure 3.2: Haar wavelet and its Fourier spectrum

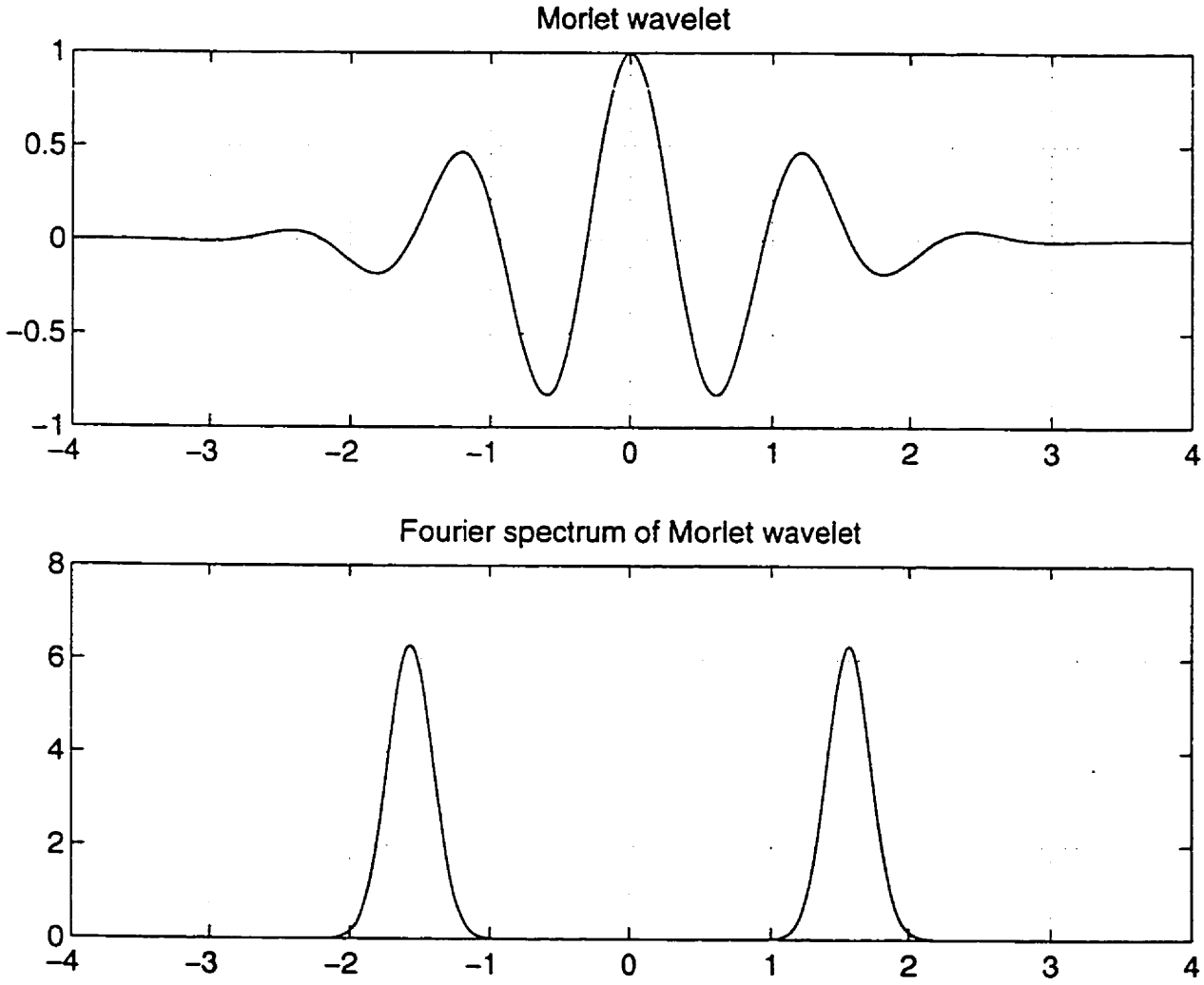

Figure 3.3: Morlet wavelet and its Fourier spectrum

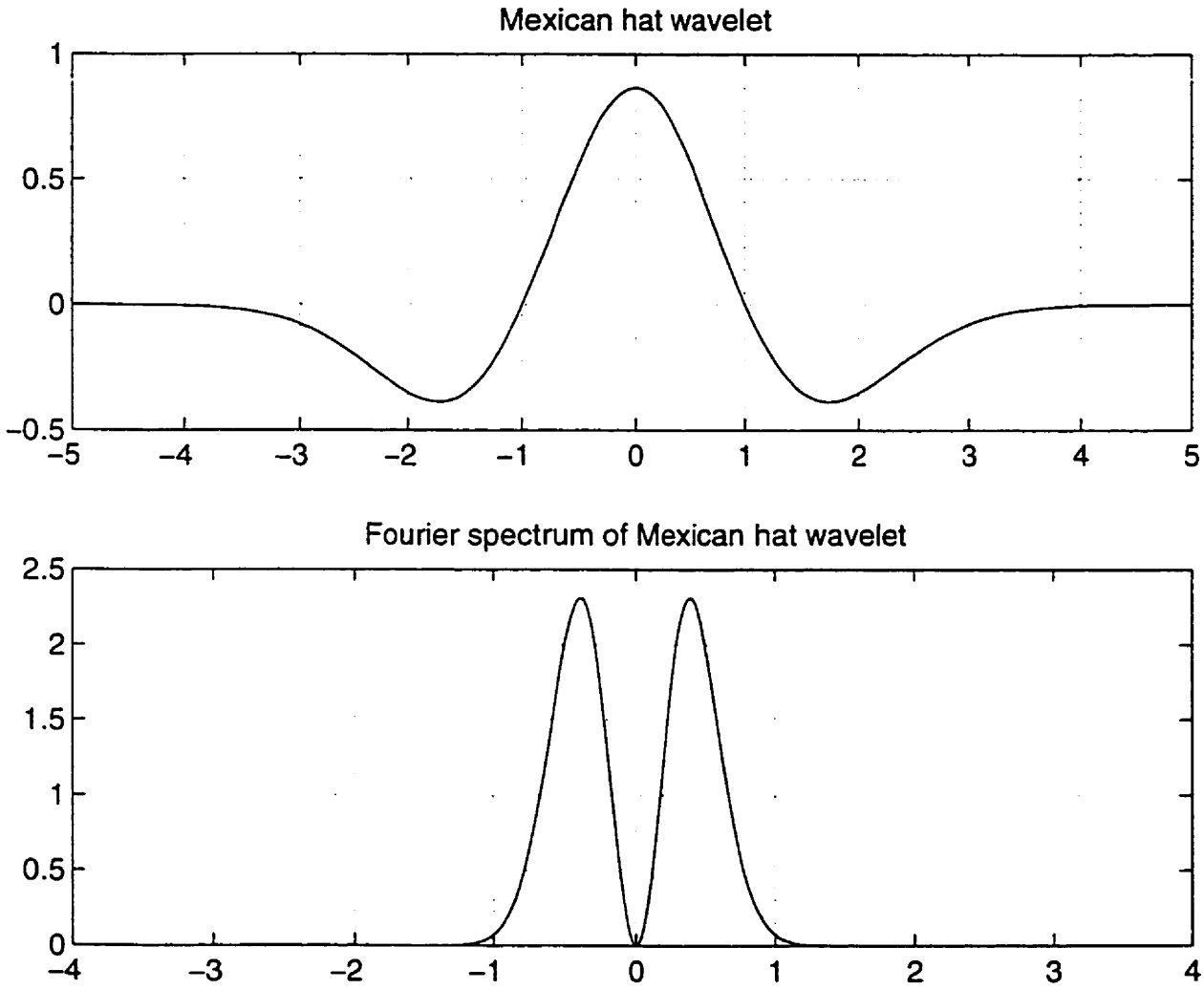

Figure 3.4: Mexican-hat wavelet and its Fourier spectrum

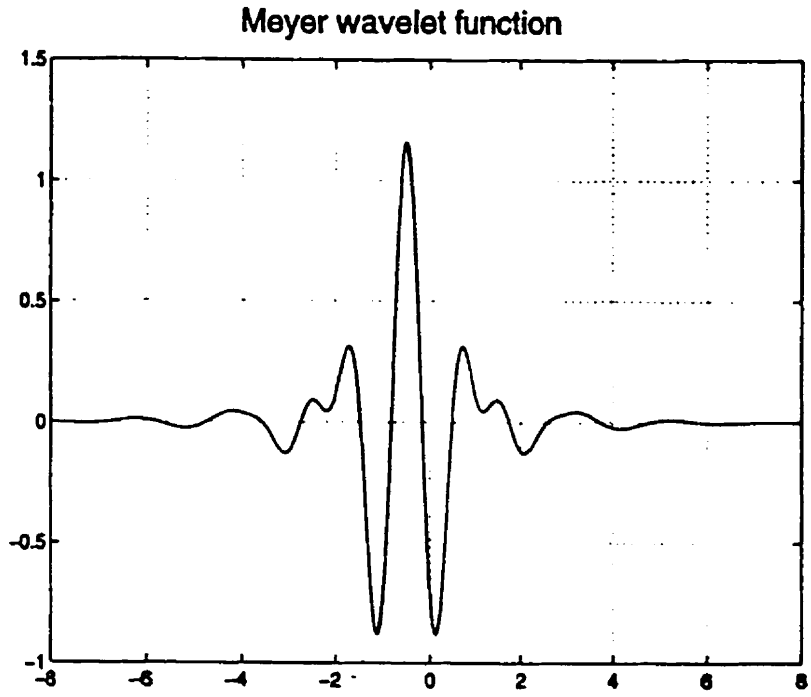

Figure 3.5: Meyer Wavelet function

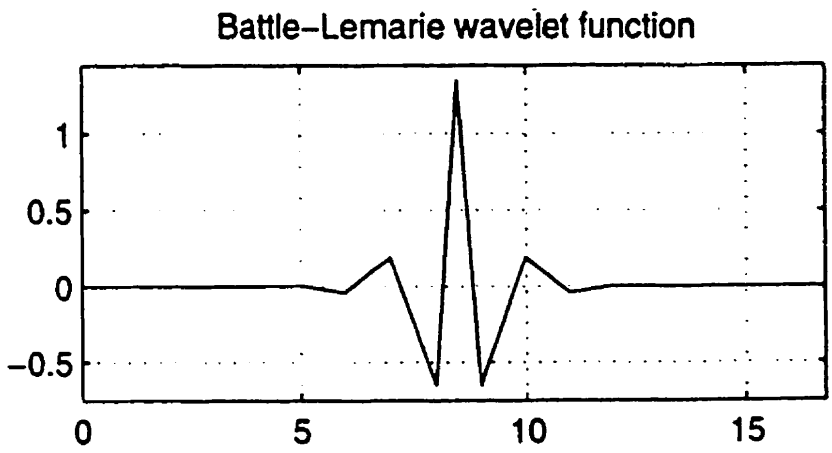

Figure 3.6: Lemarie-Battle wavelet function

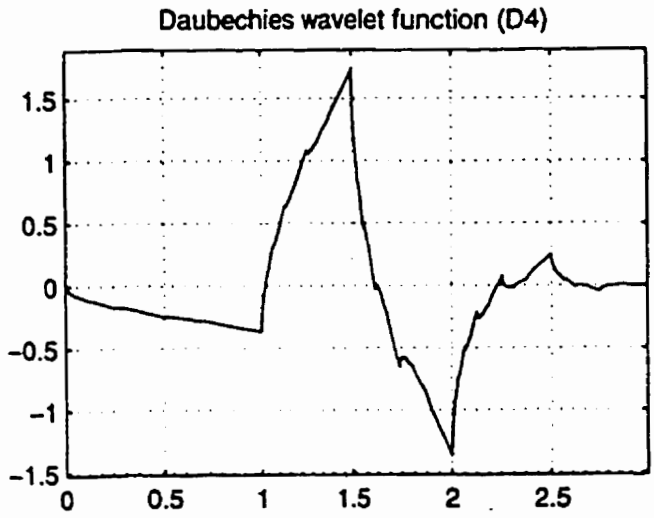

Figure 3.7: Daubechies wavelet function

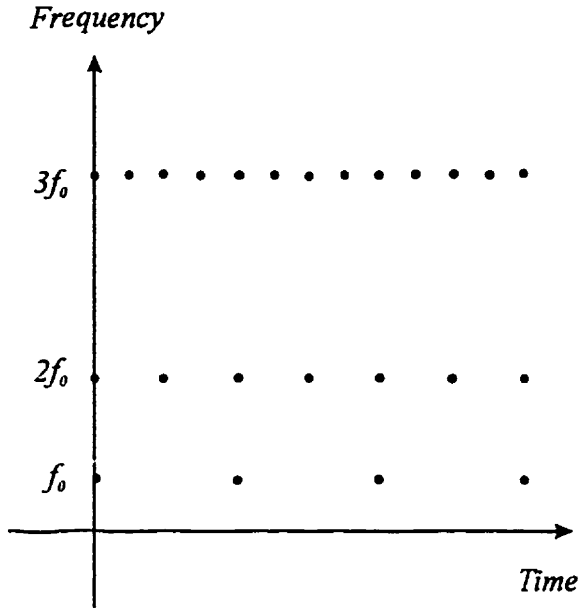

(a)

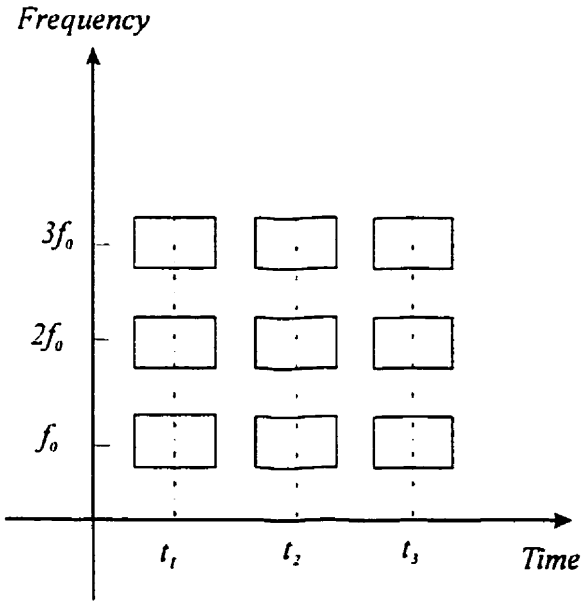

(b)

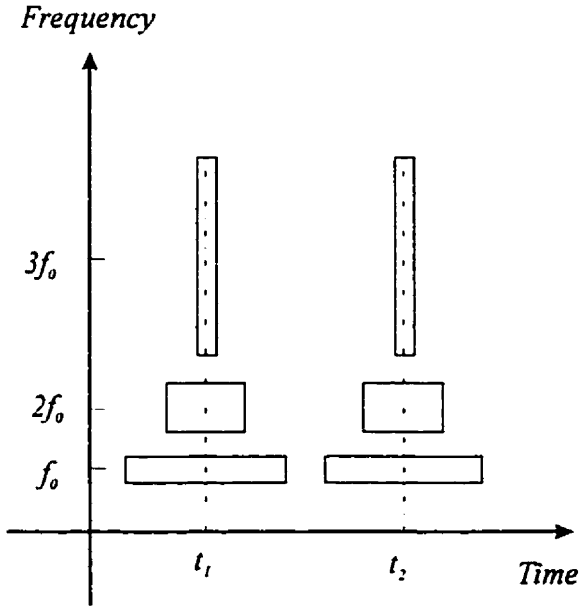

(c)

Figure 3.8: (a)Dyadic sampling grid in the time-scale plane;
(b)Time-frequency plane of the short-time Fourier transform;
(c) Time-frequency plane of the wavelet transform.

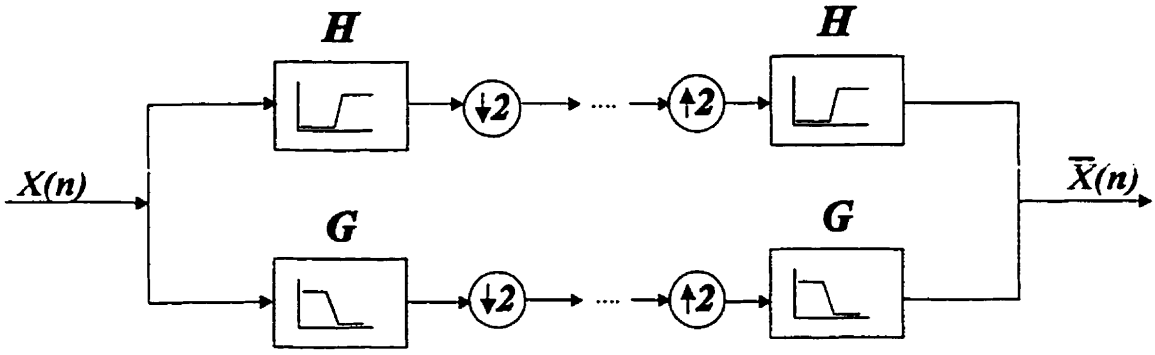

(a)

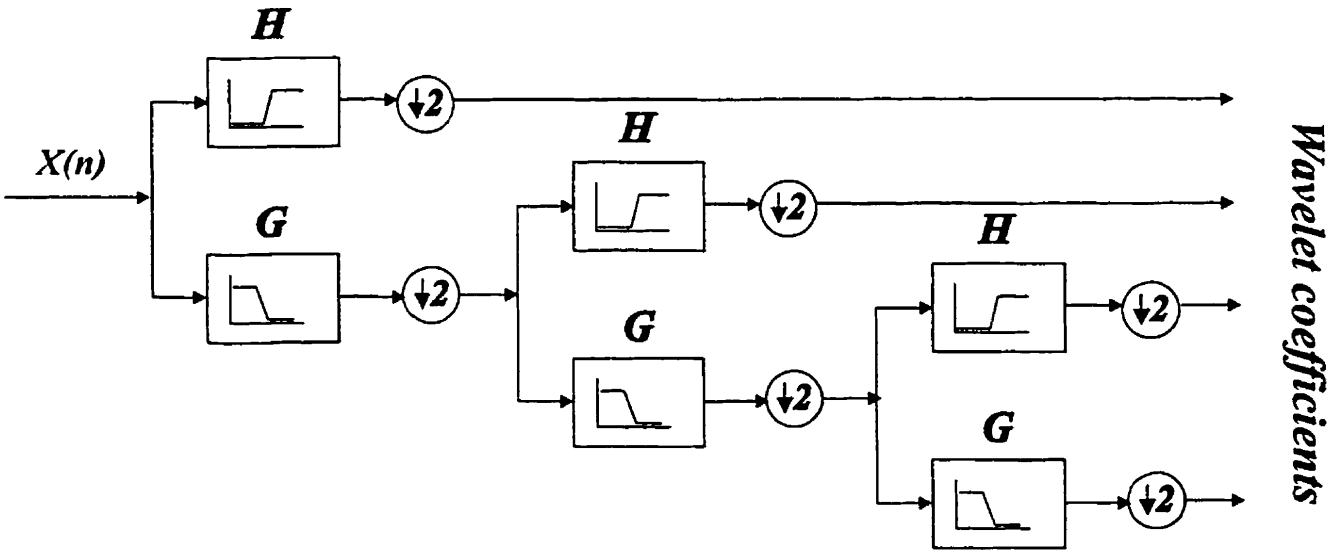

(b)

Figure 3.9: (a) Subband coding scheme H: high pass filter and G: low pass filter;
(b) Filter bank tree of the discrete wavelet transform.

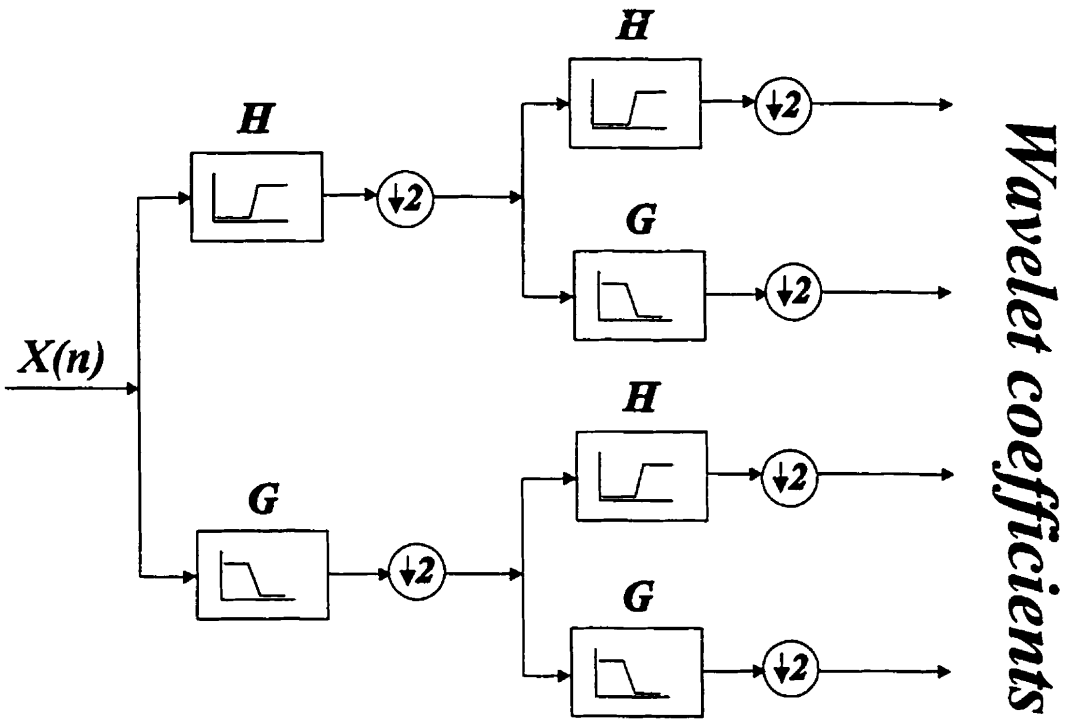

Figure 3.10: Filter bank tree of the wavelet packet transform.

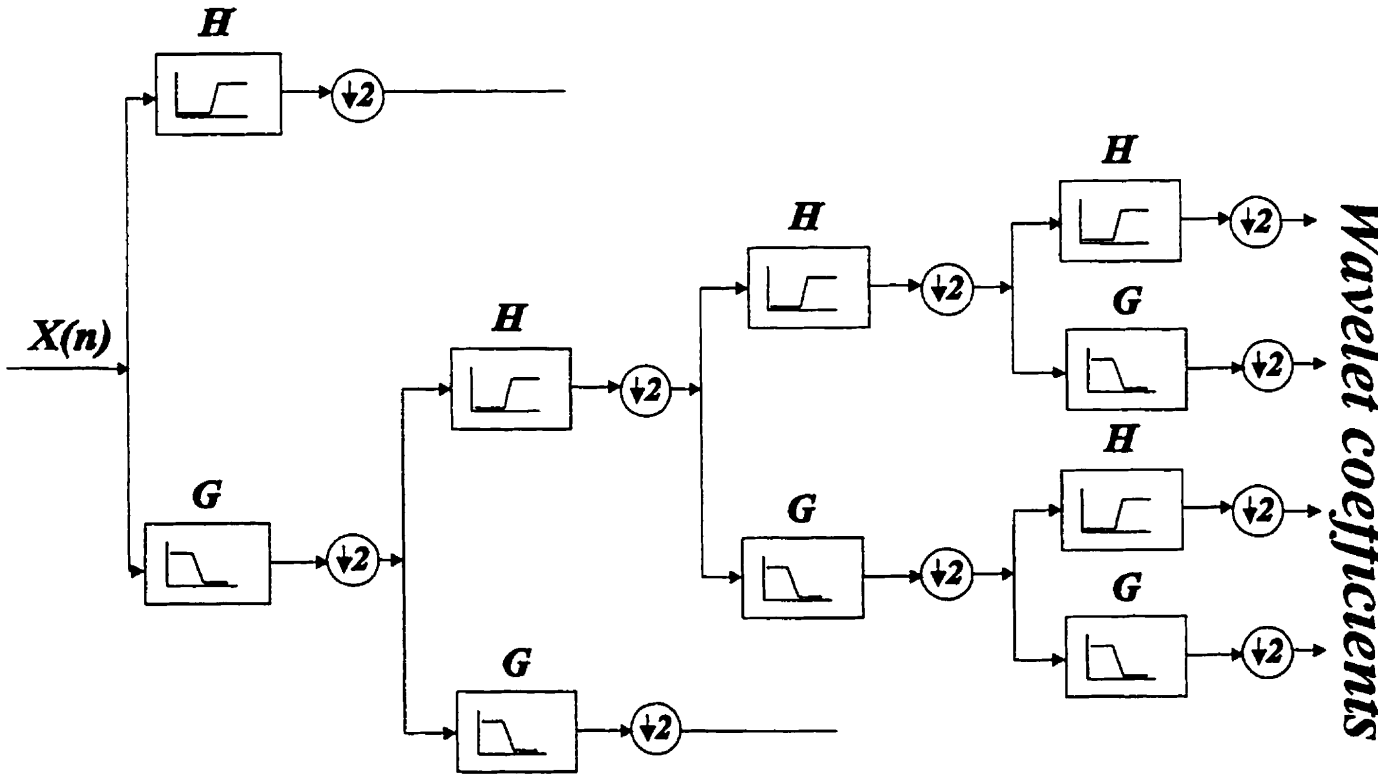

Figure 3.11: Block diagram of the zoom in wavelet transform.

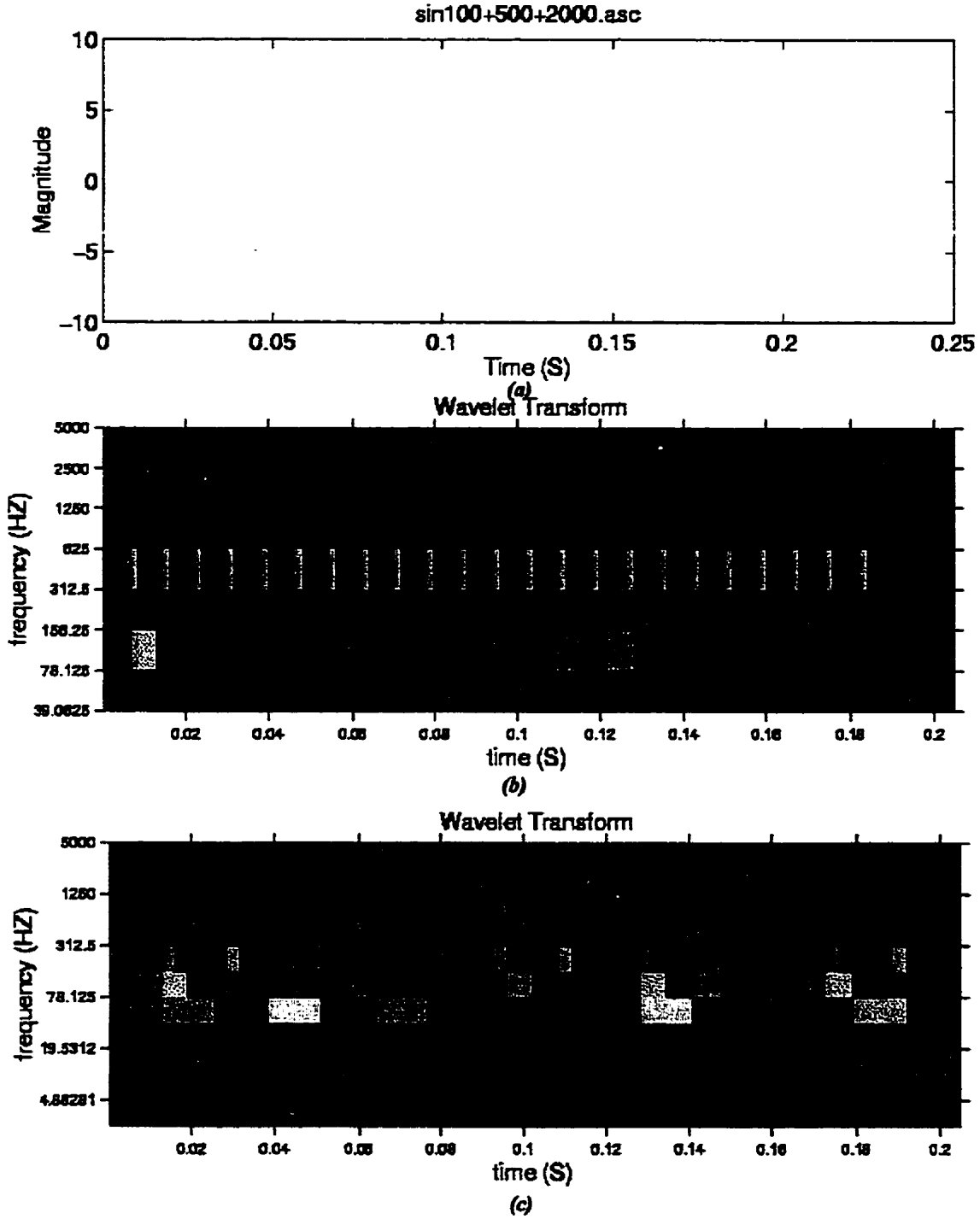

Figure 3.12: (a) Time representation of the sum of sine waves
(b) The wavelet transform of the sum of sine waves by Daubechies filter (D20)
(c) The wavelet transform of the sum of sine waves by Daubechies filter (D2)

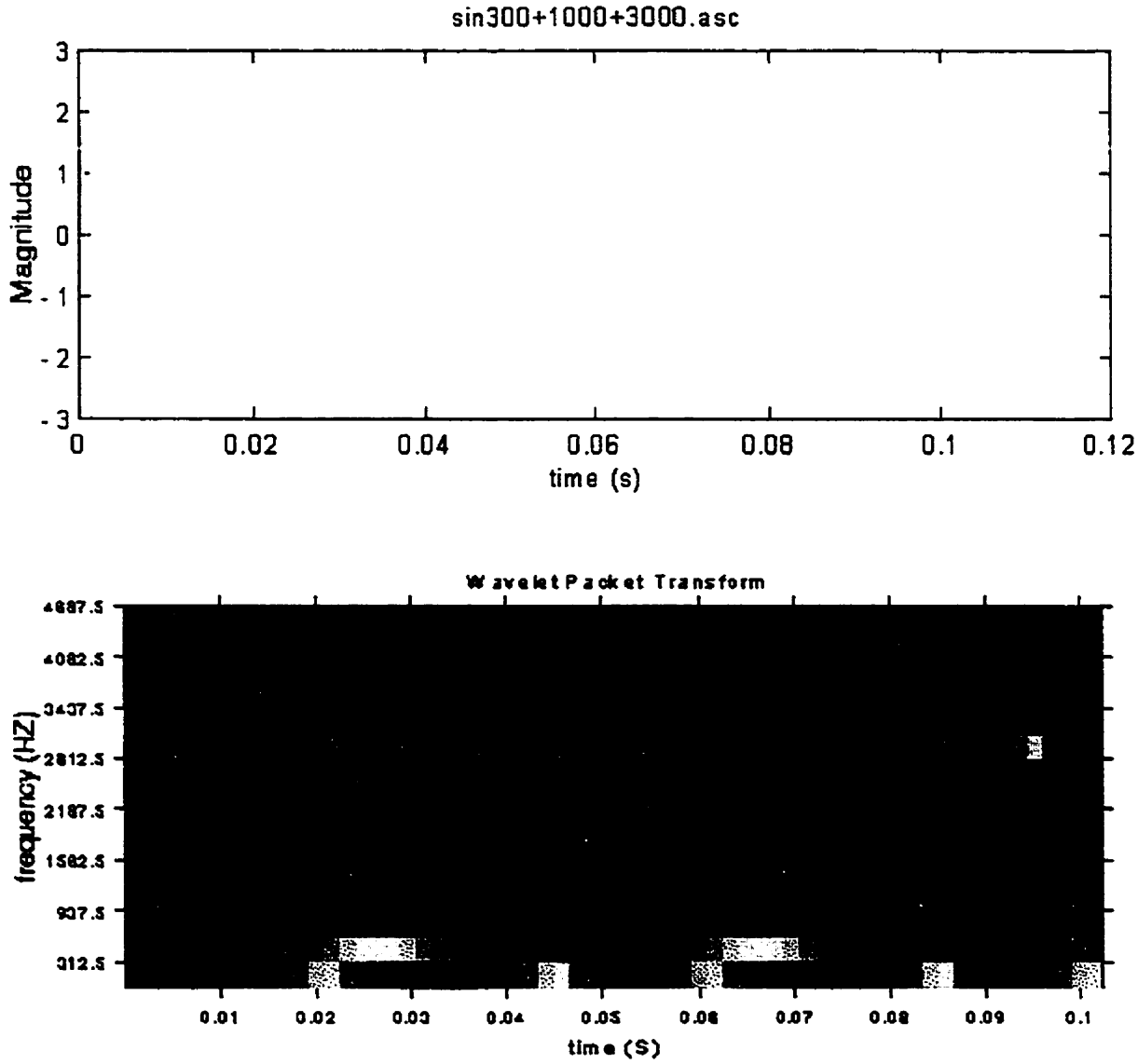

Figure 3.13: Wavelet packet transform of a sum of sine waves.

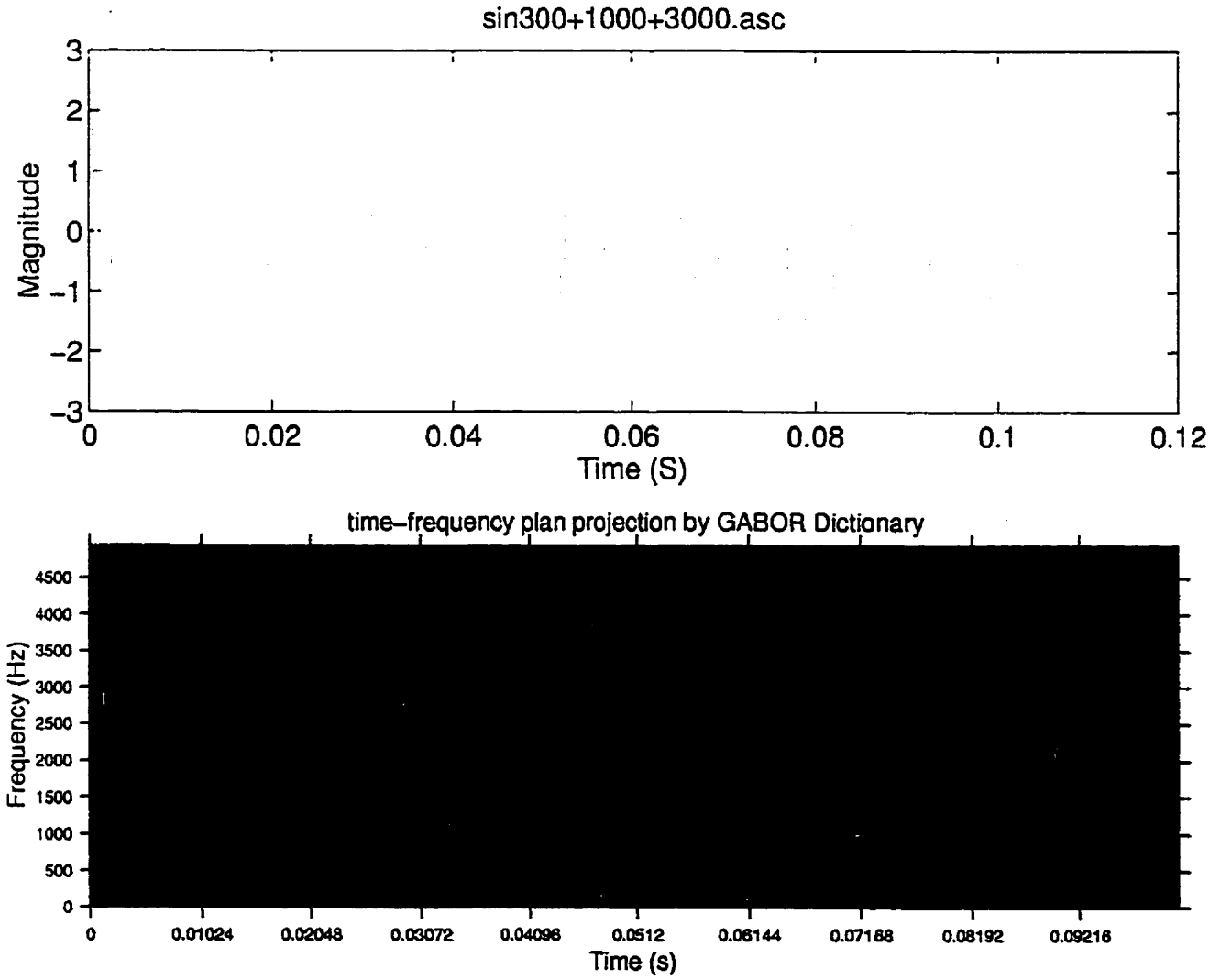

Figure 3.14: Time-frequency representation of a sum of sines wave by the Gabor dictionary.

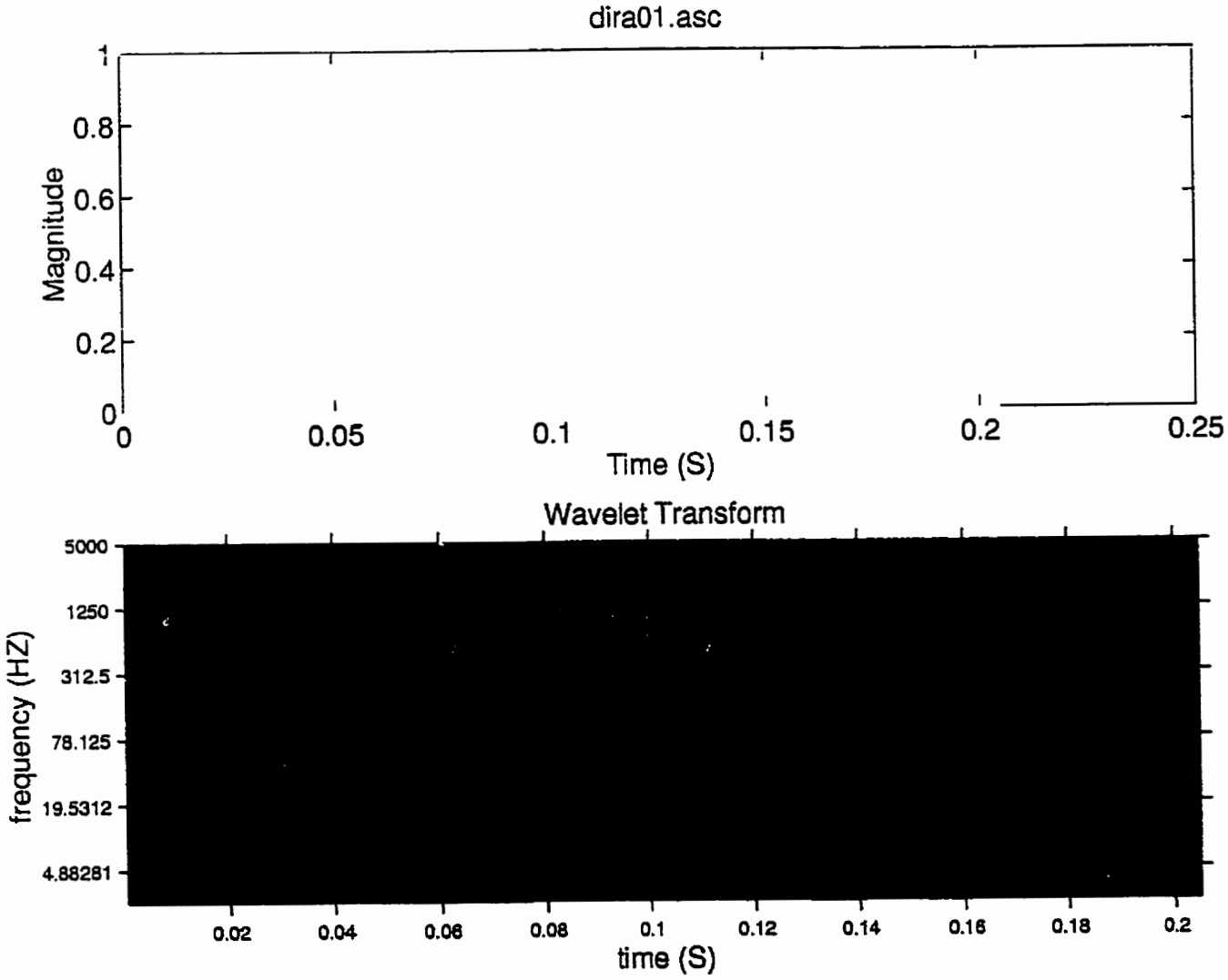

Figure 3.15: Wavelet transform of a Dirac function.

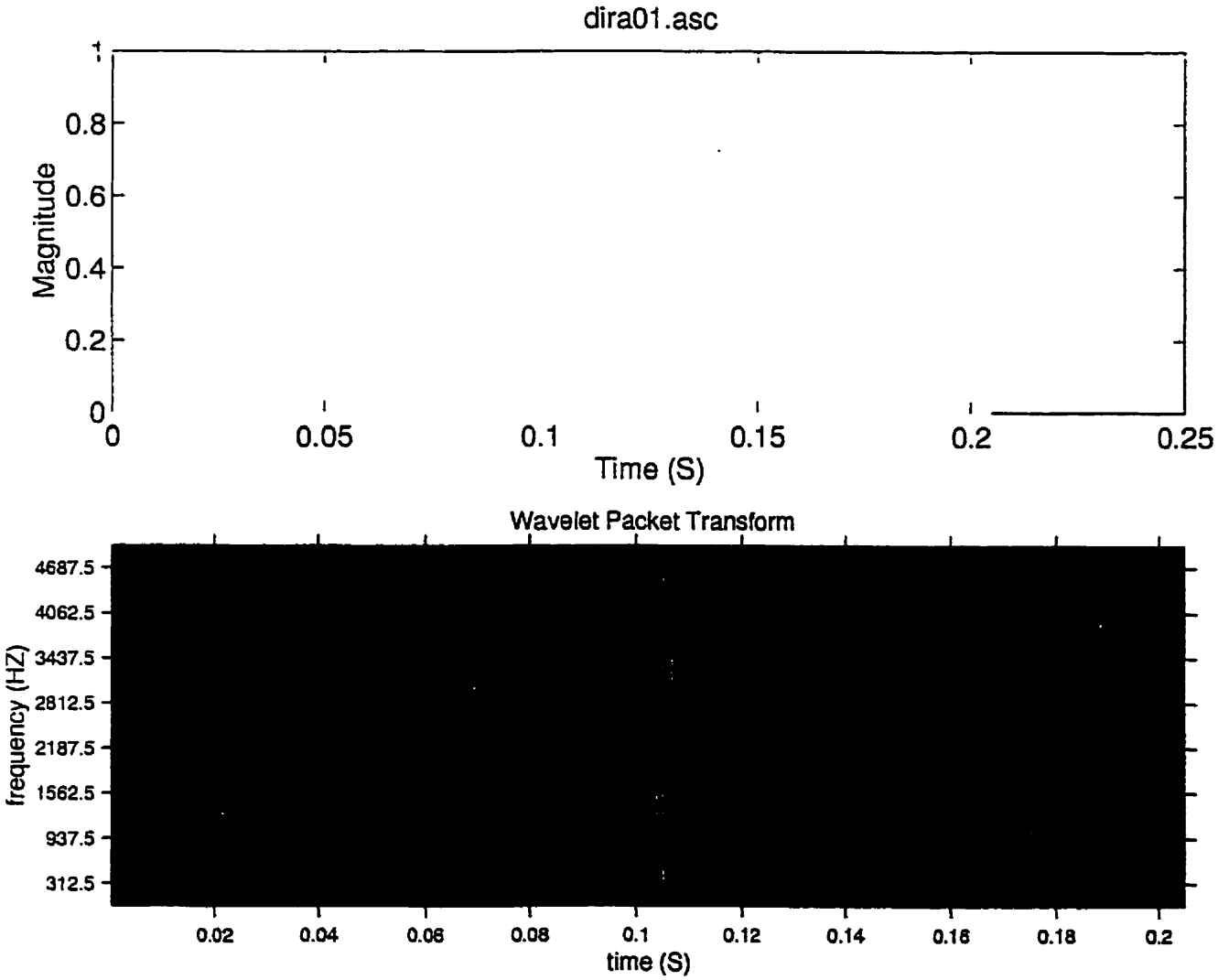

Figure 3.16: Wavelet packet transform of a Dirac function.

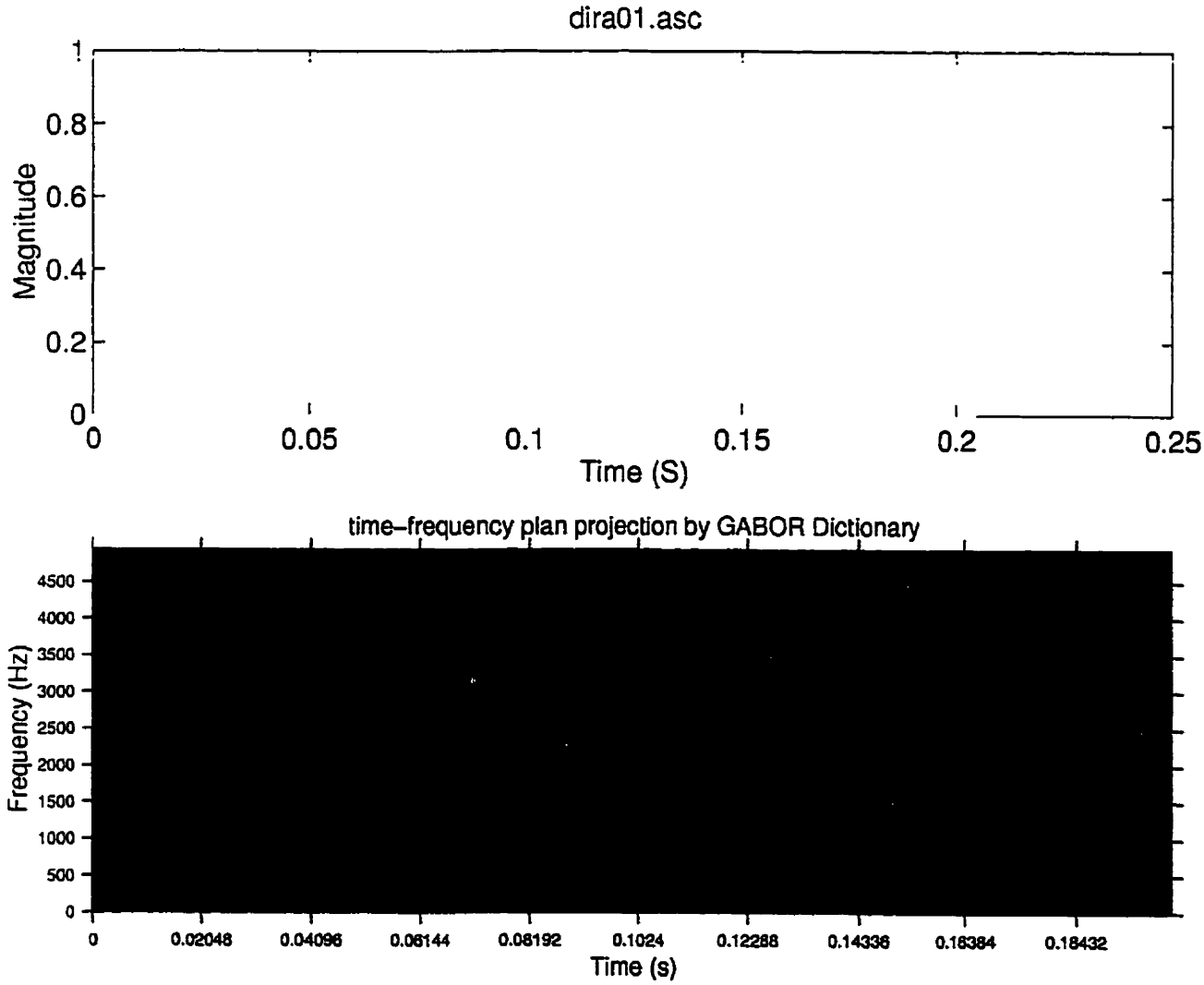

Figure 3.17: Time-frequency representation of a Dirac function by the Gabor dictionary.

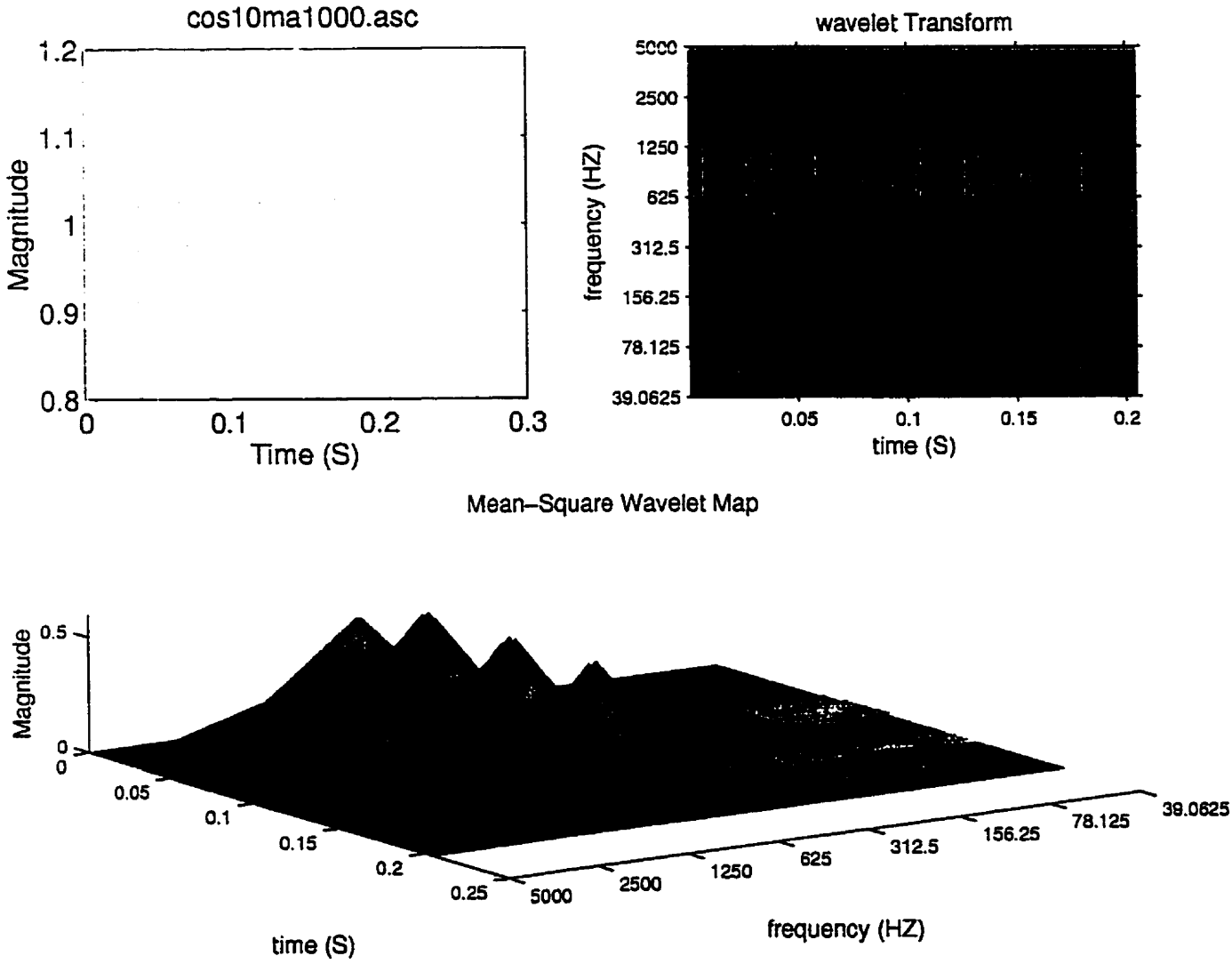

Figure 3.18: Wavelet transform and mean-square wavelet map of an amplitude-modulated sine.

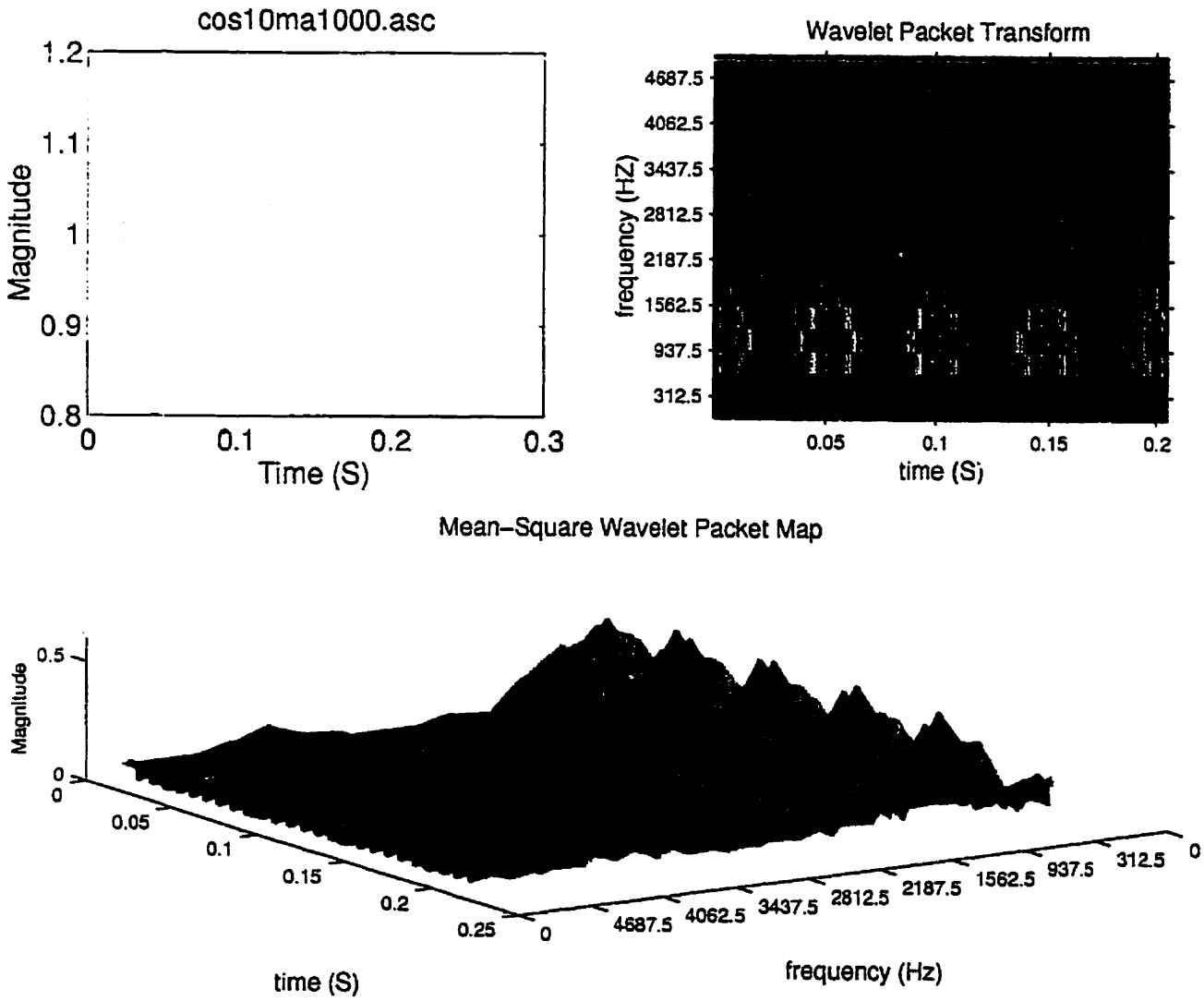

Figure 3.19: Wavelet packet transform and mean-square wavelet packet map of an amplitude-modulated sine.

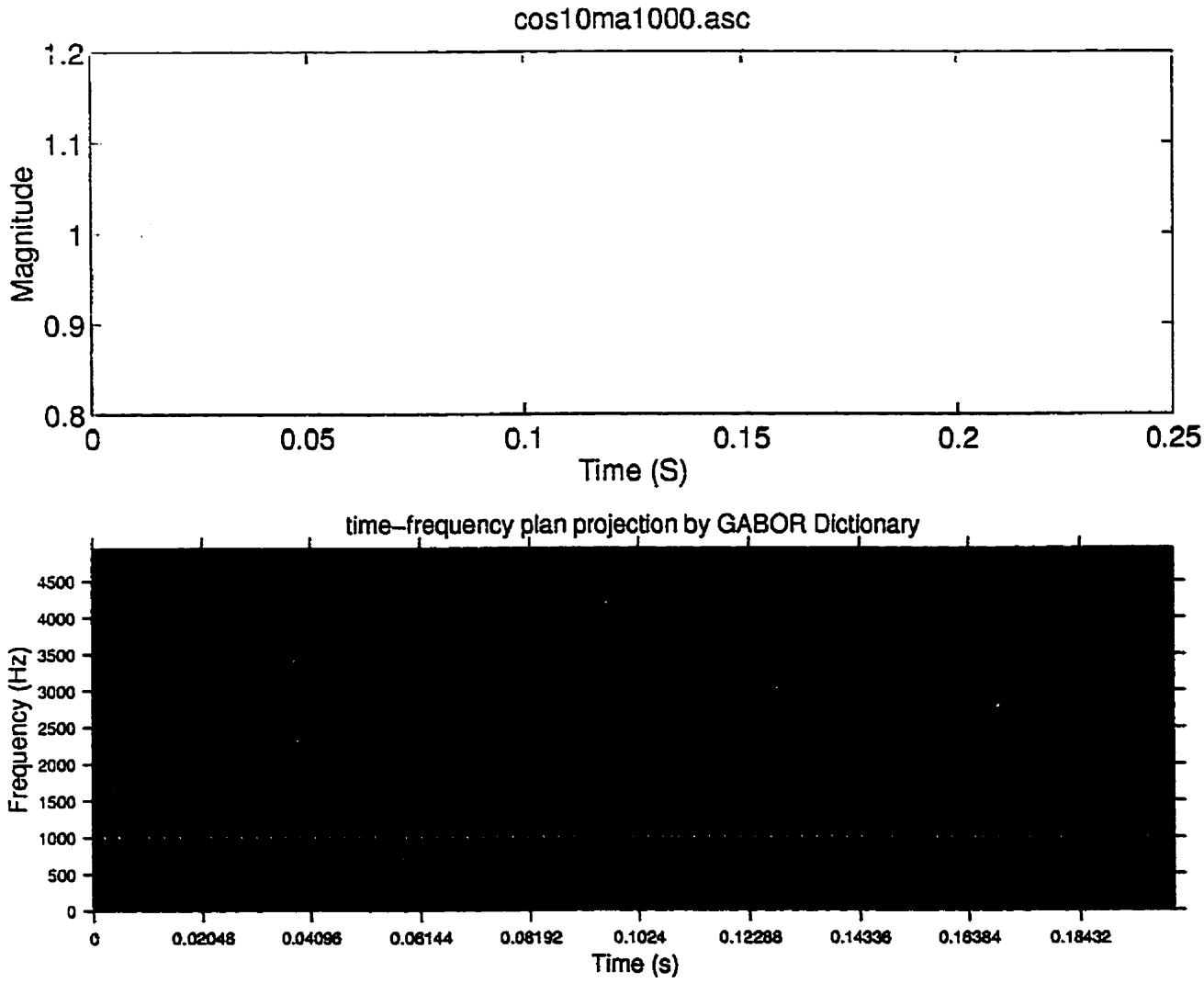

Figure 3.20: Time-frequency representation of an amplitude-modulated sine by the Gabor dictionary.

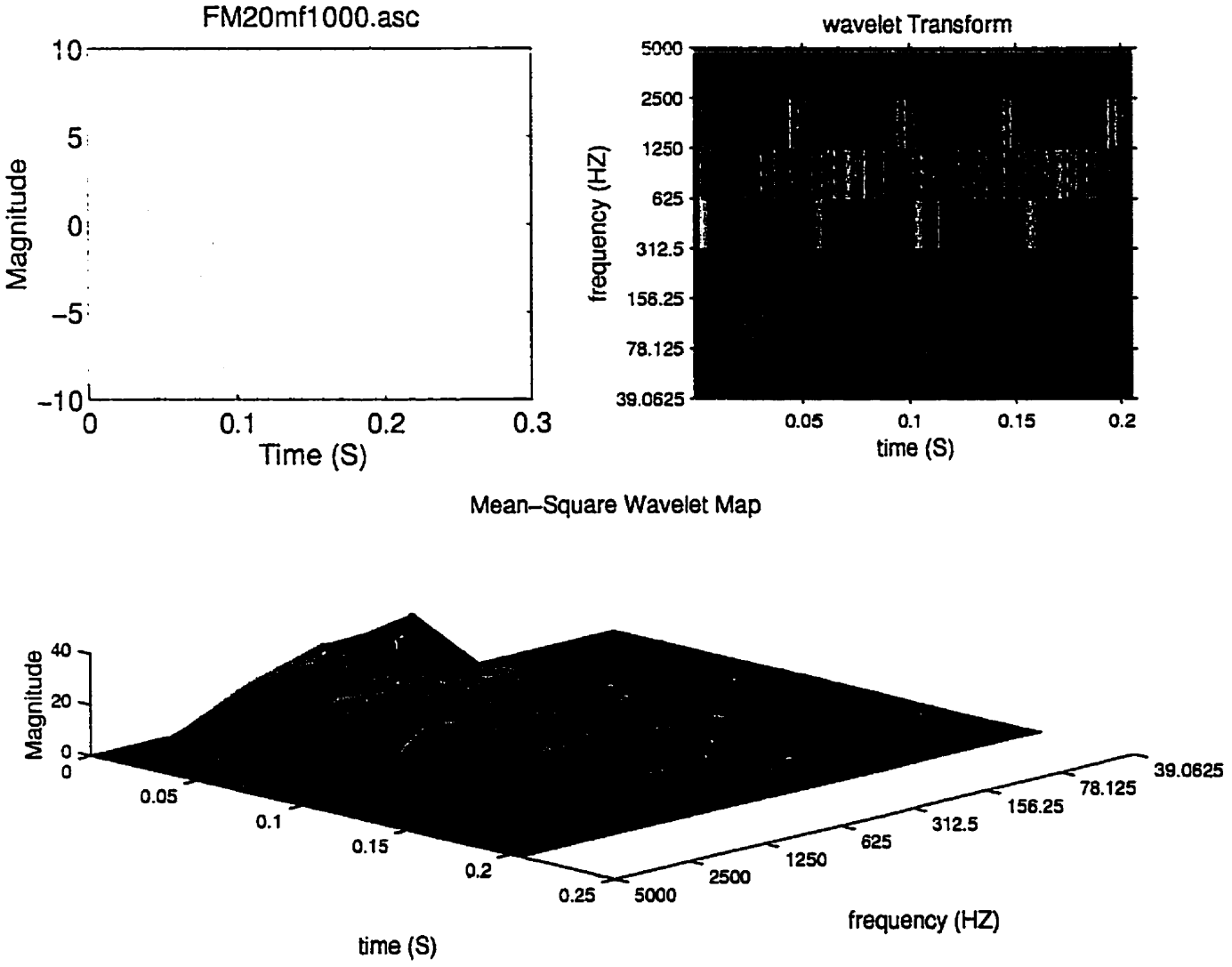

Figure 3.21: Wavelet transform and mean-square wavelet map of a frequency-modulated sine.

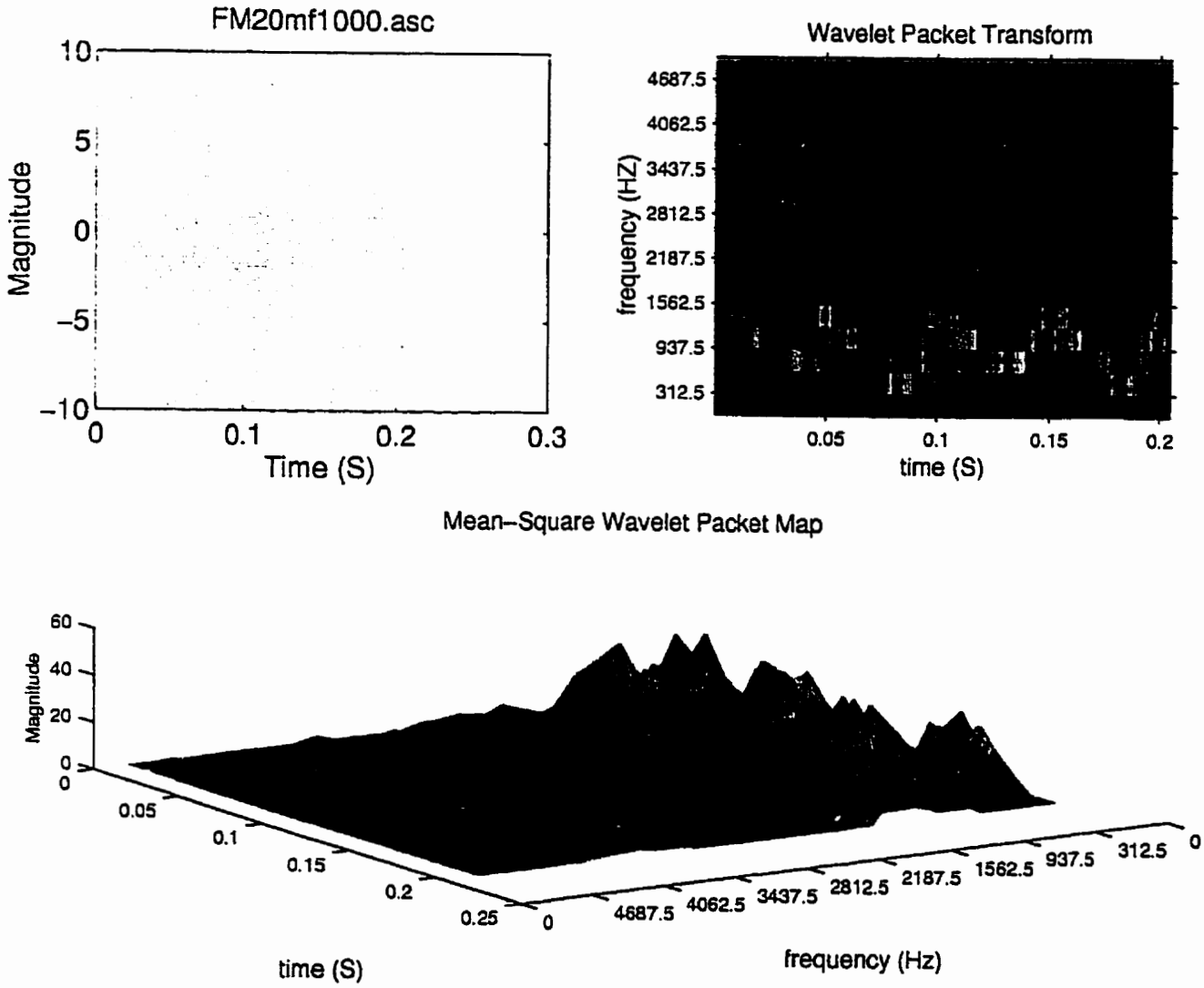

Figure 3.22: Wavelet packet transform and mean-square wavelet packet map of a frequency-modulated sine.

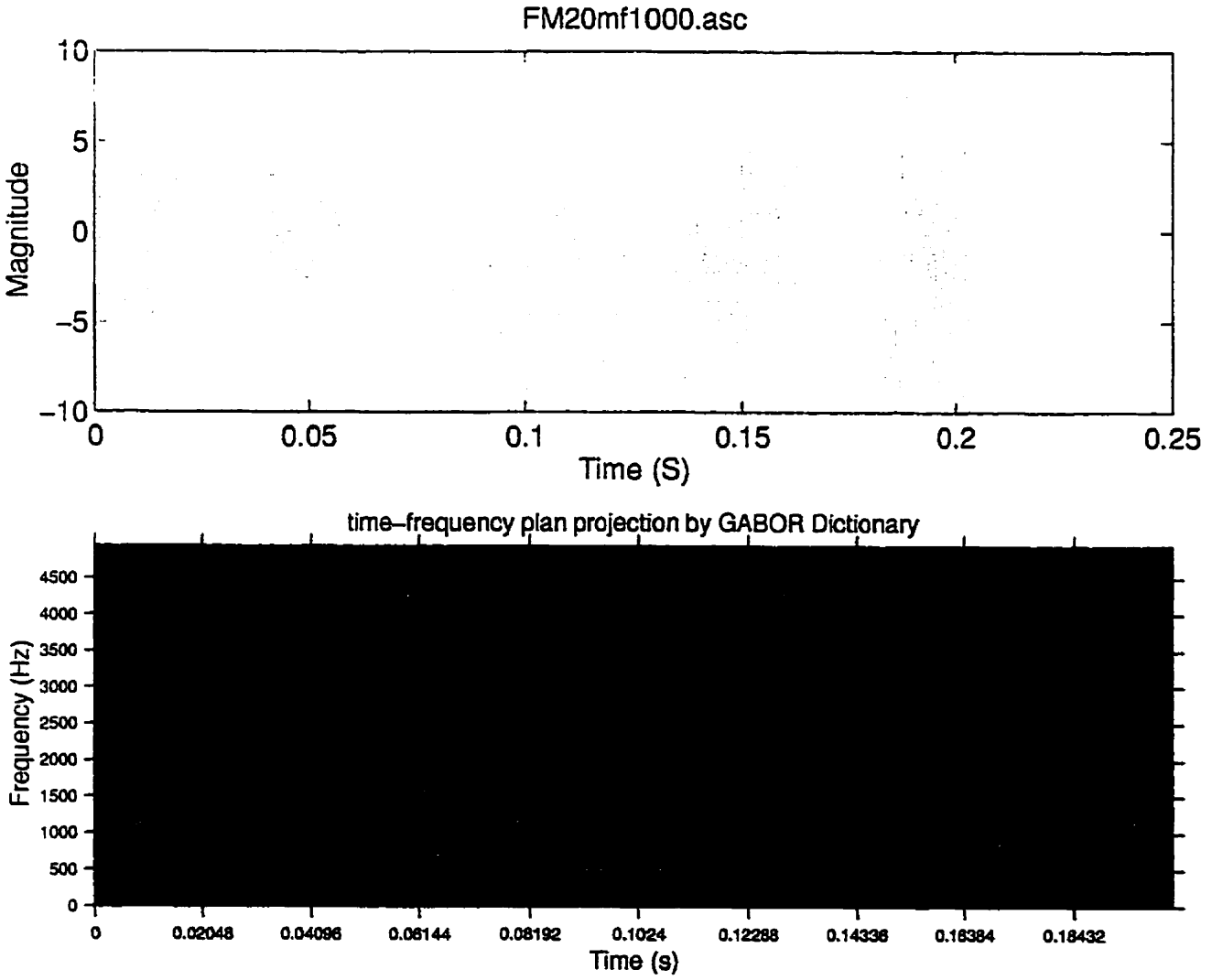

Figure 3.23: Time-frequency representation of a frequency-modulated sine by the Gabor dictionary.

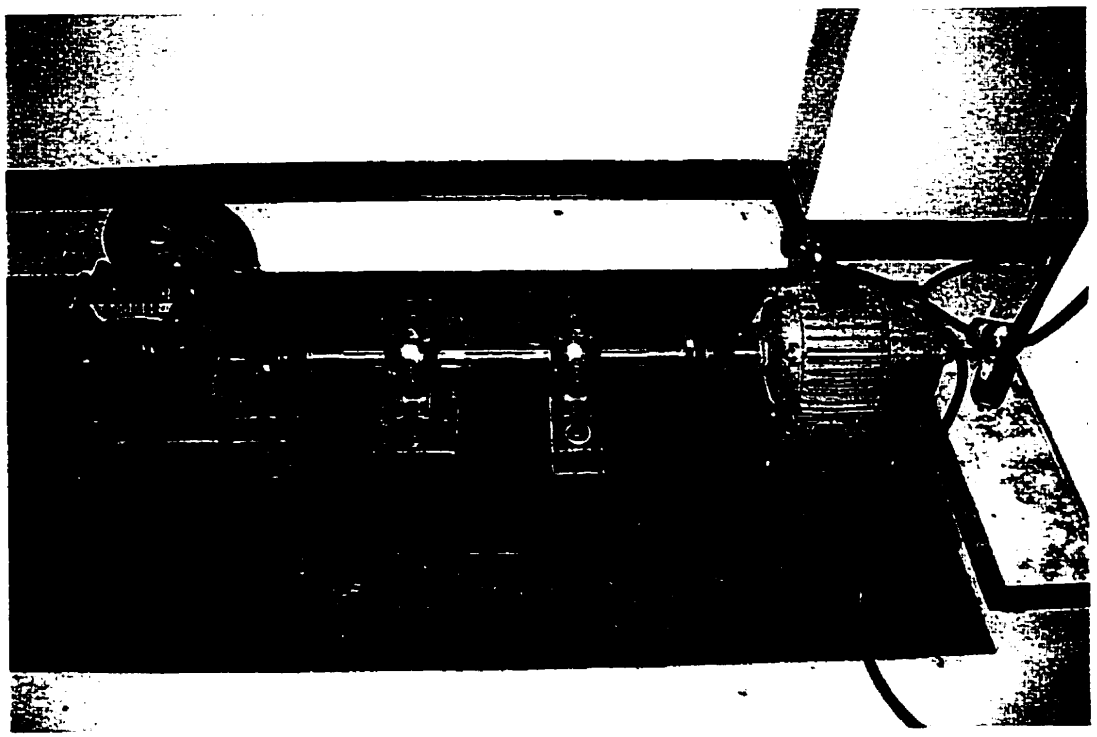

Figure 3.24: Test setup.

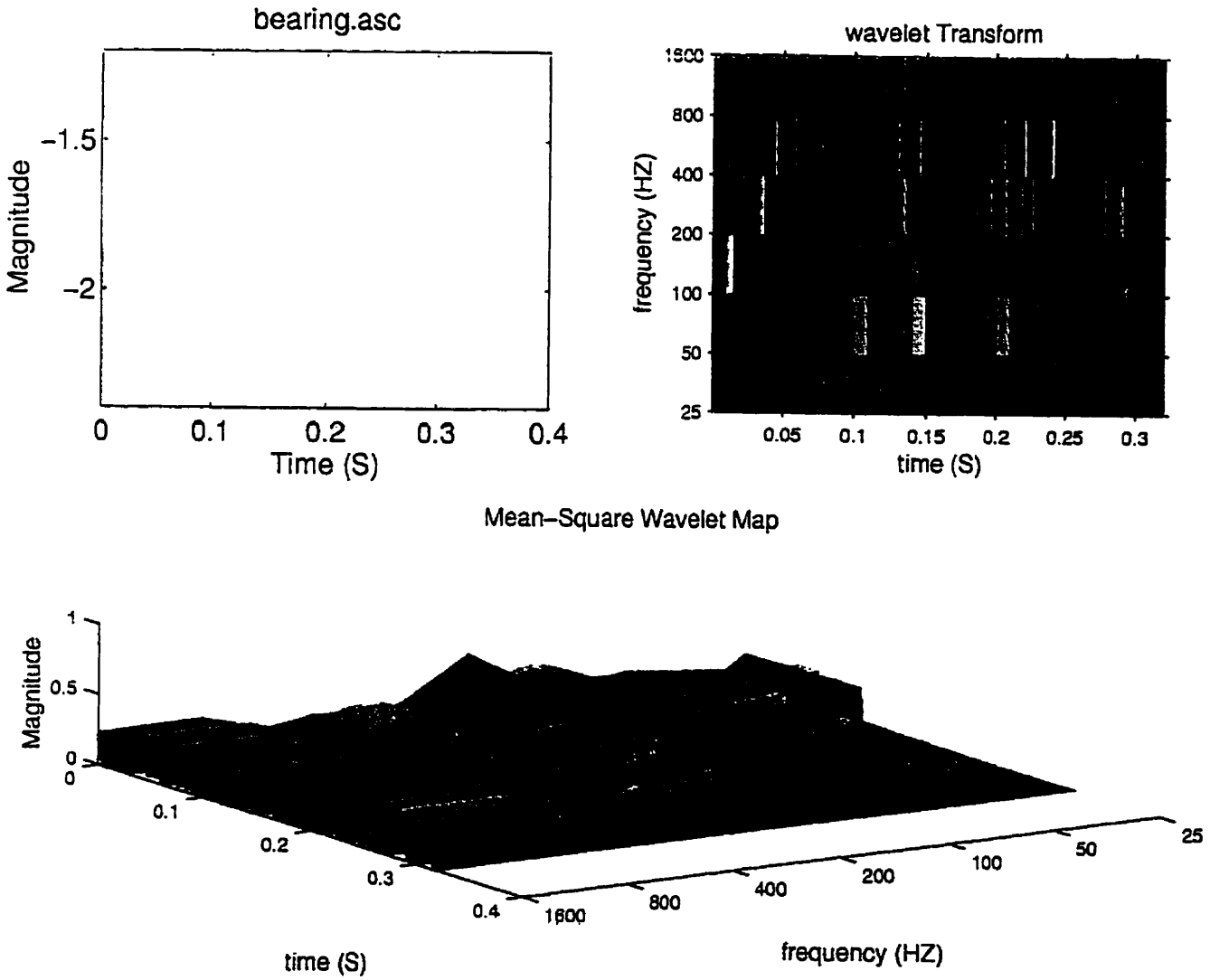

Figure 3.25: Wavelet transform and mean-square wavelet map of the measured signal on a defective bearing.

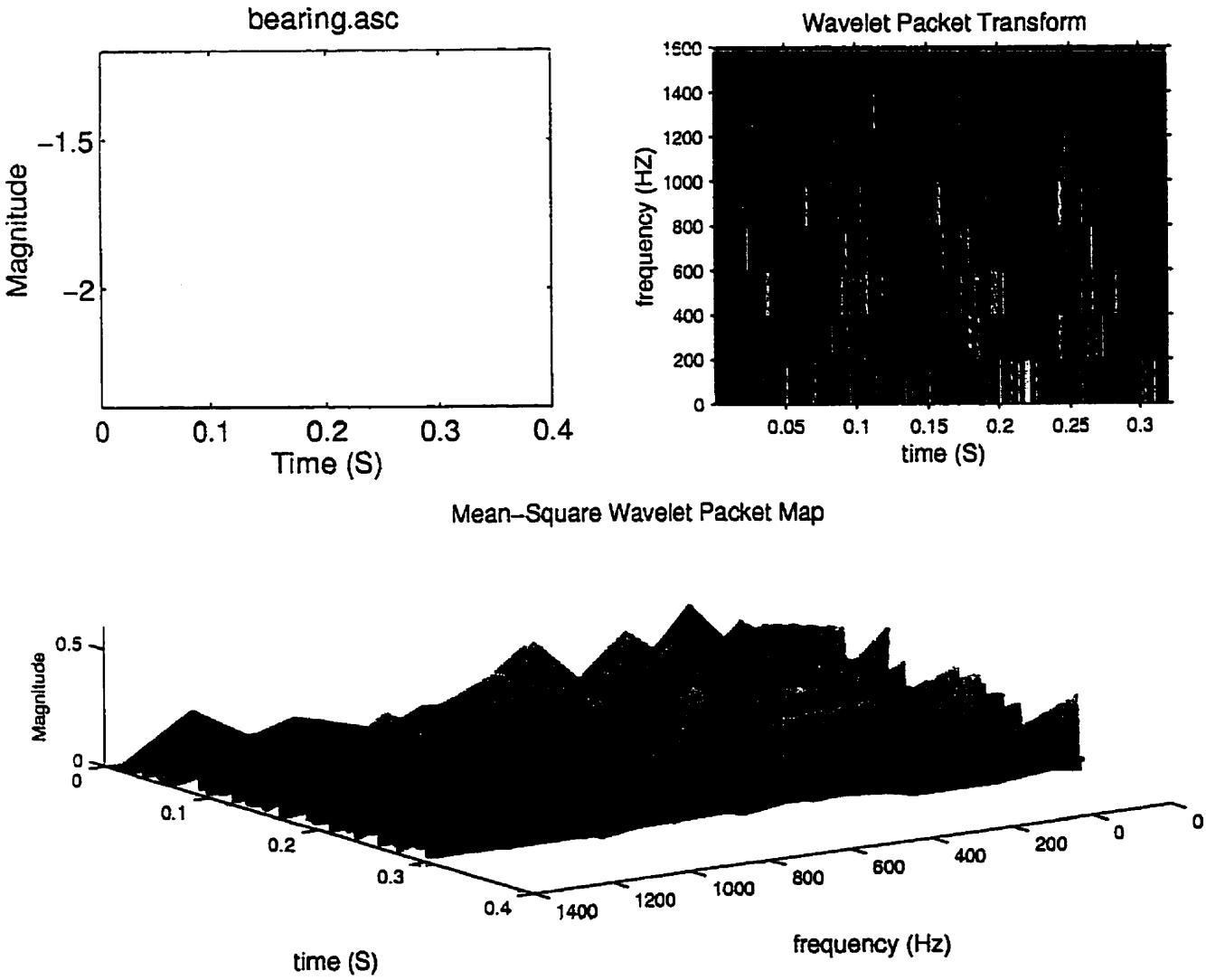

Figure 3.26: Wavelet packet transform and mean-square wavelet packet map of the measured signal on a defective bearing.

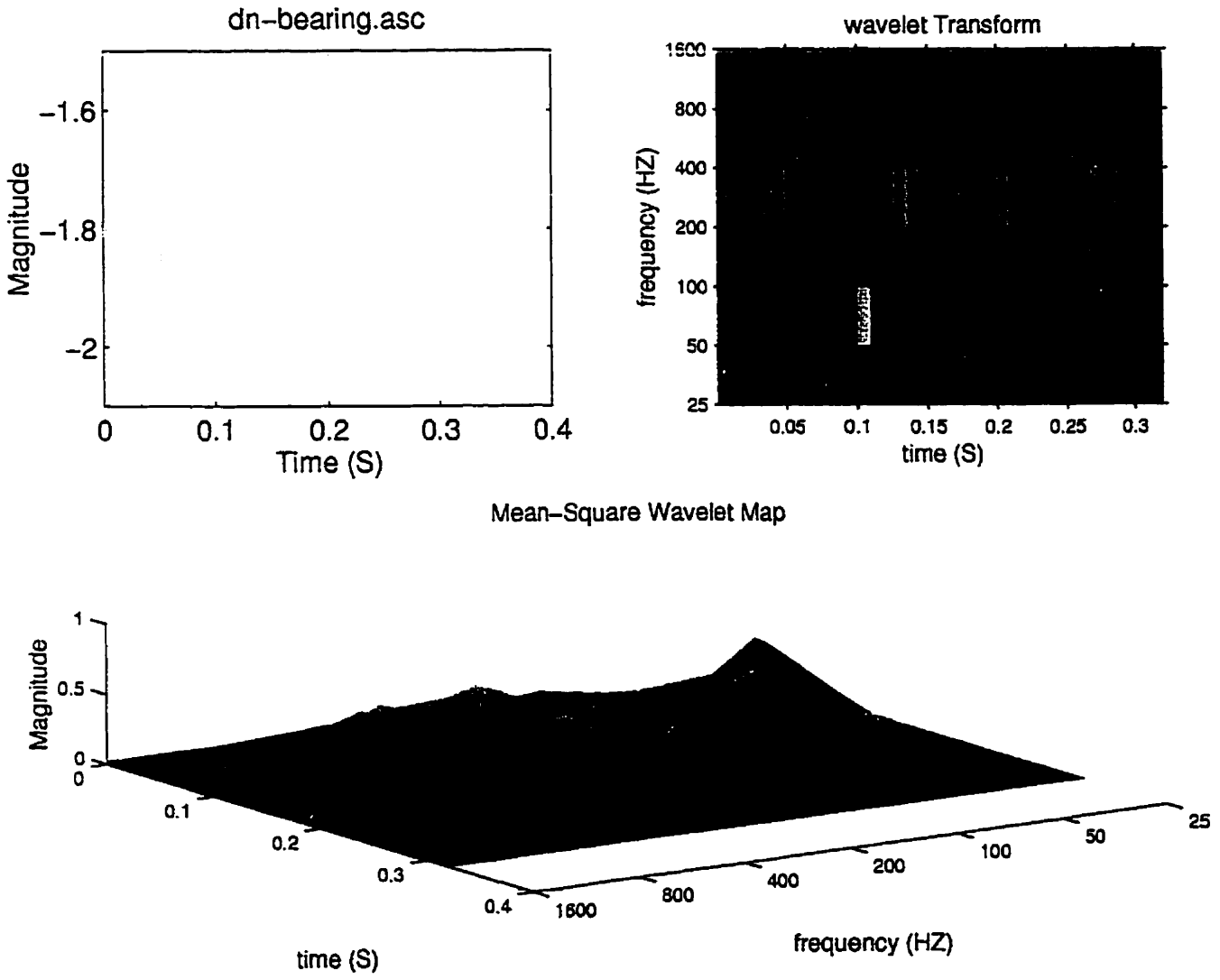

Figure 3.27: Wavelet transform and mean-square wavelet map of the de-noised signal of the defective bearing.

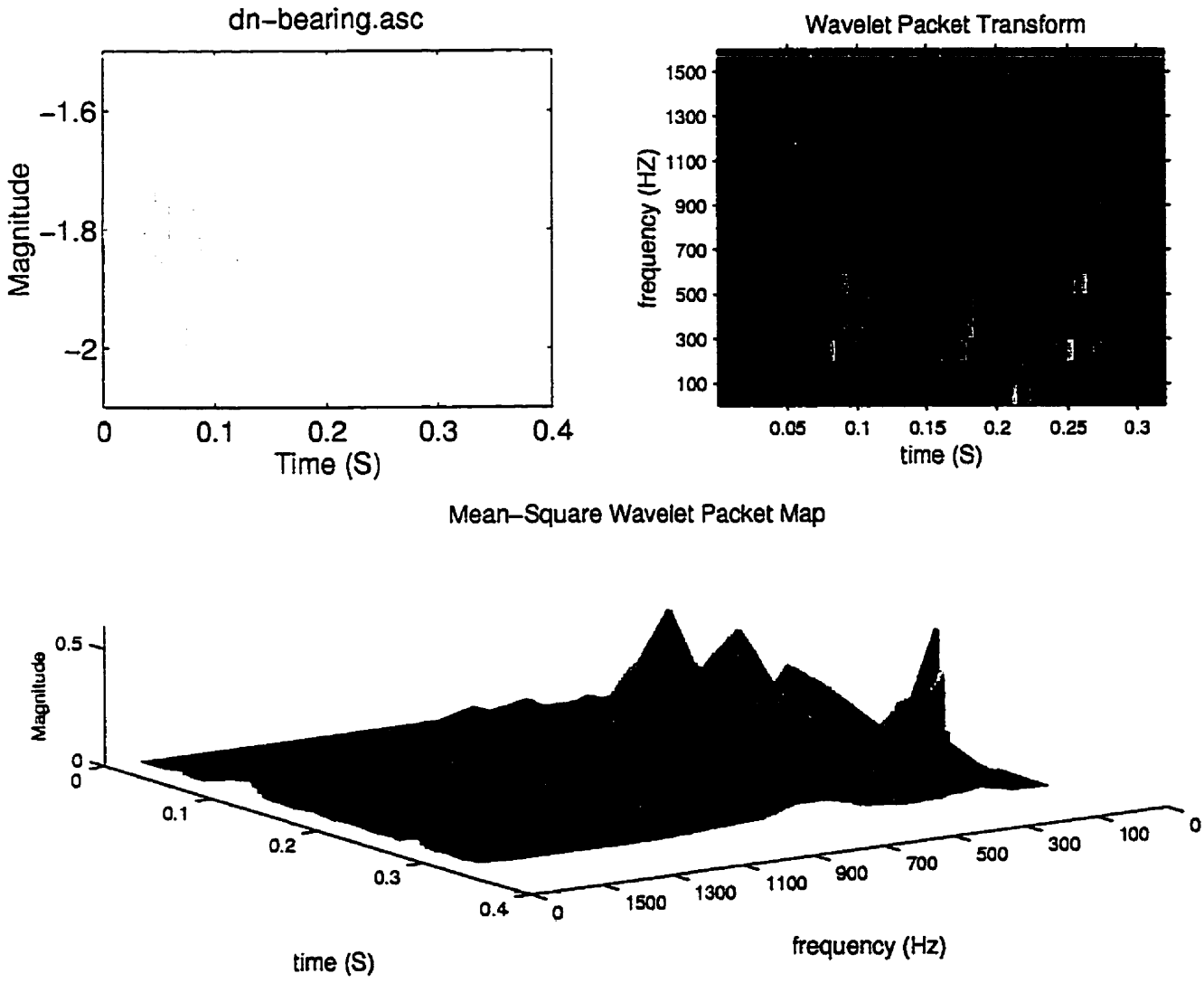

Figure 3.28: Wavelet packet transform and mean-square wavelet packet map of the de-noised signal of the defective bearing.

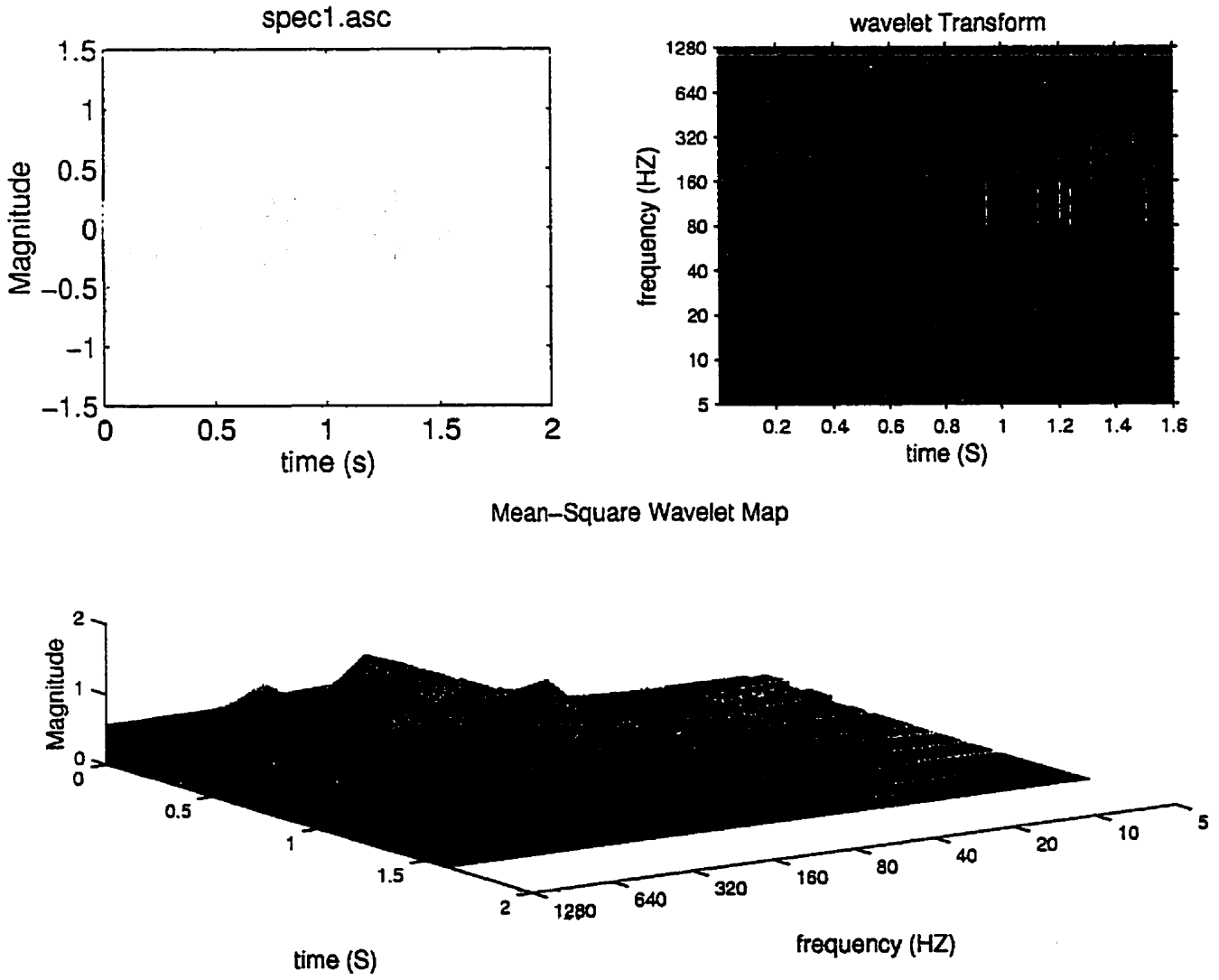

Figure 3.29: Wavelet transform and mean-square wavelet map of the signal measured on a defective gearbox.

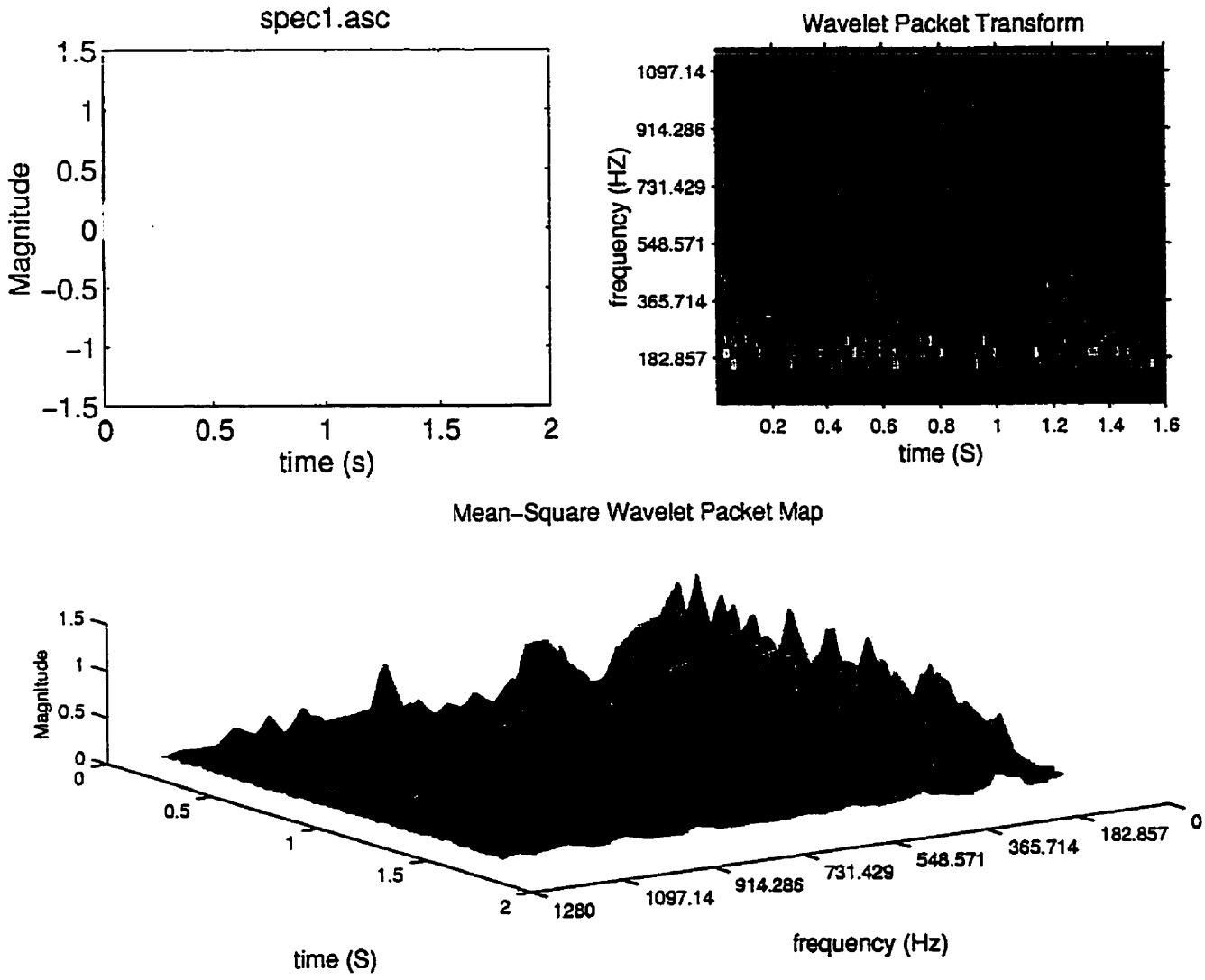

Figure 3.30: Wavelet packet transform and mean-square wavelet packet map of the signal measured on a defective gearbox.

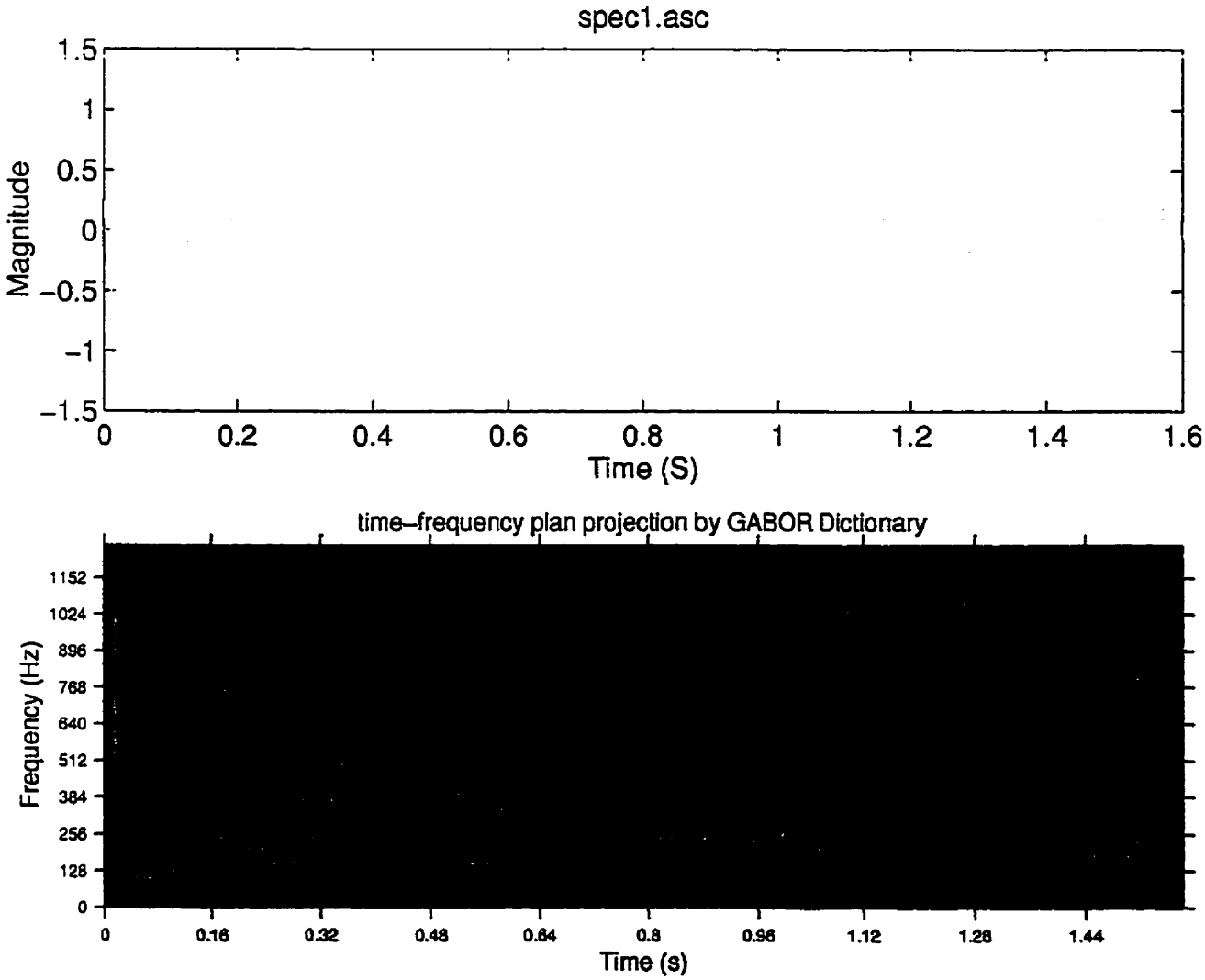

Figure 3.31: Time-frequency representation of the signal measured on a defective gearbox by the Gabor dictionary.

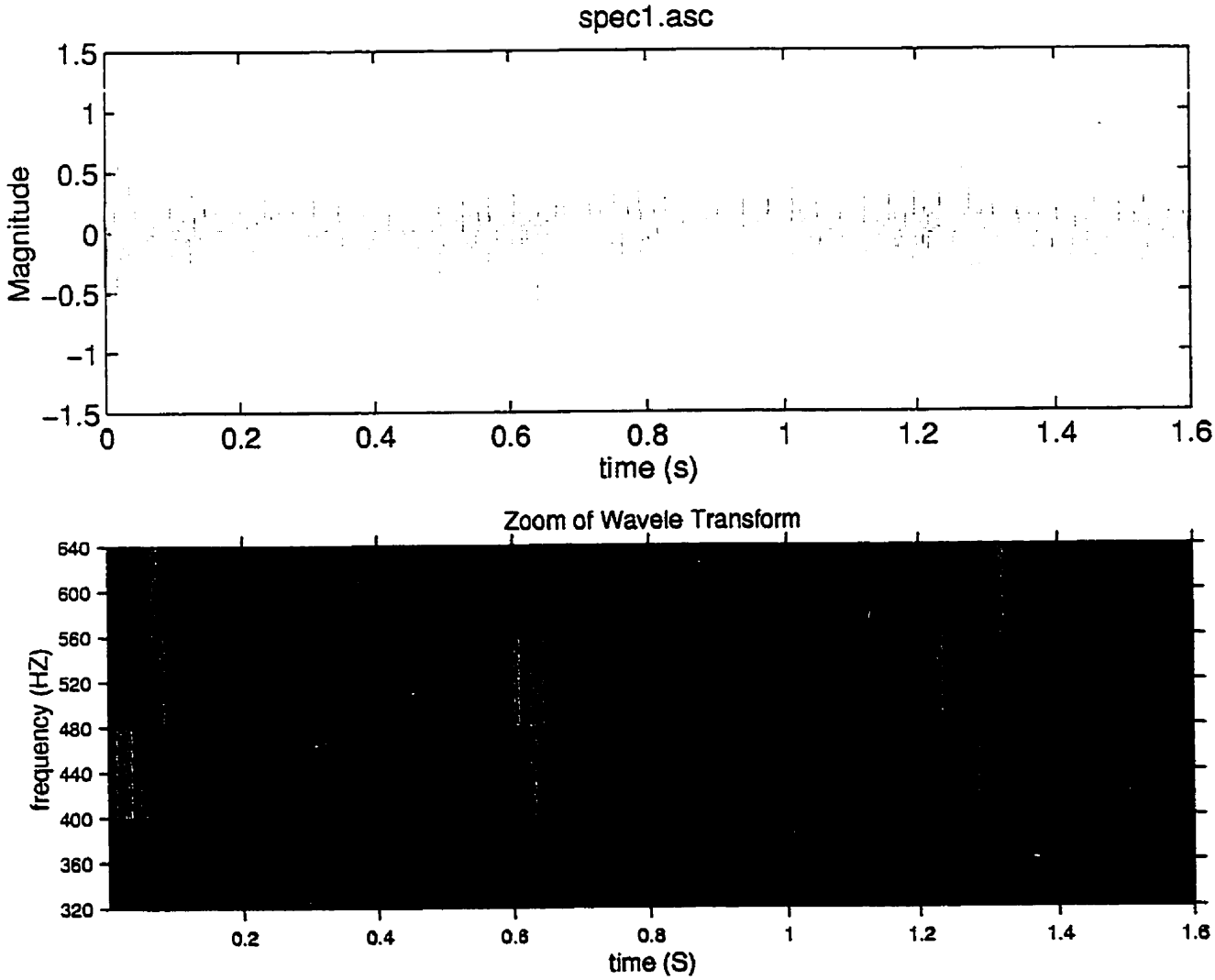

Figure 3.32: Zoom in wavelet transform of the signal measured on a defective gearbox between the frequency band 320 Hz and 640 Hz.

CHAPTIRE IV

TIME-FREQUENCY ALGORITHMS AND THEIR APPLICATIONS*

[1]M.S. Safizadeh, [1]A.A. Lakis and [2]M. Thomas

1: Département de Génie Mécanique, École Polytechnique de Montréal

Case Postale 6079, Succ. Centre-ville, Montréal, Canada H3C 3A7

2: Département de Génie Mécanique, École de Technologie Supérieure

1100, rue Notre-Dame Ouest, Montréal, Canada H3C 1K3

4.1 Abstract

Time-frequency software is designed to be a bridge between theoretical research into methods of time-frequency analysis and the practical applications of these methods in different domains. The lack of an easy-to-use time-frequency software has tended to reduce the likelihood that those engineers with little or no knowledge of time-frequency will use this method of analysis. One of the most important applications of this type of analysis is in the detection of defects in machinery.

This paper presents a user-friendly software designed to perform time-frequency analysis.

---

*: Soumis pour publication dans "International Journal of Computers and Their Applications"

The software reads a time signal from its data file, and then calculates and displays different time-frequency transforms of the signal. The software contains a number of time-frequency algorithms, such as, for example: the Short-Time Fourier transform, the Wigner-Ville distribution, the smoothed Wigner-Ville distribution, the Choi-Williams distribution, the Born-Jordan-Cohen distribution, the Rihaczek-Marginau distribution, the Wavelet transform, the Wavelet packet transform, and the Adaptive Wavelet transforms.

The results are displayed in colour in a graphical interface, which provides a clear and easy-to-interpret time-frequency representation. The window environment of this program and the menu commands make it a powerful, professional tool for time-frequency analysis.

In the first section, existing problems in the diagnostics of machinery and the importance of the application of time-frequency methods in the detection and identification of defects are studied. In the second section, a presentation of the time-frequency software is given. In the third section, each time-frequency method is briefly described and examples are given to show the advantages and disadvantages of each method for different types of signal, in particular for current signals in the diagnostics of machinery. Finally, we show some results for an industrial case.

4.2 Introduction

The purpose of using vibration analysis to monitor machines has changed considerably in recent years. Initially, machines were monitored for purposes of security: if a machine was subjected to significant damage, and the vibration amplitude (displacement, velocity, acceleration) exceeded the permissible limit, the machine was stopped or an alarm rang.

Today, the monitoring of machinery is seen more in the light of preventive maintenance. It is, therefore, expected that the monitoring will not only achieve the initial purpose of security, but will also detect the beginning of a defect and follow its development over time. Such early detection makes it possible to plan and to schedule repairs for a suitable time in order to avoid production interruption. An engineer is able to determine the nature of the defect, monitor its development, estimate the significance of the damage, and finally decide on the most opportune time for repairs.

The diagnostic techniques incorporated in the software have, therefore, been developed in response to the requirements of preventive maintenance. The techniques are based on the methodical analysis of defects and their symptoms. To identify these symptoms, it is necessary to systematically analyze recorded vibration signals obtained from machinery. The analysis of signals in order to extract the hidden information is known as the signal processing method.

Signal processing methods are the principal tools used in the diagnostics of machinery. The complexity of the signal processing operation and the time required to analyze the signal, extract and analyze the relevant information is frequently too great for on-line signal processing. For this reason, the off-line approach to machinery diagnostics has become one of the fastest-growing sectors of the machinery maintenance industry. Vibration and performance data may be measured and stored directly in a hand-held unit, such as a tape recorder or portable data collector. These data can either be gathered directly in digital form, or can be gathered in analog form and converted later to digital form.

From the information obtained, it is possible to diagnose the defect in the machine, determine the severity of the problem, and thus estimate how long the machine can safely be left in service. This requires experience, quality instrumentation and, ideally, a computer to assist in the identification of the frequencies and perform the comparisons between the results of the various transformations.

A number of transformations can be performed to aid in the analytical process. One of the most powerful techniques is spectrum analysis, which relates each rotating element in a machine to identifiable frequencies. By subtracting a "healthy" baseline spectrum from measurements made on new machinery, it is possible to identify changes quickly. Cepstrum analysis, which extracts periodicity from a spectrum, is another technique and one which has proven to be very useful in bearings and gearbox analysis. A complete review of

conventional vibration-based techniques is available [1]; however, the techniques covered in that review can only be applied to stationary signals. It is necessary, therefore, to examine ways to analyse non-stationary signals.

Nowadays, technology is progressing very quickly, and machinery diagnostics plays a major role in plant maintenance. For this reason, it has become necessary to take advantage of the new generation of more powerful methods of signal analysis. These methods, called time-frequency representations, enable us to analyse the non-stationary or the cyclo-stationary signals. Time-frequency representation maps a 1-D signal to a 2-D time-frequency image that displays ways in which the frequency content of the signal changes over time. In time-frequency representation, time runs horizontally and frequency vertically, and the energy level is indicated by color.

While each signal has a unique Fourier spectrum, the time-frequency representation of a signal is non-unique. In other words, many different time-frequency representations can be obtained from the same data. There are several time-frequency representations, such as the Short-Time Fourier transform, the Wigner-Ville distribution, and the Wavelet transform. The choice of representation will depend on the details to be observed, in time or in frequency.

The calculations involved in most of the above methods would not be possible without a computer. It is a known fact that the most important phase of maintenance is the period when

the operator is studying the measured signals to determine the condition of the machine. During this phase, the operator needs as many tools as possible, since the simple spectrum display is often not sufficient. A computer can be used to perform spectrum analysis, various time-frequency analyses, and other complex calculations, all of which contribute to easy fault-frequency identification. The results can be displayed in a convenient format on the computer screen. Thus, a computer is not only able to carry out spectrum analysis, but can also provide a great number of time-frequency representations, to highlight different aspects of the signal.

However, certain difficulties which limit the efficiency of the diagnosis, are listed below:

- The majority of engineers have little or no knowledge of advanced signal processing techniques;
- An easy-to-use software that includes all the time-frequency methods in addition to conventional methods does not exist;
- No program which includes all methods of time-frequency analysis has yet been developed specifically for machinery diagnostics. The majority of programs provide only one method, and that is for general rather than specific application.

For these reasons, it is more practical to have a user-friendly software which includes both

advanced and traditional methods of signal analysis, and having the following properties:

- It should require a minimum of knowledge of the theory of time-frequency analysis on the part of the operator, and should pose a minimum number of queries that need a response from the operator;
- It should provide the best graphic representations with the possibility of rotating the figures;
- It should include the possibility of comparing different methods by displaying several time-frequency representations simultaneously in one figure;
- Colours should be used in the representations to facilitate interpretation;
- No additional equipment or new tools should be required;
- It should use methods of signal analysis which are adapted with current signals in the field of machinery diagnostics.

In this paper, we present a new, user-friendly software which allows the user to conduct time-frequency analyses by the various methods listed above. This software may be applied

to any type of signal emanating from a rotating machine, but it is more useful when it is applied to non-stationary signals.

In addition. two-dimensional and three-dimensional displays of the time-frequency representations in color give the user an excellent opportunity to compare details of each of the different representations of the signal.

In the next section, the theory behind each method of time-frequency analysis is briefly described, and examples are given.

4.3 Time-frequency software

4.3.1 Description of the software

The software program samples a variety of different signals and calculates and displays the time-frequency-energy plane projection. It is a user-friendly program and almost all commands may be entered by a mouse. The researcher selects the signal and the chosen method of analyzing the signal. It is then necessary to enter, depending on the selected decomposition method, information such as sampling frequency, type and length of the window for cutting the signal, and the name of the wavelet function to use in the wavelet transform.

The portion of the program that does the calculating is written in '*C*' language. The window displays and menus are written using Matlab functions. Working in a Windows environment with menus gives great flexibility to the program and makes the displays very easy to manipulate.

For each method of analysis, the program displays the chosen signal, the time-frequency plane projection of the signal and a three-dimensional representation of the signal in the time-frequency-energy plane projection.

4.3.2 Software capability

Figure 4.1 shows a flow chart of the time-frequency software package which supports computer-aided monitoring and diagnosis of defects in rotating machinery. This software has four principal menus: *Calculation, Show, Signal and Wavelet function.*

The process of analyzing a signal is as follows:

a) A particular signal is selected in the *Signal* menu using the mouse. A mother wavelet function for the wavelet transform may be chosen in the *Wavelet function* menu. In this menu a list of several mother wavelets is available from which one can select a wavelet function using the mouse;

b) A time-frequency method is selected in the *Calculation* menu. The *Calculation* menu has six submenus, from which one can make selections using the mouse:

(i) *Calculation of "STFT & WT"* this calculates the fast Fourier transform (FFT), the short-time Fourier transform (STFT), the wavelet transform and the wavelet packet transform of the selected signal;

(ii) *Calculation of WVD-Cohen*: this calculates the Wigner-Ville distribution, the smoothed Wigner-Ville distribution, the Choi-Williams distribution, the Born-Jordan-Cohen distribution, and the Rihaczek-Margenau distribution;

(iii) *Zoom in wavelet transform*: this calculates one of the adaptive wavelet transforms;

(iv) *Calculation of WT by Gabor dictionary*: this part of the program uses the Matching Pursuit algorithm developed by S. Mallat [2], which is one of the adaptive wavelet transforms;

(v) *De-noising*: this is carried out by classical wavelet transform and by the Matching Pursuit algorithm;

(vi) *Quit*: exit from program.

After the different types of time-frequency transforms in this part of the program have been calculated, the results are saved in separate files.

c) The obtained results from different time-frequency transforms are displayed in a graphics window. The presentation of the time-frequency transforms is critical because it must be absolutely clear and able to be understood even by a technician with minimal knowledge of the theory of time-frequency analysis. This part of the program is written using Matlab functions; these are simple functions with which it is possible to create a very good graphical environment without using complicated algorithms.

On the principal screen the visualization menu is called *Show*. When *Show* is selected, we see a series of sub-menus which, in combination with other facilities such as zooming or rotating a figure, enable us to see the time-frequency representation in two- and three-dimensional color images. Each time-frequency representation can be printed and saved in a file.

4.4 Time-frequency techniques

4.4.1 Fourier transform

Fourier analysis may be the best-known mathematical technique for transforming the signal *x(t)* from the time domain to the frequency domain $X(\omega)$.

$$X(\omega) = \int_{-\infty}^{\infty} x(t)e^{-j\omega t}dt \tag{4.1}$$

This is not a time-frequency method, but it is a fundamental transform in signal processing and provides a great deal of important information about the signal. However, it has a serious drawback. The Fourier transform supplies information only on the frequency of the signal; information on the time of the signal is lost. Thus it is not possible to say when a particular event took place. In the diagnostics of machinery, signals are sometimes transitory or non-stationary and it is important to find the time of transition or the beginning and ending times of an event. In this case, the Fourier transform is not able to furnish us with the required information. It becomes necessary, therefore, to apply time-frequency methods to obtain the information.

4.4.2 Short-Time Fourier Transform

To estimate the time of events by the Fourier transform, Gabor [3] introduced a new method, called the Short-Time Fourier Transform. To represent a time-varying signal by the Fourier transform, we can cut the signal around a particular time t by a window and calculate its Fourier transform. Then, we can shift this window on the time axis and recalculate the Fourier transform until we have covered the whole signal. In this way, a signal is mapped into a two- dimensional function of time and frequency. The Short-Time Fourier Transform is defined as

$$STFT_x(\omega,t) = \int_{-\infty}^{\infty} x(\tau)h(\tau - t)e^{-j\omega\tau}d\tau \tag{4.2}$$

where $h(\tau)$ is a window function which is centered at time t, and τ is time delay.

Finally, the squared modulus of the STFT is represented in a time-frequency plane and is called a Spectrogram which is the spectral energy of the locally windowed signal. For example, we consider the spectrum and the STFT of two parallel chirps, as shown in figure 4.2. We can see how the STFT shows clearly the characteristic of the signal in the time and frequency domains, while the signal and its spectrum are unable to display the behavior of the signal.

The major disadvantage of the STFT is the resolution trade-off between time and frequency

[1]. Figures 4.3 and 4.4 illustrate the effect of a short window and a long window on time-frequency resolution. A long window provides good resolution in the frequency domain, but poor resolution in the time domain. Conversely, a short window provides good resolution in the time domain and poor resolution in the frequency domain. This method, therefore, gives time-frequency information with limited precision and, for more precision, we must look for a more flexible approach.

4.4.3 Wavelet Transform

The wavelet transform is another linear time-frequency representation, similar to the spectrogram but with more flexibility in time and frequency resolution. In the STFT, the length of window function will remain constant during the analysis of the signal. In the wavelet transform, by translation and dilation / contraction of a window function called the mother wavelet function, we build up a family of window functions of variable lengths:

$$\psi_{s\tau}(t) = \frac{1}{\sqrt{s}}\psi\left(\frac{t-\tau}{s}\right) \tag{4.3}$$

where $\psi(\cdot)$, s, and τ are, respectively, a mother wavelet function, the scale of wavelet transform, and time shift. The variable window length property of the wavelet transform gives us the possibility of having the time and frequency resolutions dependent on the

frequency under consideration [4]. Figure 4.5 illustrates this point by showing the cells of resolution in the time-frequency plane for the STFT and the wavelet transform. One important advantage of the wavelet transform is its ability to carry out local analysis. This property is of significant value in revealing any small change in the signal and distinguishes the wavelet transform from other signal analysis techniques. If we consider the result obtained by applying the wavelet transform on a Dirac pulse at time t_0=*0.1 sec* (Figure 4.6), we see a figure of triangular shape which points at $t=t_0$ in the time-frequency plane. It is more localized in high frequencies than in low frequencies.

The wavelet transform is defined as

$$W_{\psi}x(s,\tau) = \int_{-\infty}^{\infty} x(t)\overline{\psi}_{s\tau}(t)dt \tag{4.4}$$

where $W_{\psi}x(s,\tau)$ is called the wavelet coefficients.

It is known that the Fourier analysis decomposes a signal into sine waves of various frequencies. Similarly, analysis by the wavelet transform decomposes a signal into a shifted and scaled version of the mother wavelet.

The process of decomposition is similar; we take a wavelet and compare it to the first section of the signal. The wavelet coefficients represent the correlation between the wavelet function and this section of the signal. In the next step, we shift the wavelet along the time axis and

re-calculate the correlation. When we do it for the whole signal, we scale (stretch or compress) the wavelet in repeating the above steps.

The choice of the wavelet function is an important factor in the wavelet transform and is dependent on the signal to be analyzed. For this reason, a list of different wavelet functions [5] is available in the *Wavelet function* section of the principal menu of this program. The possibility also exists of adding to the list a new wavelet function: one created by the researcher. Figure 4.7 shows the wavelet transform of the sum of three sines and the effect of using different wavelet functions on the time-frequency representation of the wavelet transform. In Figure 4.7(b), we select the wavelet function of Daubechies 20, which has considerable support, while in Figure 4.7(c), we select the wavelet function of Haar (or Daubechies 2), which has little support. We observe that the wavelet function of Daubechies 20 provides better localization in frequency than the wavelet function of Haar. Here it is noted that, in Figure 4.6, we selected the wavelet function of Haar for the presentation of Dirac because this wavelet function is better adapted to temporal phenomena. Henceforth, we will choose the best wavelet function for a given signal.

This program computes the wavelet coefficients by using the Fast Wavelet Transform proposed by S. Mallat [6]. The Fast Wavelet Transform algorithm is based on multiresolution analysis and filter banks derived from older methods of telecommunication, called sub-band coding. This technique calculates the wavelet coefficients rapidly [5].

The variable time and frequency resolution of the wavelet transform is one of its advantages; however, in the discrete wavelet transform the frequency axis has logarithmic scale (basic 2) which means that the frequency band is divided by 2 in each iteration. The logarithmic scale of the frequency axis does not permit either fine frequency resolution of the high frequencies or fine time resolution of the low frequencies. This characteristic of the frequency axis in the wavelet transform makes it a specialized method to be used for signals which contain long-duration events at the low frequencies and short-duration events at the high frequencies. The logarithmic scale of the frequency axis in the wavelet transform may at times be considered to be a disadvantage of this method.

To resolve the inconvenience of the wavelet transform, another method based on the principle of the wavelet transform has been introduced. This method is called the wavelet packet transform [7,8], and gives a frequency axis with linear scale at the expense of losing the excellent time resolution of the high frequencies of the wavelet transform. The algorithm of the wavelet packet transform is based on a completed tree of filter banks [5], but the program includes an option to select the required number of levels (couples of filters) for calculating the wavelet packet transform. For example, if we select "number of levels = 3", this means that there are $2^3 = 8$ frequency bands in the time-frequency representation of the wavelet packet transform. This option makes it possible to avoid too much complexity in the time-frequency representation of the wavelet packet transform. For example, let us look at the wavelet packet transform of the sum of three sines shown in Figure 4.8. If we compare

this figure to Figure 4.7, we observe that the wavelet packet transform is more effective than the wavelet transform for signals localized in frequency. The emphasis is on the linear scale of the frequency axis of the wavelet packet transform.

4.4.4 Zoom-in wavelet transform

As mentioned above, the wavelet transform is recommended for signals with transient phenomena in high frequencies and is not recommended for arbitrary signals. On the other hand, the wavelet packet transform is a modified version of the wavelet transform and is missing one important property of the wavelet transform: perfect time resolution of the high frequencies.

To improve the performance and, at the same time, to preserve the properties of the wavelet transform, it is necessary to use the signal-adaptive transformation. With this, the resolution exchange between time and frequency in the wavelet transform is dependent on the signal under analysis.

The zoom-in wavelet transform is an interesting technique for optimizing the time and frequency resolutions by filter bank selection.

To continue the program using this technique, we choose the *Zoom-in wavelet transform*,

which is a submenu in the *Calculation* section. This submenu has two other submenus: *Show wavelet transform* and *Calculation of zoom-in WT*, as shown in Figure 4.1. If we select the *Show wavelet transform* submenu, a time-scale representation of the wavelet transform of the signal is displayed. From this representation, we can select the scale in which we want to have more resolution. Then, we go to another submenu (*Calculation of zoom- in WT*) and, in response to the on-screen queries, we indicate the required scale to zoom and the number of levels we wish to obtain. Finally, we go to the *Show* menu of the program to display the result. The result will be a time-frequency representation of the chosen band. It is noted that we must have a sufficient number of wavelet coefficients in the scale (frequency band) to execute a zoom, otherwise we will not obtain a good representation. Figure 4.9 shows the zoom-in wavelet transform for frequency band 1250-2500 Hz of the sum of three sines. This figure shows that precision increases significantly in the frequency domain if we use the *Zoom-in wavelet transform* technique. In the wavelet transform (Figure 4.7(b)), the $\omega_3 = 2000\ Hz$ is located in frequency band 1250-2500 Hz, while in Figure 4.9, the ω_3 is located in frequency band 1875-2031 Hz.

4.4.5 Calculation of WT by the Gabor dictionary

The next signal-adaptive transformation of the wavelet transform is the calculation of the

wavelet transform by the Gabor dictionary. The principle of this method is to optimize the wavelet functions with respect to the structure of the signal. In contrast to the wavelet transform, in which the wavelet function is fixed during analysis of the signal, in this method, the best adapted wavelet function with respect to the signal structure is chosen from a vast waveform library during the analysis of the signal. Such waveforms are called time-frequency atoms and the library of these waveforms is called the dictionary of time-frequency atoms.

In order to calculate the wavelet transform by this method, the program makes use of the Matching Pursuit algorithm developed by Mallat [2]. In the *Calculation* menu of the program, there is a submenu inviting us to do the wavelet analysis by the Gabor dictionary. In order to see the results, we must go to the *Show* menu. Figures 4.10 and 4.11 show two examples of the wavelet transform by the Gabor dictionary. As shown in these figures, this method provides very high resolution in time and in frequency for signals having components parallel with the time axis or the frequency axis. However, in the case of signals showing variation in the time-frequency plane, such as two parallel chirps (Figure 4.12), signals with frequency modulation (Figure 4.13), or even amplitude modulation (Figure 4.14), this technique gives poor representations.

4.4.6 De-noising

Removing noise from a signal by wavelet analysis is one of the most recent applications of wavelets [9]. It consists of decomposing the signal by wavelet transform, removing noise from components, and reconstructing the signal.

Wavelet analysis is a linear method; therefore the wavelet coefficients of the linear combination of two signals are equal to the linear combination of their wavelet coefficients.

$$W(x_1 + x_2) = W(x_1) + W(x_2) \tag{4.5}$$

A noisy signal can be modeled in the following form:

$$x(t) = s(t) + e(t) \tag{4.6}$$

where $x(t)$ is a noisy signal, $s(t)$ is the original signal, and $e(t)$ is the noise. The noise part of the signal may be eliminated by taking the following three steps:

a) Computing the wavelet decomposition of the signal $x(t)$

b) Determining a limit for optimal de-noising and suppressing only the portion of the wavelet coefficients that exceeds this limit;

c) Reconstruction of the signal with the help of modified wavelet coefficients $s(t)$. In practice, the decomposition and reconstruction procedures are accomplished by the

fast wavelet transform and the inverse fast wavelet transform respectively;

It is clear that the performance of the de-noising method depends mostly on step ***(b)***. The suppression of a part of a signal, called the thresholding procedure, is carried out using different optimization techniques, which give different threshold values [10].

To de-noise a signal, we go to the *De-noising* submenu in the *Calculation* menu of the program. The *De-noising* menu has two other submenus: **I)** *De-noising by classical wavelet transform* and **II)** *De-noising by Matching Pursuit*. The program uses Matlab Mat-files for part **(I)**, and the Matching Pursuit Algorithm for part **(II)**.

Figures 4.15-4.21 show examples of de-noising using the classical wavelet transform accompanied by the STFT, and the wavelet transform of an original, noisy and de-noised signal. Figures 4.22-4.28 show an example of de-noising using the Matching Pursuit algorithm accompanied by the STFT and the wavelet transform of original, noisy, and de-noised signal.

4.4.7 The Wigner-Ville distribution and Cohen's class time-frequency distributions

One interesting time-frequency energy distribution is the Wigner-Ville distribution (WVD) [11], which has recently been applied to the field of mechanical signal analysis [12]. This

distribution is a bilinear function, in contrast to the transforms discussed above, which are linear transforms. In a linear transform, the similarity of the signal to a window function is measured using the correlation function; on the other hand, the Wigner-Ville distribution is the Fourier transform of the instantaneous auto-correlation of the signal. Thus, its time-frequency representation is independent of the window function.

If the instantaneous correlation, $R_x(\tau, t_0)$, at time t_0 with a time lag τ, is defined as

$$R_x(x, t_0) = \lim_{T \to \infty} \frac{1}{T} \int_{t_0}^{t_0 + T} x(t - \tau/2) x(t + \tau/2) dt \tag{4.7}$$

its Fourier transform may be written as follows:

$$S_x(\omega, t_0) = WVD_x(\omega, t_0) = \int_{-\infty}^{\infty} R_x(\tau, t_0) e^{-j\omega\tau} d\tau \tag{4.8}$$

The WVD satisfies a large number of desirable mathematical criteria and has excellent resolution in the time and frequency domains, but it has two major problems. First, it is not always non-negative, which, since energy is always positive, makes it difficult to interpret the Wigner-Ville representation as the energy distribution of the signal in the time-frequency plane. Secondly, because it is bilinear, it produces interference terms or cross terms for multicomponent signals [13, 14]. The interference term is located between two components of a multicomponent signal in the time-frequency representation, and it oscillates with a frequency proportional to the distance between these two components, as shown in Figure

4.29 for two parallel chirps.

In the numerical method, we cannot use a signal from $-\infty$ to $+\infty$, and therefore we use a window function to cut the signal in the time domain. This time-window version of the WVD is called the pseudo-WVD [11]. Windowing in the time domain provides some smoothing in the frequency direction of the WVD and reduces the interference terms oscillating perpendicularly to the frequency axis, but at the expense of loosing many properties of the WVD.

In addition to the interference terms, the alias problem may affect the discretization of WVD if the signal is real-valued and sampled at the Nyquist rate. To prevent this problem, Ville [15] suggested using the analytical signal, a complex signal in which the imaginary part is equal to the Hilbert transform of the real part. With the analytical signal, the spectral domain will be [0, ½] of the real signal and consequently the aliasing will not happen. On the other hand, since the spectral domain is divided by two, the number of components in the time-frequency plane is also reduced by half. In addition, application of the analytical signal eliminates the negative part of the frequency axis, so that the interference terms generated between negative- and positive-frequency components are eliminated, leading to a considerable decrease in the number of interference terms.

Since the development of the WVD, there have been several attempts to find other formulae to express the energy of the signal in the time-frequency plane. Cohen classified these

formulae by giving a general formula for all time-frequency energy distributions [16]. This formula is defined as

$$WD_x(t,\omega) = \iiint x(u+\tau/2)x(u-\tau/2)\varphi(\theta,\tau)e^{j(\theta u-\theta t-\tau\omega)}\,du\,d\tau\,d\theta \qquad (4.9)$$

where θ and τ are respectively a frequency lag and a time lag. In addition, $\varphi(\theta,\tau)$ is a kernel function that, when changed, gives different time-frequency distributions with different properties.

One desirable choice for the kernel function is a separable smoothing function in both the time and frequency domains which attenuates the interference terms of the WVD in both the frequency and time directions. The distribution attained in this way is called the smoothed-WVD [17], and is defined as

$$SWVD_x(t,\omega) = \iint WVD_x(u,\xi)\Phi(t-u,\omega-\xi)dud\xi \qquad (4.10)$$

where $\Phi(t,\omega)$ is a two-dimensional smoothing function.

The smoothed-WVD may be considered as an intermediate distribution between the STFT and the WVD. It has some of their advantages and none of their problems. The WVD provides the best resolution in time and in frequency, but produces some significant interference terms in the time and in frequency directions. The STFT is a linear transform and does not suffer from interference terms, but it is unable to give satisfactory resolution

simultaneously in time and in frequency. The smoothed-WVD provides the best compromise between these two problems: interference terms and resolution in time and frequency. Figure 4.30 shows the smoothed Wigner-Ville distribution of two parallel chirps. If this figure is compared with the STFT of the same signal (Figure 4.2), we can see that the smoothed-WVD provides better resolution and clearer representation of the signal than the STFT.

In addition to the WVD, other energy distributions have been developed to give the time-frequency representation of the signal. One interesting distribution is the Rihaczek distribution [18], which presents a complex energy density of the signal. This distribution is also a member of Cohen's class and corresponds to Cohen's general formula. Its kernel function is $e^{j\theta\tau/2}$.

In practice, however, the Margenau-Hill distribution, which is, in fact, the basis of the Rihaczek distribution, $\cos(\theta\tau/2)$, is preferred to the Rihaczek because it satisfies a number of the same desirable mathematical properties as does the WVD. The interference terms are also present in the Margenau-Hill time-frequency representation, but with a different structure (Figure 4.31). However, the specific structure of the interference terms in the Margenau-Hill distribution is such that, if the signal is composed of synchronized components in time and in frequency, the application of the Margenau-Hill distribution is not recommended.

Interference terms are present in all members of Cohen's class distributions because of the bilinear property. Mathematicians and physicists have been seeking a kernel function which is capable of eliminating, or reducing, the interference terms whilst at the same time preserving the desirable properties.

One interesting group of kernel functions is the exponential kernel function [19]. The general form of these kernel functions is defined as

$$\varphi(\theta,\tau) = e^{\frac{-|\theta|^p|\tau|^q}{\sigma}} \tag{4.11}$$

where p, q and σ are the parameters which are adjusted to produce a compromise between the amplitudes of the interference terms and the resolution. The distributions obtained by using this type of kernel function are known as Exponential distributions (ED).

An example of the ED is the Choi-Williams distribution [20] where the kernel function is defined as

$$\varphi(\theta,\tau) = e^{-\theta^2\tau^2/\sigma} \tag{4.12}$$

when $\sigma \rightarrow +\infty$, the CWD becomes the WVD. Inversely, when $\sigma \prec\prec \infty$, the interference terms diminish, but resolution is lost. The performance of this distribution is dependent on the analyzed signal. For example, if the signal is composed of multicomponents located at

the same position in time or in frequency, the efficiency of the CWD will be relatively poor and a great number of interference terms will be present in the time-frequency plane. Figure 4.32 shows the Choi-Williams distribution of two parallel chirps. It is noted that this representation is produced by choosing the best value of the parameter σ.

There is another type of kernel function that reduces the interference terms. This kernel function produces time-frequency distributions known as Reduced Interference distributions (RID). The RID has the desirable properties of the WVD, but the WVD is not a member of the RID. The RID kernel satisfies some conditions, as discussed by Jeong and Williams [21].

An example of the RID is the Born-Jordan distribution [22] whose kernel function is a sinc defined as

$$\varphi(\theta,\tau) = \frac{\sin(\theta\tau/2)}{\theta\tau/2} \tag{4.13}$$

Although it appears that the RID is a satisfactory distribution, it has many disadvantages. One of its main disadvantages is the fact that the RID is only able to reduce the amplitude of the interference terms and spread them over a larger time-frequency area. It is not able, particularly when the interference terms are located on the time or frequency axis, to suppress the interference terms.

Figure 4.33 shows the Born-Jordan distribution of two parallel chirps. The time and frequency resolutions in this representation are very poor.

With regard to the advantages and the disadvantages of each distribution, we conclude that there is no perfect distribution. In fact, while one distribution gives the best representation for a certain type of signal, other time-frequency distributions give the best representation for other types of signal.

For this reason, we put the various time-frequency distributions into the program. In this way, when the researcher selects the *Calculation of WVD-Cohen* option from the *Calculation* menu, all the time-frequency distributions are calculated. Then, in the *Show* section, each of the distributions can be selected to represent the time-frequency domain. The possibility exists to see all the time-frequency distributions and to compare them.

4.4.8 Quit

The last submenu of the *Calculation* menu is *Quit*: the command to exit from the program.

4.5 Industrial application of the time-frequency algorithm

In this section, the efficiency of the time-frequency software in an industrial case is demonstrated. The case is that of the defective gear of a hoist drum in a large shovel

operating at an open-pit iron mine. Two types of defect which tend to be produced in a gearbox are shaft-related problems, such as misalignment and imbalance, and tooth-related problems, such as wear, scuffing, and cracking. The detection of a defect in a single tooth will be investigated in this section.

Vibration signals measured in a gearbox include tooth-meshing frequency, transient events caused by defects, gearbox resonance vibrations, and system and sensor transmission characteristics. The vibration signals are non-stationary signals and require specific techniques because it is often difficult to apply conventional methods, such as Fourier analysis, to gearbox fault-detection [1]. Time-frequency methods provide new techniques for the analysis of non-stationary signals, and have advanced capabilities for the separation of different phenomena in non-stationary signals.

Figures 4.34-4.43 show, respectively, the time signal of the damaged gearbox measured by IMS company and its spectrum, the STFT, the wavelet transform, the wavelet packet transform, the wavelet transform by the Gabor dictionary, the Wigner-Ville distribution, the smoothed Wigner-Ville distribution, the Rihaczek-Margenau distribution, the Choi-Williams distribution and the Born-Jordan-Cohen distribution.

- The spectrum of the signal displays some large peaks around 200 Hz and some smaller peaks in the vicinity of 400 Hz, 800 Hz and 1200 Hz. However, it is very difficult to assume or confirm any defects;

- The Short-Time Fourier transform clearly displays time-frequency representation of the signal . There are a gear meshing frequency at approximately 220 Hz and some pulses at approximately 440 Hz. It has known that pulses are appeared in the vibration signal of a gearbox if there is a broken tooth.

  Then we may conclude that there is a broken tooth in this gearbox. It is also possible to find the location of the fault in gearbox. The frequency of repetition of the pulses $(\frac{1}{\approx 2.65 \text{ sec}} = 1.5 \text{ Hz})$ determines the rotating speed of the shaft with faulty gear in gearbox. As well as, in frequency domain the frequency of pulses (≈ 440 Hz) is equal to the meshing frequency of faulty gear.

  In following, we will compare the resolution and quality of representation of this signal which can be obtained by other time-frequency methods;

- The wavelet transform of the signal shows the three repetitive pulses in the frequency band 320-640 Hz. The frequency of the periodicity of the signal may be calculated from the wavelet transform more precisely than from the STFT, because the time resolution in this band of the wavelet transform is finer than in the STFT. But in the three-dimensional representation of the signal, the STFT provides better representation than does the mean square wavelet;

- The wavelet packet transform provides not only better frequency resolution, but also better time-frequency representation (three-dimensional) than does the wavelet transform;

- The time-frequency plane projection of the signal by the Gabor dictionary is shown in Figure 4.38, but it is not easy to obtain the characteristics of the signal from this figure;

- The Wigner-Ville distribution cannot provide a good representation of the signal due to the cross terms, which are generated between the signal components;

- The smoothed Wigner-Ville shows the characteristics of the signal even more clearly than the STFT and we can calculate the frequency of repetition of pulses with more precision by the smoothed Wigner-Ville than by the STFT;

- The Rihacezk-Margenau cannot give a good representation of the signal and the second peak vanishes completely;

- Although the Choi-Williams, with an appropriate value of σ, shows a representation of the signal in which a part of energy of the first peak is dispersed between the second peak and the third peak, but after the smoothed Wigner-Ville distribution, it gives the best representation of the signal in Cohen's class distribution;

- In the Born-Jordan-Cohen, the second peak virtually disappears and it is difficult to obtain satisfactory information about the signal;

4.6 Conclusion

A time-frequency software package has been presented in this paper. A number of time-frequency methods that can be used to analyze non-stationary and time-varying signals have been described. The advantages and disadvantages of each method of time-frequency analysis have been discussed, and the benefits to be obtained from the application of these techniques in the monitoring and fault-detection of machinery have been highlighted. The comprehensive representation and user-friendly way in which the information is made available in this software package make it particularly useful for other applications of signal processing. It is stressed, that, while it is important to have a certain level of knowledge of signal analysis techniques in order to understand all the details of the results, the software has been designed so that it can be used by an operator-technician with relatively little knowledge of the techniques of time-frequency analysis.

4.7 References

[1] M. S. Safizadeh, A. A. Lakis and M. Thomas, "Application of the Short-Time Fourier Transform in Machine Fault Detection," École Polytechnique de Montréal, Technical Report No. EPM/RT-99/05, 1999.

[2] S. Mallat, "Matching Pursuits with Time-Frequency Dictionaries," IEEE Trans. Signal Processing, 41 (12): 3397-3415, 1993.

[3] D. Gabor, "Theory of Communication," J. IEEE (London), 93: 429-457, 1946.

[4] J. Morlet and Al, "Wave Propagation and Sampling Theory-part II: Sampling Theory and Complex Waves," Geophysics, 47 (2), February 1982.

[5] M. S. Safizadeh, A. A. Lakis and M. Thomas, "Condition Monitoring and Diagnostic of Rotating Machinery by Means of Wavelet Transform," École Polytechnique de Montréal, Technical Report No. EPM/RT-99/07, 1999.

[6] S. Mallat, "A Theory for Multi Resolution Signal Decomposition: The Wavelet Representation," IEEE Transaction on Pattern Analysis and Machine Intelligence, 11(7): 674-693, 1989.

[7] N. Hess-Nielsen and M. V. Wickerhauser, "Wavelets and Time-Frequency Analysis," Proceedings of the IEEE, 84 (4): 523-539, April 1996.

[8] K. Ramchandran and M. Vetterli, "Wavelets, Subband Coding and Best Bases," Proceeding of the IEEE, 84(4): 541-560, April 1996.

[9] D. L. Donoho and I. M. Johnstone, "Idea De-noising in an Orthonormal Basis Chosen from a Library of Bases," CRAS Paris, t. 319, Ser I, PP. 1317-1322, 1994

[10] D. L. Donoho, "De-noising by Soft-thresholding," IEEE Trans. On Inf. Theory, 41 (3): 613-627, 1995.

[11] T. A. C. M. Classen and W. F. G. Mecklenbrauker, "The Wigner Distribution - A Tool for Time-Frequency Signal Analysis Part I: Continuous Time Signals," Philips J. Res., 35 (3): 217-250, 1980.

[12] M. S. Safizadeh, A. A. Lakis and M. Thomas, "Fault Detection and Identification Using Wigner-Ville Distribution," École Polytechnique de Montréal, Technical Report No. EPM/RT-99/06, 1999.

[13] F. Hlawatsch, " Interference terms in the Wigner distribution," in Proc. Int. Conf. Signal Processing (Florence, Italy), PP. 363-367, Sept. 1984.

[14] P. Flandrin, " Some Features of Time-Frequency Representation of Multicomponent Signals, " in Proc. IEEE 1984 Int. Conf. Acoust., Speech, Signal Processing (San Diego, CA), PP. 41.B.4.1-4, Mar. 1984.

[15] J. Ville, "Théorie et Applications de la Notion de Signal Analytique," Cables et Transmission, 2A: 61-74, 1948.

[16] T. A. C. M. Classen and W. F. G. Mecklenbrauker, "The Wigner Distribution - A Tool for Time-Frequency Signal Analysis Part II: Discrete Time Signals," Philips J. Res., 35 (4/5): 276-300, 1980.

[17] L. Jacobson and H. Wechsler, " The Composite Pseudo Wigner Distribution (CPWD): A Computable and Verstaile Approximation to the Wigner distribution (WD), " in Proc. IEEE ICASSP-83 (Boston, MA), 254-256, 1983.

[18] W. Rihaczek, "Signal Energy Distribution in Time and Frequency," IEEE Trans. Informat. Theory, IT-14: 369-374, 1968.

[19] E. J. Diethorn, "The Generalized Exponential Time-Frequency Distribution," IEEE Trans. Signal Processing, 42 (5): 1028-1037, 1994.

[20] H. I. Choi and W. J. Williams, "Improved Time-Frequency Representation," IEEE Trans. Acoust., Speech, Signal Processing, ASSP-37: 862-871, 1989.

[21] J. Jeong and W. Williams, "Kernel Design for Reduced Interference Distributions," IEEE Trans. Sig. Proc., 40: 402-412, 1992.

[22] L. Cohen, " Generalized Phase-Space Distribution Functions," J. Math. Phys., 7: 781-786, 1966.

4.8 Nomenclature

$x(t)$	Magnitude of the signal
$X(\omega)$	Spectrum of the signal $x(t)$
$STFT_x(\omega,t)$	Short-time Fourier transform of the signal $x(t)$
$\psi_{s,\tau}(t)$	Mother wavelet function
$W_\psi x(s,\tau)$	Wavelet coefficients of the signal $x(t)$
$R_x(\tau,t_0)$	Instantaneous correlation function of $x(t)$
$S_x(\omega,t_0)$	Instantaneous spectrum density function of $x(t)$
$WVD_x(\omega,t_0)$	Wigner-Ville distribution of $x(t)$
$\varphi(\theta,\tau)$	Kernel function
$SWVD_x(\omega,t)$	Smoothed Wigner-Ville distribution of $x(t)$

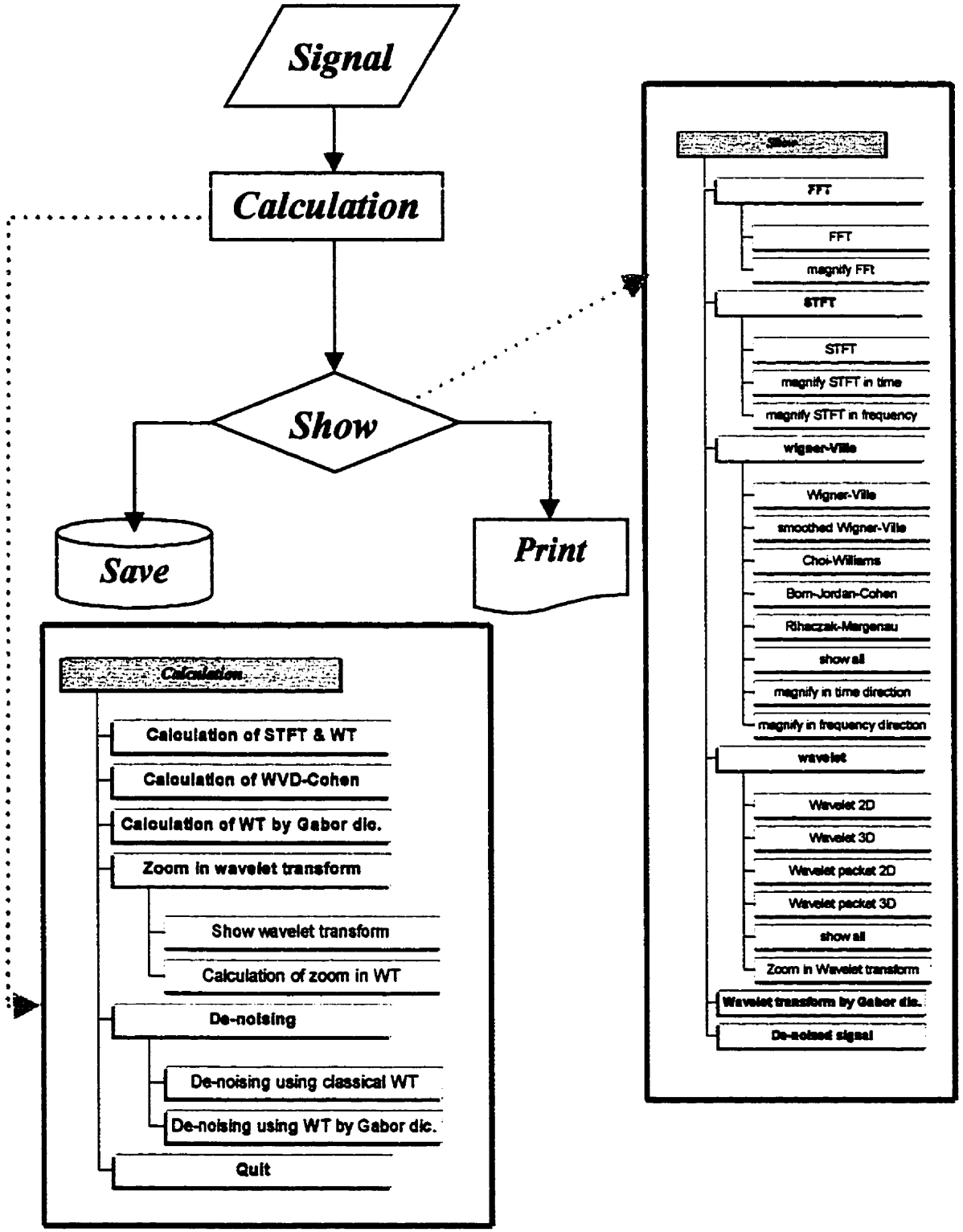

Figure 4.1: Flow chart of the time-frequency software package.

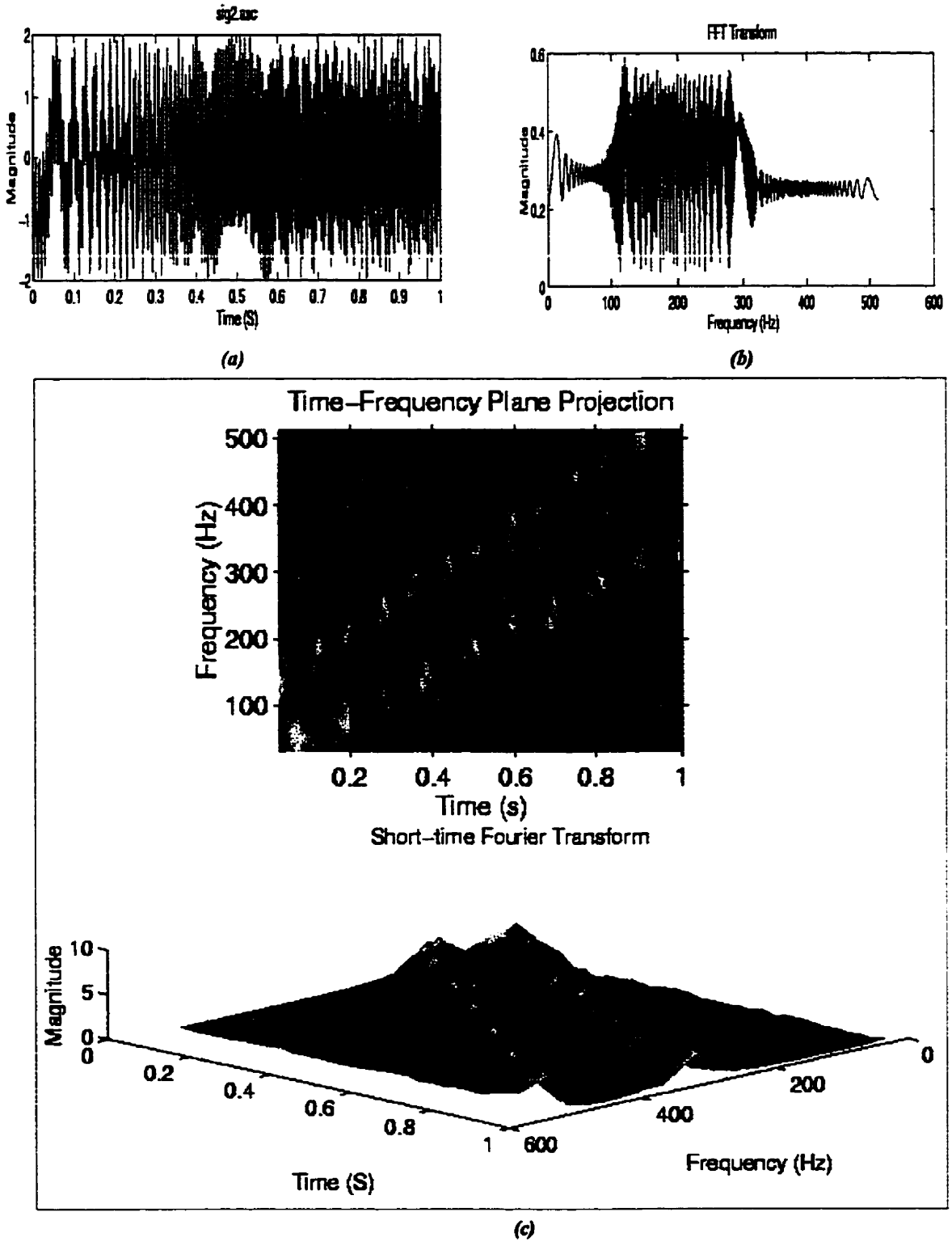

Figure 4.2: a) Time representation of two parallel chirps; b) Spectrum representation of two parallel chirps; c) Short-time Fourier transform of two parallel chirps.

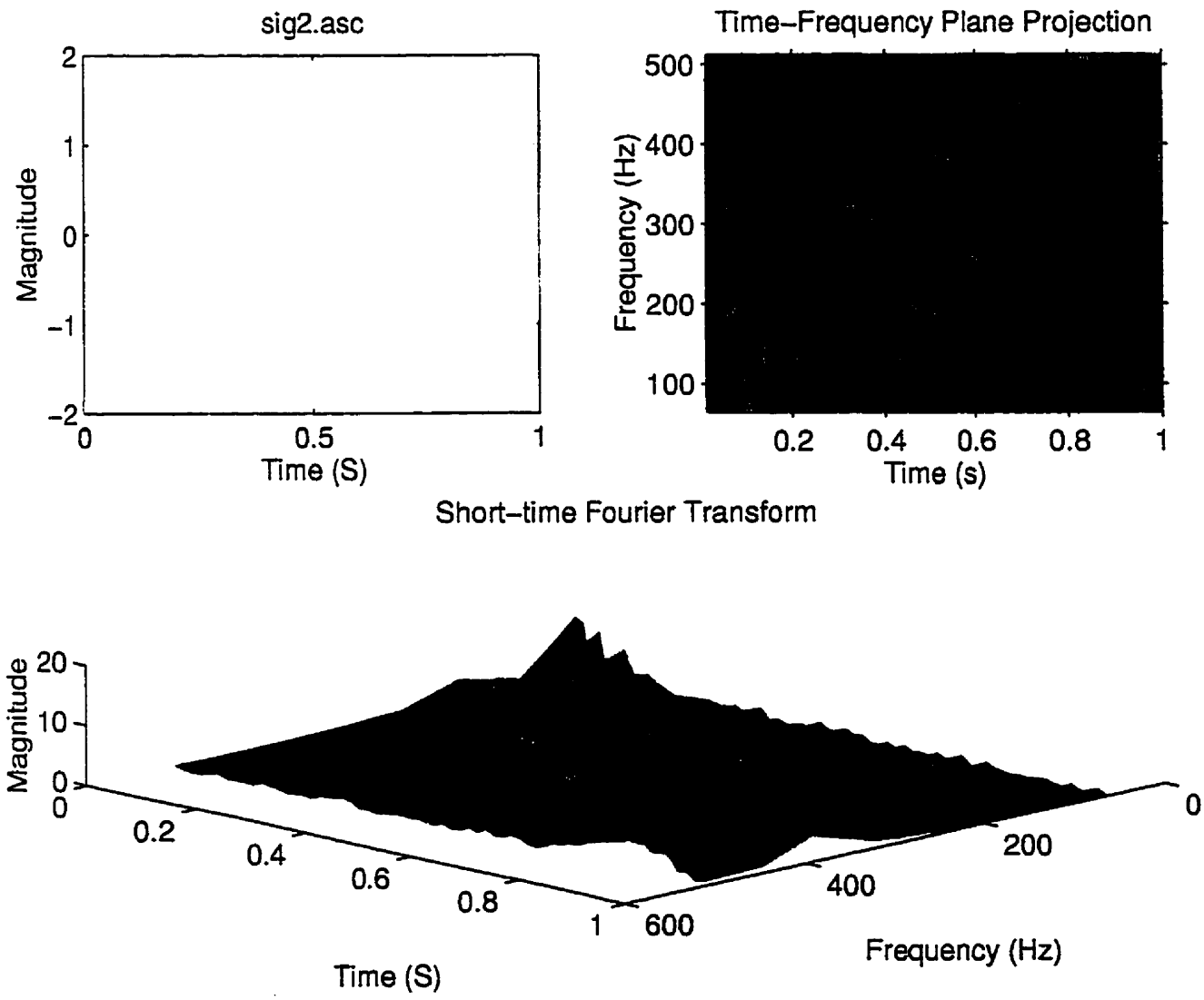

Figure 4.3: Short-Time Fourier transform of two parallel chirps with a short window.

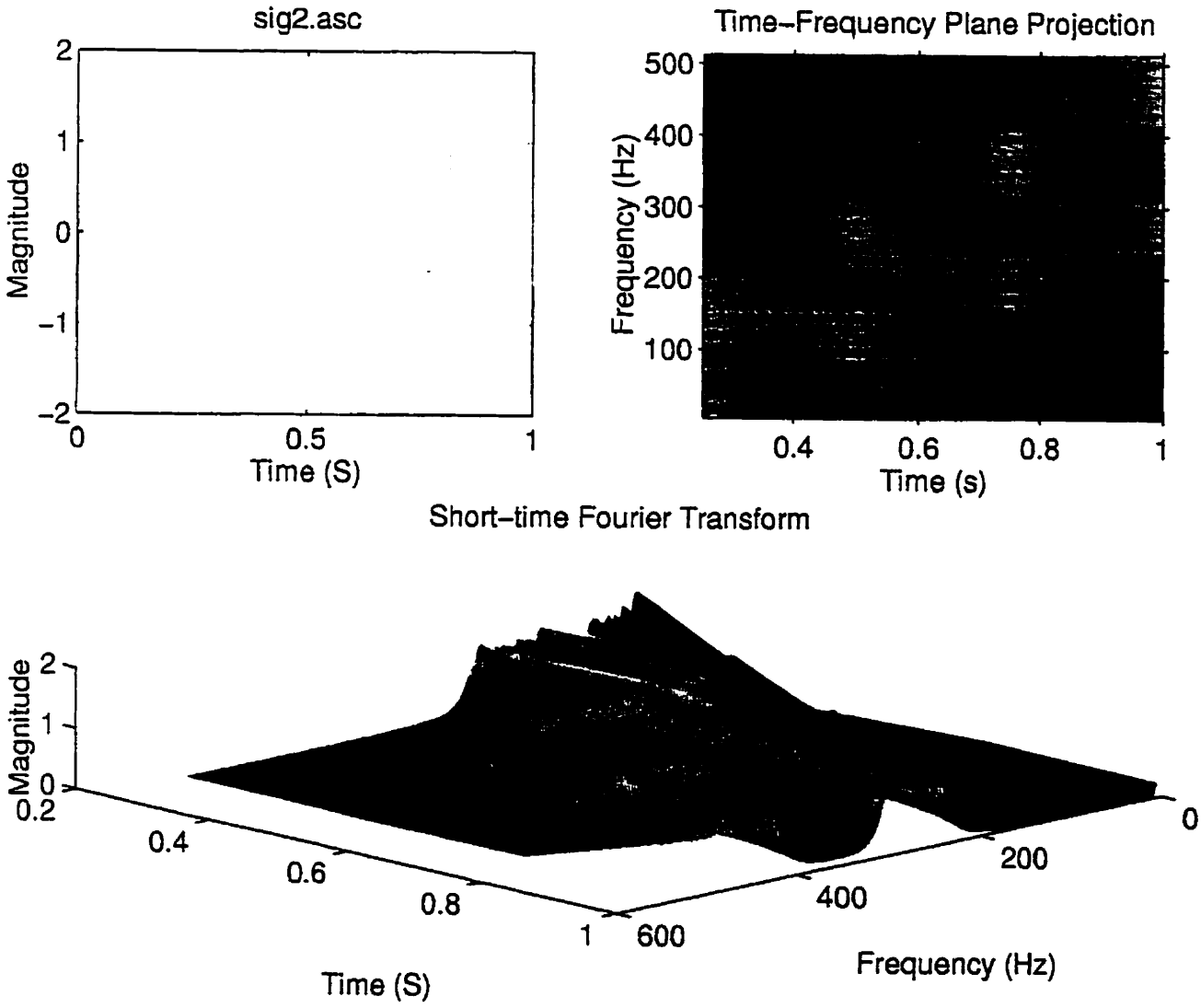

Figure 4.4: Short-time Fourier transform of two parallel chirps with a long duration window.

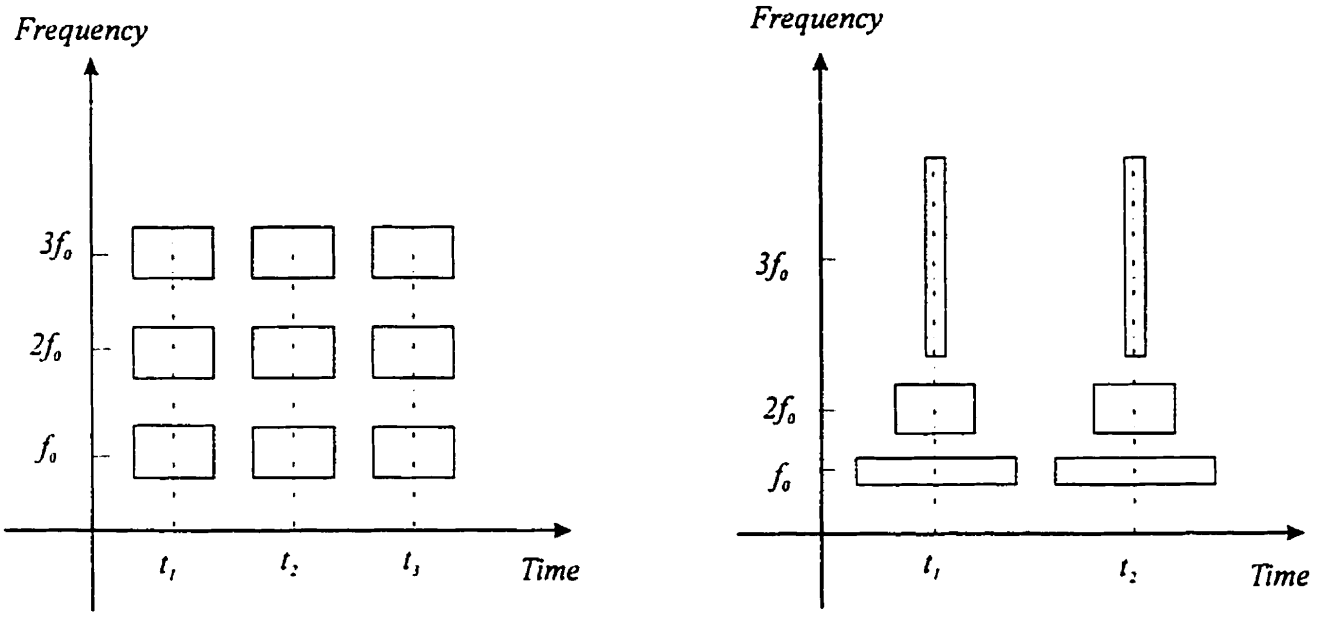

Figure 4.5: (a) Time-frequency plane of the short-time Fourier transform;
(b) Time-frequency plane of the wavelet transform.

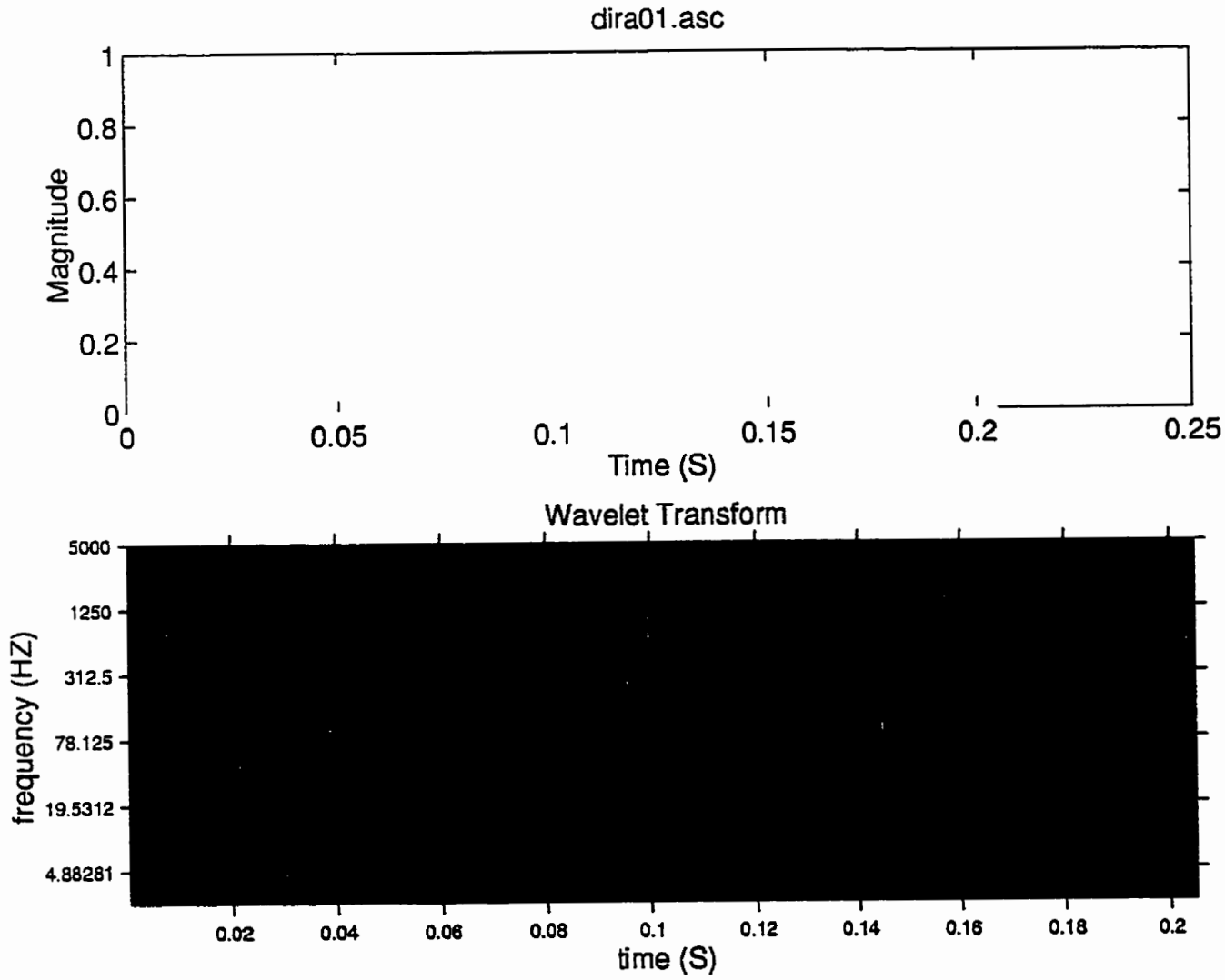

Figure 4.6: Wavelet transform of a Dirac function.

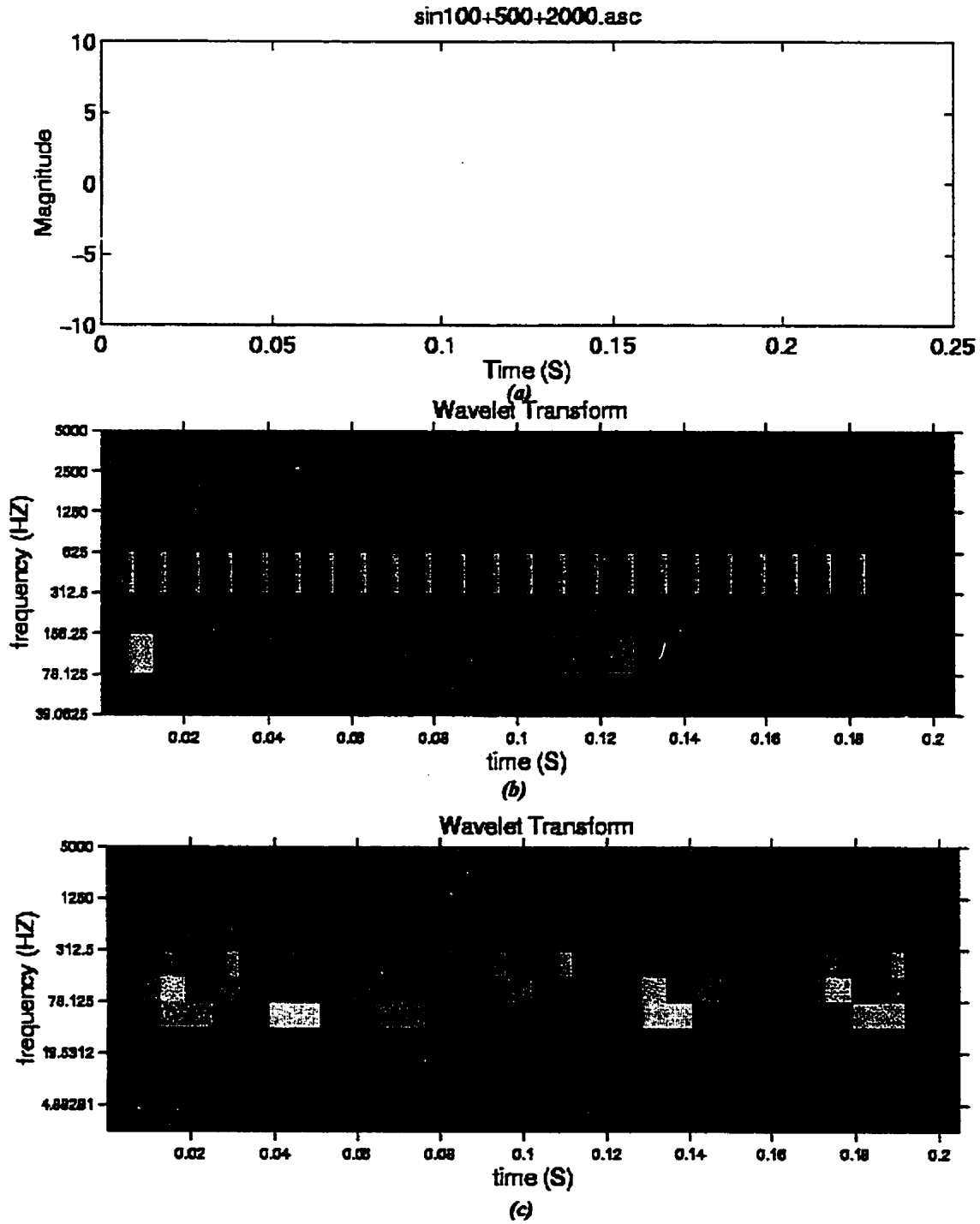

Figure 4.7: (a) Time representation of the sum of sine waves
(b) The wavelet transform of the sum of sine waves by Daubechies filter (D20)
(c) The wavelet transform of the sum of sine waves by Daubechies filter (D2)

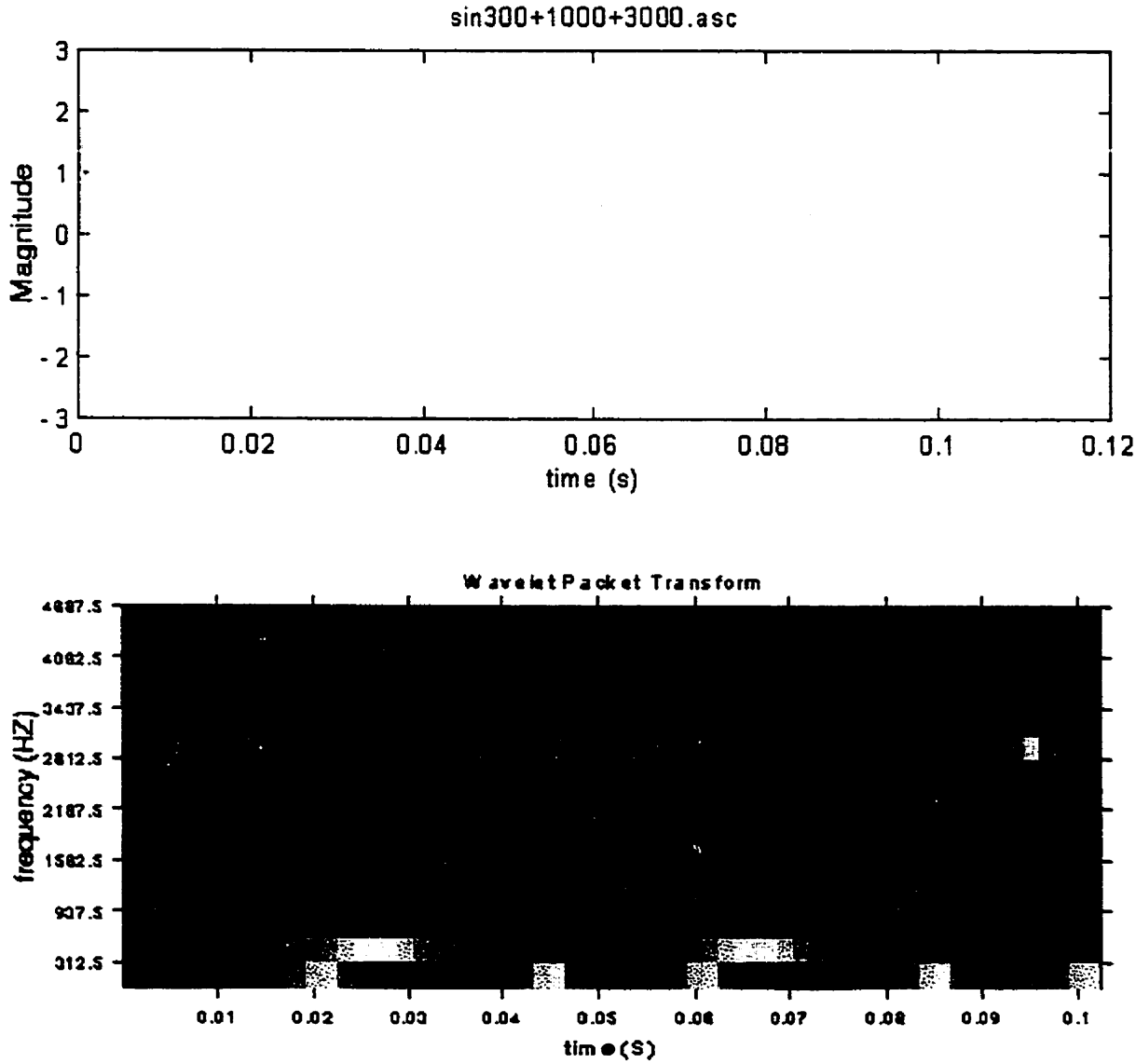

Figure 4.8: Wavelet packet transform of sum of three sines

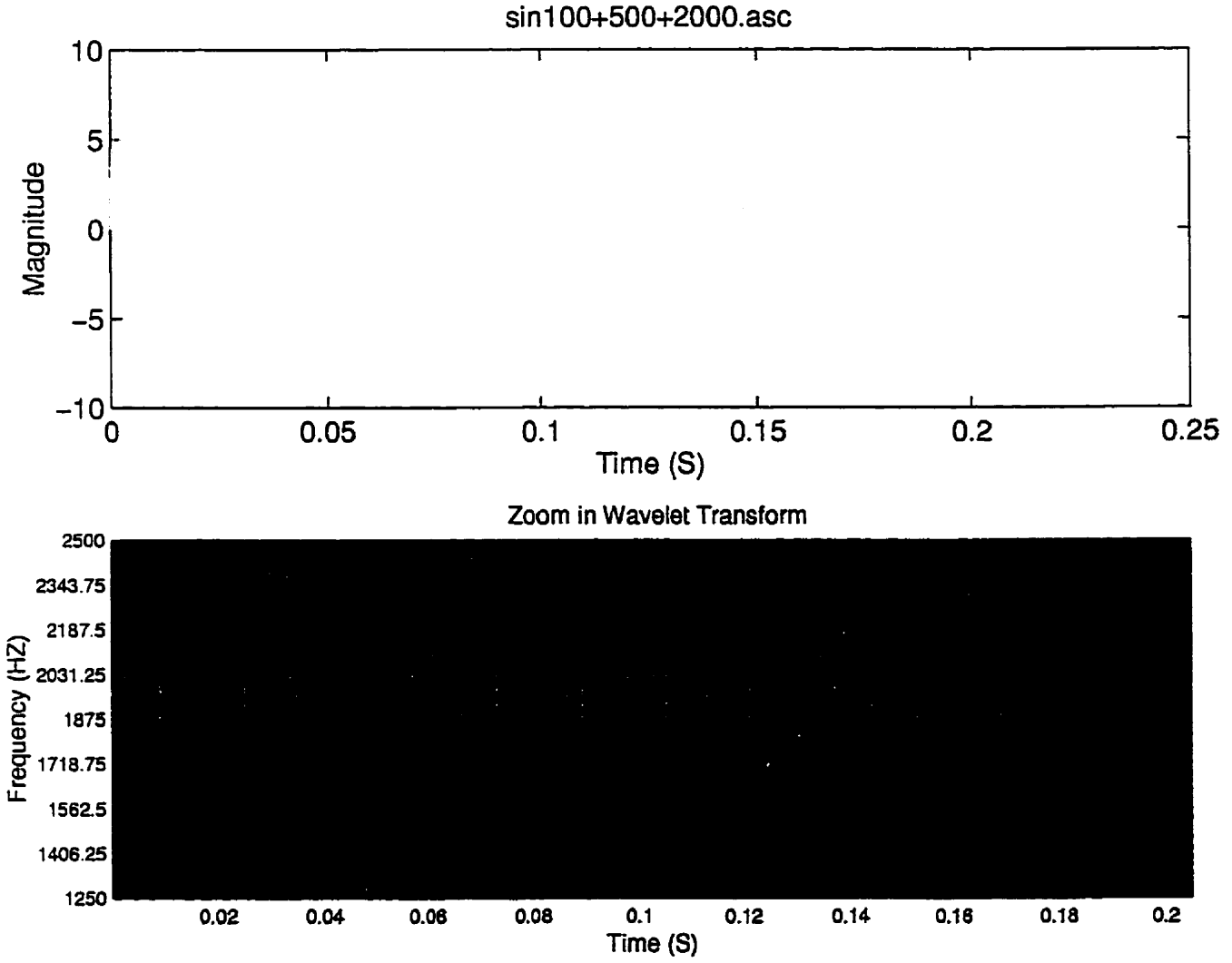

Figure 4.9: zooming in wavelet transform for frequency band 1250-2500 Hz of the sum of three sines.

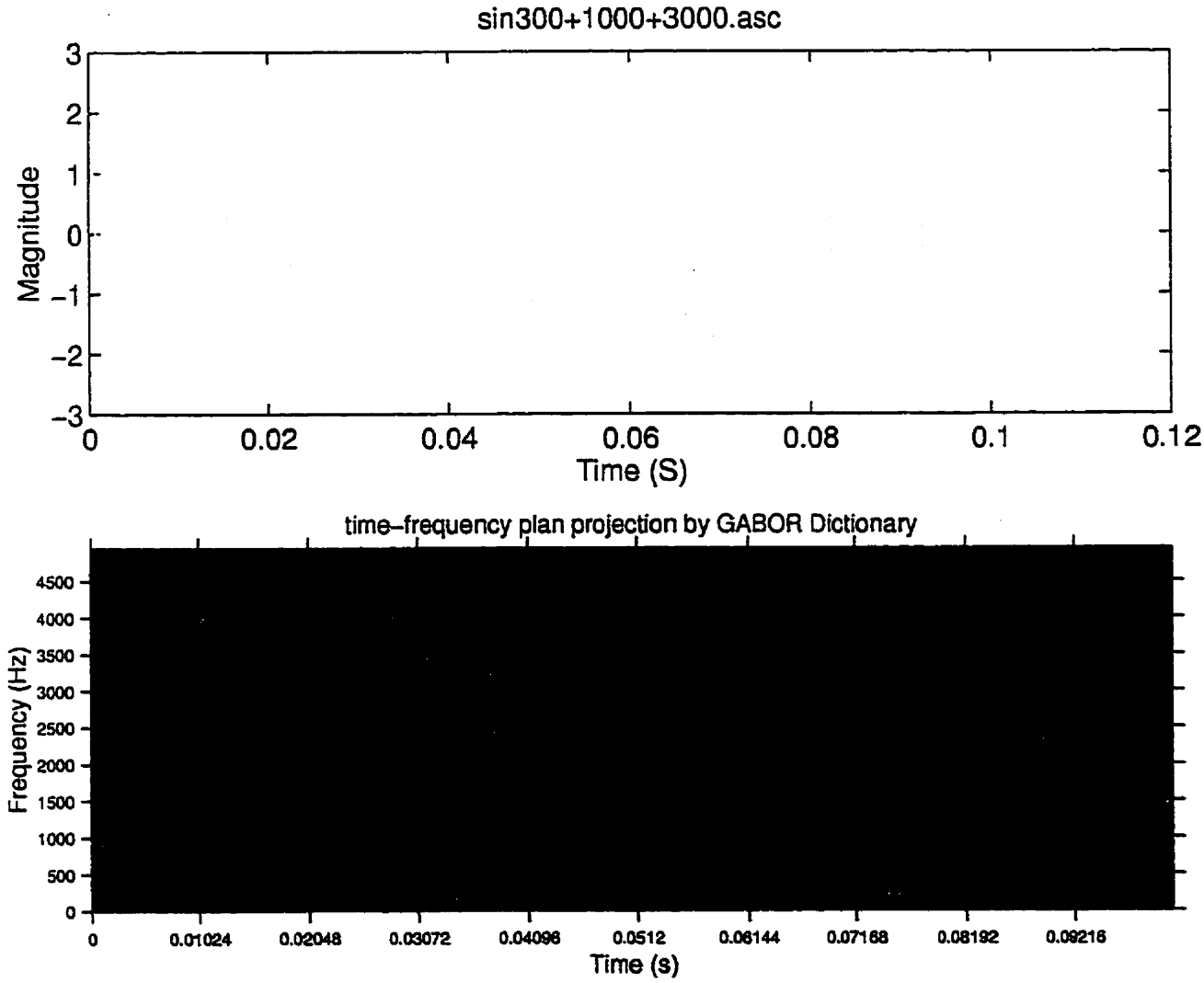

Figure 4.10: Time-frequency representation of sum of three sines by the Gabor dictionary.

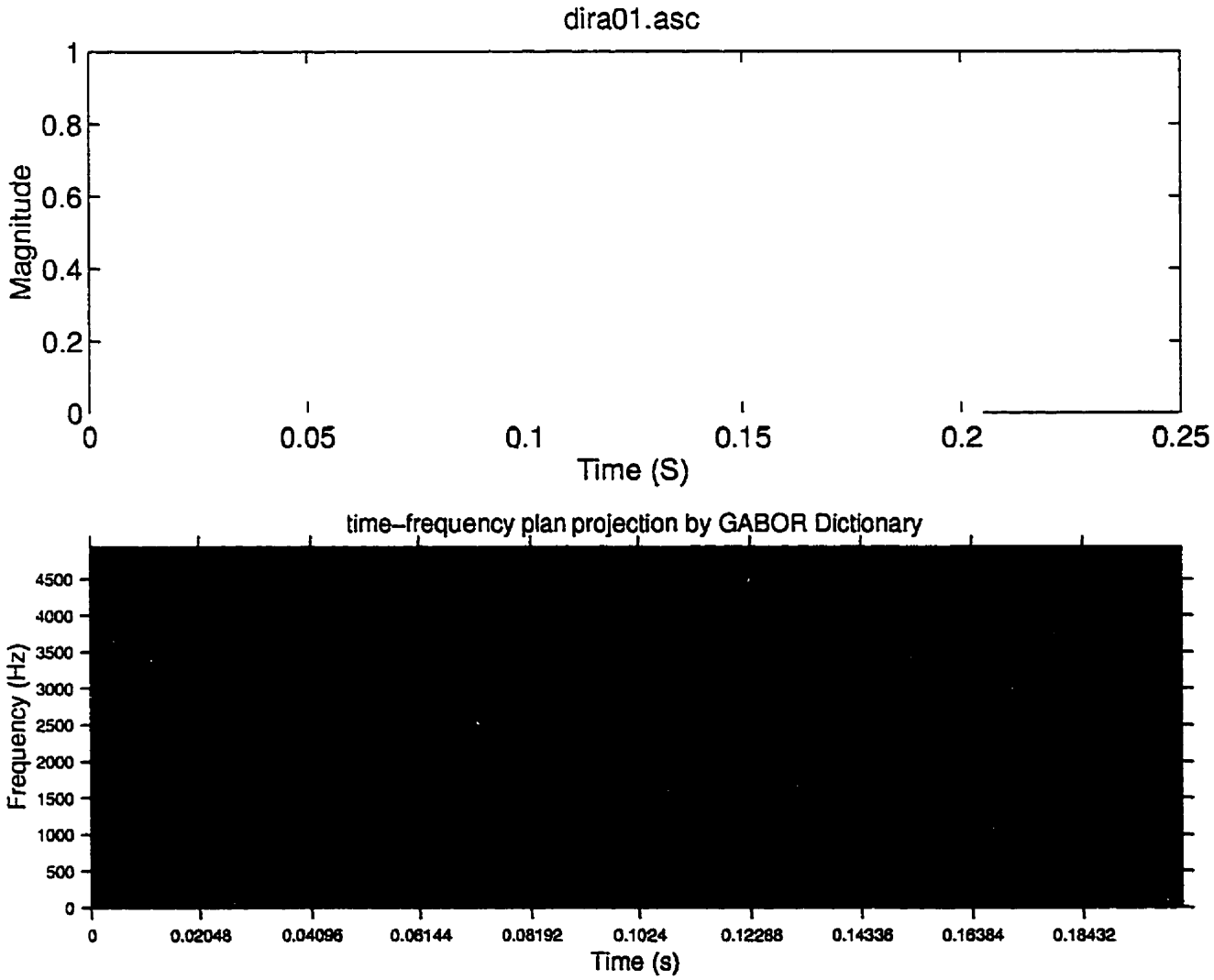

Figure 4.11: Time-frequency representation of a Dirac function by the Gabor dictionary.

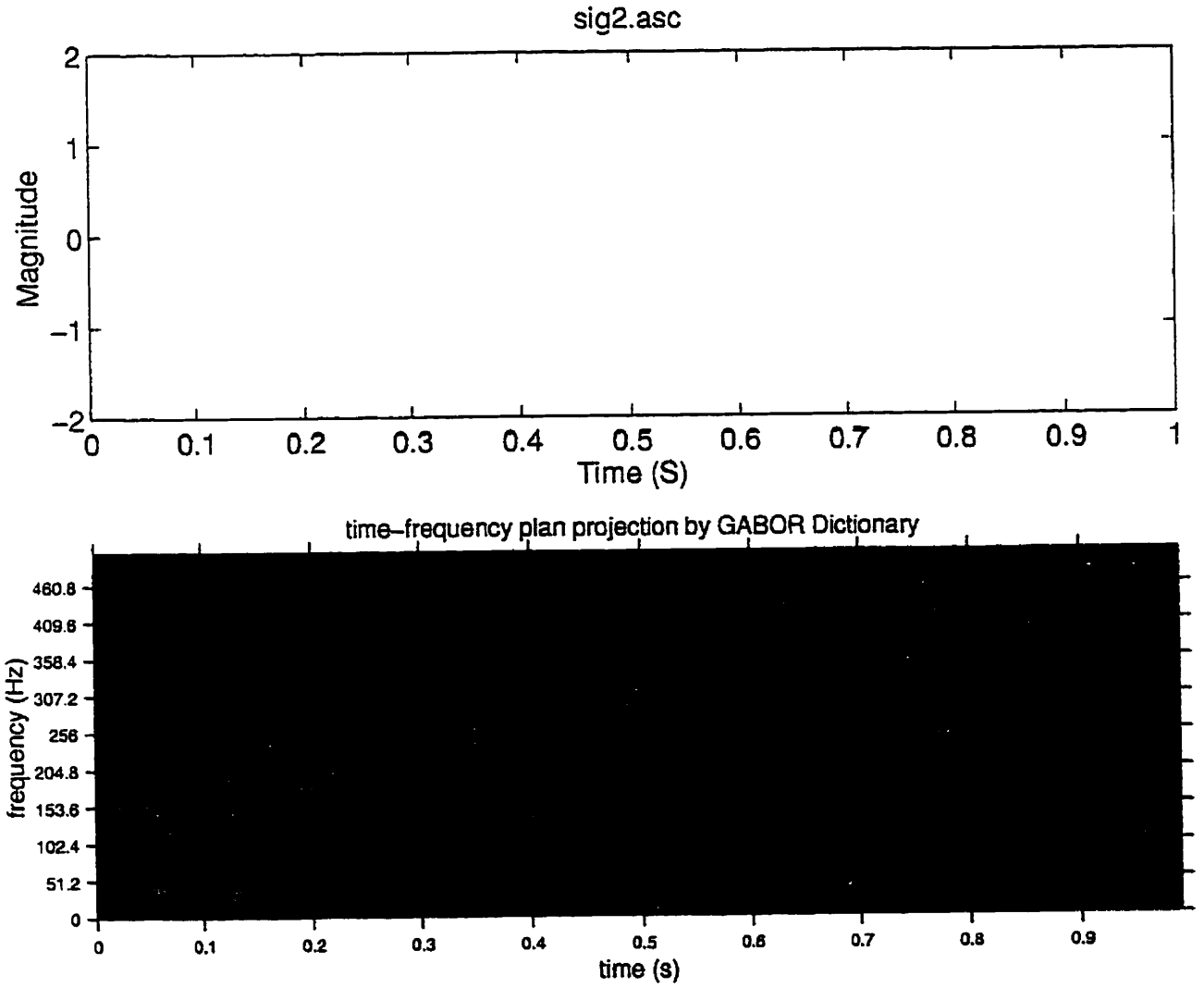

Figure 4.12: Time-frequency representation of two parallel chirps by the Gabor dictionary.

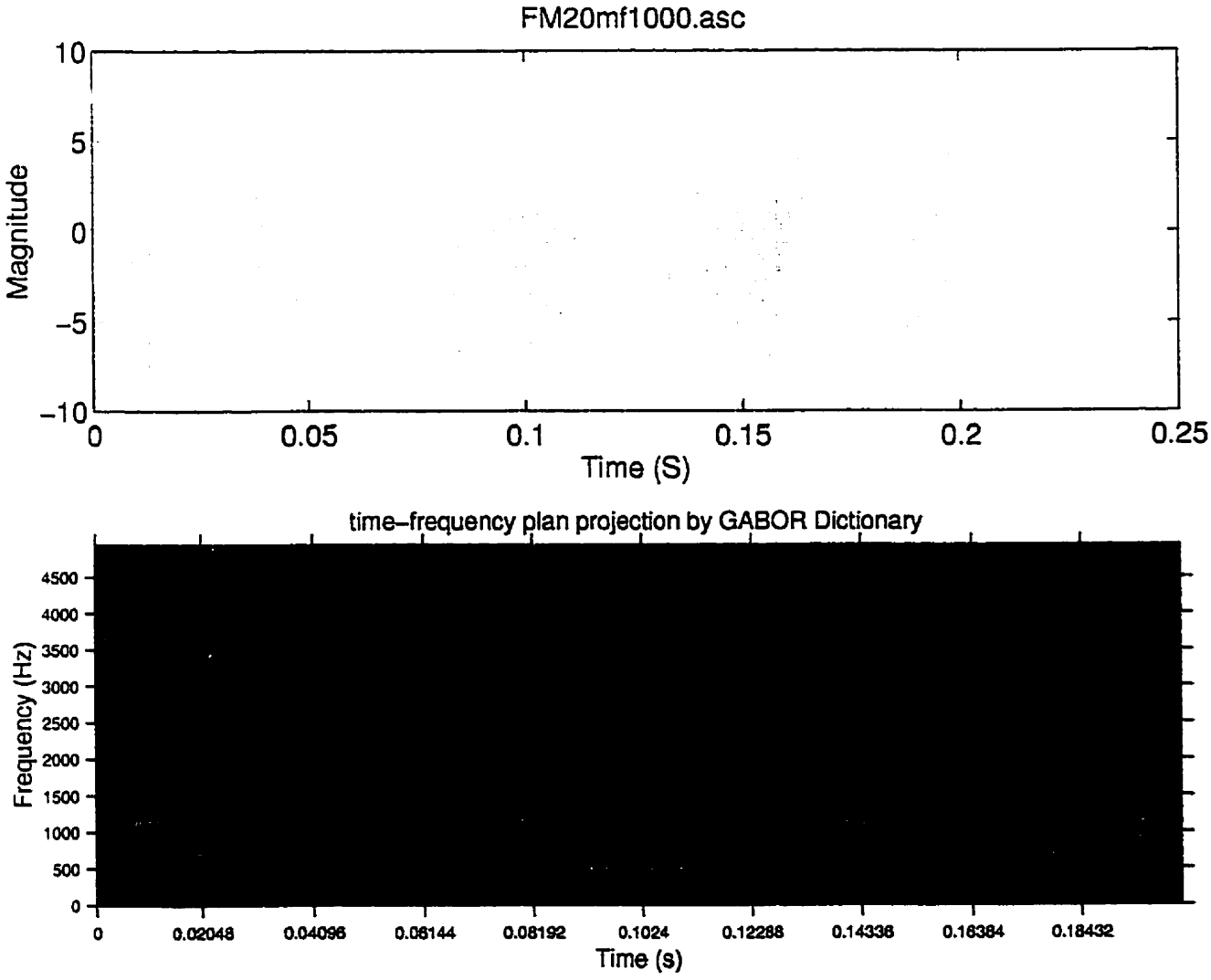

Figure 4.13: Time-frequency representation of a frequency-modulated sine by the Gabor dictionary.

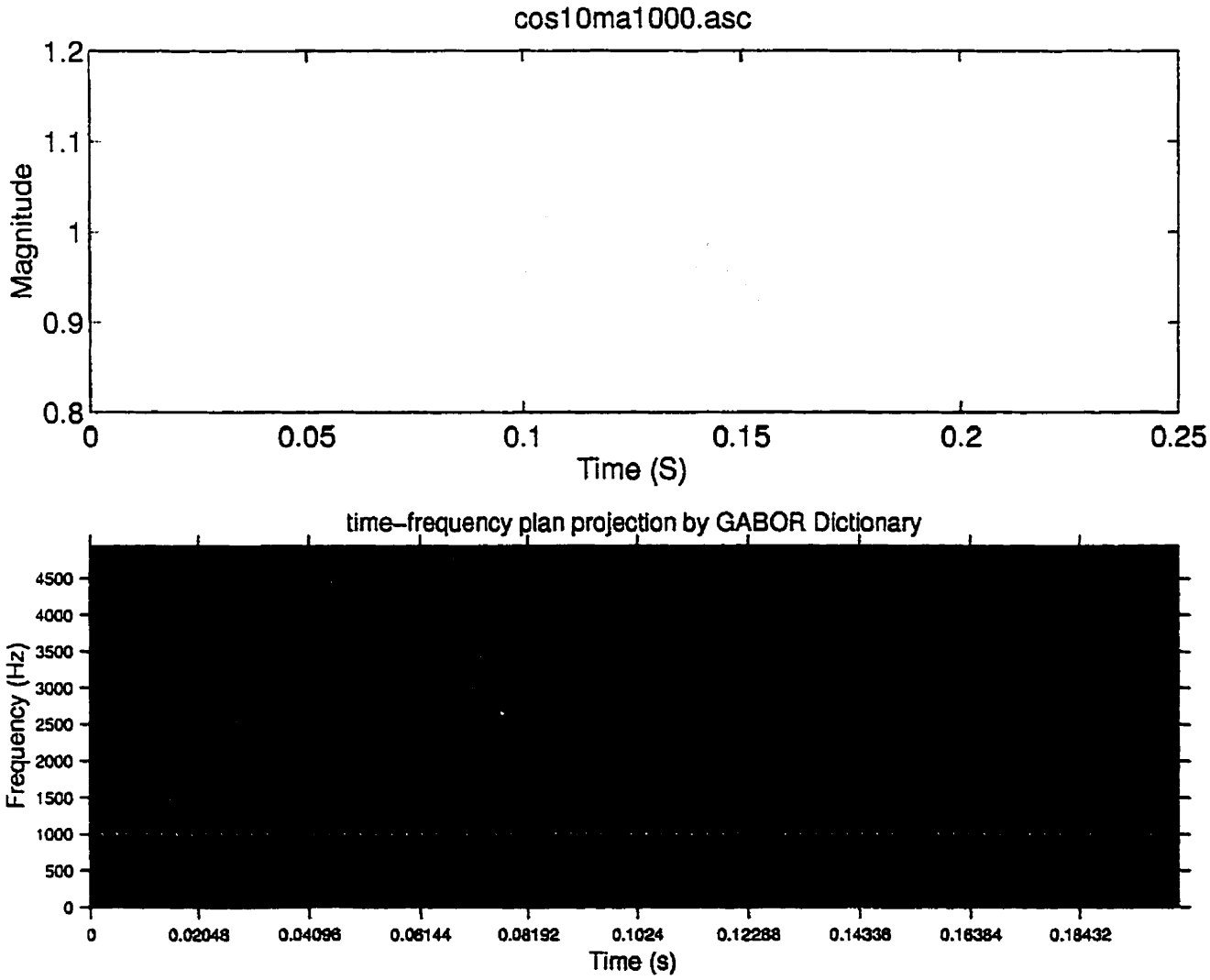

Figure 4.14: Time-frequency representation of an amplitude-modulation cosine by the Gabor dictionary.

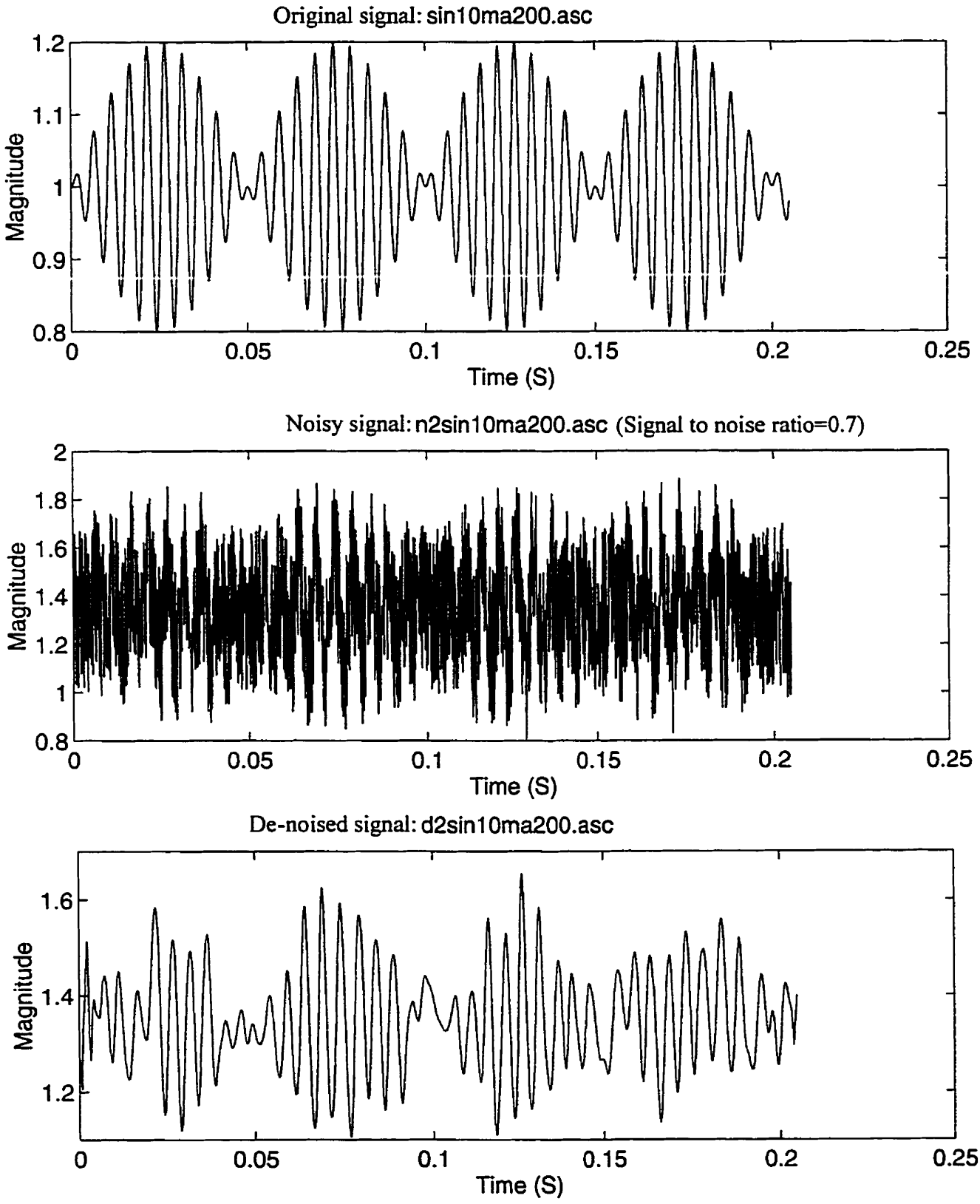

Figure 4.15: Signal de-noised by wavelet transform.

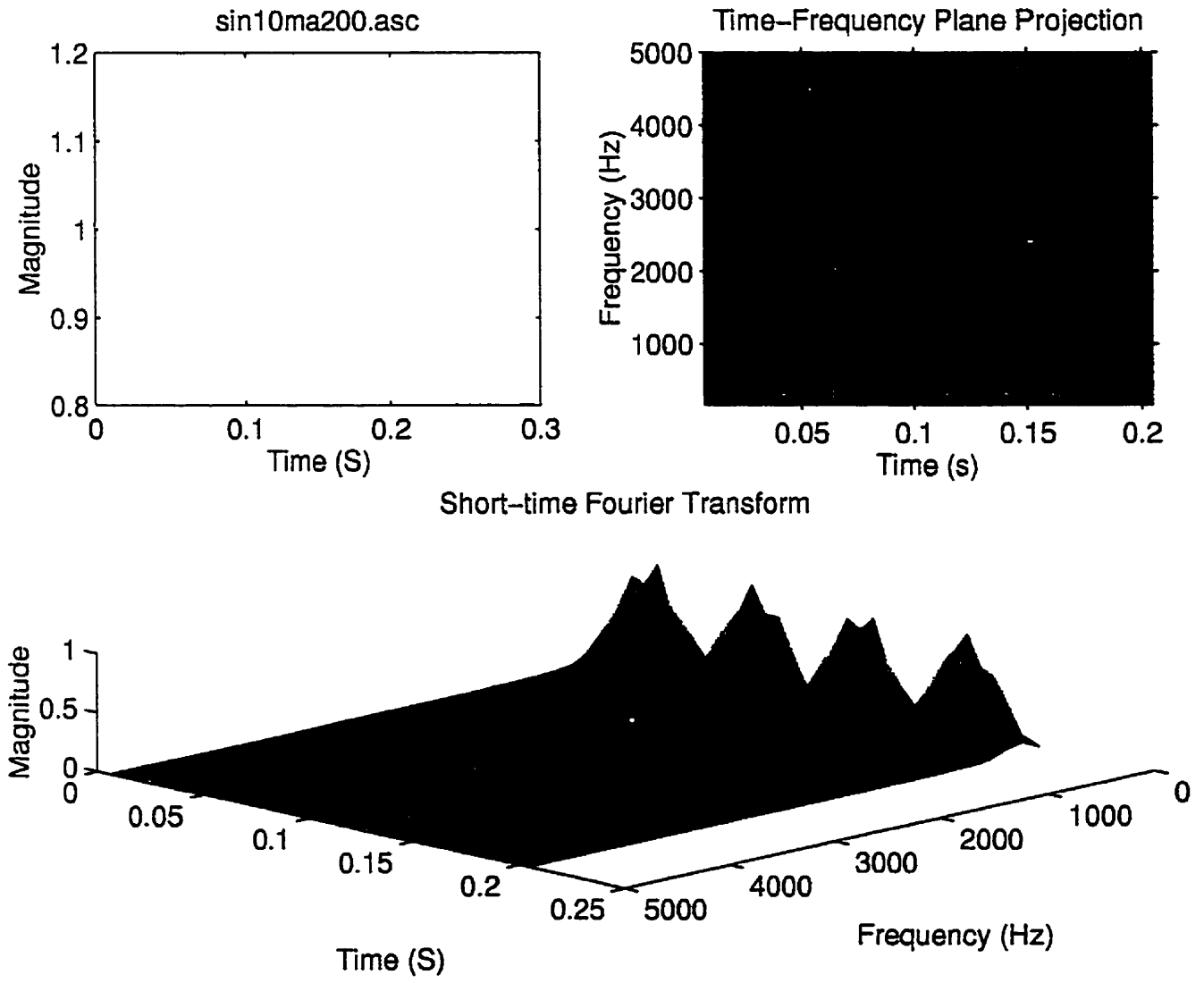

Figure 4.16: Short-time Fourier transform of the original signal.

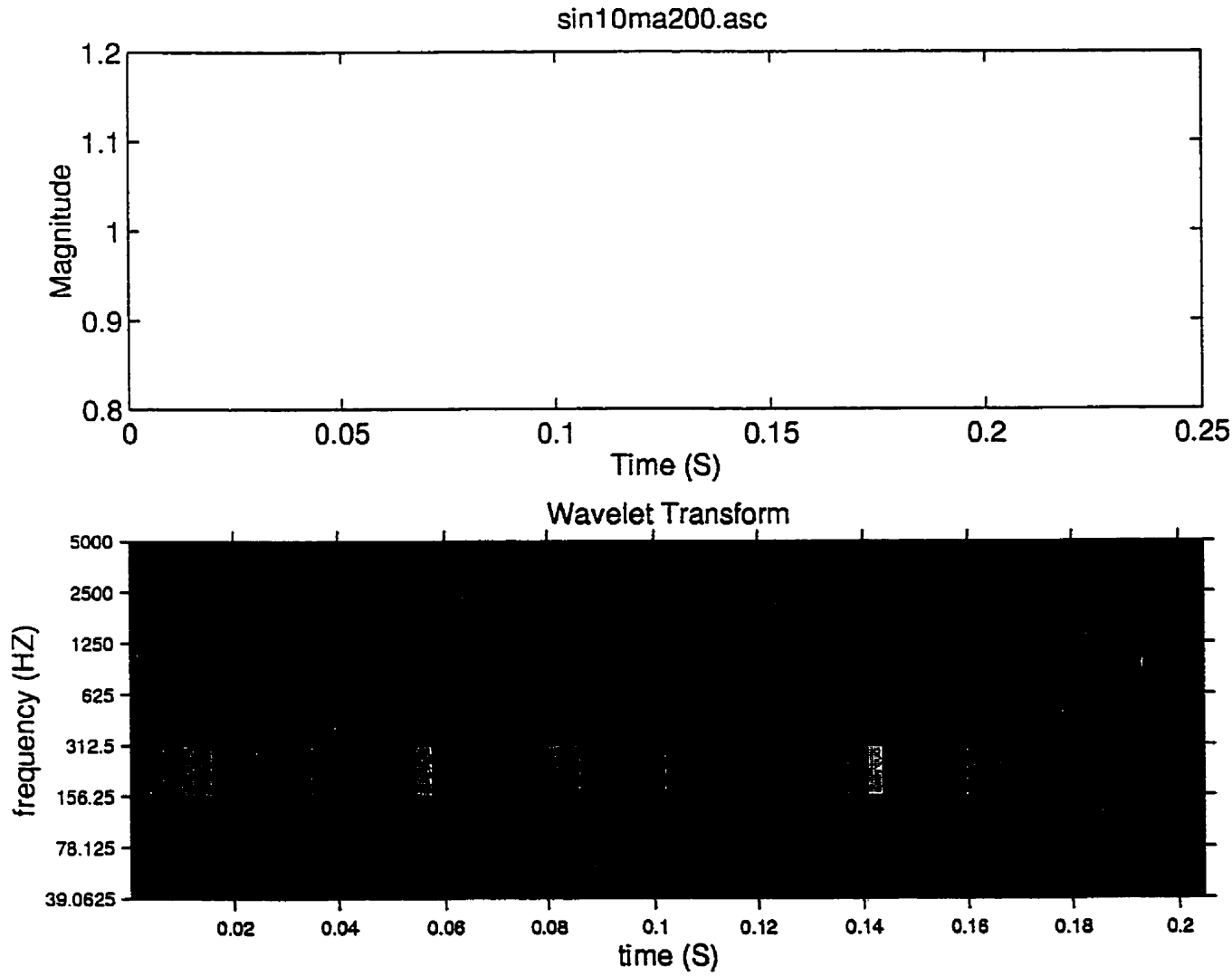

Figure 4.17: Wavelet transform of the original signal.

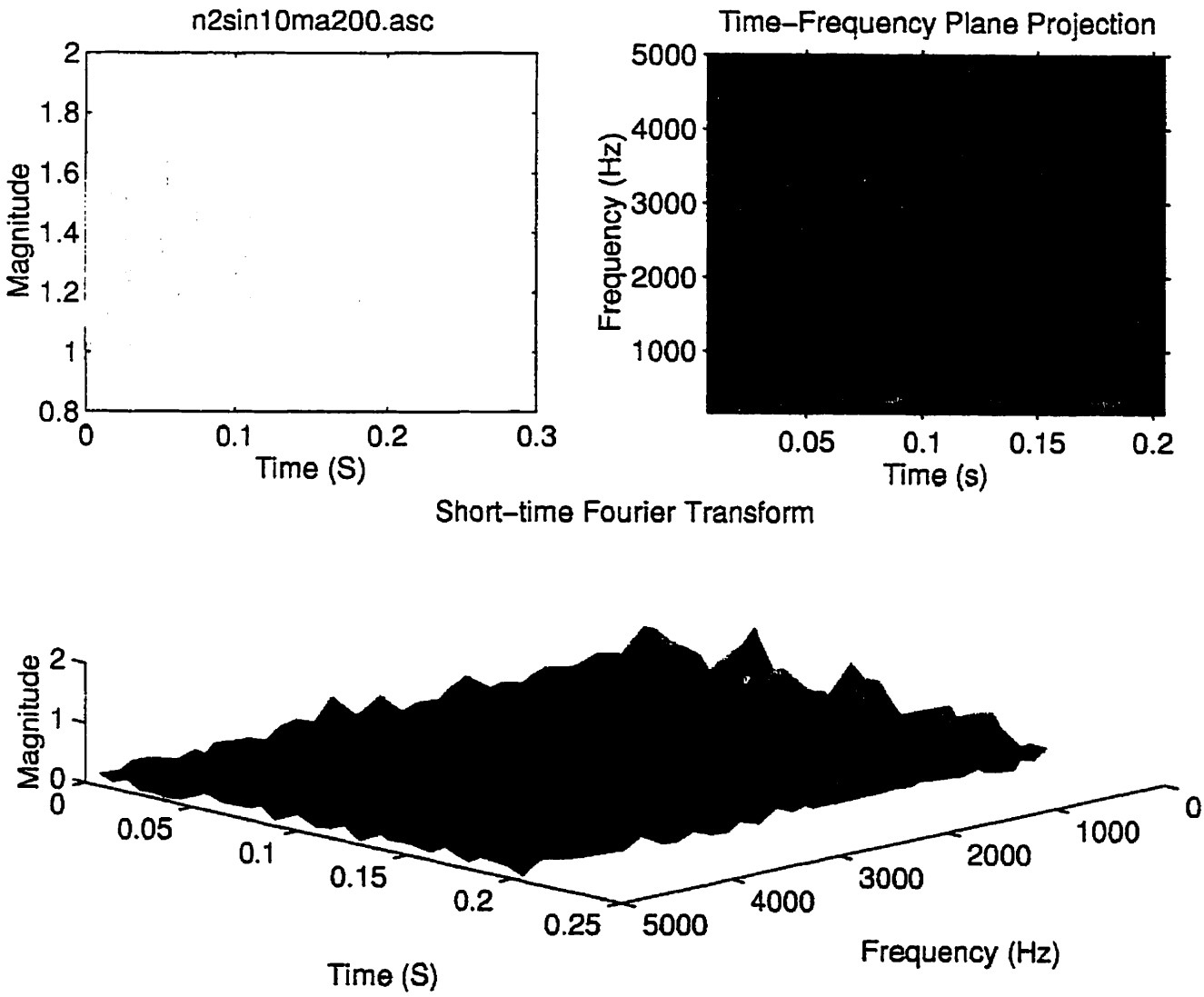

Figure 4.18: Short-time Fourier transform of the noisy signal.

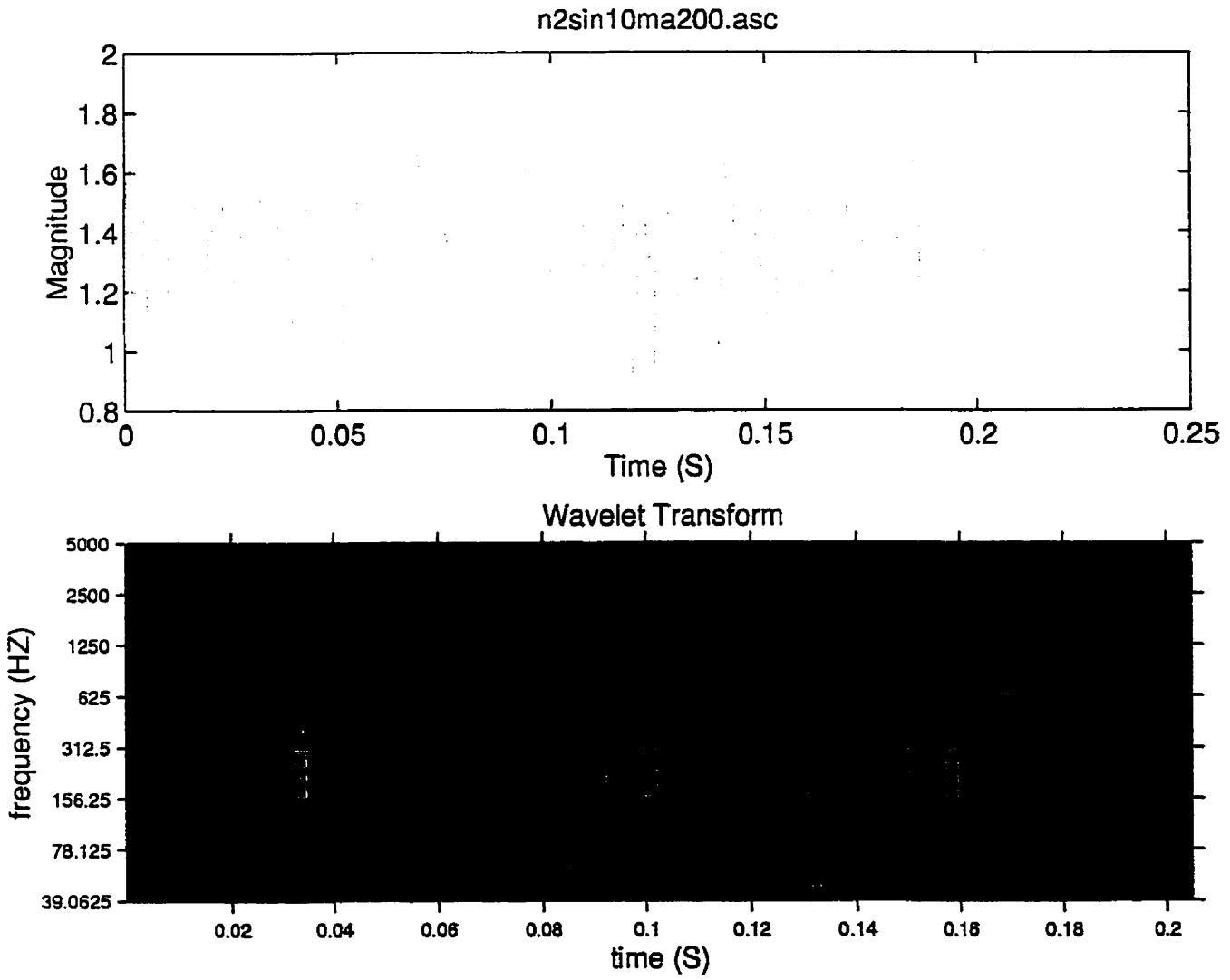

Figure 4.19: Wavelet transform of the noisy signal.

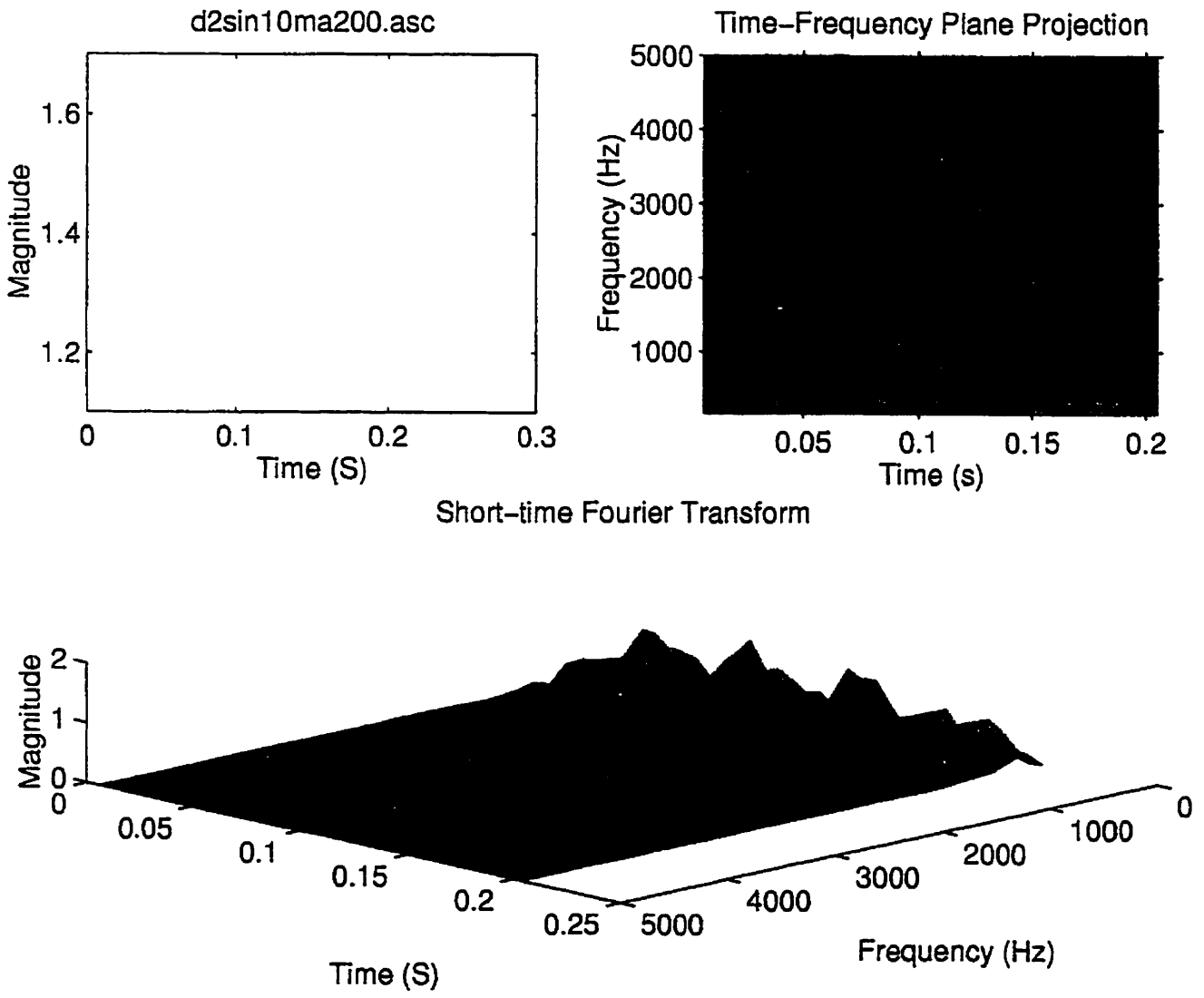

Figure 4.20: Short-time Fourier transform of the de-noised signal.

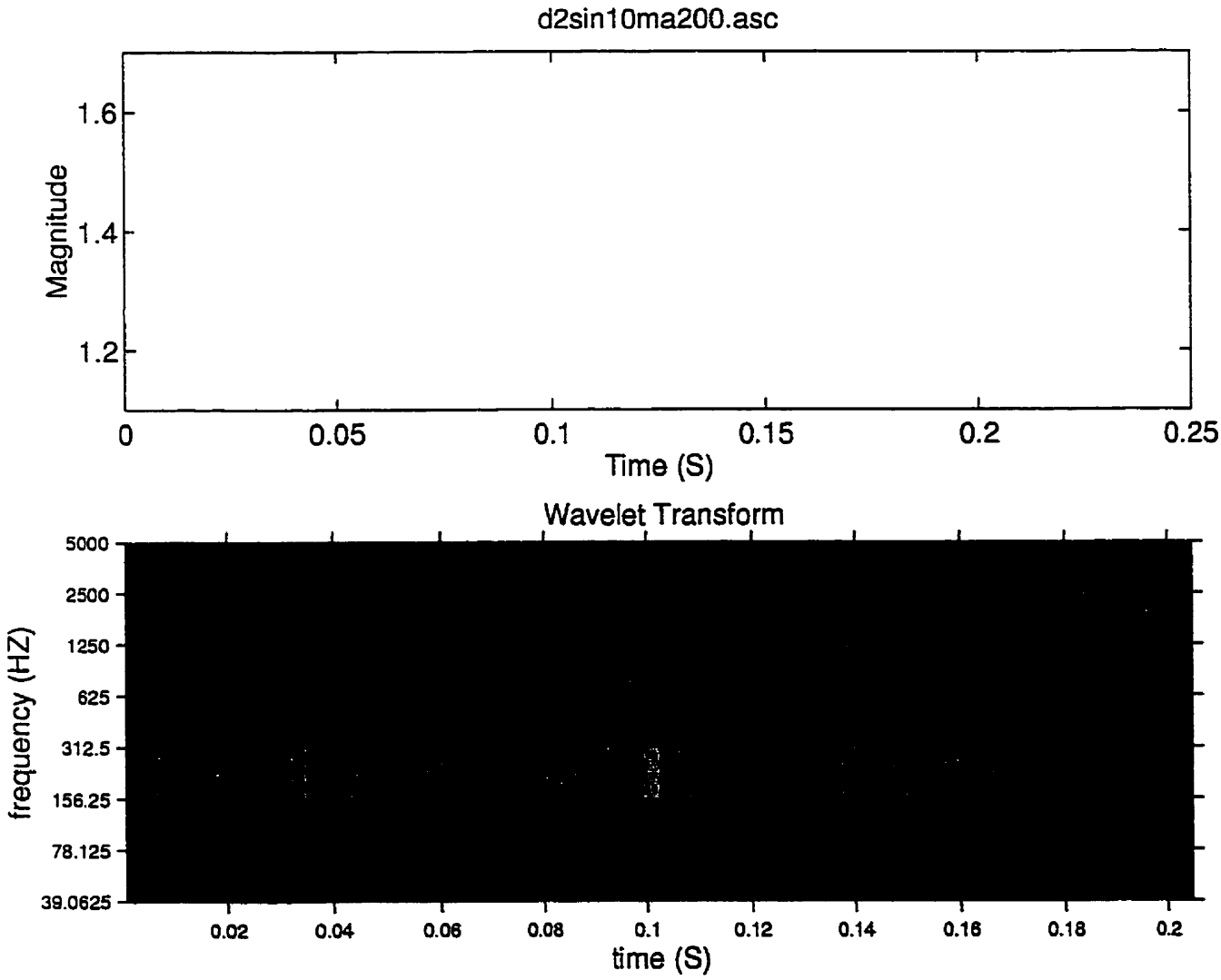

Figure 4.21: Wavelet transform of the de-noised signal.

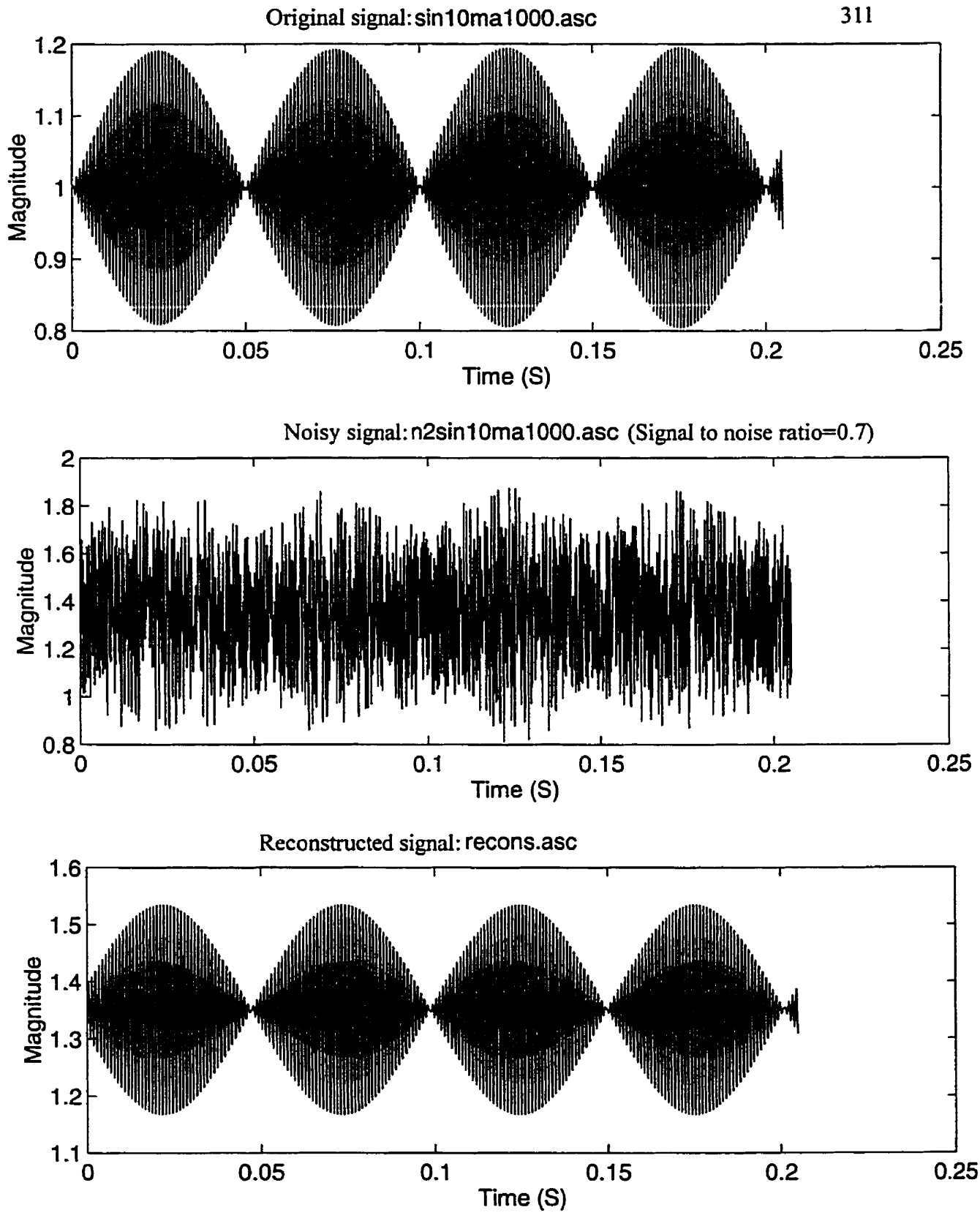

Figure 4.22: Signal de-noised by Matching Pursuit algorithm.

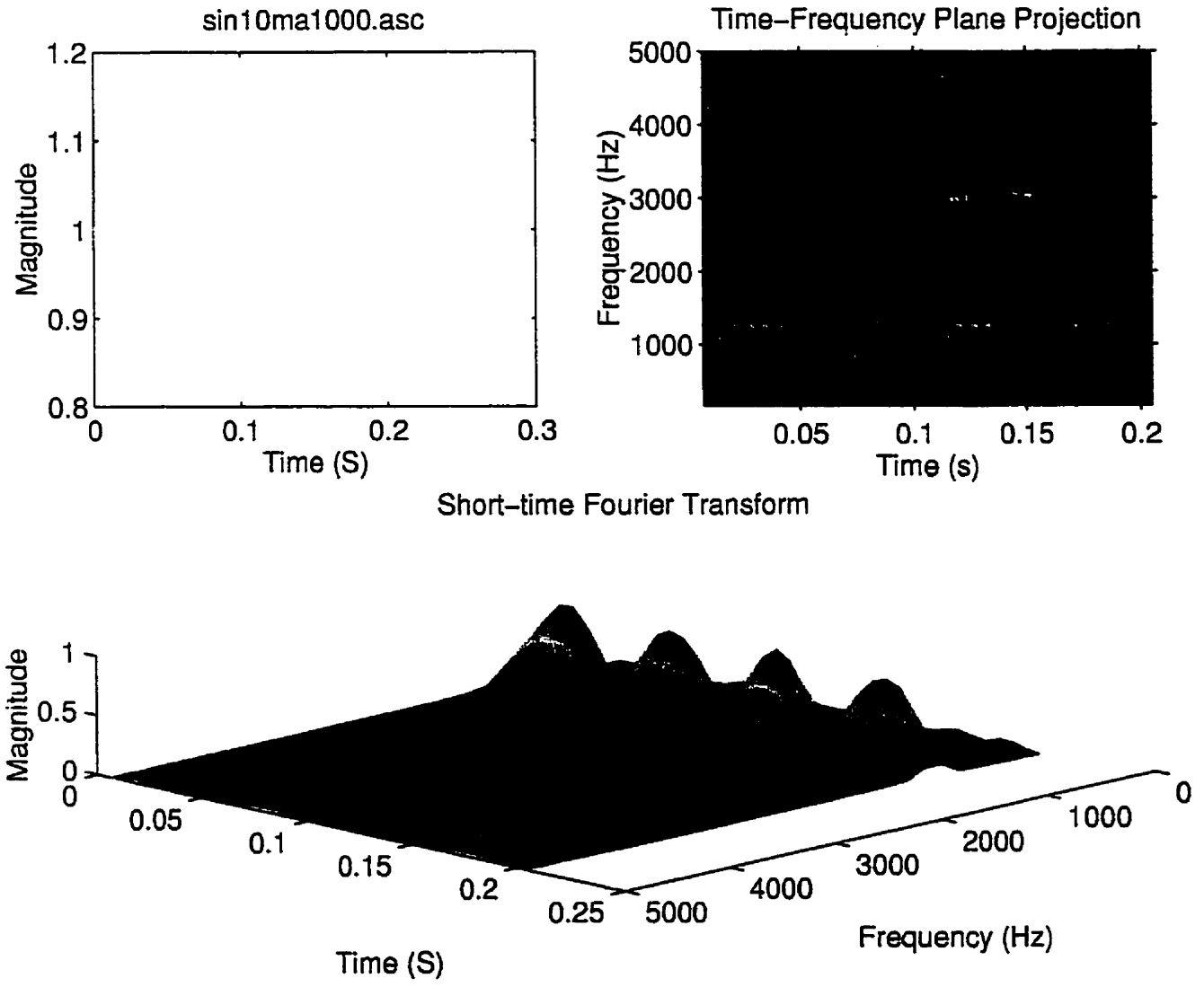

Figure 4.23: Short-time Fourier transform of the original signal.

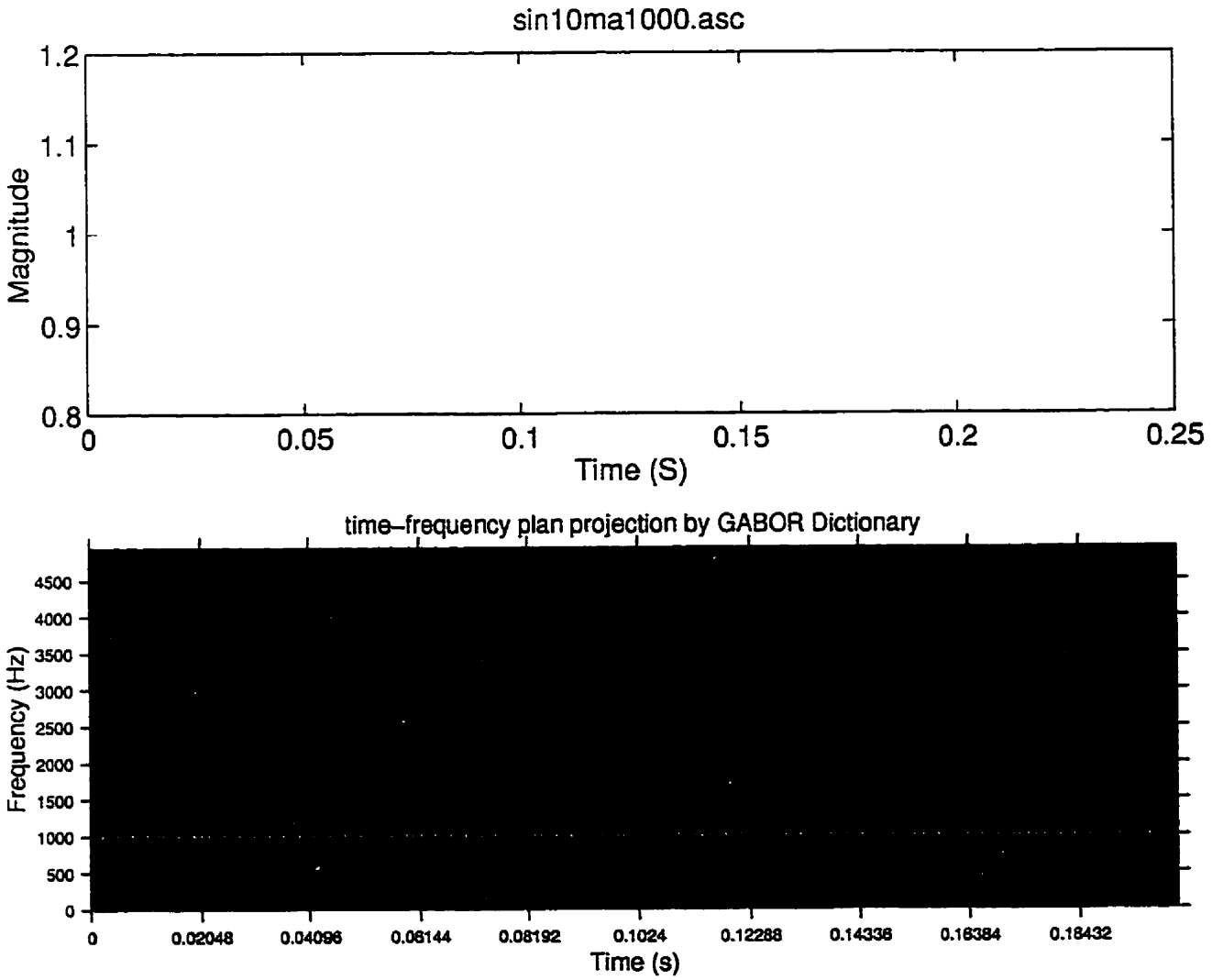

Figure 4.24: Time-frequency representation of the original signal by the Gabor dictionary.

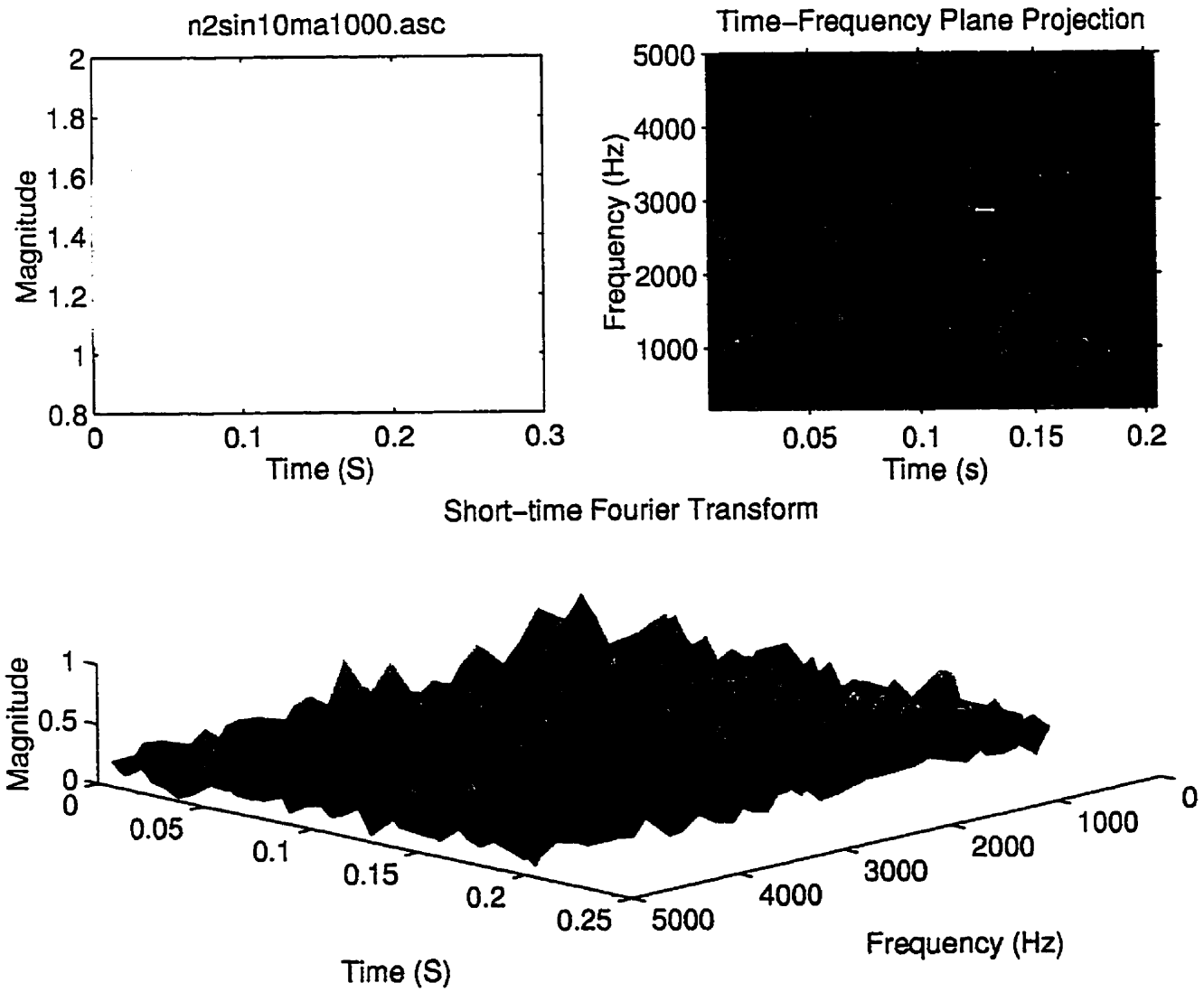

Figure 4.25: Short-time Fourier transform of the noisy signal.

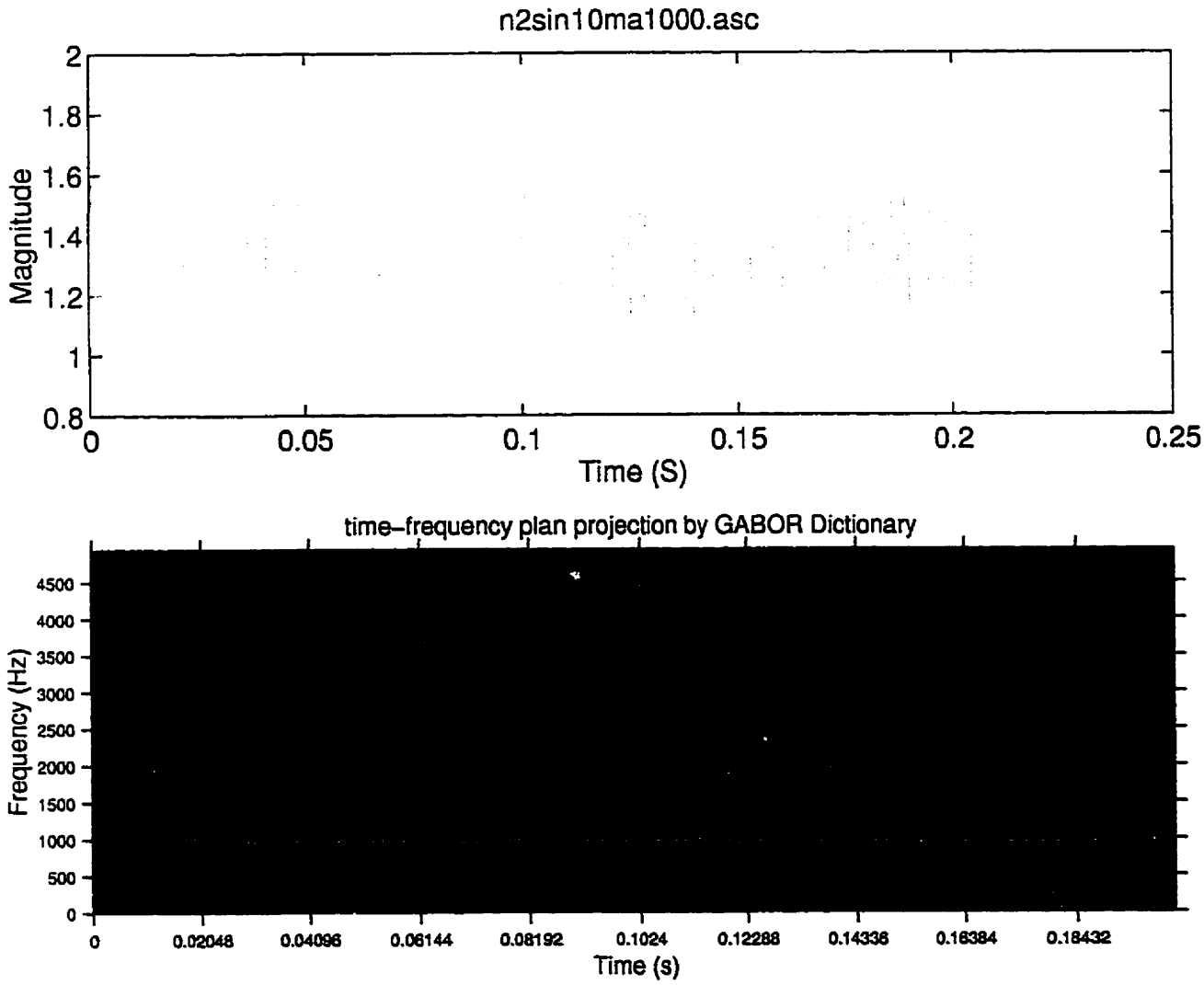

Figure 4.26: Time-frequency representation of the noisy signal by the Gabor dictionary.

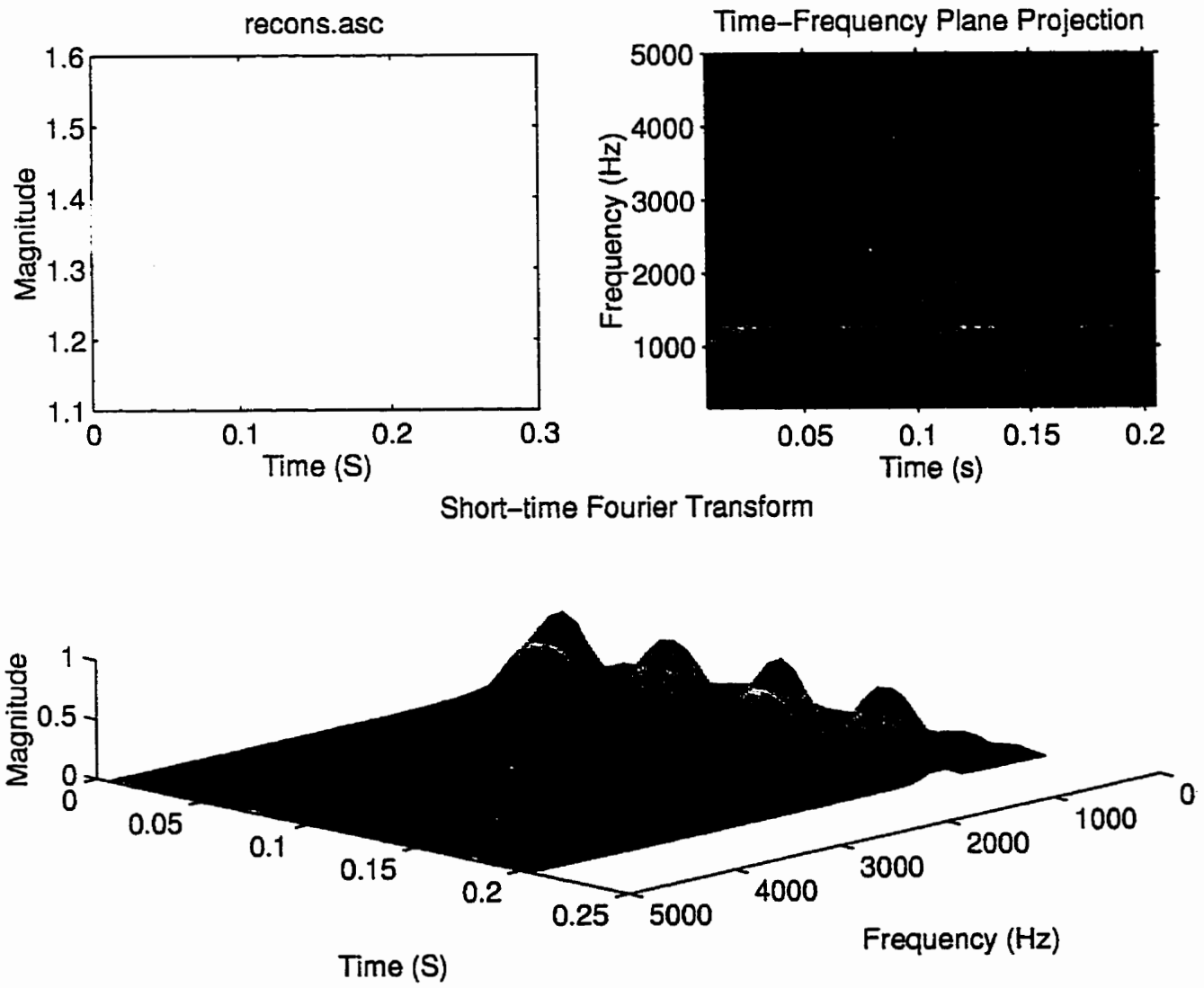

Figure 4.27: Short-time Fourier transform of the de-noised signal.

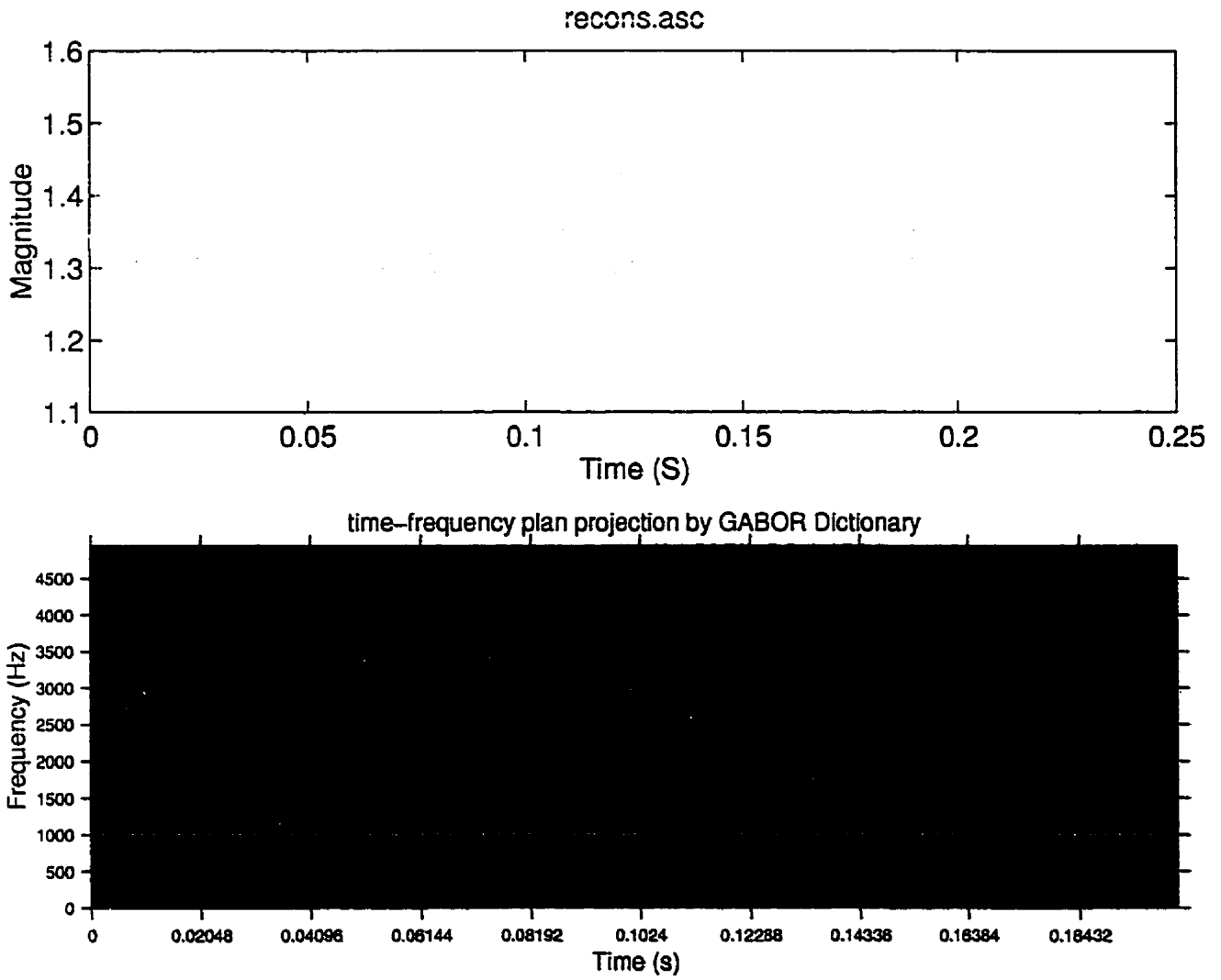

Figure 4.28: Time-frequency representation of the de-noised signal by the Gabor dictionary.

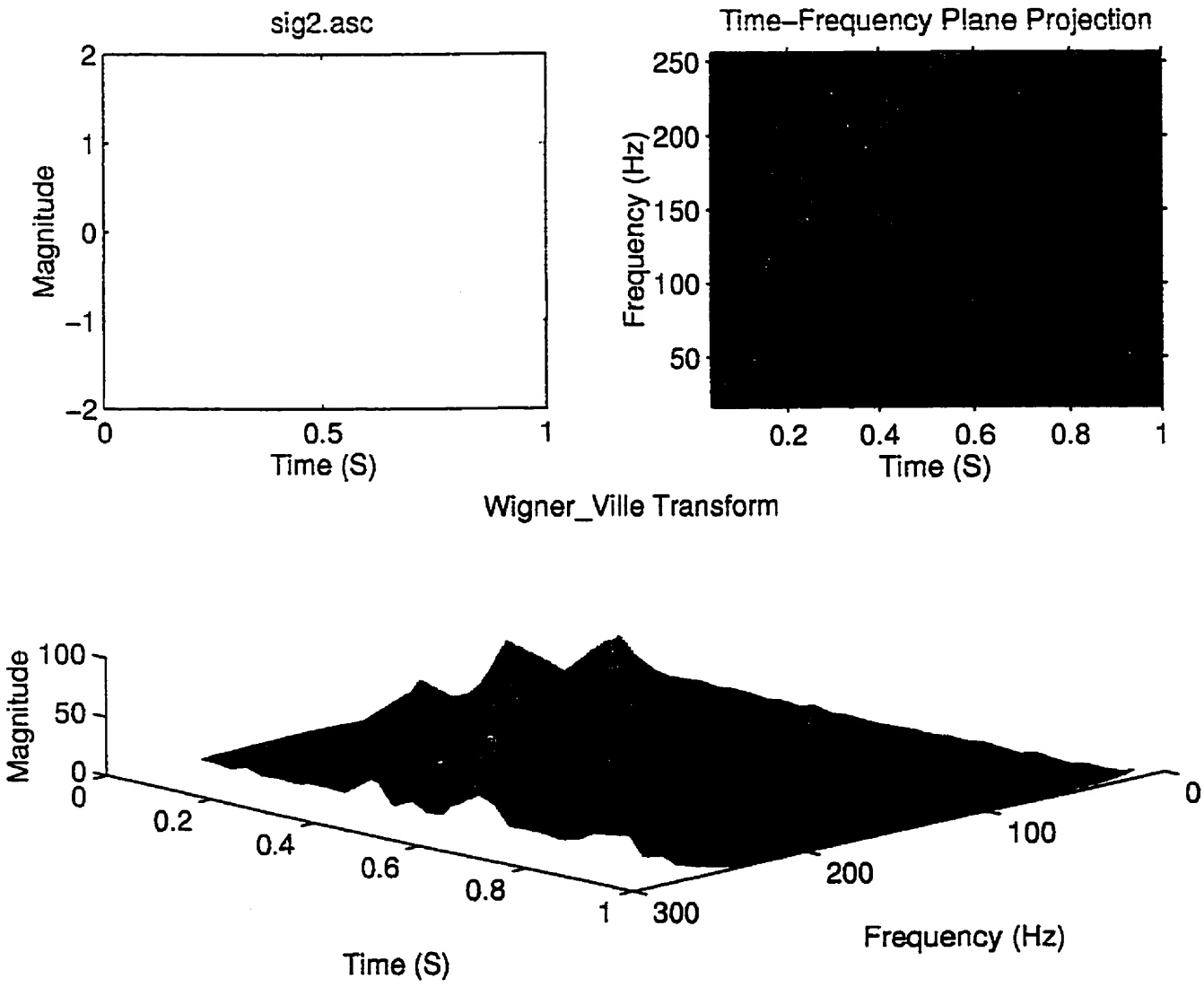

Figure 4.29: Wigner-Ville distribution of two parallel chirps.

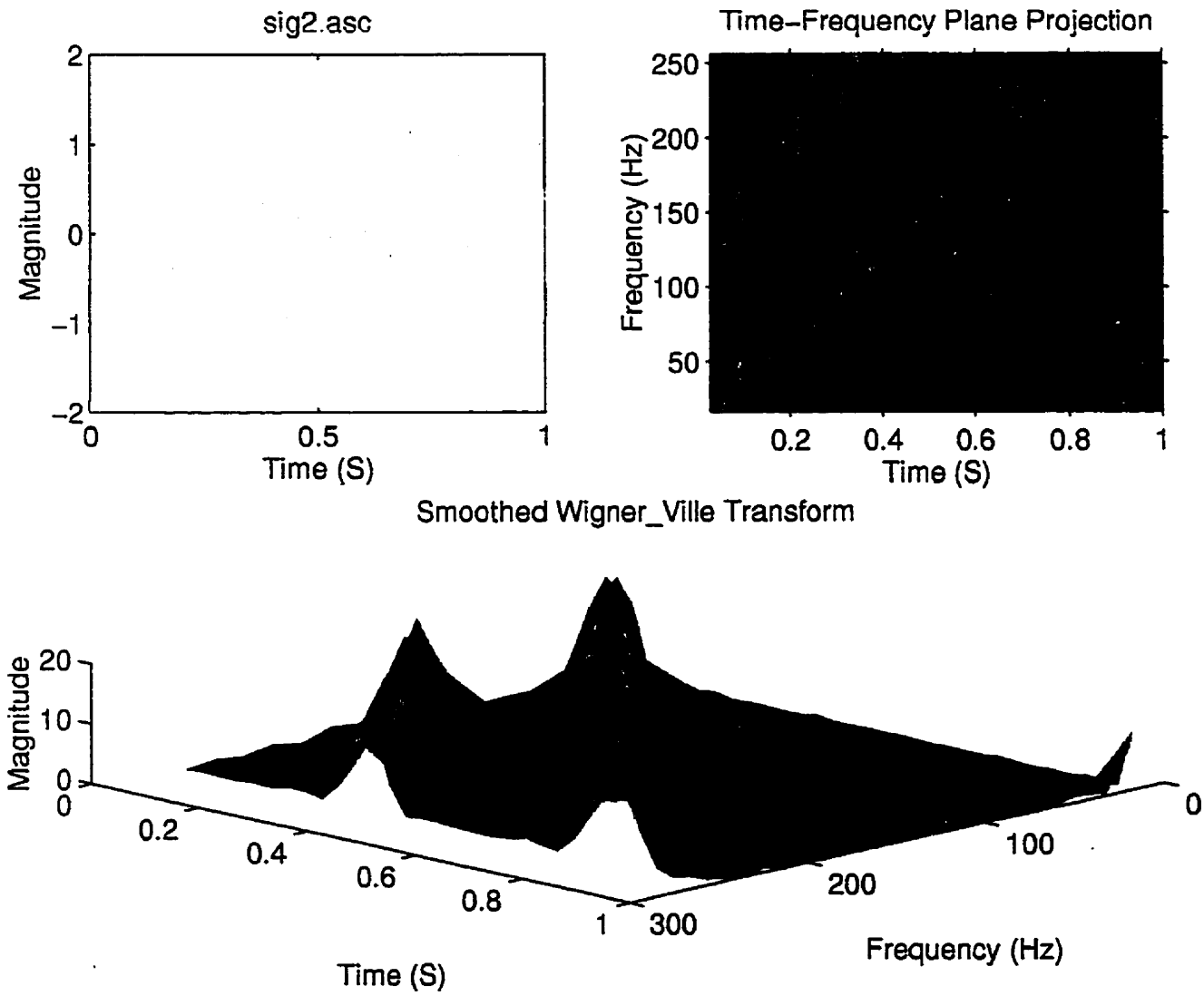

Figure 4.30: Smoothed Wigner-Ville distribution of two parallel chirps.

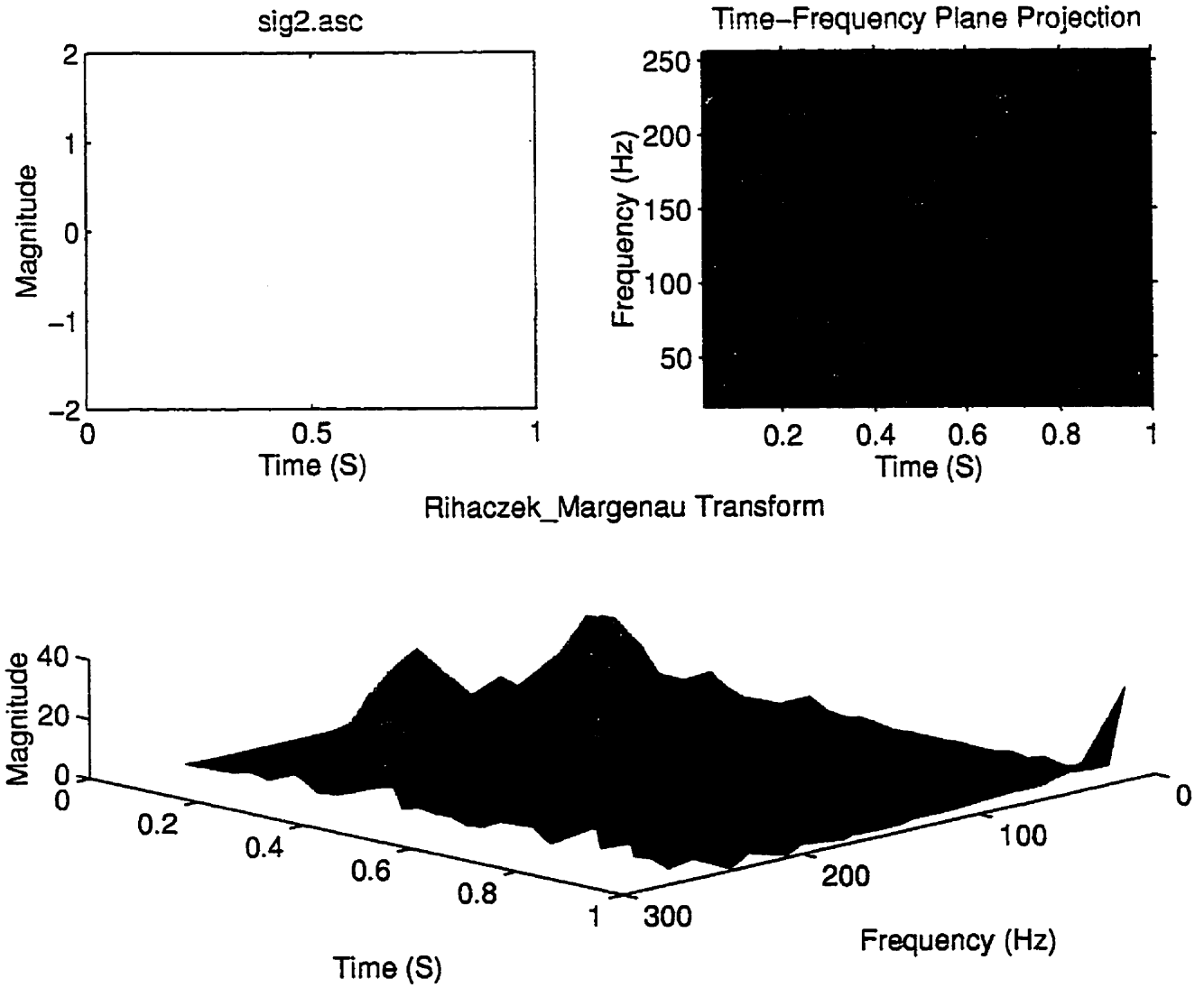

Figure 4.31: Rihaczek-Margenau distribution of two parallel chirps.

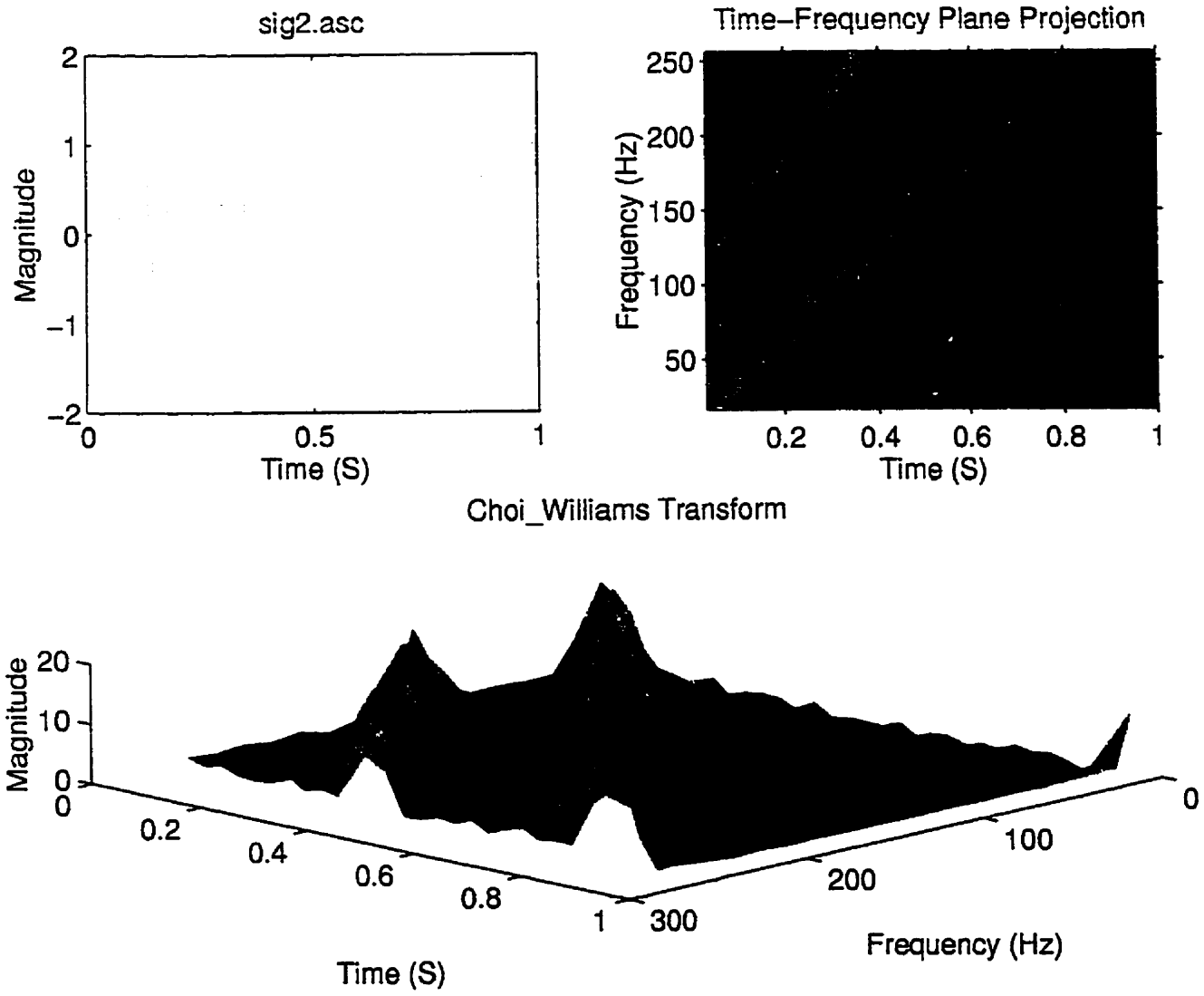

Figure 4.32: Choi-Williams distribution of two parallel chirps.

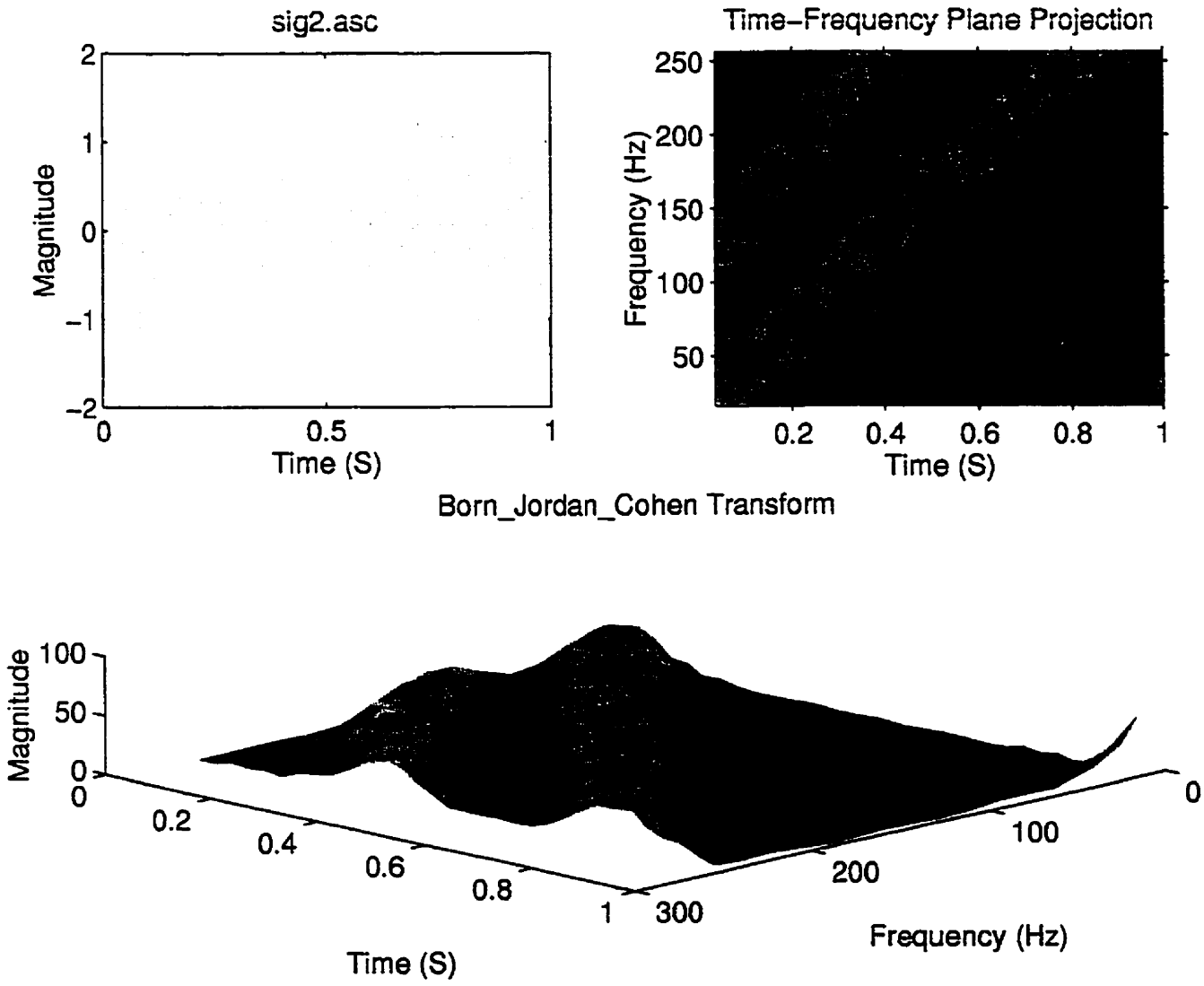

Figure 4.33: Born-Jordan-Cohen distribution of two parallel chirps.

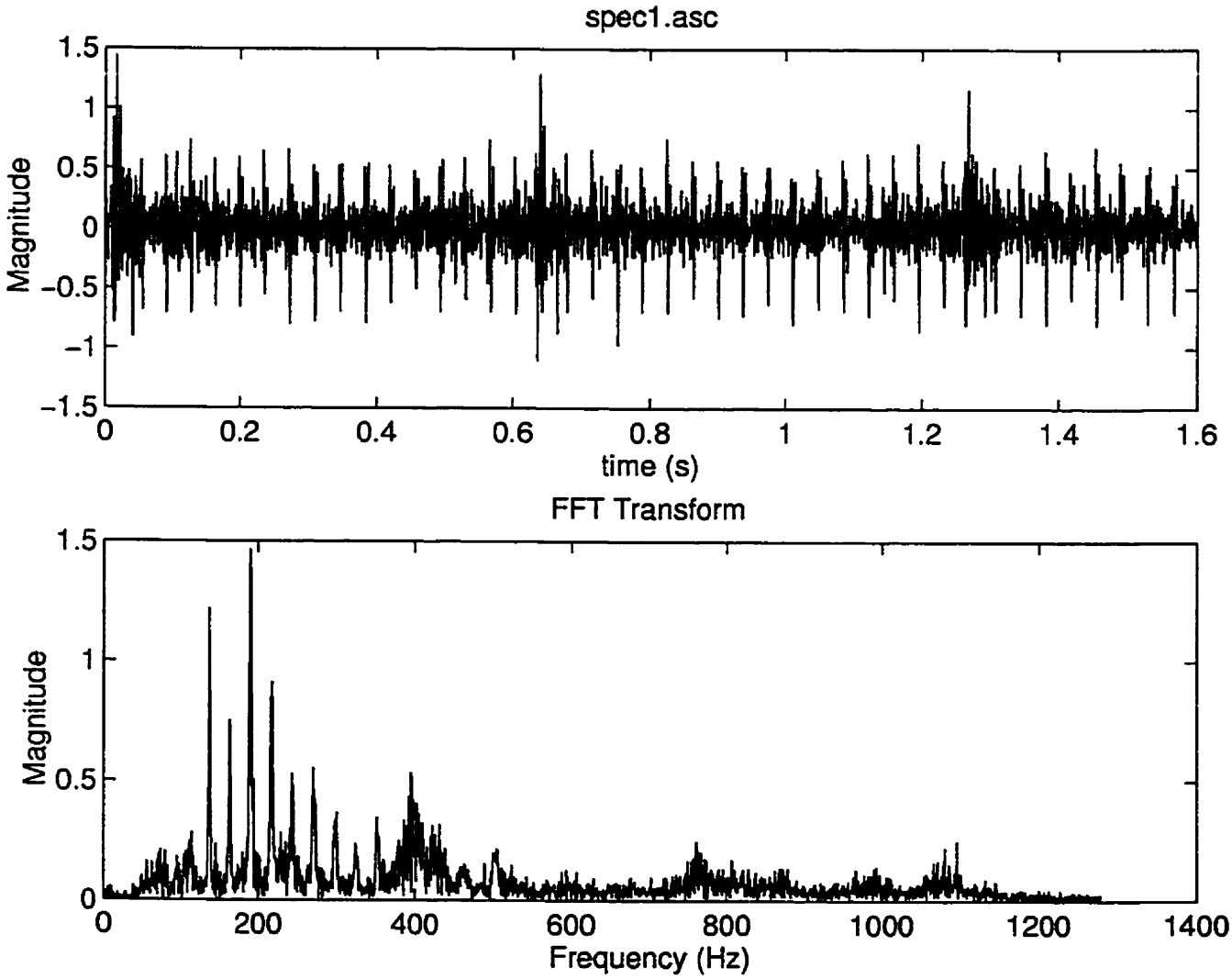

Figure 4.34: Time and spectrum representation of the signal measured on a defective gearbox.

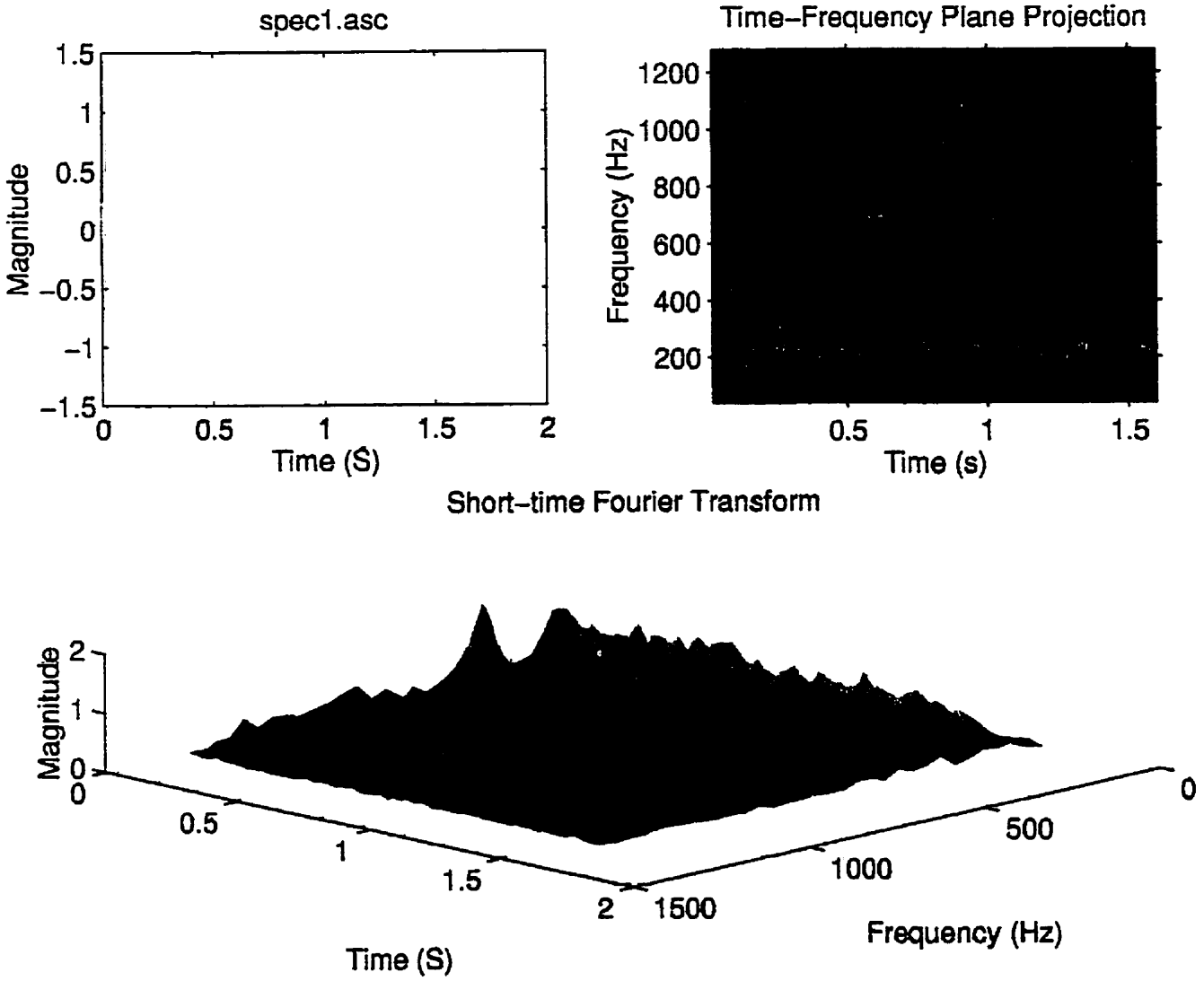

Figure 4.35: Short-time Fourier transform of the signal measured on a defective gearbox.

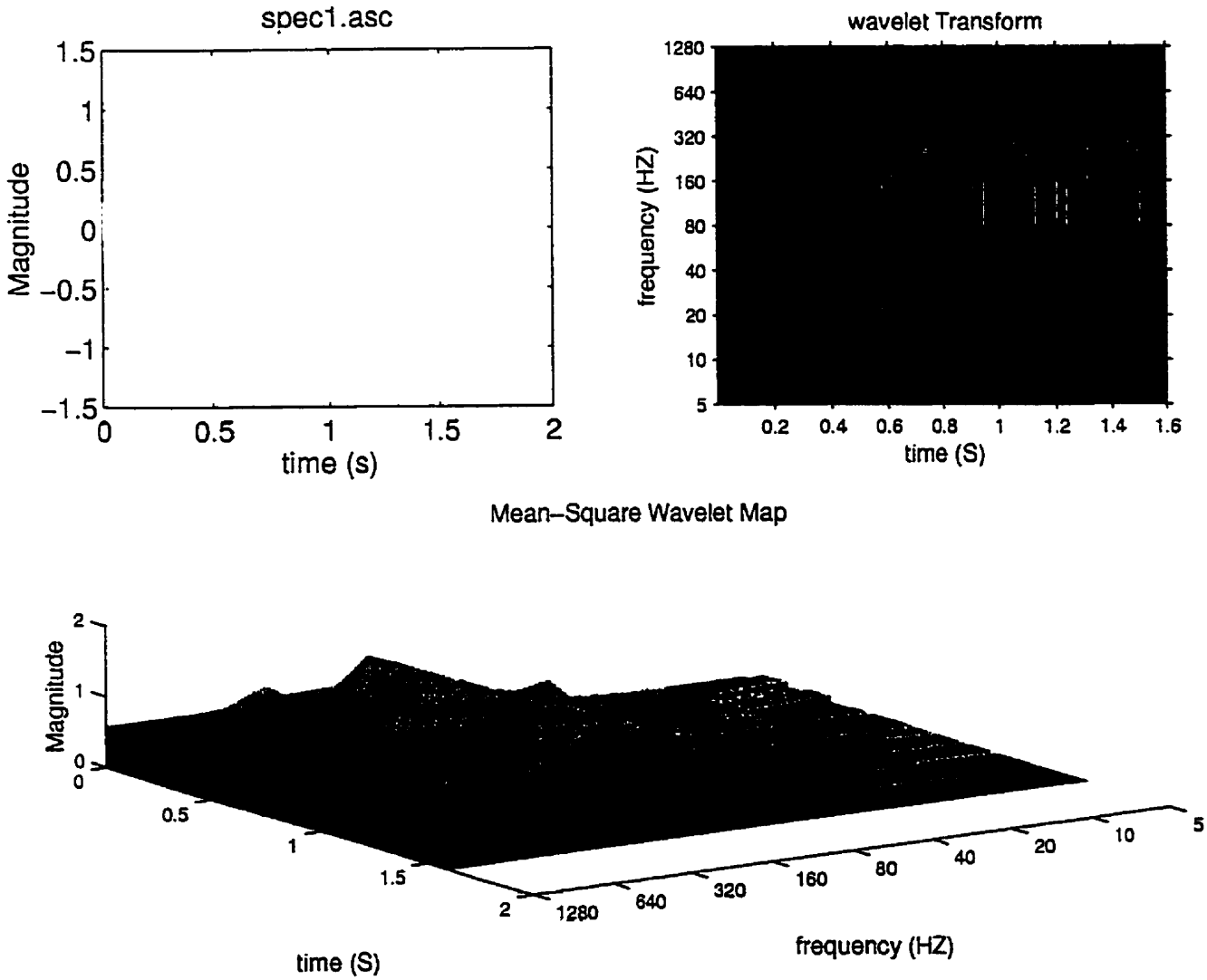

Figure 4.36: Wavelet transform and mean-square wavelet map of the signal measured on a defective gearbox.

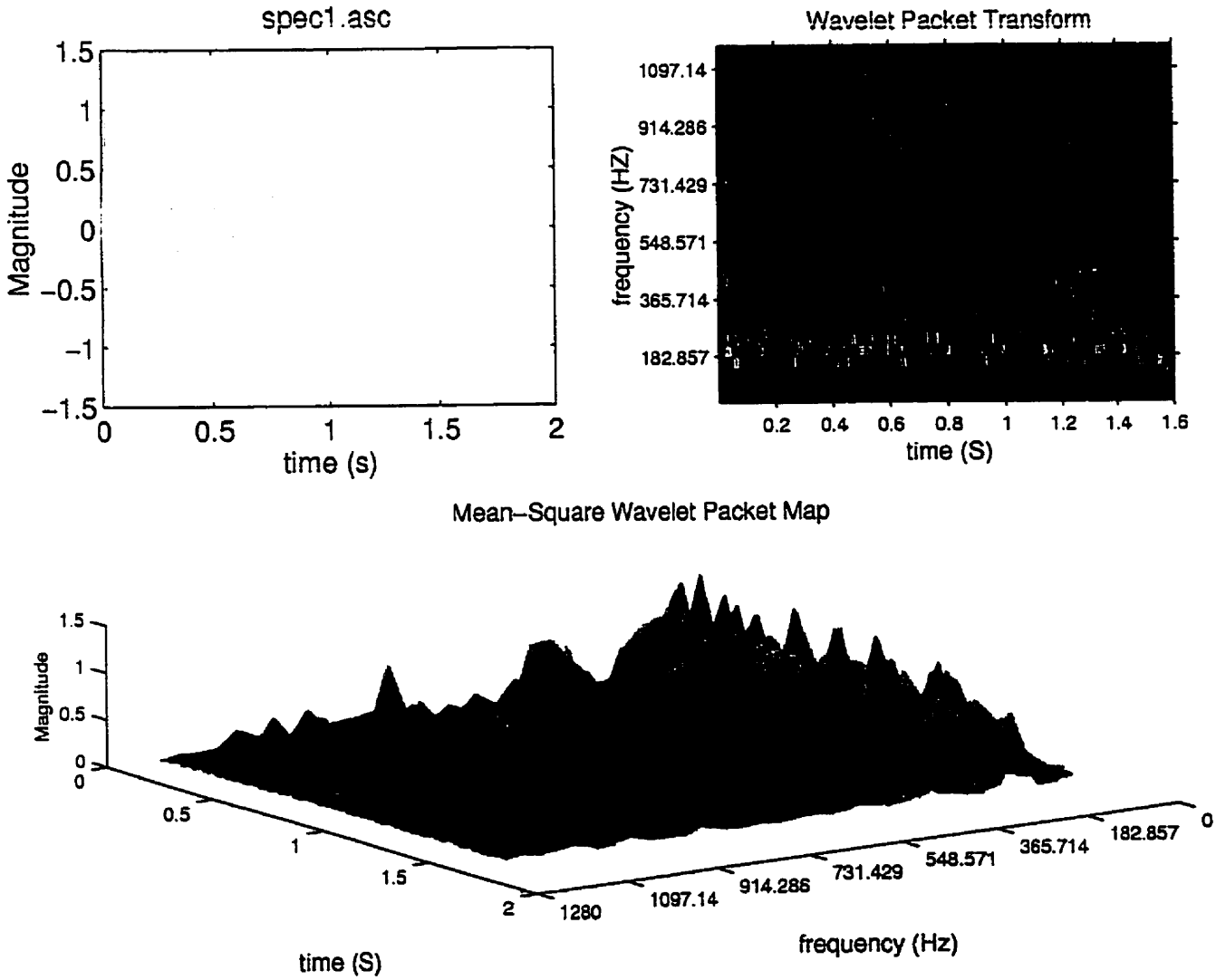

Figure 4.37: Wavelet packet transform and mean-square wavelet packet map of the signal measured on a defective gearbox.

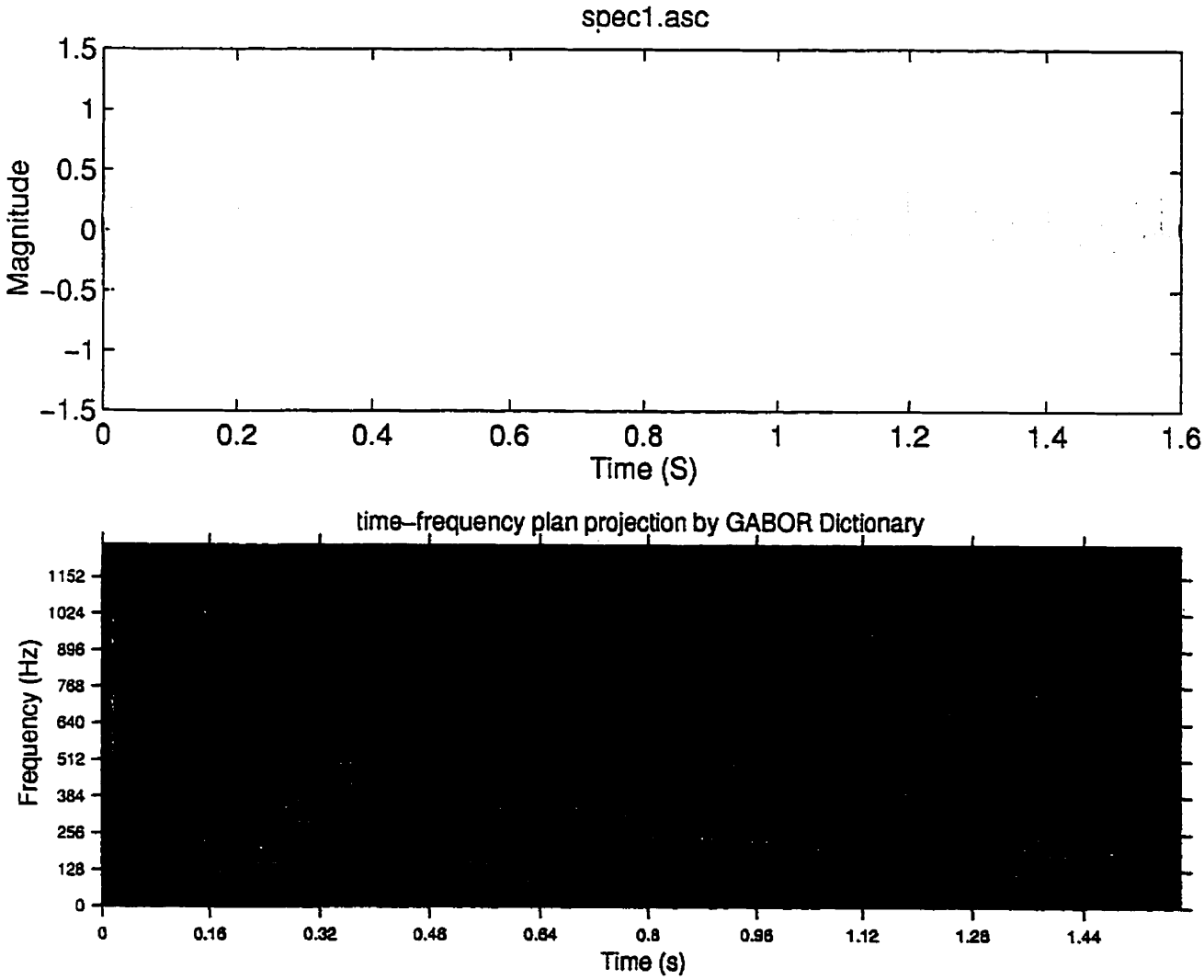

Figure 4.38: Time-frequency representation by the Gabor dictionary of the signal measured on a defective gearbox.

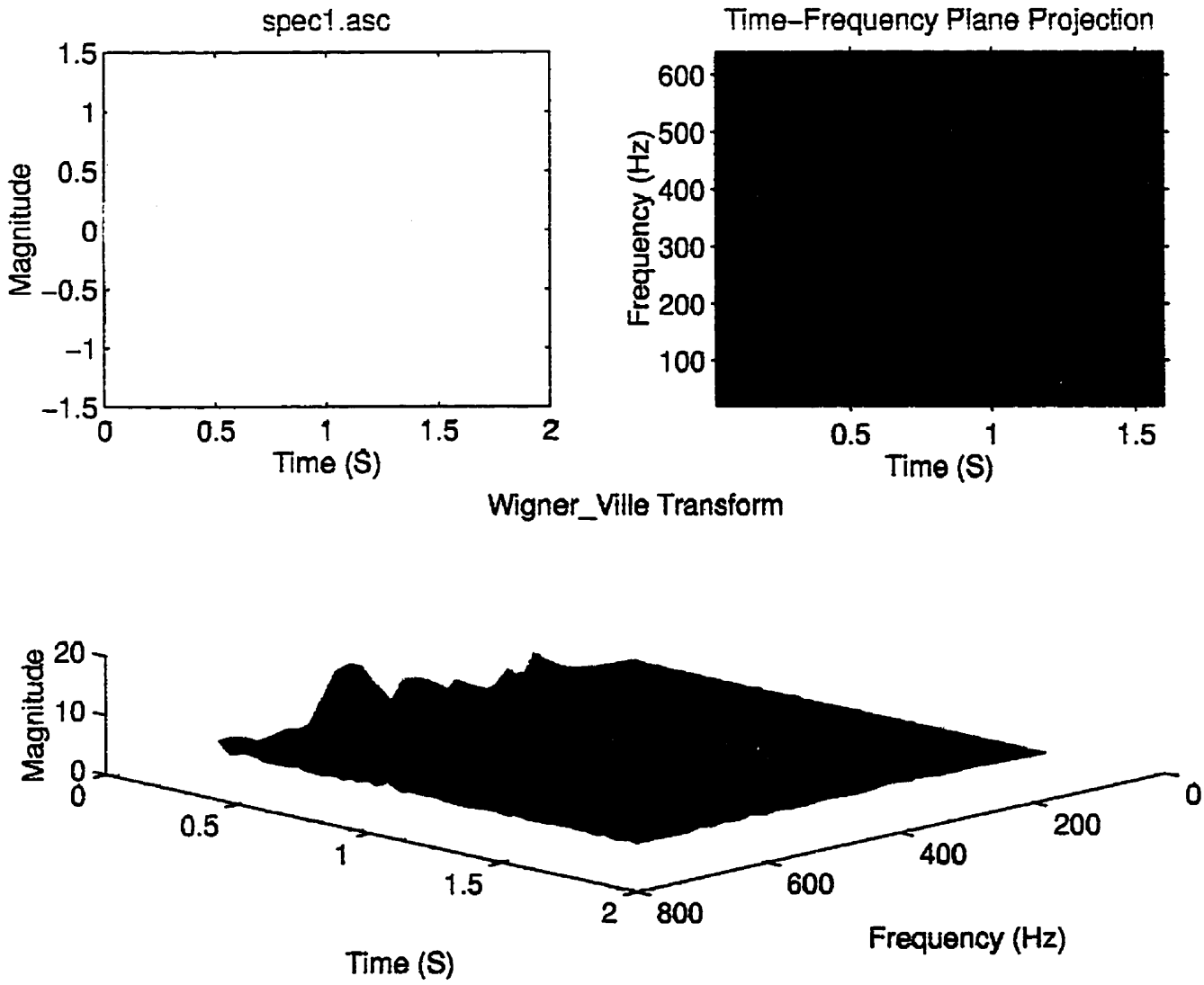

Figure 4.39: Wigner-Ville distribution of the signal measured on a defective gearbox.

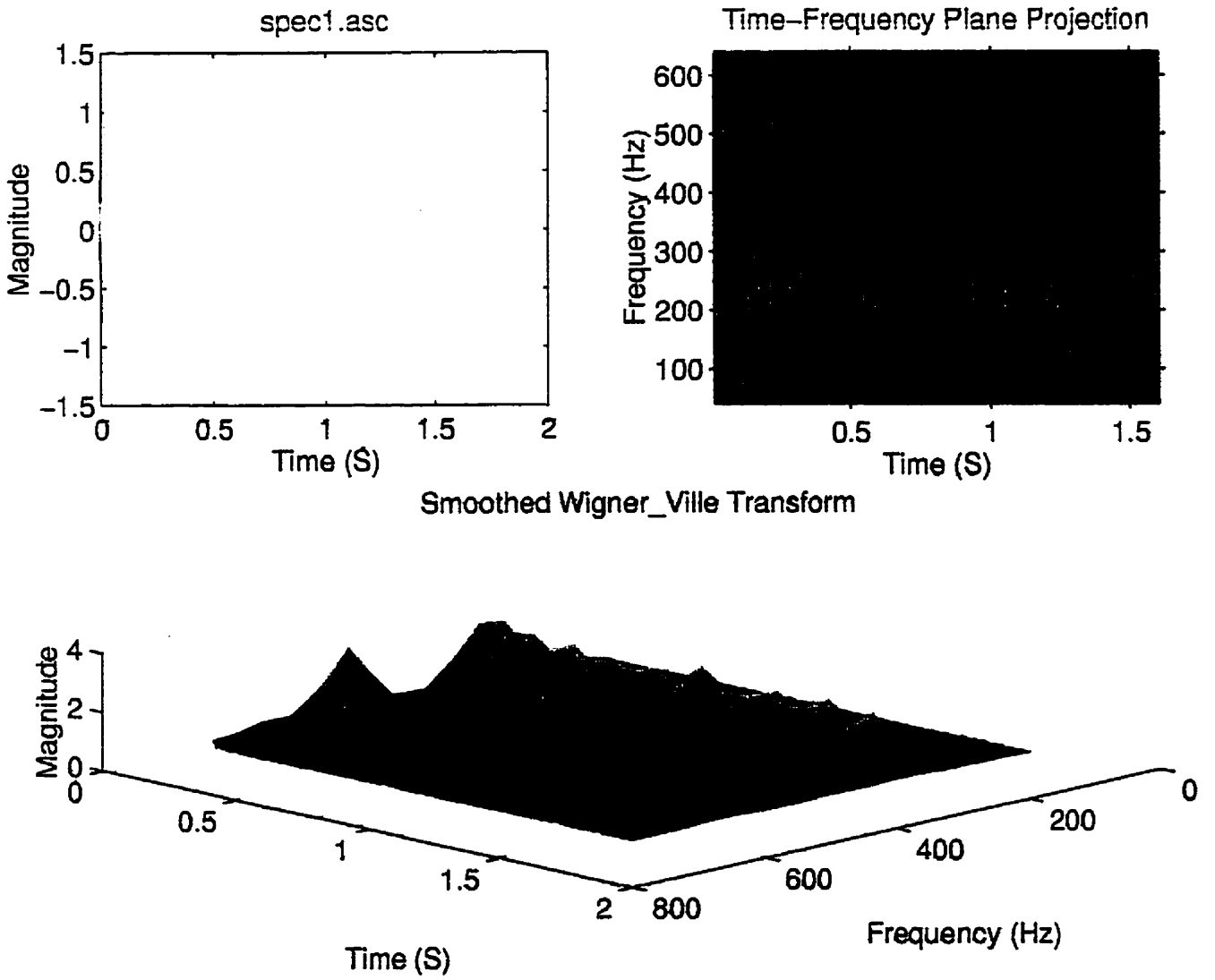

Figure 4.40: Smoothed Wigner-Ville distribution of the signal measured on a defective gearbox.

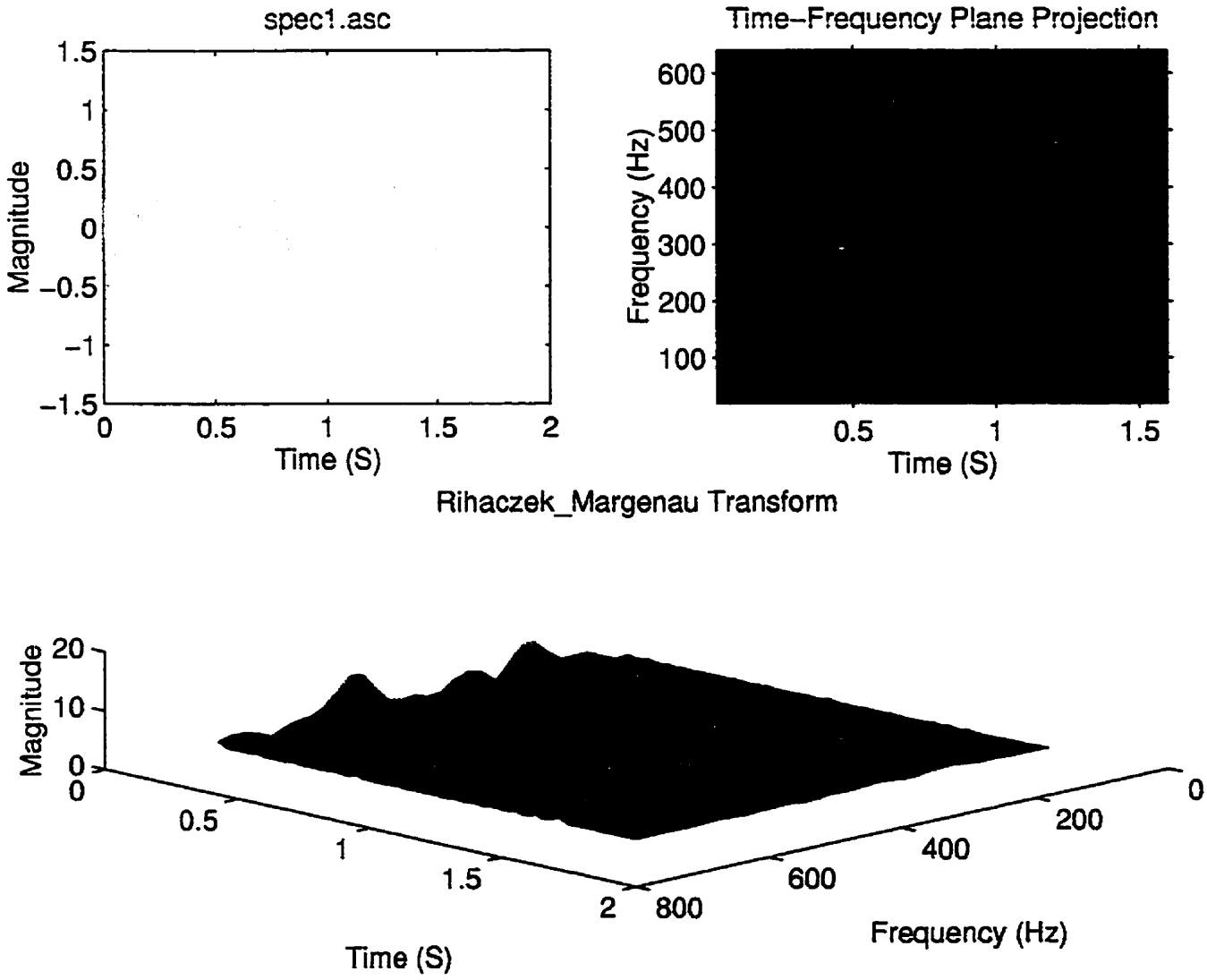

Figure 4.41: Rihaczek-Margenau representation of the signal measured on a defective gearbox.

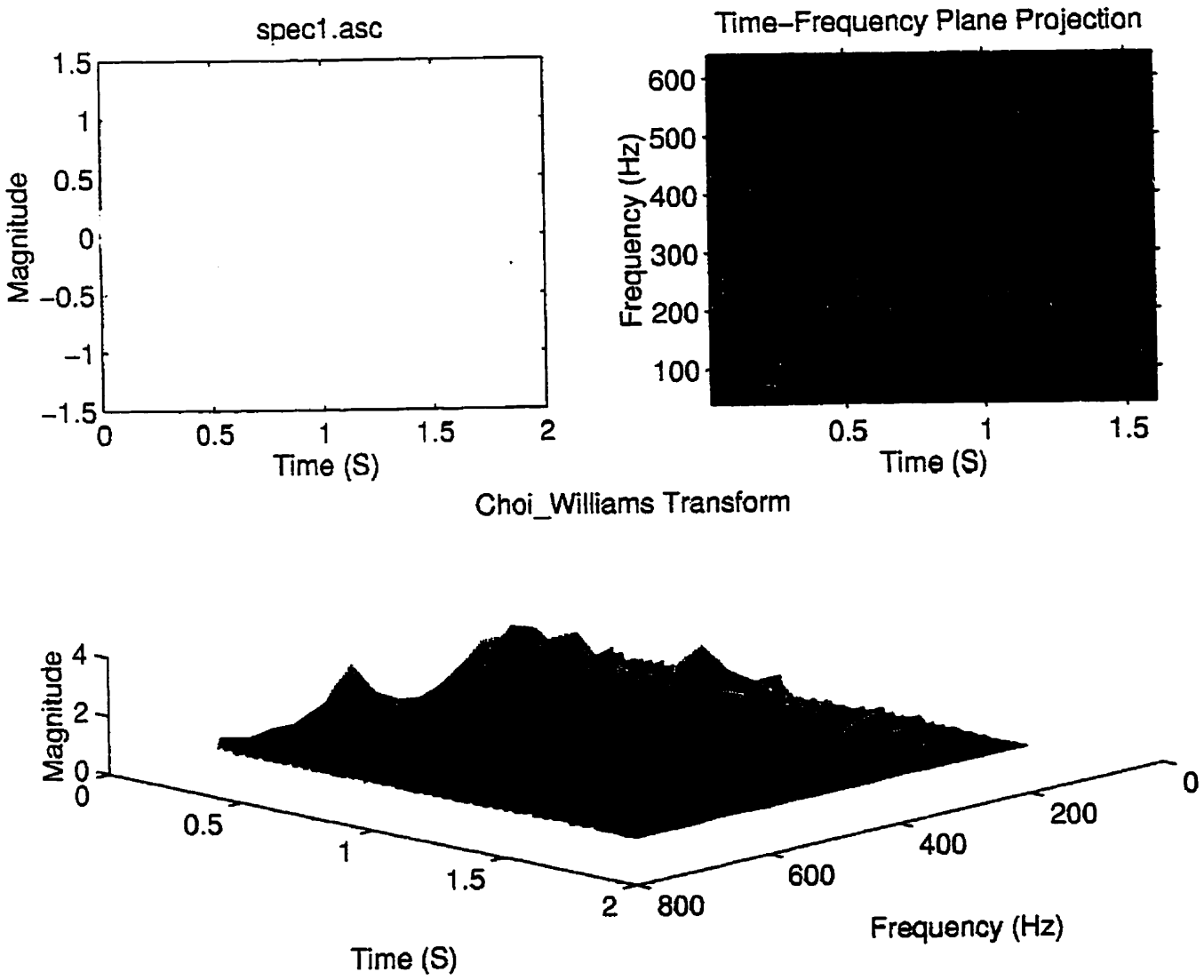

Figure 4.42: Choi-Williams representation of the signal measured on a defective gearbox.

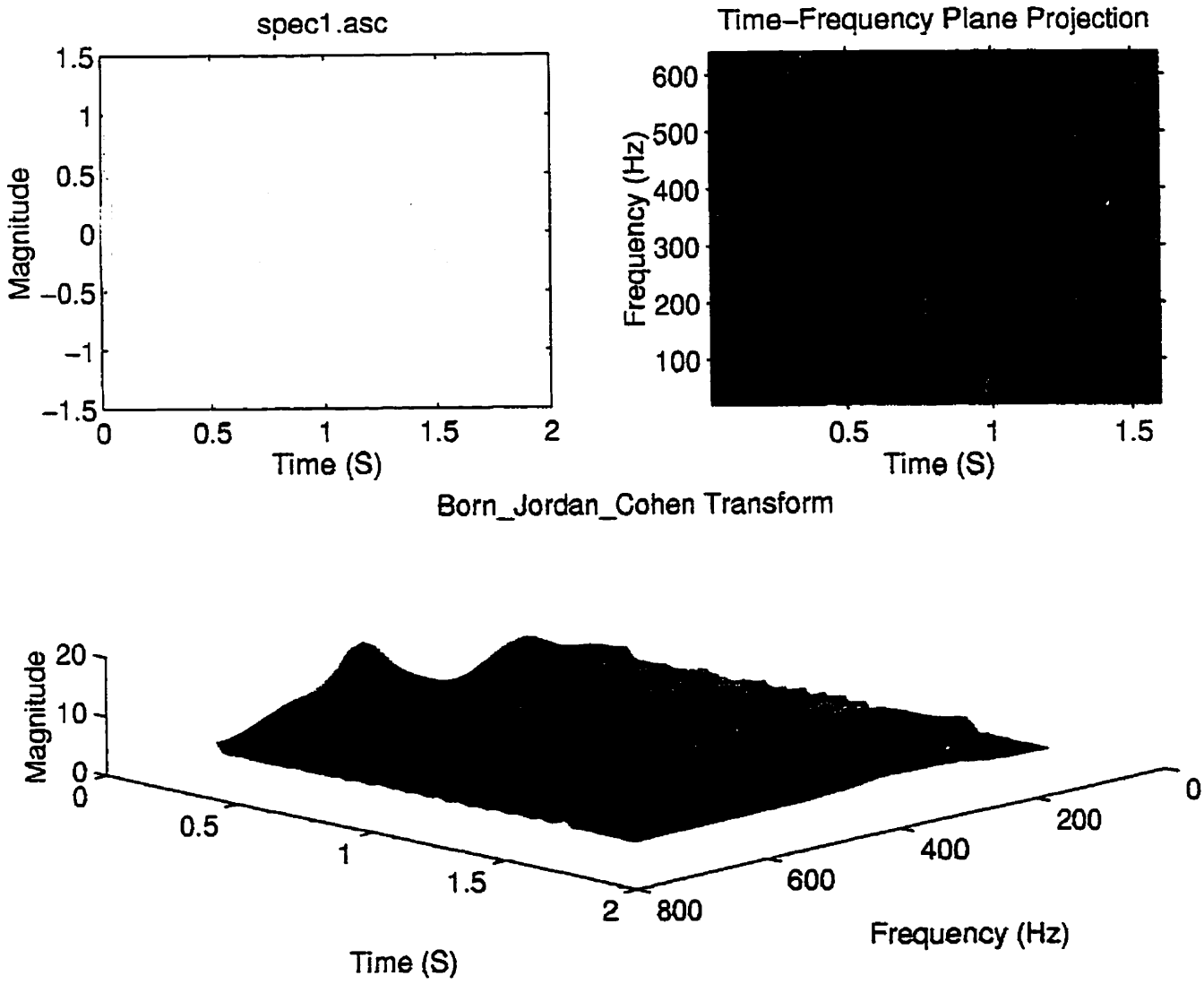

Figure 4.43: Born-Jordan-Cohen representation of the signal measured on a defective gearbox.

CONCLUSION

Dans ce travail de thèse, nous avons :

a) résolu le problème du manque de résolution dans la représentation temps-fréquence en développant une nouvelle technique appelée *Zoom in wavelet transform*, et en proposant une nouvelle méthode de STFT.

b) appliqué des nouvelles méthodes de "de-noising" par la méthode en ondelettes et par l'algorithme de Matching Pursuit.

c) développé un logiciel de traitement du signal en temps-fréquence.

d) procédé à des essais expérimentaux.

e) procédé à des essais industriels.

Nous avons bien montré que la majorité des méthodes conventionnelles sont applicables pour un seul défaut sur un élément de machine simple et qu'aucune de ces méthodes ne peut fournir la réponse pour tous les problèmes de diagnostic de machines. Il est très difficile de décider laquelle parmi ces méthodes est la plus efficace avant d'identifier le type de défaut. Ces problèmes des méthodes conventionnelles nous obligent à aller vers les méthodes de

traitement de signal plus avancées.

La représentation temps-fréquence est une solution qui peut apporter beaucoup d'avantages et faciliter le diagnostic des machines. La plus simple méthode pour obtenir une représentation temps-fréquence est la transformée de Fourier à fenêtre glissante (TFFG). Cette méthode peut facilement être utilisée dans la surveillance de machines. La méthode TFFG peut nous donner une représentation temps-fréquence de signal vibratoire capté sur une machine, lequel peut être interprété facilement par un technicien pour vérifier l'état général de machines. Malgré tous les avantages de cette méthode, elle a un défaut fondamental qui nous empêche d'obtenir une bonne résolution simultanément dans le temps et dans la fréquence. Pour obtenir plus de précision, nous nous sommes tournés vers les méthodes un peu plus complexes comme les distributions de Wigner-Ville, Choi-Williams et RID. En comparant ces distributions, nous avons conclu que :

- La distribution de Wigner-Ville peut fournir la fréquence instantanée, qui est très importante dans le diagnostic des machines, mais malheureusement elle n'est pas capable de produire une représentation temps-fréquence correcte du signal à cause des termes rectangulaires (cross terms) qui sont créés artificiellement entre les terms carrés.

- La distribution de smoothed Wigner-Ville donne une meilleure représentation temps-fréquence que les autres distributions et fournit une résolution satisfaisante

dans le temps et dans la fréquence. Dans cette méthode, les termes rectangulaires sont éliminés par le fenêtrage.

- La distribution de Choi-Williams peut nous fournir une aussi bonne représentation temps-fréquence que la distribution smoothed Wigner-Ville, à condition qu'on puisse choisir une valeur adéquate pour le paramètre σ . Cette distribution est un membre de la classe générale de distribution ayant un noyau exponentiel.

- La distribution Born-Jordan-Cohen nous donne une représentation temps-fréquence avec une résolution moins bonne que celle de smoothed Wigner-Ville ou Choi-Williams. Cette distribution est un membre de la distribution de RID.

- La distribution Rihaczek-Margenau pour les signaux industriels bruités n'est pas très efficace.

En somme, le choix d'une distribution dans une application pratique dépend du problème concerné et aucune de ces distributions ne peut résoudre avec précision tous les problèmes.

Les méthodes les plus récentes qui sont utilisées pour obtenir une représentation temps-fréquence sont les méthodes temps-échelle. Contrairement aux méthodes précédentes qui ont une résolution constante dans le plan temps-fréquence, ces méthodes nous permettent d'avoir une résolution flexible dans le plan temps-fréquence.

-La transformée en ondelettes est une méthode temps-échelle qui produit une très bonne résolution temporelle pour les hautes fréquences et une très bonne résolution fréquentielle pour les basses fréquences. Cette propriété la rend très puissante pour l'étude des phénomènes transitoires qui sont très courants dans le diagnostic de machines. Mais le choix de la fonction de base d'ondelettes (mother wavelets) joue un rôle très important dans la qualité de la représentation temps-fréquence. Donc, la transformée en ondelettes peut être utilisée accompagnée des autres méthodes pour fournir les informations qui peuvent être manquées par les autres méthodes.

-La transformée en paquet d'ondelettes est un autre membre des méthodes temps-échelle qui essaie de résoudre le problème de résolution fréquentielle de la transformée en ondelettes. Dans cette méthode, l'échelle logarithmique de l'axe de fréquence de la transformée en ondelettes est remplacée par l'échelle linéaire de l'axe de fréquence, mais au détriment de l'excellente résolution temporelle de la transformée en ondelettes.

-Parfois, même la résolution fréquentielle de la transformée en paquet d'ondelettes n'est pas satisfaisante, surtout dans l'identification des défauts. Dans ce cas, la nouvelle méthode appelée "*Zoom in Wavelet transform*" est très utile. Par cette méthode, on peut diviser une bande de fréquences en plusieurs bandes de fréquences. Cette méthode a été testée pour une boîte d'engrenage et elle a donné un très bon

résultat.

-Une autre technique relevant des méthodes temps-échelle et qui a été présentée dans ce travail est la transformée en ondelettes adaptatives (par l'algorithme de "Matching Pursuit"). Cette technique donne une bonne résolution pour les signaux ayant des composantes parallèles à l'axe de temps ou à l'axe de fréquence. Mais, pour les signaux ayant une modulation en amplitude ou une modulation en fréquence, elle ne donne pas une bonne représentation.

Pour mettre en oeuvre toutes les méthodes temps-fréquence et temps-échelle, un logiciel facile à utiliser a été développé. Ce logiciel permet à un ingénieur ou à un technicien ayant peu d'expérience dans le traitement de signal d'obtenir différentes représentations temps-fréquence d'un signal en deux et trois dimensions, en couleurs et de différents points de vue. Ce logiciel est très pratique dans les cas expérimentaux et industriels, surtout avec les différentes options qui y sont ajoutées, comme la technique de "De-noising". On sait qu'on ne peut pas utiliser les méthodes habituelles de "De-noising" pour des signaux non stationnaires et transitoires. On a donc utilisé les méthodes du "Wavelet De-noising" qui donnent des résultats très satisfaisants.

Il faut noter qu'il existe depuis 1995 un nouveau logiciel pour exécuter la transformée en ondelette qui s'appelle "Wavelet Toolbox" mais la programmation de notre logiciel a été faite en 1994 et le logiciel était en marche à la fin de 1995. De toute façon, notre logiciel

possède les avantages suivants que Matlab ne serait pas en mesure d'exécuter, entre autres:

a) Exécuter de la distribution de Wigner-Ville et différentes distribution de classe Cohen, de classe Exponentielle et de classe RID.

b) Exécuter de la transformée de Fourier à fenêtre glissante adaptative pour ajuster la résolution dans le plan temps-fréquence.

c) Exécuter de "Zoom in Wavelet Transform" qui permet d'obtenir une précision désirable dans une bande de fréquence choisie.

d) Fournir la transformée en ondelettes adaptatives par l'algorithme de "Matching Pursuit" qui nous permet d'avoir des décompositions plus flexible pour la représentation d'un signal ayant de propriétés très différentes.

e) Appliquer la méthode de "De-noising" par l'algorithme de "Matching Pursuit".

Enfin le logiciel a été vérifié avec plusieurs signaux théoriques, expérimentaux et industriels. Dans tous les cas, le logiciel a montré une efficacité supérieure aux méthodes conventionnelles.

En somme, malgré le fait que toutes les méthodes temps-fréquence et temps-échelle nous fournissent beaucoup plus d'information sur un signal que les autres méthodes traditionnelles aucune de ces méthodes n'est parfaite. Croire en l'existence d'une méthode universelle

unique capable de détecter à un stade précoce n'importe quel défaut susceptible d'affecter une machine et d'en suivre l'évolution dans le temps est une pure utopie. Il faut plutôt prendre avantages de chacune de ces méthodes pour obtenir le plus d'information possible d'un signal.

Ce travail qui a été effectué pour la première fois dans notre groupe de recherche nous a donné un très bon outil pour avancer dans le domaine de la surveillance et du diagnostic de machines. Il nous a ouvert une nouvelle voie non seulement dans le domaine du génie mécanique mais aussi dans le domaine de la biomécanique pour la cardiographie et dans le domaine du génie électrique pour le traitement du signal.

Le logiciel pourra servir à d'autres essais sur différents autres défauts mécaniques, pourra également servir à enseigner les représentations temps-fréquence aux ingénieurs en mécanique qui connaissent très peu de ces méthodes.

La suite logique de ce travail consisterait à améliorer certains noyaux par des méthodes d'optimisation dans le but d'obtenir un noyau plus adapté au signal vibration de machines.

RÉFÉRENCES

ARCHAMBAULT, R. (1989). Getting more out of vibration signals: using the logarithmic scale, Proceedings of the 1st International Machinery Monitoring & Diagnostic Conference & Exhibit, 567-571.

ATLAS, L., BERNARD, G. et NARAYANAN, S.B. (1966). Applications of time-frequency analysis to signal from manufacturing and machine monitoring sensors. Proceedings of the IEEE, 84(9), 1319-1329.

BARKOV, A., BARKOVA, N. et MITCHELL, J.S. (1995). Condition assessment and life prediction of rolling element bearing - Part 1, Sound and Vibration, 29(6), 10-17.

BAZELAIRE, E. et VIALLIX, J.R. (1978). Theory of seismic noise. Proc. 49th Eur. Ass. Explor. Geophys. Mtg. (Belgrade, Yugoslavia), 1-2.

BENTLY, D.E., ZIMMER, S., PALMATIER, G.E. et MUSZYNSKA, A. (1986). Interpreting vibration information from rotating machinery. Sound and Vibration, 20(2), 14-23.

BERRY, J.E. (1986). Diagnostic evaluation of machinery using vibration signature analysis.

Sound and Vibration, 20(6), 10-17.

BOUACHACHE, B. (1978). Représentation temps-fréquence. Soc. Nat. ELF Aquitaine, Pau, France, Publ. Recherches, 373-378.

BOASHASH, B. (1992). Time-frequency signal analysis. John Wiley & Sons, Inc.

BRENNAN, M.J., CHEN, M.H. et REYNOLDS, A.G. (1997). Use of vibration measurements to detect local tooth defects in gears. Sound and Vibration, 31(11), 12-17.

CHOI, H.I. et WILLIAMS, W.J. (1989). Improved time-frequency representation of multicomponent signal exponential kernels. IEEE Trans. Acoust., Speech, Signal Processing, 37(6), 862-871.

CLASSEN, T.A.C.M. et MECKLENBRAUKER, W.F.G. (1980). The wigner distribution - A tool for time-frequency signal analysis part I: continuous time signals. Philips J. Res., 35, 217-250.

CLASSEN, T.A.C.M. et MECKLENBRAUKER, W.F.G. (1980). The wigner distribution - A tool for time-frequency signal analysis part II: discrete time signals. Philips J. Res., 35, 276-300.

CLASSEN, T.A.C.M. et MECKLENBRAUKER, W.F.G. (1980). The wigner distribution - A tool for time-frequency signal analysis part III: relations with other time-frequency signal transformations. Philips J. Res., 35, 372-389.

COHEN, L. (1966). Generalized phase-space distribution functions. J. Math. Phys., 7, 781-786.

COHEN, L. (1989). Time-frequency distribution - A review. Proc. IEEE, 77(7), 941-981.

COIFMAN R.R. et WICKERHAUSER M.V. (1992). Entropy-based algorithms for best basis selection. IEEE Trans. Inform. Theory, Special Issue on Wavelet Transforms and Multires. Signal Anal., 38, 713-718.

COLLACOTT, R.A. (1979). Vibration monitoring diagnosis, John Wiley & sons.

D'AMATO, E. et RISSONE, P. (1989). Using the envelope method to monitor rolling bearings. Proceedings of the 1st International Machinery Monitoring & Diagnostic Conference & Exhibit, 560-566.

DALPIAZ, G. et RIVOLA, A. (1995). Fault detection and diagnostics in cam mechanisms. 2nd International Symposium Acoustical and Vibratory Surveillance Methods and

Diagnostic Techniques, 327-339.

DAUBECHIES, I. (1988). Orthonormal based of compactly supported wavelets. Commun. Pure Appl. Math., XLI, 909-996.

DAUBECHIES, I. (1992). Ten lectures on wavelets. Philadelphia: SIAM.

DEBAO, L., HONGCHENG, Z., YUANYUN, Z. et BO, W. (1989). Cepstrum analysis and the fault diagnosis of rotating machine. Proceedings of the 1st International Machinery Monitoring & Diagnostic Conference & Exhibit, 596-598.

DIETHORN, E.J. (1994). The generalized exponential time-frequency distribution. IEEE Trans. Signal Processing, 42(5).1028-1037.

ESHLEMAN, R.L. (1983). Machinery diagnostics and your FFT, Sound and Vibration, 17(4), 12-18.

FORRESTER, B.D. (1989). Use of the Wigner-Ville distribution in helicopter fault detection. Proc. ASSPA89, 78-82.

GABOR, D. (1946). Theory of communication. J. IEEE (London), 93, 429-457.

GASQUET, G. et WITMOSKI, P. (1992). Analyse de Fourier et applications: filtrage, calcul numérique, ondelettes. Masson, Paris, 307-308.

GRIVELET, P. (1990). Monitoring of reciprocating compressors by vibration. Proceedings of the IMMDC Congress, Los Angeles. 393-399.

GROSSMANN, A. et MORLET, J. (1984). Decomposition of hardy functions into square integrable wavelets of constant shap. SIAM J. Math. Anal., 15, 723-736.

HESS-NIELSEN, N. et WICKERHAUSER, M.V. (1996). Wavelets and time-frequency analysis. Proceedings of the IEEE, 84(4), 523-539.

HLAWATSCH, F. et BOUDREAUX-BARTELS, G.F. (1992). Linear and quadratic time-frequency signal representations. IEEE Signal Processing Magazine, 9, 21-67.

HONGBIN, M. (1995). Application of wavelet analysis to detection of damages in rolling element bearings. Proc. of the Int. Conf. on Structural Dynamics, Vibration, Noise and Control, Hongkong, 1334-1339.

JAMES LI, C. et MA J. (1992). Bearing localized defect detection through wavelet decomposition of vibrations. Sensors and Signal Processing for Manufacturing, ASME

Winter Annu. Meet. 187-196.

JEONG, J. et WILLIAMS, W. (1992). Kernel design for reduced interference distributions. IEEE Trans. Sig. Proc., 40, 402-412.

JONES, R.M. (1994). A guide to the interpretation of machinery vibration measurements - part I. Sound and Vibration, 28(5), 24-35.

JONES, R.M. (1994). A guide to the interpretation of machinery vibration measurements - part II. Sound and Vibration, 28(9), 12-20.

JONES, R.M. (1996). Enveloping for bearing analysis. Sound and Vibration, 30(2), 10-15.

KIRKWOOD, J.G. (1933). Quantum statistics of almost classical ensembles. Phys. Rev., 44, 31-37.

LE BLEU, J. et MING, X. (1995). Vibration monitoring of sealess pumps using spike energy. Sound and Vibration, 29(12), 10-16.

LEON, R.L. (1985). Is your periodic machinery monitoring program telling you the truth, the whole truth, and nothing but ...?. Sound and Vibration, 19(6), 24-26.

LEURIDAN, J., VAR DER AUWERAER, H. et VOLD, H. (1994). The analysis of nonstationary dynamic signals. Sound and Vibration, 28(8), 14-26.

LIANGSHEN, Q., YAODONG, C. et XIONG, L. (1989). A new approach to computer aided vibration surveillance of rotating machinery. International Journal of Computer Applications in Technology, 2(2), 108-117.

LIANGSHEN, Q., YAODONG, C. et JIYAO, L. (1989). The Holospectrum: A new FFT based rotor diagnostic method. Proceedings of the 1st International Machinery Monitoring & Diagnostic Conference & Exhibit, 196-201.

LIPOVSZKY, G., SOLYOMVARI, K. et VARGA, G. (1990). Vibration testing of machines and their Maintenance , Elsevier.

LOPEZ, J.E., TENNEY, R. et DECKERT, J. (1994). Fault detection and identification using real-time wavelet feature extraction. Proc. IEEE-SP Int. Symp. on Time-Frequency and Time-Scale Analysis, 217-220.

LOUGHLIN, P., ATLAS, E.L. et PITTON, J. (1993). Advanced time-frequency representations for speech processing. Visual Representations of Speech Signals, M. Cooke, S. Beete and M. Crawford (eds.), John Wiley & Sons.

LOUGHLIN, P., ATLAS, L., BERNARD, G. et PITTON, J. (1995). Application of time-frequency analysis to the monitoring of machining. Life Extension of Aging Machinery and Structures: Proc. of the 49th Meet. of MFPT Soc., 49, Vibration Inst.: Virginia Beach, 305-314.

LOUGHLIN, P.J. et BERNARD, G.D. (1997). Cohen-Posch (Positive) time-frequency distributions and their application to machine vibration analysis. Mechanical Systems and Signal Processing, 11(4), 561-576.

LOUGHLIN, P., PITTON, J. et ATLAS E. (1994). Construction of positive time-frequency distributions. IEEE Trans. Sig. Proc., 42, 2697-2705.

MALLAT, S. (1989). A theory for multiresolution signal decomposition: The wavelet representation. IEEE Transaction on Pattern Analysis and Machine Intelligence, 11(7), 674-693.

MALLAT, S. (1993). Matching pursuits with time-frequency dictionaries. IEEE Trans. Signal Processing, 41(12), 3397-3415.

MAJOVSKY, B. et SALAMONE, D.J. (1988). Dynamic analysis of a steam turbine vibration problem. Sound and Vibration, 22(9), 24-33.

MARGENAU, H. et HILL, R.N. (1961). Correlation between measurements in quantum theory. Prog. Theor. Phys., 26, 722-738.

MARTIN, A. (1987). Vibration monitoring of machines. Brueel & Kjaer Technical Review, 1, 1-36.

MCFADDEN, P.D. et WANG, W. (1990). Time-frequency domain analysis of vibration signals for machinery diagnostics. 1: Introduction to the Wigner-Ville distribution. Report No. : OUEL-1859/90; ETN-91-98957, Department of Engineering Science, Oxford University.

MCFADDEN, P.D. et WANG, W. (1991). Time-frequency domain analysis of vibration signals for machinery diagnostics. 2: The weighted Wigner-Ville distribution. Report No. : OUEL-1891/91; ETN-92-91087, Department of Engineering Science, Oxford University.

MCFADDEN, P.D. et WANG, W. (1992). Time-frequency domain analysis of vibration signals for machinery diagnostics. 3: The present power spectral density. Report No. : OUEL-1911/92; ETN-92-92063, Department of Engineering Science, Oxford University.

MCFADDEN, P.D. et WANG, W. (1992). Time-frequency domain analysis of vibration signals for machinery diagnostics. 4: Interpretation using image processing techniques.

Report No. : OUEL-1953/92; ETN-94-95148, Department of Engineering Science, Oxford University.

MCFADDEN, P.D. et SMITH, J.D. (1983). Vibration monitoring of rolling element bearings by the high-frequency resonance technique. C-Mech TR 30.

MEYER, Y. (1992). Les ondelettes algorithmes et applications. Armand Colin, Paris, 127-133.

MORLET, J., ARENS, G., FOURGEAU, E. et GIARD, D. (1982). Wave propagation and sampling theory-part II: sampling theory and complex waves. Geophysics, 47(2), 203-236.

PAGE, C.H. (1952). Instantaneous power spectra. J. Appl. Phys., 23, 103-106.

RAMCHANDRAN, K. et VETTERLIi, M. (1996). Wavelets, subband coding and best bases. Proceeding of the IEEE, 84(4), 541-560.

REYNOLDS, A.G. (1995). The detection of local tooth defects in gearing by vibration analysis. M. Sc. Dissertation, Royal Naval Engineering College, Manadon.

RIHACZEK, W. (1968). Signal energy distribution in time and frequency. IEEE Trans.

Informat. Theory, IT-14, 369-374.

RIOUL, O. et VETTERLI, M. (1991). Wavelet and signal processing. IEEE SP Magazine, 14-38.

ROBINSON, J.C., CANADA, R.G. et PIETY, K.R. (1996). Peakvue analysis - new methodology for bearing fault detection. Sound and Vibration, 30(11), 22-25.

ROHRBAUGH, R. (1993). Application of time-frequency analysis to machinery condition assessment. Soc. Proceedings of the 27th Asilomar Conference on Signal, Systems & Computer, 2, 1455-1458.

ROHRBAUGH, R.A. et COHEN, L. (1995). Time-frequency analysis of a cam operated pump. Life Extension of Aging Machinery and Structures: Proc. Of the 49th Meet. of MFPT Soc., 49, Vibration Inst.: Virginia Beach, 349-361.

SCULTHORPE, B.R., et JOHNSON, K.M. (1987). Vibration monitoring techniques on reactor coolant pumps. Sound and Vibration, 21(9), 18-21.

SHENSA, M.J. (1992). The discrete wavelet transform: Wedding the À Trous and Mallat algorithms. IEEE Trans. Signal Processing, 40(10), 2464-2482.

SMITH, D.R. et WOODWARD, G.M. (1988). Vibration analysis of vertical pumps. Sound and Vibration, 22(6), 24-30.

SWARUP, J. (1990). Vibration analysis of centrifugal pumps. Sound and Vibration, 24(5), 12-15.

TREVILLION, B., PARGE, P., CARLE, P. et GOOD, M. (1989). Machinery interactive display and analysis system description and applications. Proceedings of the 1st International Machinery Monitoring & Diagnostic Conference & Exhibit, 176-182.

ULIERN, D. (1993). Diagnosis by measurement of internal vibration and vibration analysis on maintenance of rotating machinery as turbo chillers. Proceedings, Annual Technical Meeting - Institute of Environmental Sciences, 2, 525-530.

VETTERLI, M. (1992). Wavelets and filter banks : theory and design. IEEE Trans. Signal Processing, 40(9), 2207-2232.

VILLE, J. (1948). Théorie et applications de la notion de signal analytique. Cables et Transmission, 2A, 61-74.

WANG W.J. et MCFADDEN, P.D. (1993). Early detection of gear failure by vibration

analysis - I. calculation of the time-frequency distribution. Mechanical Systems and Signal Processing, 7(3), 193-203.

WANG, W.J. et MCFADDEN, P.D. (1993). Application of the wavelet transform to gearbox vibration analysis. American Society of Mechanical Engineers, Petroleum Division (Publication) PD Structural Dynamics and Vibrations Proceedings of the 16th Annual Energy - Sources Technology Conference and Exhibition Jan 31-Feb 4 1993, 52, 13-20.

WANG W.J. et MCFADDEN, P.D. (1995). Application of wavelets to early gear damaged detection. Mechanical Systems and Signal Processing, 9, 497-507.

WIGNER, E.P. (1932). On the quantum correction for thermodynamic equilibrum. Phys. Rev., 40, 749-759.

ZHANG, B. et SATO, S. (1994). A time-frequency distribution of cohen's class with a compound kernel and its application to speech signal processing. IEEE Trans. Signal Processing, 42(1), 54-64.

ZHAO, Y., ATLAS, L.E. et MARKS, R.J. (1990). The use of cone shaped kernels for generalized time-frequency representations of nonstationary signals. IEEE Trans. Acoust., Speech, Signal Process., 38(7), 1084-1091.

ZHONGXING, G. et LIANGSHENG, Q. (1994). Vibrational diagnosis of machine parts using the wavelet packet technique. British Journal of Non-Destructive Testing, 36(1), 11-15.

ZHONYU, G., DAURAND, L. et HOWARD, C.L. (1994). The time-frequency distributions of non stationary signals based on a Bessel kernel. IEEE Transactions on Signal Processing, 42(7), 1700-1706.